Understanding the contribution of inositol phosphate signalling to class-1 HDAC complex function

Thesis submitted for the degree of

Doctor of Philosophy

at the University of Leicester

by

Grace Emily Adams BSc (Hons)

College of Medicine, Biological Sciences, and Psychology

Department of Molecular and Cell Biology

University of Leicester

March, 2018

Grace Emily Adams

Understanding the contribution of inositol phosphate signalling to class-1 HDAC complex function

Abstract:

Class 1 histone deacetylases (HDACs) regulate chromatin confirmation and gene expression through recruitment to co-repressor complexes. Recently, it was shown that HDAC3/SMRT binds and is regulated by inositol phosphates (IP) *in vitro*. Additionally, complex activity of HDAC1/MTA1 and HDAC1/MIDEAS is enhanced by the addition of IPs *in vitro*, indicating conserved regulation. In this work, I aimed to alter the level of IPs present in the cells through overexpression of a kinase, IPMK, and two phosphatases, PTEN and SopB, and determine the effect on HDAC activity *in vivo*. In addition, I utilised an IPMK knockout embryonic stem (ES) cell line and generated inducible rescues through a PiggyBac TET system to establish if large scale depletions of IP levels alter HDAC activity.

We revealed that manipulation of IP through the overexpression of IPMK, PTEN and SopB does not influence global HDAC activity or histone acetylation levels. Isolation of overexpressed HDAC3/SMRT in concert with these enzymes, revealed differences in HDAC3/SMRT complex activity, however, these differences did not correlate with altered IP levels. Analysis of global HDAC activity, isolated complex activity and HDAC3 target genes in IPMK knockout and rescue ES cell lines further revealed minimal changes. In conclusion, we were unable to show that IPs regulated the activity of class I HDAC complexes *in vivo.* IPMK, HDAC1 and HDAC3 null mice all exhibit early embryonic lethality suggesting they play essential roles in embryogenesis. Upon differentiation of TET-IPMK cells, embryoid bodies revealed loss of IPMK leads to increased cardiomyocyte markers and decreased formation of neuroectoderm progenitors. Therefore, emphasizing IPMKs important role in gene regulation during embryogenesis. Our data suggests, that this is not through direct regulation of HDAC activity, thus highlighting an undiscovered nuclear role for IPMK.

Acknowledgments

I firstly wish to thank my supervisor, Professor Shaun Cowley, for his endless support, guidance, encouragement and faith throughout my time at the University of Leicester. I would also like to thank my co-supervisor Professor John Schwabe for his advice and invaluable discussion during my project. My thanks also go to my committee members Professor Ian Eperon and Dr Tom Webb for their helpful and thought provoking comments and discussion. I would like to extend my gratitude to Dr Peter Watson for his irreplaceable advice, valuable discussion and help in the lab and in establishing the inositol phosphate quantitation method with me. My thanks go to all members of labs 3/37, you've made me feel welcome since my first day with your friendship, encouragement and help. Special thanks go to Claire Barnes for sharing the ups and downs of a PhD with me, your support and friendship have kept me sane during this process. Without the unconditional support, love and patience provided by my family, especially my mother, father, brother, sister-in-law and my adorable nephews, this process would have been so much harder, thank you for everything you do for me. Finally, to my husband Cam, you may not understand the contents of this thesis as I do not understand geotechnical engineering; but I could not have got to this stage without your constant love, patience, motivational speeches and simply being there for me.

List of Contents

Table of Contents

List of figures

List of tables

Abbreviations

A	Alanine
Ala	Alanine
Akt	Protein kinase B
Arg	Arginine
Ascl-1	Achaete-scute homolog 1
ATP	Adenosine triphosphate
BMP4	Bone morphogenic protein 4
bp	base pair
BPTF	Bromodomain PHD Finger Transcription Factor
C	Cysteine
CaMK	Calcium/calmodulin-dependent protein kinase
CBP	Histone acetyltransferase CREB-binding protein
cDNA	Complementary DNA
CDS2	CDP-diacylglycerol synthase 2
CD68	Cluster of differentiation 68
ChIP	Chromatin immunoprecipitation
CK2	Casein kinase 2
CoA	Co-enzyme A
COMPASS	Complex of protein associated with Set1
IP	Immunoprecipitation
CoREST	Co-repressor of RE1-silencing transcription factor (REST)
CpG	Cytosine—phosphate—Guanine
Ct	Threshold cycle
CtBP	C-terminal binding protein
D	Aspartate
DAD	Deacetylase activation domain
DMSO	Dimethyl sulfoxide
DNA	Deoxyribose nucleic acid
DNMTs	DNA (cytodine-5)-methyltransferase
DNTTIP1	Deoxynucleotidyltransferase, terminal, interacting protein 1
Dox	Doxycycline hyclate
DPBS	Dulbecco's Phosphate Buffered Saline
E	Embryonic day
EBs	Embryoid bodies
EDTA	Ethylenediaminetetraacetic acid
ES	Mouse embryonic stem cells
ESI	Electrospray ionisation
FACS	Fluorescently activated cell sorting
Fam35a	Family with sequence similarity 35 member A
FGF5	Fibroblast growth factor 5
FoxA2	Forkhead transcription factor A2
G	Glycine

G1	Gap 1 phase
G2	Gap 2 phase
GAL4-UAS	GAL4-upstream activating sequence
GAL4-DBD	GAL4-DNA binding domain
GATA4/6	GATA binding protein 4/6
GFP	Green fluorescent protein
Gly	Glycine
GNAT	Gcn5-related N-acetyltransferase
GPS2	G-protein pathway suppressor 2
GSK3	Glycogen synthase kinase-3
H	Histone
HAT	Histone acetyltransferase
HDAC	Histone deacetylase
HDLP	Histone deacetylase like protein
HEK	Human embryonic kidney cells
HID	Histone interaction domain
Hnf1β	Hepatic nuclear factor 1-beta
Hnf4α	Hepatic nuclear factor 4-alpha
His	Histidine
Hist1h2bq	Histone cluster 1, h2bq
HMT	Histone methyl transferases
HOP	Homeodomain only protein
HoxB2	Homeobox B2
HPLC	High-performance liquid chromatography
HP1	Heterochromatin protein 1
ICM	Inner cell mass
Id	Inhibitor of differentiation factors
IEG	Immediate early genes
IL-10	Interleukin-10
ING1	Inhibitor of growth protein 1
INNP5	Inositol phosphate 5-phosphatase
INO1	Inositol-3-phosphate synthase
Ins(3,4,5)P_3	Inositol-3,4,5-trisphosphate
Ins(1,4,5,6)P_4	Inositol-1,4,5,6-tetrakisphosphate
Ins(3,4,5,6)P_4	Inositol-3,4,5,6-tetrakisphosphate
IP/s	Inositol phosphate/s
IP_4	Inositol tetrakisphosphate
IP_5	Inositol pentakisphosphate/ Inositol-1,3,4,5,6-pentakisphosphate
IP_6	Inositol hexakisphosphate/ Inositol-1,2,3,4,5,6-hexakisphosphate
IPMK	Inositol polyphosphate multikinase
IPPK	Inositol-Pentakisphosphate 2-Kinase
ISWI	Imitation SWI
IP3 5/6-kinase	Ins(1,3,4)P_3 5/6Kinase
JAK	Janus-associated kinases
JmjC	Jumonji C

JMJD2A	JmjC histone demethylase 2A
K	Lysine
LB	Lysogeny broth
LIF	Leukaemia inhibitory factor
LSD1	Lysine specific demethylase
Lys-Ac	Acetylated lysine
Lys	Lysine
M	Mitotic phase
MAPK/ERK	Mitogen activated protein kinase
MBD	Methyl CpG binding domain
MBD2/3	Methyl-CpG-binding domain proteins 2/3
MECP2	Methyl-CpG-binding protein 2
Mef2c	Myocyte enhancer factor 2c
MEFs	Mouse embryonic fibroblasts
MEK	MAPK/ERK kinase
MiDAC	Mitotic deacetylase complex
MIDEAS	Mitotic deacetylase-associated SANT domain protein
Mi-2	Chromodomain-helicase-DNA-binding protein Mi-2 homolog
MLL	Mixed lineage leukaemia
MRG15	MORF (mortality factor) -related gene on chromosome 15
mRNA	Messenger RNA
MSK1/2	Mitogen and stress-activated protein kinases 1 and 2
MTA1/2/3	Metastasis associated proteins 1/2/3
Myf5	Myogenic factor 5
Myf6	Myogenic factor 6
MyoD	Myogenic differentiation 1
MyoG	Myogenic Factor 4
NCoR	Nuclear receptor corepressor
NES	Nuclear export signal
Neurog1	Neurogenin 1
Nkx2.5	Homeobox protein NK-2 homolog E
NLS	Nuclear localisation signal
nm	Nanometer
NODE	Nanog- and Oct4- associated deacetylase
NuRD	Nucleosome remodelling and histone deacetylation complex
NURF	Nucleosome remodelling factor
P	Proline
PAGE	Polyacrylamide gel electrophoresis
PAH	Paired amphipathic helices
Pax3/6	Paired box protein 3/6
PBS	Phosphate buffered saline
PBST	Phosphate buffered saline – tween
PCR	Polymerase chain reaction
PEI	Polyethylenimine
PHD	Plant homeodomain
PI	Propidium iodide
PIPs	Phosphoinositide’s

PI(4,5,)P_2	Phosphatidylinositol 4,5-bisphosphate
PI(3,4,5)P_3	Phosphatidylinositol (3,4,5)-trisphosphate
PP1	Protein phosphatase 1
PP4	Protein phosphatase 4
PRC1	Polycomb repressive complex 1
PRC2	Polycomb repressive complex 2
PRMT	Protein arginine methyltransferases
PTB	Polypyrimidine tract binding
PTEN	Phosphatase and tensin homolog
PTM	Post translational modifications
P300	Histone acetyltransferases p300
qRT-PCR	Quantitative Real Time - PCR
R	Arginine
RA	Retinoic acid
RAR	Retinoic acid receptor
RbAp48/46	Retinoblastoma associated protein 48/46
REST	RE1-silencing transcription factor
RING1B	Really Interesting New Gene 1B (E3 ubiquitin ligase)
RNA	Ribonucleic acid
Rpgrip1	retinitis pigmentosa GTPase regulator-interacting protein 1
rtTA3	3rd generation reverse tetracycline transactivator
S	Serine
S phase	Synthesis phase
SAHA	Suberanilohydroxamic acid
SAM	S-adenosyl-L-Methionine
SANT	Swi3, Ada2, N-Cor, and TFIIIB domain
SAP18/30	Sin3-asscoiated protein 18/30
SDS3	Suppressor of defective silencing 3
S.Dublin	*Salmonella Dublin*
Ser	Serine
SET	Su(var)3-9, Enhancer of Zeste and Trithorax
SMRT	Silencing mediator for retinoid and thyroid hormone receptors
Sox1/2/17	SRY-box HMG-like transcription factor 1/2/17
SRE	Serum response element
SRF	Serum response factor
SRM	Selected reaction monitoring
STAT3	Signal-transducer and activator of transcription 3
SUMO	Small ubiquitin-related modifier protein
SWI/SNF	SWItch/Sucrose non-fermentable
T	Threonine
TAF1	Transcription initiation factor TFIID subunit 1
TAF3	Transcription initiation factor TFIID subunit 3
TBL1	Transducin β-like 1
TBLR1	TBL1-related protein
Tbx5/20	T-box transcription factor 5/20
Tbx3os2	T-box 3 opposite strand 2
TCA	Trichloroacetic acid

TET	Ten Eleven Translocation
Tet	Tetracycline
TEV	Tobacco Etch Virus nuclear-inclusion-a endopeptidase
TFIID	Transcription factor II D
TRE	Minimal tetracycline response element
TSA	Trichostatin A
Tyr	Tyrosine
unHDAC3	untagged HDAC3
UTX	Ubiquitously transcribed tetratricopeptide repeat, X chromosome, also known as Lysine-specific demethylase 6A
Xt DAD	Extended deacetylase activation domain
Y	Tyrosine
5hmC	5-hydroxymethyl-cytsoines
[^{3}H]Inositol	Tritiated inositol

Chapter 1 Introduction

1.1 Structure and function of chromatin

Cell identity is dependent on cell type specific transcription, regulated in eukaryotes through organisation of the genome as well as transcription factor access and DNA modifications. DNA encoding the genetic material is packaged into chromatin in a highly-organized manner enabling regulation of gene transcription, DNA replication and repair (Luger & Richmond, 1998a).

DNA associates with histone proteins making up the basic unit of chromatin termed nucleosomes. The core nucleosome comprises of 146 base pairs (bp) of DNA wrapped 1.65 times around a histone octamer consisting of two molecules of each class of histone protein, H2A, H2B, H3 and H4 (Figure 1-1) (Luger et al, 1997). These four histone proteins associate to form two H2A:H2B dimers and a tetramer of H3 and H4 (Luger et al, 1997). Histone proteins are largely globular proteins containing an unstructured N-terminal tails, rich in basic residues, which protrude from the chromatin structure (Luger et al, 1997; Luger & Richmond, 1998b). These tails can be covalently modified which enables the alteration of chromatin compaction (discussed later).

Following formation of the nucleosome, the chromatin condenses through histone/histone and histone/DNA interactions leading to the generation of polynucleosome arrays (Figure 1-1) (Hubner et al, 2013; Luger et al, 1997). The nucleosomes are joined by approximately 20-60 base pairs (bp) of linker DNA to which a linker histone protein H1 binds to ensure stability (Thoma et al, 1979). This formation of the polynucleosome array is considered the 10nm fibre often termed “beads on a string” conformation due to the 200bp repeating units (Olins & Olins, 1973; Thoma et al, 1979). *In vitro,* further organization results in a compacted structure termed the 30nm fibre, which is a flexible helical structure containing 6 nucleosomes per turn

(Figure 1-1) (Hubner et al, 2013; Thoma et al, 1979; Widom & Klug, 1985). During metaphase, the 30nm fibre forms radial loops which are secured by proteins called condensins resulting in a higher order structure which is tightly compacted (Maeshima & Eltsov, 2008; Widom & Klug, 1985). During interphase, the formation of the 30nm fibre is undetected, instead a more variable chromatin structure containing two distinct conformations, heterochromatin and eurchromatin is visible (Fussner et al, 2011; Maeshima & Eltsov, 2008; Maeshima et al, 2010). Heterochromatin is considered the closed form of chromatin and is associated with transcriptionally silent regions, such as tissue specific loci or X inactivation. Euchromatin is characterised by an open conformation and is transcriptionally permissive thus correlating with active genomic loci.

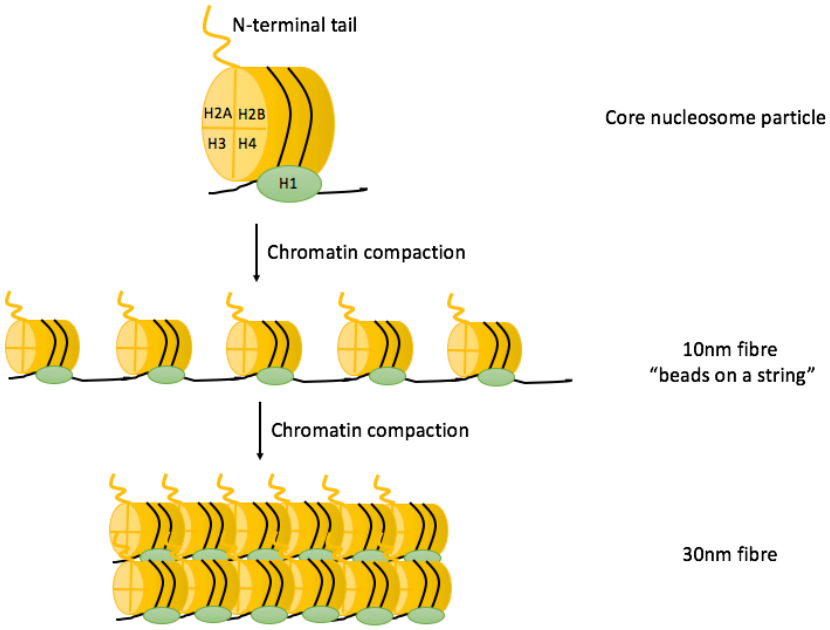

Figure 1-1 Schematic of chromatin condensation. *The core nucleosome particle is shown with 146 base pairs of DNA wrapped 1.65 times around the histone octamer consisting of two of each histone protein H2A, H2B, H3 and H4. The linker H1 histone, binds to DNA in between the nucleosomes enabling the stability of the 10nm fibre upon chromatin compaction and assembly of polynucleosome arrays. Further compaction of the 10nm fibre results in formation of the 30nm fibre, associated with the mitotic chromosome.*

1.2 Epigenetic regulation of chromatin

The organisation of chromatin into higher order structures is not permissive towards transcription due to the inability of transcription machinery to access critical sequence motifs in the underlying DNA. Consequently, the cell requires mechanisms to allow the alteration of the chromatin conformation to regulate DNA accessibility. Multiple processes have been shown to alter chromatin state *in vivo* including ATP-dependent chromatin remodelling, DNA methylation, incorporation of histone variants and post-translational modifications of histone proteins (introduced later) (Goldberg et al, 2007). These various processes work together to alter the structure of the chromatin leading to the inheritance of modifications which alter the phenotype observed without affecting the genetic code, commonly termed epigenetics (Berger et al, 2009; Dupont et al, 2009).

ATP-dependent chromatin remodelling complexes enable the interconversion of transcriptionally permissive and non-permissive chromatin thus enabling both transcriptional repression and activation (Varga-Weisz, 2001). These complexes utilise energy generated by ATP hydrolysis to reposition nucleosomes through nucleosome sliding (Vignali et al, 2000). ATP-dependent chromatin remodelling complexes can be classified into four groups, SWI2/SNF2, imitation SWI (ISWI) the Mi-2 group and the INO80 family (Hota & Bruneau, 2016). The SWI2/SNF2 family contains yeast SWI/SNF complex and human BRM and BRG1 complexes which all contain a homologous ATPase domain containing protein with a C-terminal bromodomain (Varga-Weisz, 2001; Vignali et al, 2000). The ISWI family consists of NURF in *Drosophila* and RSF in humans in which the SNF2h protein contains the ATPase domain. The INO80 family contains the INO80 complex which is involved in many developmental processes including the regulation of pluripotency through nucleosome remodelling (Hota & Bruneau, 2016). Mi-2 containing complexes on the other hand contain both ATPase remodelling capabilities and histone deacetylase activity. In humans, the NuRD complex contains HDAC1/2 and Mi2α/β, which have deacetylase and nucleosome remodelling activity respectively (Torchy et al, 2015; Xue et al, 1998; Zhang et al,

1998). Accordingly, NuRD couples the two activities together, the nucleosome remodelling is believed to promote histone deacetylation and repression of gene transcription through increasing DNA accessibility for transcriptional repressors (Xue et al, 1998; Zhang et al, 1998).

DNA methylation at CpG dinucleotides is a common epigenetic mark associated with transcriptional repression, transposon and X chromosome inactivation and gene imprinting (Law & Jacobsen, 2010). Individual CpG dinucleotides are dispersed throughout the genome, although CpG islands (regions of GC rich DNA containing clusters of CpG dinucleotides approximately 200-2000bp in length) are located at gene promoters where they are primarily un-methylated (Bird, 2002). The cytosine residue is methylated at the 5' position in the cytosine ring by the action of de-novo or maintenance DNA methyltransferases (DNMTs) which transfer the methyl moiety from S-adenosyl-L-Methionine (SAM) (Jin et al, 2011; Law & Jacobsen, 2010). Methylation of CpGs is associated with transcriptional repression, due to the inability of transcription factors to bind methylated DNA or through the binding of methyl CpG binding domain (MBD) proteins (Bird, 2002). MBD family proteins include MECP2 and MBD2/3 of which the latter are found in the NuRD complex therefore linking histone deacetylases to methylated DNA sites (Bird, 2002; Torchy et al, 2015). In 2009, a ground-breaking discovery led to the identification of Ten Eleven Translocation proteins (TET) which convert 5-methyl-cytosines to 5-hydroxymethyl-cytsoines (5hmC) (Tahiliani et al, 2009). Consequently, de-methylating the DNA due to passive dilution through DNA-replication, or active conversion to cytosine via DNA glycosylation and base excision repair (He et al, 2011; Tahiliani et al, 2009; Valinluck & Sowers, 2007).

1.3 Post translational modifications of histones

The post translational modification (PTM) of histones is a key epigenetic method of regulating gene expression and chromatin accessibility. Histones had previously been shown to block transcription prior to the identification of modifications, and removal

of histones led to increased RNA synthesis (Allfrey et al, 1963). In 1964, covalent modifications, in the form of acetyl and methyl groups, were shown to occur on histones (Allfrey et al, 1964). Furthermore, analysis of histone acetylation indicated that RNA expression and thereby transcriptional activation correlated with the addition of acetyl groups (Allfrey et al, 1964). The determination of the structure of histones indicated a globular core domain with a basic unstructured N-terminal tail (Luger et al, 1997). These N-terminal tails extend out of the core nucleosome structure and create contacts with DNA and adjacent nucleosomes (Luger et al, 1997). This led to the idea that due to their numerous acetylation sites, histone modifications in the N-terminal tails are able to alter chromatin structure (Luger et al, 1997). It is believed that PTMs manipulate histone/histone, histone/DNA and histone/non-histone protein electrostatic interactions, subsequently altering chromatin compaction and accessibility, leading to modulation of gene transcription (Hansen et al, 1998; Luger et al, 1997; Wolffe & Hayes, 1999).

Since their initial discovery, multiple sites of PTMs on histones have been discovered including: acetylation, methylation, phosphorylation, sumoylation, ubiquitination and most recently crotonoylation (Berger, 2007; Kouzarides, 2007; Tan et al, 2011). These modifications occur primarily on the N-terminal tails and are summarised in Table 1-1 (Berger, 2007). Due to the co-localisation of different marks and their ability to recruit different protein complexes, the "histone code hypothesis" was proposed (Strahl & Allis, 2000). The combination of histone marks present on a particular nucleosome defines the chromatin state of the underlying DNA sequence and whether or not it is likely to be accessible to the transcription machinery. Certain marks are associated with heterochromatin including H3K9, K27 and H4K20 trimethylation, whilst others are associated with euchromatin including Lys acetylation (always a positive mark independent of context) and H3K4, K36 and K79 trimethylation (Table 1-1) (Kouzarides, 2007). The histone code anticipates that the combination of PTMs act as a language to be 'read' by protein complexes which can modulate their effect on chromatin structure therefore specifying downstream functions and reflecting transcriptional states (Strahl & Allis, 2000).

Modification	Histone	Residue	Functional role
Acetylation	H2A	K5, K9	Activation
	H2B	K5, 12, 15, 16, 20, 120	Activation
	H3	K4, 9, 14, 18, 23, 27 36, 56	Activation
	H4	K5, 8, 12, 16, 20, 91	Activation
Methylation	H3	K4, 36, 79	Activation
		R2, 17, 26	Activation
		K9, 27	Repression
	H4	K20	Repression
		R3	Activation
Phosphorylation	H2A	T119	Mitotic compaction
	H2AX	S139	DNA damage response
	H2B	S32, S36	Activation
	H3	S10, 28, T3, 6, 11, Y41	Activation
		S10, 28	Mitotic compaction
	H4	S1	Activation
Ubiquitinylation	H2A	K119	Repression
	H2B	K120	Activation
Sumoylation	H2A	K126	Repression
	H2B	K6, 7, 16, 17	Repression
Crotonylation	H2A	K36, 118, 119, 125	Activation
	H2B	K5, 12, 16, 20, 23, 24, 34	Activation
	H3	K4, 9, 18, 23, 27, 56	Activation
	H4	K5, 8, 12, 16	Activation

Table 1-1 Function of post translation modifications. *H2A=histone 2A, H2AX = histone 2A variant X, H2B = histone 2B, H3 = histone 3, H4, Histone 4, K= Lysine, R=Arginine, S= Serine, T=Threonine, Y=Tyrosine. Adapted and summarised from Banerjee & Charkravarti 2011, Berger et al 2007; Kouzarides 2007, Musselman et al 2012, Rossetto et al 2012 and Tan et al 2011*

1.3.1 Sumoylation and Ubiquitinylation

Sumoylation is the addition of a small ubiquitin-related modifier protein (SUMO) of 100 amino acids to Lys residues, and generally correlates with transcriptional repression (Nathan et al, 2006). Sumoylation has been detected on H2AK126 and H2BK6/7/16/17 and several Lys in the N-terminus of H4 and is thought to recruit histone deacetylsaes (HDACs) and heterochromatin protein 1 (HP1) to repress transcription (Nathan et al, 2006). Ubiquitinylation of histones involves the addition of a single ubiquitin moiety of 76 amino acids to a Lys (Cao & Yan, 2012). While

polyubiquitination can occur, the most common modification is mono-ubiquitination of H2AK119 and H2BK120 which are associated with repression and activation of transcription respectively (Cao & Yan, 2012; Kouzarides, 2007). The E3 ubiquitin ligase RING1B part of the polycomb repressive complex 1 (PRC1) mediates H2AK119 ubiquitination (Wang et al, 2004). Deletion of RING1B decreases H2AK119 ubiquitination and increases expression of repressed polycomb genes such as Pax3 in mouse embryonic stem cells (Endoh et al, 2012; Wang et al, 2004). H2BK120 ubiquitination is catalysed by the E3 ligase complexes RNF20/40 and UbcH6 and is associated with gene activation due to its disruption of chromatin compaction and ability to promote RNA polymerase II elongation (Fierz et al, 2011; Pavri et al, 2006).

1.3.2 Phosphorylation

Phosphorylation of histones involves the addition of a phosphate moiety to serine, threonine or tyrosine residues, and correlates with transcriptional activation in interphase cells through the addition of a negative charge (Rossetto et al, 2012). Several phosphorylated residues have been shown to result in transcriptional activation including, H3S28, H2T11, H3S210 and H3Y41 (Rossetto et al, 2012). Perhaps the most interesting of the histone phosphorylation sites is H3S10, this residue has been shown to be phosphorylated by numerous kinases such as mitogen and stress-activated protein kinases 1 and 2 (MSK1/2) and de-phosphorylated by type 1 phosphatases (PP1) (Banerjee & Chakravarti, 2011; Nowak & Corces, 2004). Phosphorylation of H3S10 results in transcriptional activation and is able, although not necessary, to recruit the histone acetyl-transferase GCN5 to histone H3 and promote H3K14 acetylation subsequently enhancing transcriptional activation (Nowak & Corces, 2004). On the other hand, phosphorylation of H3S10 by Aurora B kinase has been shown to be essential for chromatin condensation in mitosis as yeast lacking the modification fail to divide effectively (Banerjee & Chakravarti, 2011; Wei et al, 1999). These two conflicting activities at the same residue suggest a potentially context dependent effect whereby the proteins recruited by the modification affect the outcome of phosphorylation (Nowak & Corces, 2004).

1.3.3 Crotonylation

In 2011, crotonylation of Lys was identified as a novel histone modification (Tan et al, 2011). This modification occurs at 28 sites located at active promoters and enhancers thus correlating with gene expression, and has since been shown to be enriched at Oct4, Sox2 and Nanog in mouse embryonic stem cells (Tan et al, 2011; Wei et al, 2017). p300, a traditional histone acetyltransferase (HAT) can also utilise crontyl-CoA to cronotylate Lys residues in histones and promote transcription (Sabari et al, 2015). Furthermore, class I HDACs, HDAC1, 2, 3 and 8 have also been shown to de-crontonylate Lys in addition to their classical deacetylase roles (Madsen & Olsen, 2012; Wei et al, 2017). Although this modification over laps with many acetylation sites (Table 1-1) and is now believed to utilise the same enzymes for its addition and removal, it may play a unique role in transcriptional activation and maintenance of embryonic stem cell renewal (Tan et al, 2011; Wei et al, 2017).

1.3.4 Methylation

Histone methylation is a complex mark occurring on either lysine or arginine residues which can result in transcriptional activation (H3K4) or repression (H3K9, 27) (Ruthenburg et al, 2007; Shi & Whetstine, 2007; Zhang & Reinberg, 2001). Arginine residues including H4R20 can be mono-methylated or asymmetrically/symmetrically di-methylated through the action of either type 1 protein arginine methyltransferases (PRMTs) which catalyse mono and asymmetrical methylation, or type 2 PRMTs which catalyse mono to symmetrical di-methylation (Zhang & Reinberg, 2001). Lysine residues such as H3K4 and K9 can be mono, di, or tri-methylated via the action of histone methyltransferases (HMTs) which mediate the addition of a methyl group from SAM to the lysine residue (Shi & Whetstine, 2007). HMTs contain a catalytically crucial SET (Su(var)3-9, Enhancer of Zeste and Trithorax) domain which shows a high level of conservation (Rea et al, 2000). Individual HMTs also show a high degree of substrate specificity. For example, SUV39H1 mediates the methylation of H3K9, G9a methylate's H3K9 and H3K27, whilst H3K4 is methylated by mixed lineage leukaemia (MLL)

MLL1/2/3/4 (Rea et al, 2000; Ruthenburg et al, 2007; Zhang & Reinberg, 2001). These signals can be removed through the action of histone demethylases. The first histone demethylase identified was the amine oxidase containing lysine specific demethylase 1 (LSD1) which was shown to de-methylate mono or di-methylated H3K4 (Shi et al, 2004). Since the identification of LSD1, numerous Jumonji (JmjC) domain containing histone demethylases have been identified all of which show high levels of specificity (Shi & Whetstine, 2007). JHDM1 is able to demethylate H3K36Me2 (associated with transcriptional elongation), whist JMJD2A is able to mono- or di- demethylate both H3K9 and H3K36 and UTX demethylates H3K27 (Agger et al, 2007; Klose et al, 2006; Tsukada et al, 2006; Whetstine et al, 2006).

Since addition of methyl groups does not alter the charge of the nucleosome, it is believed that histone methylation exerts its functionality through recruitment of proteins containing chromodomains, plant homeodomain (PHD) fingers or tudor domains which all bind methyl groups (Shi & Whetstine, 2007). Following methylation of H3K9, which is associated with transcriptional repression, HP1 binds H3K9me3 via its chromodomain and helps mediate gene silencing (Bannister et al, 2001; Jacobs et al, 2001). On the other hand, methylation at H3K4 results in recruitment of nucleosome remodelling factor (NURF) via the PHD domain containing BPTF subunit, promoting nucleosome remodelling and transcriptional activation (Wysocka et al, 2006). Conversely, H3K4Me also enables binding of ING1 a member of the Sin3/HDAC1/2 complex via a PHD domain, therefore promoting deacetylation and transcriptional repression, indicating that the recruitment of different protein complexes can alter the outcome of the methylation signal (Pena et al, 2008).

1.3.5 Acetylation

Histone acetylation was the first histone modification to be identified and was seen to correlate with transcriptional activation (Allfrey et al, 1964). The N-terminal tails of histones are positively charged due to the presence of numerous Lys residues thus enabling histone/DNA and histone/histone interactions resulting in a compact chromatin conformation. Lys-Ac neutralises the positive charge on Lys residues, resulting in decreased histone/DNA interactions, histone/histone interactions and prevention of H1 binding, leading to an open chromatin conformation, increased accessibility for transcription factors and RNA polymerase (Figure 1-2) (Hebbes et al, 1988; Hong et al, 1993; Lee et al, 1993; Norton et al, 1989; Ridsdale et al, 1990). Histone acetyl transferases (HAT) catalyse the addition of an acetyl group to the ε-amino group on Lys residues using the donor acetyl-CoA (Figure 1-2) (Sterner & Berger, 2000). HATs are categorised based on their cellular localisation and role, type A HATs acetylate histones in the nucleus, whilst type B HATs acetylate histones in the cytoplasm, however, recent research indicates HATs have overlapping functions (Brownell & Allis, 1996; Garcea & Alberts, 1980; Ruizcarrillo et al, 1975). Type A HATs can be further categorised into three groups; GNAT (Gcn5-related N-acetyltransferase), MYST and p300/CBP (Sterner & Berger, 2000). The GNAT family of HATs contains the first HAT identified, Gcn5 as well as the human homologs hGCN5 and PCAF all of which show homology with a conserved glutamic acid in the HAT domain (Brownell et al, 1996; Sterner & Berger, 2000). The MYST family contains the HAT Tip60 which has been shown to have modulated activity upon binding to HIV-1 Trans-Activator of Transcription (TAT) protein (Creaven et al, 1999; Sterner & Berger, 2000). The final family is the p300/CBP family in which p300 and its homolog CREB-binding protein (CBP) associate together to acetylate histones thus promoting transcriptional activation (Bannister & Kouzarides, 1996; Ogryzko et al, 1996).

Addition of an acetyl group via HATs primarily occurs at the N-terminal tails of histones including H3 K4, 9, 14, 18, 36 and H4 K5, 12, 16 and correlates with gene expression. The distribution of these marks varies across the genome with H3K9 and H3K27

showing increased acetylation at transcriptional start sites of genes whilst H3K4 and H4K5/12/16 are acetylated at promoters and transcribed regions of active genes (Wang et al, 2008). Moreover, acetylation of H4K16 has since been shown to disrupt higher order chromatin and thus preventing formation of the 30nm fibre (Shogren-Knaak & Peterson, 2006). Acetylation of histones is not just associated with increased gene expression. Acetylation of H3K56, H4K5/12 has been shown to occur on histones in the cytoplasm thus promoting incorporation of the histones into newly synthesized chromatids (Li et al, 2008). Furthermore, acetylated H4K5 has been linked to re-activation of transcription post-mitosis indicating it as an epigenetic bookmark whilst H3K56Ac is involved in the DNA damage response (Vempati et al, 2010; Zhao et al, 2011).

The removal of acetyl groups is catalysed through the action of histone deacetylase enzymes (HDACs) (discussed later) (Figure 1-2) (Yang & Seto, 2008). HDACs were first identified in mammals in 1996 and are associated with transcriptional repression due to the removal of the acetyl groups from Lys-Ac resulting in a more compact chromatin through the reinstatement of the positive charge on histone tails (Brownell & Allis, 1996; Yang & Seto, 2008). Accordingly, the opposing actions of HATs and HDACs maintain the steady-state balance of Lys-Ac in cells and therefore regulate transcriptional activation at specific loci.

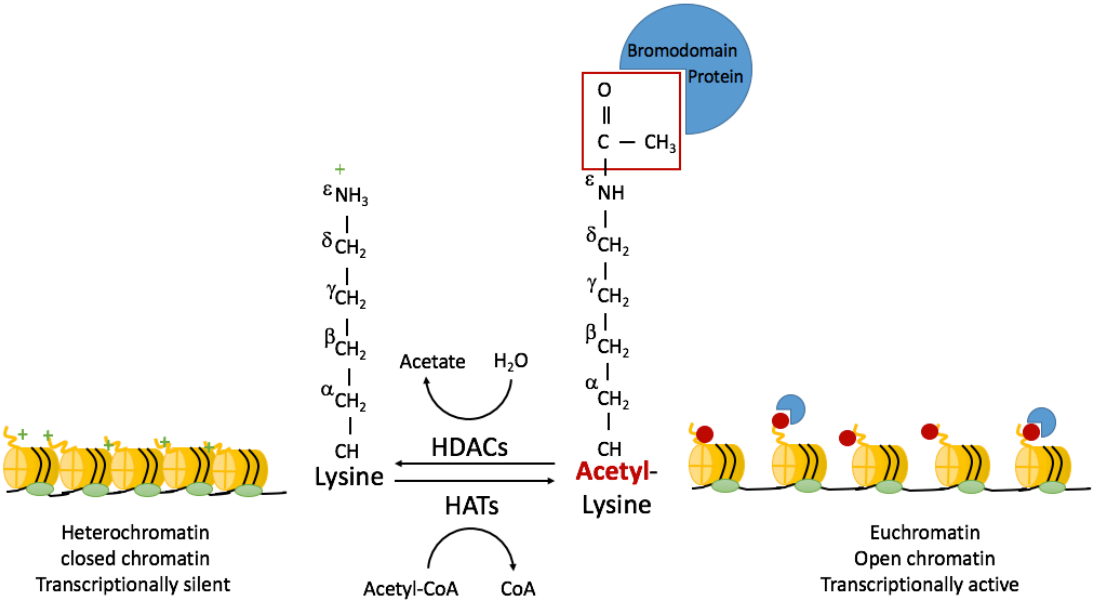

Figure 1-2 Removal and addition of acetyl groups to lysine residues on histones alters chromatin state. *The addition of acetyl groups (red circles and box) to lysine residues by histone acetyltransferases (HATs) using Acetyl-CoA as a donor, removes the positive charge from the lysine resulting in open chromatin state (euchromatin) and transcriptionally active genes. The acetyl group can be bound by a bromodomain containing protein as shown in blue. Removal of the acetyl group by histone deacetyalses (HDACs) reveals the positive charge on the lysine (green +), resulting in chromatin compaction and the transcriptional silencing of genes. Adapted from Yang and Seto, 2008*

1.3.6 Readers of histone modifications

As well as their ability to alter the electrostatic interactions of chromatin, histone modifications also act as signals to recruit proteins to chromatin. These histone reader proteins enable the histone modification to be interpreted and alter downstream processes through recruitment of protein complexes (Musselman et al, 2012; Taverna et al, 2007).

The first bromodomain was identified in the histone acetyltransferase, PCAF and was found to bind acetylated histones and tether the HAT enzyme to active chromatin (Dhalluin et al, 1999). Since its initial discovery, several other bromodomain containing proteins have been identified including, TAF1, a member of the transcriptional initiation complex TFIID which binds H4K5/K12Ac via a double bromodomain (Taverna et al, 2007). Binding of epigenetic readers to methylated histones is involved in

transcriptional activation via the binding of TFIID via TAF3 to H3K4Me3 (Musselman et al, 2012; Vermeulen et al, 2010). Histone readers can also have dual capacity to bind epigenetic marks for example BPTF binds H4K16Ac and H3K4Me2/3 thus tethering the ATP-dependent chromatin remodelling complex NURF to genes and regulating transcription (Ruthenburg et al, 2011; Wysocka et al, 2006). Those outlined above a just a few examples of proteins which are able to interpret the histone code through recognition of PTMs.

1.4 Interplay of epigenetic modifications

Whilst it is possible that histone modifications work independently, they are more likely to act in concert to alter the chromatin state (Berger, 2007). Cross-talk between histone modifications and their interactors can occur in several different ways, some of which are outlined here. Cross-talk between modifications can be in the form of one modification promoting the occurrence of another. For example, H2B and H2A ubiquitination are required for H3K4 methylation by the COMPASS (complex of protein associated with Set1) complex and methylation of H3K27 by PRC2 respectively (Kalb et al, 2014; Kim et al, 2009). Furthermore, phosphorylation of H3S10 results in transcriptional activation through the recruitment of GCN5 thus promoting H3K14 acetylation (Nowak & Corces, 2004). As well as being required for additional PTMs, they are also able to collaborate to recruit factors. For example, TFIID and BPTF bind more strongly to H3K4Me3 when flanked by H3K9Ac/K14Ac (Vermeulen et al, 2010). Moreover, histone modifications can coordinate different histone modifying enzymes through the recruitment of multi-component complexes. For example, LSD1 is a member of the CoREST complex which contains HDAC1/2 thus coupling demethylation of H3K4 and deacetylation of Lys-Ac, thus promoting transcriptional repression (Lee et al, 2006a). The lysine demethylase UTX associates with MLL2, a H3K4 histone methyltransferase, enabling the removal of the repressive H3K27me3 mark and deposition of the activating H3K4Me3 mark causing transcriptional activation (Agger et al, 2007).

An alternative form of cross-talk between modifications is in the form of competition for modification sites and recruitment of histone readers. The same Lys residue could potentially be modified with different modifications such as acetylation, crotonylation or methylation (see Table 1-1), suggesting antagonism between different PTMs since they are bound by unique readers. Furthermore, several histone binding factors can bind at the same residue but have different effects, however, generally their affinity for the modified residue is comparable suggesting competition between the binders can determine the outcome (Rothbart & Strahl, 2014).

The final form of cross-talk between histone modifications is their ability to modulate adjacent modifications or the binding of effector proteins. The most well-known example of this form of interplay is phosphorylation of H3S10 during mitosis which induces dissociation of heterochromatin protein 1 (HP1) bound to adjacent H3K9Me3 sites despite the level of H3K9Me3 remaining constant (Fischle et al, 2005). Phosphorylation of H3T6 has also been shown to disrupt LSD1 binding to H3K4Me3 residues therefore preventing demethylation of the active mark (Metzger et al, 2010). The mechanisms outlined above, provide evidence that histone marks are highly likely to cooperate in their modulation of chromatin. Consequently, the histone code proposed by Strahl and Allis in 2000, is now thought to resemble a language whereby modifications and recruitment of effectors are interpreted together in a context and cell dependent manner leading to functional interplay of downstream processes.

1.5 Histone deacetylase (HDAC) family of proteins

HDACs catalyse the removal of acetyl groups from Lys-Ac on histone and non-histone proteins (Grozinger & Schreiber, 2002; Yang & Seto, 2008). Affinity chromatography using the HDAC inhibitor trapoxin led to the identification of the first mammalian HDAC, now known as HDAC1 (Taunton et al, 1996). HDAC1 is an orthologue of the yeast protein Rpd3 which had previously been identified as a transcriptional regulator

(Kadosh & Struhl, 1998; Vidal & Gaber, 1991). HDACs have since been shown to regulate transcription as well as cellular processes such as cell cycle, metabolism and differentiation (Bhaskara et al, 2008; Dovey et al, 2010b; Jamaladdin et al, 2014; Montgomery et al, 2007; Montgomery et al, 2008). Since the identification of Rpd3, 18 mammalian deacetylase enzymes have been identified and grouped into two main families based on their catalytic domains. The sirtuins (class III) require NAD^+ for their catalytic activity, whilst the "classical" HDACs (class I, IIa, IIb and IV) are dependent on Zinc for the removal of the acetyl moiety (De Ruijter et al, 2003; Gregoretti et al, 2004; Grozinger & Schreiber, 2002; Yang & Seto, 2008).

1.5.1 Classification of histone deacetylases

Following classification into the HDACs and sirtuins, HDACs are characterised based on their homology to yeast Rpd3 (Class I) and Hda1 (Class IIa and IIb) and class IV which shows homology to both Rpd3 and Hda1, with sirtuins forming class III (Figure 1-3). These HDACs differ in structure, function, size and cellular localisation thus enabling specific interactions and substrates.

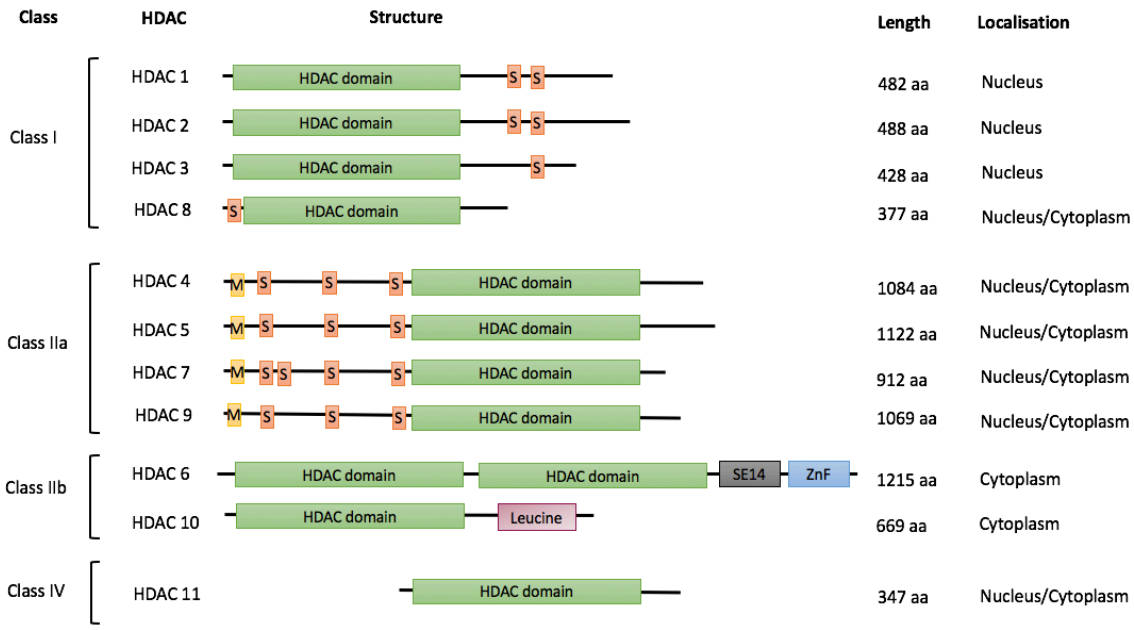

Figure 1-3 Schematic of the classification of classical HDAC family members. *The eleven human classical HDACs are represented according to their classification. Histone deacetylase catalytic domain is denoted by the green boxes and is highly conserved. Serine phosphorylation sites observed in Class I and Class IIa HDACs are denoted by the orange boxes and class IIa MEF2 binding sites are indicated by the yellow boxes. Class Iib contains HDAC6 with 2 HDAC domains and a SE14 motif important in cytoplasmic localisation (grey box) and a ubiquitin binding Zinc finger domain (blue box). HDAC 10 contains a Leucine rich domain (red box). HDAC11 is the only HDAC in class IV and is the simplest HDAC consisting of just a HDAC domain. Adapted from Yang and Seto 2008*

As depicted in Figure 1-3, the Zn^{2+} dependent deacetylase catalytic domain is highly conserved across class I, II and IV enzymes and is approximately 390 amino acids in length (De Ruijter et al, 2003). The crystal structure of bacterial histone deacetylase like protein (HDLP) which has homology to HDAC1, indicated that the catalytic core has a tubular pocket with an adjacent internal cavity (Finnin et al, 1999). The pocket becomes narrow in the middle and widens again at the bottom, this coupled with the hydrophobic and aromatic walls enables efficient binding of the Lys-Ac (Finnin et al, 1999). A Zn^{2+} cation is found at the bottom of the pocket coordinated by two conserved histidine-aspartic acid (His-Asp) pairs which act as a charge relay mechanism during catalysis (Finnin et al, 1999). A conserved tyrosine residue is also present which coordinates the intermediate produced during catalysis, this tyrosine is mutated in class II HDACs thus accounting for their decreased activity (Lahm et al, 2007). In 2004 and 2005 the structures of class I HDAC8 and class II HDAC homologue were resolved and revealed that the structure of the catalytic core is comparable to HDLP and largely

conserved between the classes (Nielsen et al, 2005; Somoza et al, 2004; Vannini et al, 2004).

The class I HDAC group comprises HDAC1, 2, 3, and 8 and are ubiquitously expressed nuclear proteins (Figure 1-3) (De Ruijter et al, 2003). HDAC1 and HDAC2 are the most closely related with 82% identity, resulting in functional redundancy in most tissues. As well as the conserved catalytic domain, HDAC1/2 contain two-tandem casein kinase 2 (CK2) phosphorylation sites in the C-terminus which have been shown to increase HDAC activity and incorporation into co-repressor complexes (Pflum et al, 2001; Tsai & Seto, 2002). *In vivo*, HDAC1/2 are found in 4 co-repressor complexes, Sin3, NuRD, CoREST and MiDAC (Table 1-2). The incorporation of HDAC1/2 into a complex is essential for catalysis (discussed later) (Bantscheff et al, 2011; Yang & Seto, 2008). HDAC3 shares 53% identity with HDAC1 and contains the conserved catalytic domain and a single serine-phosphorylation site which is regulated by the action of CK2 and protein phosphatase 4 (PP4) which increase and decrease activity respectively (Yang et al, 2002; Zhang et al, 2005). Despite the similarities to HDAC1/2 it is incorporated into a unique co-repressor complex SMRT/NCoR and shows exclusive roles in liver metabolism and embryogenesis (Bhaskara et al, 2008; Montgomery et al, 2008). HDAC8 is the most diverse class I HDAC and is active in isolation (Yang & Seto, 2008). Like HDAC1/2/3 it contains a serine-phosphorylation site but at the N-terminus and phosphorylation occurs by protein kinase A at ser-39 resulting in inactivation of the enzyme (Lee et al, 2004a; Vannini et al, 2004).

The second group of HDACs is class II which is split into two sub groups, class IIa (HDAC4, 5, 7 and 9) and class IIb (HDAC6 and 10) (Figure 1-3) (Gregoretti et al, 2004). Unlike class I, class IIa HDACs are expressed in a tissue specific manner and are found in both the nucleus and the cytoplasm (De Ruijter et al, 2003). Class IIa HDACs have a large extended N-terminal domain, making them almost twice as large as class I HDACs (Figure 1-3). This N-terminal domain contains binding sites for myocyte enhancer factor-2 (MEF2) and 14-3-3 proteins important in their localisation. Phosphorylation of the serine residues by calcium/calmodulin-dependent protein kinase (CaMK) creates a binding site for 14-3-3 proteins which shuttle HDAC4, 5, 7 and 9 out of the nucleus

leading to de-repression of their target genes (Grozinger & Schreiber, 2000; Wang et al, 2000). Removal of the phosphorylation sites results in loss of interaction with 14-3-3 proteins enabling sequestration in the nucleus (Grozinger & Schreiber, 2000). Binding of MEF2 to the N-terminal domain promotes nuclear localization and subsequent transcriptional repression at MEF2 target genes, this is inhibited by 14-3-3 export resulting in myogensis (Lu et al, 2000; McKinsey et al, 2000; Miska et al, 1999). However, due to a natural tyrosine to histidine substitution within the catalytic site class IIa HDACs have little enzymatic activity against Lys-Ac substrates, it is thought that their role in cells is to recruit HDAC3/SMRT/NCoR to target genes, since they retain an affinity for Lys-Ac (Fischle et al, 2001; Fischle et al, 2002; Lahm et al, 2007).

HDAC6 and HDAC10 make up class IIb. HDAC6 is distinct from other HDACs due to a duplicated HDAC domain, both of which are functional (Grozinger et al, 1999). Furthermore, it contains a C-terminal SE14 domain (Ser-Glu containing tetradecapeptide) which is important in its localisation to the cytoplasm and a C-terminal ubiquitin binding Zinc finger domain (Figure 1-3) (Bertos et al, 2004; Hook et al, 2002). HDAC6 is a cytoplasmic protein, therefore indicating it has non-histone substrates, accordingly, it has been shown to deacetylate α-tubulin in microtubules thus promoting their stabilisation (Hubbert et al, 2002). HDAC10 contains the conserved deacetylase domain and a pseudo-repeat region with high homology to the catalytic domain (designated leucine rich in Figure 1-3) (Kao et al, 2002). An emerging role for HDAC10 is in tumorigenesis, with recent evidence suggesting that it promotes lung cancer proliferation by interacting with Akt and promoting its phosphorylation (Yang et al, 2016).

The final group, class IV, consists of HDAC11 alone which has homology to both class I and class II HDACs (Gao et al, 2002). HDAC11 contains a conserved catalytic domain and localises to the nucleus with tissue specific expression (Figure 1-3) (Gao et al, 2002). Recent studies indicate it negatively regulates IL-10 in myeloid cells preventing their expansion (Sahakian et al, 2015).

1.5.2 Recruitment of Class I HDACs to DNA via co-repressor complexes

Due to the lack of an intrinsic DNA binding domain and their inactivity in isolation (HDAC8 excepted), class I HDACs require recruitment to multiprotein co-repressor complexes for targeting to histones (Kelly & Cowley, 2013). The main class I HDAC co-repressor complexes include Sin3, NuRD, CoREST, MiDAC and NCoR/SMRT (Delcuve et al, 2012). HDAC1/2 form the catalytic core of all but N-CoR/SMRT where HDAC3 is the primary HDAC (Table 1-2). Incorporation of HDAC1/2/3 into these multi-protein complexes enables recruitment to histones via proteins containing PTM reader domains and methyl-DNA binding domains (Table 1-2). Furthermore, whilst HDAC1/2 and 3 can associate directly with transcription factor YY1, co-repressor complexes are able to interact with transcription factors thus targeting them to specific loci (Kelly & Cowley, 2013; Yang et al, 1996; Yang et al, 1997). For example, CoREST interacts with RE1-silencing transcription factor (REST), NuRD interacts with Foxp, Sin3 interacts with Mad/Max and NCoR/SMRT interacts with many unliganded nuclear receptors including RevErb (Andres et al, 1999; Ayer et al, 1995; Chokas et al, 2010; Zamir et al, 1996).

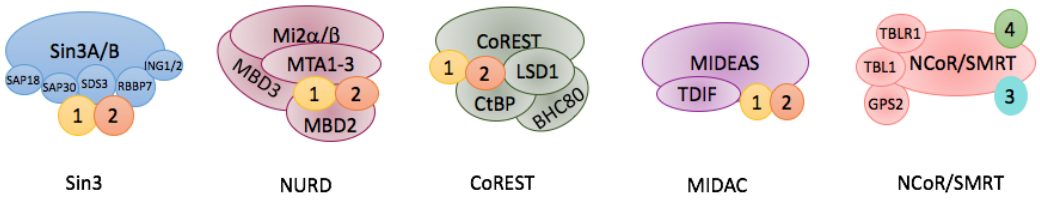

Complex	Component	Enzymatic function/interacting domain
Sin3	HDAC1 / 2	Histone deacetylase domain
	RbAp46/48	WD40 domain
	Sin3A/B	PAH motifs
	SDS3	
	RBP1	
	SAP18	Ubiquitin fold
	SAP30	Zinc finger
	ING1/2	PHD finger
NuRD	HDAC1 / 2	Histone deacetylase domain
	RbAp46/48	WD40 domain
	Mi2α/β	ATP-dependent chromatin remodelling domain
	MDB2/3	Methyl CpG binding domain
	MTA1/2/3	ELM2-SANT domain
	p66α/β	
CoREST	HDAC1 / 2	Histone deacetylase domain
	CoREST 1/2/3	ELM2-SANT domain
	LSD1	Lysine demethylase
	BHC80	PHD finger
	BRAF35	high mobility group (HMG)- box domain
	CtBP	NAD+ regulated dehydrogenase
MiDAC	HDAC1 / 2	Histone deacetylase domain
	MiDEAS	ELM2-SANT domain
	TDIF/DNTTIP1	SKI/SNO/DAC domain
N-CoR/SMRT	HDAC3	Histone deacetylase domain
	HDAC4, 5, 7	Class IIa HDAC
	SMRT/N-CoR	SANT domain and DAD domain
	TBL1/TBLR1	WD40 domain
	GPS2	
	JMJD2A	Histone lysine demethylase/ PHD finger/tudor domain
	Kasio	Methyl CpG binding domain

Table 1-2 Components of the class I co-repressor complexes. *The schematic at the top of the figure denotes the core components of the co-repressor complexes. The table below indicates the functional domains and enzymatic function of the components of the complexes as adapted from Yang and Seto 2008.*

1.5.2.1 Sin3

The two mammalian Sin3 isoforms A and B are 60% identical to each other and 35% identical to the conserved yeast homolog, with the highest homology present in the 4 paired amphipathic helices (PAH) domains (Ayer et al, 1996). The mammalian Sin3A/B complex was first identified as a mediator of transcriptional repression through its PAH2 mediated interaction with Mad-Max (Figure 1-4) (Ayer et al, 1995). The transcription factor Mad is upregulated during differentiation and associates with Max, resulting in the transcriptional silencing of Myc-Max regulated genes via Sin3 (Ayer et al, 1995). The interaction of Sin3 with HDAC1/2 via the histone deacetylase interaction domain (HID) was later shown to be responsible for Sin3 mediated repression (Figure 1-4) (Hassig et al, 1997; Laherty et al, 1997; Zhang et al, 1997). It is believed that Sin3 acts as a scaffold for interaction with the core-components; Sin3-associated protein 18 (SAP18) and SAP30, suppressor of defective silencing 3 (SDS3) and retinoblastoma associated protein 48 and 46 (RbAp48/46) (Alland et al, 2002; Hassig et al, 1997; Zhang et al, 1997). SDS3 interacts with a region overlapping the HID (Figure 1-4) and has been shown to be important for the integrity of the Sin3 complex and activation of HDAC1/2 (Alland et al, 2002).

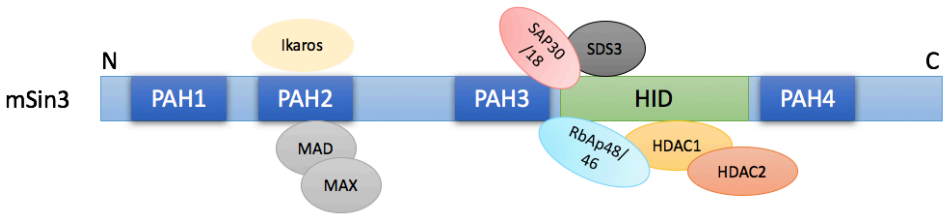

Figure 1-4 Schematic indicating the structure of Sin3 and its interacting domains. *A schematic of mSin3 with the paired amphipathic helices (PAH) denoted by dark blue boxes. Transcription factors such as Mad-Max and Ikaros bind to PAH2 and core components of the complex including SDS3 and SAP30/18 bind at the histone deacetylase interaction domain (HID) (green box) along with HDAC1/2 and RbAp48/46. N and C denote the terminus.*

Sin3 does not encode a DNA binding domain and as such requires interacting proteins to target it to the chromatin (Wang & Stillman, 1990). RbAp48/46 interact with both HDAC1 and Sin3 and contain WD40 repeats which have been shown to interact with H4 suggesting they play a role in targeting HDACs to chromatin (Hassig et al, 1997;

Taunton et al, 1996; Verreault et al, 1996). Additionally, SAP30 contains an N-terminal Zinc finger domain which has been shown to bind DNA and enhance Sin3/HDAC1 mediated repression (Viiri et al, 2009). Moreover, interaction of ING1 with H3K4me3 via its PHD domain recruits Sin3 to the chromatin (Pena et al, 2008). Furthermore, the association of Sin3 with transcription factors such as Ikaros also promotes the localisation of Sin3 to gene promoters (Koipally et al, 1999). Sin3 is an essential complex as it is embryonic lethal and crucial for embryogenesis and T-cell development (Cowley et al, 2005).

1.5.2.2 NuRD

Nucleosome remodelling and histone deacetylation (NuRD) complex was first described in 1998, and was shown to have both histone deacetylation and ATP-dependent chromatin remodelling capabilities (Xue et al, 1998). NuRD contains HDAC1/2 and RbAp48/46 suggesting a conserved catalytic core shared with Sin3 (Xue et al, 1998; Zhang et al, 1999). Despite NuRDs similarity to Sin3, it contains unique components including metastasis associated proteins (MTA1, 2, 3) methyl-CpG-binding domain proteins (MBD2/3), p66α/β and ATP-dependent chromatin remodelling proteins Mi-2α/β (Fujita et al, 2003; Xue et al, 1998; Yao & Yang, 2003; Zhang et al, 1999). The MTA family proteins act as a scaffold for complex formation (Millard et al, 2013). A schematic of the structure of MTA1 is depicted in Figure 1-5 and shows that HDAC1 and HDAC2 are recruited via the ELM2/SANT domain which along with I(1,4,5,6)P_4 activates the deacetylase activity (discussed later) (Millard et al, 2013). The ELM2 also acts as a dimerization domain for the MTA containing complex (Millard et al, 2014; Millard et al, 2013). The presence of Mi-2α/β enables nucleosome remodelling at sites targeted by NuRD (Zhang et al, 1998). The complex is believed to be recruited to chromatin through several different proteins found in the complex as well as association with transcription factors. RbAp48/46 also known as RBBP4/7 have been shown to be recruited to two sites in MTA1 (R1 and R2 in Figure 1-5) leading to the recruitment of 4 RBBP4/7 proteins which can bind H3 (Millard et al, 2016). Furthermore, MBD2 can bind methylated DNA therefore tethering NuRD to the chromatin (Zhang et al, 1999). Whilst MBD3 is unable to bind methylated CpGs, it is

essential for mouse development, and deletion in mouse embryonic stem cells is associated with failure to differentiate due to increased expression of pluripotency genes, thus suggesting NuRD is an essential complex involved in the regulation of pluripotent gene silencing (Hendrich et al, 2001; Kaji et al, 2006). An alternative NuRD-like complex has been discovered in mouse embryonic stem cells which contains the core components of NuRD minus MBD3 but with Oct4 and Nanog present, this complex was termed NODE (Nanog- and Oct4- associated deacetylase) (Liang et al, 2008).

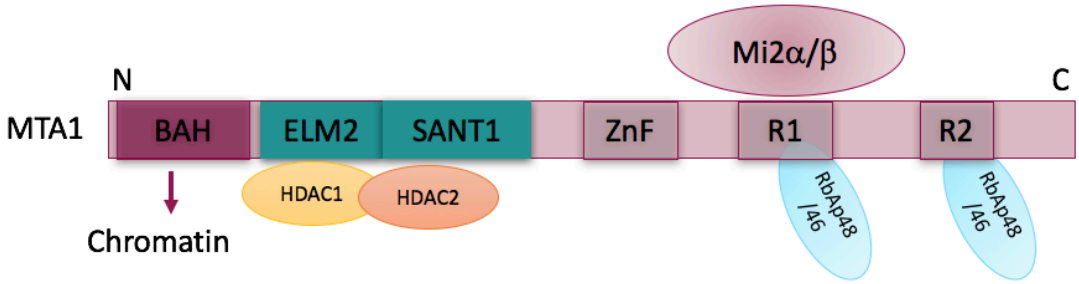

Figure 1-5 Schematic depicting the interaction domains of MTA1. *A schematic of MTA1 indicates a BAH (bromo-adjacent homology) domain which interacts with chromatin. The ELM2 domain potentiates dimerisation and activation and recruitment of HDAC1/2 with SANT and inositol phosphate. RbAp48/46 are able to bind at interacting domains R1 and R2. Mi-2α/β interact with the C-terminal domain of the protein. Adapted from Millard et al 2014 and Millard et al 2016*

1.5.2.3 CoREST

CoREST is the co-repressor of RE1-silencing transcription factor (REST), which mediates the repression of neuronal genes in non-neuronal cells, via its interaction with the C-terminus of REST (Andres et al, 1999). HDAC1 and HDAC2 were later found to be a component of the complex and interact with the ELM2-SANT1 domain at the N-terminus of the CoREST protein, most likely through a conserved ELM2/SANT domain similar to that of MTA1/HDAC1 (Figure 1-6) (You et al, 2001). BRAF35 is a high-mobility group box protein which is a structural DNA binding protein was also detected in the CoREST complex which could encourage recruitment to chromatin (Hakimi et al, 2002). The association of the co-repressor C-terminal binding protein (CtBP) with CoREST was discovered in 2003 and was shown to be recruited to target promoters via

transcription factors such as ZEB1 which targets the complex to E-Cadherin (Shi et al, 2003). The CoREST complex contains demethylase activity in the form of LSD1 which demethylates H3K4Me1/2 and interacts via its tower domain with CoREST at the C-terminal region containing the linker and SANT2 domain (Figure 1-6) (Shi et al, 2004; Shi et al, 2005). The binding of LSD1 to CoREST promotes the association of LSD1 with nucleosomes via the SANT2 domain, which can loosely bind DNA, and the complex component BHC80, a PHD finger protein which binds unmethylated H3K4, together prevent methylation of this mark at repressed loci (Lan et al, 2007; Lee et al, 2005; Yang et al, 2006). The association of LSD1 and CoREST is essential for their stability as deletion of LSD1 results in a subsequent decrease in CoREST at the protein level and embryonic lethality before e7.5 days, thus highlighting the essential role of CoREST (Foster et al, 2010; Wang et al, 2007). Furthermore, the activity of HDAC1/2 and LSD1 in CoREST are believed to be co-dependent as acetylated histones prevent demethylation of H3K4 suggesting that the HDAC activity is required for demethylation via LSD1 (Forneris et al, 2006). Moreover, inhibition of either LSD1 or HDAC1 reduces the activity of the partner enzyme indicating they function in concert (Yin et al, 2014).

Figure 1-6 Schematic indicating the interaction domains of CoREST with LSD1 and HDAC1/2. *CoREST contains an N-terminal ELM2-SANT1 domain which is responsible for interaction with HDAC1/2, a linker domain separates the two SANT domains, LSD1 binds via its SWIRM domain to the linker/SANT2 region, of which the SANT2 domain also has the capacity to bind DNA. BHC80 and CtBP are not shown as their binding sites remain unknown.*

1.5.2.4 MiDAC

The novel HDAC-containing complex, mitotic deacetylase complex (MiDAC), was identified in 2011 using a suberoylanilide hydroxamic acid (SAHA, a HDAC inhibitor) derived matrix as bait in a chemoproteomic screen (Bantscheff et al, 2011). This study indicated that MiDAC is more active in mitotic cells, correlating with the finding that it

is associated with cyclin A (Bantscheff et al, 2011; Pagliuca et al, 2011). The mitotic deacetylase-associated SANT domain protein (MIDEAS), contains an ELM2-SANT domain and forms a complex with HDAC1/2 (Itoh et al, 2015). DNTTIP1, also known as TDIF1, contains an amino-terminal dimerization domain, which interacts with HDAC1/2 and MIDEAS as well as its self and is responsible for the formation of the dimer of dimers structure of the complex (Figure 1-7) (Itoh et al, 2015). The C-terminal domain has the potential to bind both naked DNA and nucleosomes therefore enabling targeting of the MiDAC complex to chromatin (Itoh et al, 2015).

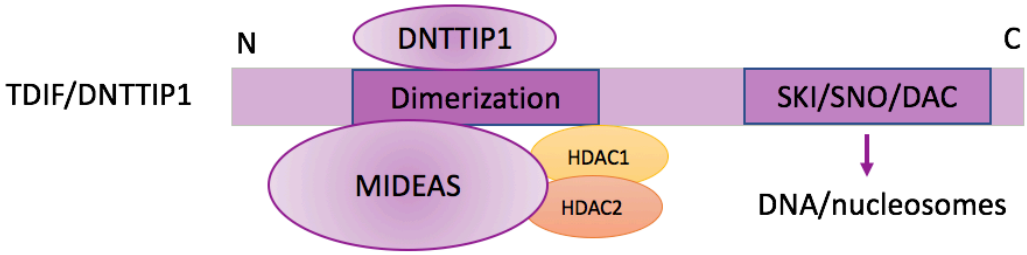

Figure 1-7 Schematic denoting the interacting domains of DNTTIP1 with HDAC1/2 and MIDEAS. *MIDEAS contains a C-terminal ELM2/SANT domain which is sufficient for interaction with HDAC1/HDAC2. TDIF/DNTTIP1 contains a dimerization domain which is responsible for interacting with HDAC1/2 and MIDEAS and the formation of the dimer of dimers structure. The N-terminal SKI/SNO/DAC domain of DNTTIP1 can bind both naked DNA and nucleosomes thus targeting the complex to chromatin. Adapted from Itoh et al, 2015*

1.5.2.5 SMRT/NCoR

Silencing mediator for retinoid and thyroid hormone receptors (SMRT) and its homolog nuclear receptor corepressor (NCoR) were first identified as corepressors of nuclear receptors such as thyroid hormone receptor and retinoic acid receptor in the absence of their ligands (Chen & Evans, 1995; Horlein et al, 1995). They were later shown to form a complex with HDAC3 which mediates transcriptional repression via hormone receptors (Guenther et al, 2000; Ishizuka & Lazar, 2003; Li et al, 2000; Wen et al, 2000). HDAC3 interacts with SMRT/NCoR via the deacetylase activating domain (DAD) which stimulates the deacetylase activity (Codina et al, 2005; Guenther et al, 2001). The minimal DAD domain is comprised of a 16 amino-acid DAD-specific motif and the SANT1 domain in the N-terminal region (Figure 1-8) and was shown to undergo large

structural rearrangements facilitating the interaction of SMRT:DAD with HDAC3 and substrate access (Codina et al, 2005; Guenther et al, 2001; Watson et al, 2012). Later, an extended DAD domain of SMRT was shown to wrap around HDAC3 in a conserved groove forming extensive interactions in a similar manner to the ELM2-SANT domain of MTA1 (Millard et al, 2013). Mutations and deletions in the DAD domain abolish the interaction and activation of HDAC3 by SMRT/NCoR, although these two processes can be separated as indicated by the K449A mutation in SMRTs DAD domain which retains binding but does not activate HDAC3 (Codina et al, 2005; Guenther et al, 2001). Furthermore, mutation of residues critical for the interaction of NCoR/SMRT with HDAC3 render HDAC3 catalytically inactive in mice, yet they are viable (You et al 2013). Catalytically inert HDAC3 has the ability to rescue the liver specific deletion phenotype thus suggesting deacetylase independent activity, mediated through the binding of NCoR/SMRT to chromatin (Sun et al, 2013).

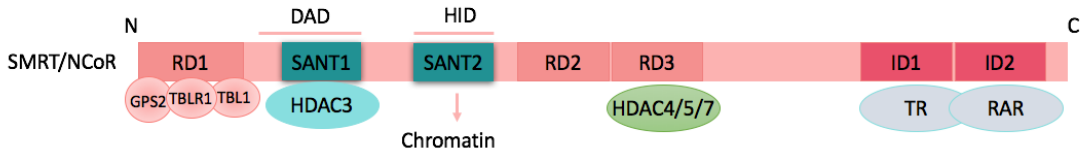

Figure 1-8 Schematic denoting the structural regions and interacting domains of SMRT/NCoR. *SMRT/ NCoR contain 3 repressive domains (RD1, 2, 3), of which RD1 interacts with GPS2, TBL1 and TBLR1. RD3 interacts with class IIa HDAC4, 5 and 7. ID1 and ID2 denote the interaction domains 1 and 2 which bind nuclear hormone receptors including thyroid receptor (TR) and retinoic-acid receptor (RAR). The deacetylase activation domain (DAD) is made up of the SANT1 domain and an N-terminal extension, which both binds and activates HDAC3. SANT2 domain of SMRT/NCoR makes up the histone interacting domain (HID) which is capable of binding to chromatin.*

It was previously thought, that the DAD was sufficient for activation of HDAC3, however, in 2012, Watson et al., resolved the crystal structure of the SMRT:DAD/HDAC3 complex and revealed Inositol-1,4,5,6-tetrakisphosphate ($Ins(1,4,5,6)P_4$) at the interface of the two proteins. The interface is depicted in Figure 1-9 and shows $Ins(1,4,5,6)P_4$ in a highly basic pocket, due to its negative charge it was believed to prevent charge repulsion therefore acting as an intermolecular glue (Watson et al, 2012). Since the initial discovery of $Ins(1,4,5,6)P_4$ at the interface it has been proposed to be a regulator of class I HDAC activity, discussed in more detail later.

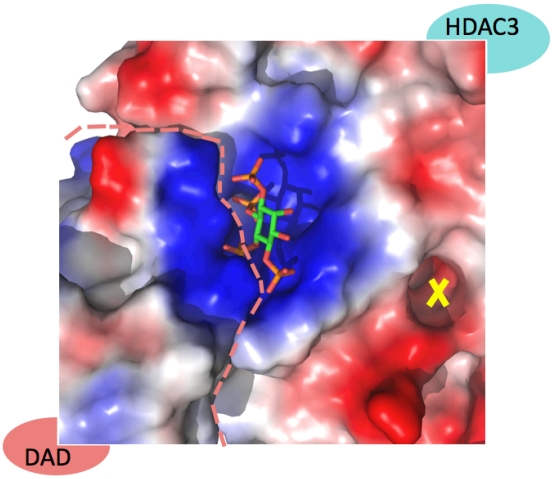

Figure 1-9 Crystal structure indicating Inositol-1,4,5,6-phosphate bound at the interface between SMRT/HDAC3. *Electrostatic surface representation of Inositol-1,4,5,6-phosphate (IP_4) binding at the interface of DAD-SMRT/HDAC3 (denoted by salmon dotted line) in a basic pocket (blue). The active site of HDAC3 is shown by the yellow cross. PDB ID: 4A69, Watson et al, 2012.*

The second SANT domain of SMRT/NCoR (Figure 1-8) has been shown to interact with histone tails, therefore presenting the SMRT/NCoR-HDAC3 complex more effectively to the nucleosome, this region is termed the histone interaction domain (HID) (Yu et al, 2003). The complex components transducin β-like 1 (TBL1) and TBL1-related protein (TBLR1) are WD40 domain containing proteins which associate with HDAC3 in a tetramer and are known to interact with histones such as H2B, H3 and H4, thus targeting the complex to chromatin (Choi et al, 2008; Guenther et al, 2000; Oberoi et al, 2011; Yoon et al, 2003). Other complex members include G-protein pathway suppressor 2 (GPS2), which stabilises the complex (Zhang et al, 2002). Interaction of SMRT/NCoR with class IIa HDACs, HDAC4, 5, 7, has also been reported at repression domain 3 (Figure 1-8) (Fischle et al, 2001; Fischle et al, 2002). Although binding does not activate their deacetylase activity, it is thought that they act as scaffolding proteins which target the complex to target genes via transcription factors such as MEF2 (Codina et al, 2005; Fischle et al, 2001; Fischle et al, 2002; Guenther et al, 2001).

Despite the high level of homology observed between SMRT and NCoR, they are not functionally redundant. Deletion of NCoR and SMRT results in embryonic lethality at

e15.5 and e16.5 days respectively, the loss of NCoR affects the development of T-cells and deletion of SMRT results in heart defects (Jepsen et al, 2000; Jepsen et al, 2007). Furthermore, whilst both NCoR and SMRT affect neural differentiation down the astrocyte pathway, only SMRT affects overall neural differentiation (Jepsen et al, 2007). These differences are also observed during tissue specific deletions, as deletion of NCoR in the liver but not SMRT results in metabolic and transcriptional alterations similar to those seen in the HDAC3 liver specific deletion (Sun et al, 2013).

1.6 HDACs and transcriptional regulation

The correlation between histone acetylation and transcriptional activation is well established and led to the general mechanism where removal of acetyl groups via the action of HDACs results in silencing of transcription (Yang & Seto, 2008). Histone acetylation correlates with transcriptional start sites, promoters, recruitment of TFIID, and disruption of higher order chromatin (Agalioti et al, 2002; Shogren-Knaak & Peterson, 2006; Wang et al, 2008). Whereas histone deacetylation is associated with repression of transcription at promoters and inhibition of cryptic transcription (Carrozza et al, 2005; Kadosh & Struhl, 1998; Li et al, 2007). Furthermore, treatment of cells with butyrate, a HDAC inhibitor, has been shown to result in increased gene accessibility and transcriptional activation (Shogren-Knaak & Peterson, 2006).

Despite the substantial evidence supporting HDACs as transcriptional repressors, evidence has emerged suggesting they may also enable transcription. Deletion of Rpd3 in yeast, an ortholog of HDAC1, resulted in the downregulation of more genes than were upregulated (Bernstein et al, 2000). This result was corroborated by inhibition of Rpd3 with trichostatin A (TSA), an HDAC inhibitor, which resulted in downregulation of a similar set of genes within 15 minutes (Bernstein et al, 2000). It was later shown by genome wide chromatin immunoprecipitation (ChIP) studies in human $CD4^+$ T cells, that HDACs co-localise with HATs such as p300 and CPB, at active loci and primed genes (Wang et al, 2009).

Since the initial indication that HDACs may enable transcriptional activation, several studies have identified specific loci to which HDACs are recruited to facilitate transcriptional activation. HDAC3 was recently shown to enable UCP-1 expression through the removal of a repressive acetyl mark on co-activator Pgc1α, which activates the transcription factor ERRα in brown adipose tissue (Emmett et al, 2017). Moreover, in mammals knockdown or inhibition of either Sin3 or HDAC1/2 resulted in decreased Nanog expression (Baltus et al, 2009). Subsequently, Sin3 and Nanog have been shown to co-occupy transcriptionally active genes in ES cells further supporting the role of HDACs in the facilitation of transcriptional activation (Saunders et al, 2017). It has been proposed that HDACs enable transcription by removal of Lys-Ac added by HATs to reset the chromatin state (Dovey et al, 2010a). Thus suggesting that gene activation requires the cyclical utilisation of HATs and HDACs between RNA polymerase II recruitment to enable subsequent rounds of transcription (Dovey et al, 2010a).

1.7 Non-histone targets of HDACs

Histones were the first identified target of HDACs, however, since their initial discovery, several non-histone targets have been identified suggesting they should be termed lysine specific deacetylates instead. Unsurprisingly, one of the most common groups of acetylated non-histone proteins are transcription factors, which recruit HDACs to chromatin. Deacetylation of p53 and E2F1 by HDAC1/2/3 results in their decreased association with target sites and downregulation of transcriptional activation (Juan et al, 2000; Martinez-Balbas et al, 2000). Furthermore, deacetylation of MyoD by HDAC1 in non-muscle cells prevents MyoD mediated myogensis. Upon differentiation, the interaction of MyoD and HDAC1 is reduced thus enabling the activation of downstream targets (Mal et al, 2001). Other examples of Lys-Ac includes the control of cyclin A stability whereby deacetylation by HDAC3 prevents its degradation during S phase (Vidal-Laliena et al, 2013). In 2009, a high-resolution mass spectrometry analysis discovered a widespread acetylome in mammalian cells, with

3,600 lysine acetylation sites on 1,750 proteins. Sites of Lys-Ac include proteins from all major cellular processes such as cell cycle, splicing, nuclear transport, chromatin remodeling and transcription (Choudhary et al, 2009). Consequently, it is clear that acetylation is not a modification unique to histones, but is an abundant post-translational modification involved in nearly all major processes in the cell.

1.8 Role of class I HDACs in cellular processes

To ascertain the role of histone deacetylases in the development of normal tissues and cell types, various germline and tissue specific knockout studies have been generated, thereby enabling the determination of which HDACs are involved in specific physiological processes.

1.8.1 Germ-line deletion of class I HDACs in mice

All the class I HDACs have been ablated in the mouse germ-line and result in lethality at various stages (summarised in Table 1-3). Genetic disruption of HDAC1 results in embryonic lethality before embryonic day (E) 10.5, due to retarded development, attributed to proliferation defects consistent with an increase in cyclin-dependent kinase inhibitors p21 and p27 (Lagger et al, 2002). Ablation of HDAC2 results in a perinatal or adult phenotype dependent on the targeting method utilised. The first study found that loss of HDAC2 in the mouse germline resulted in perinatal lethality 24 hours after birth attributed to cardiac defects due to increase cardiomyocyte proliferation (Montgomery et al, 2007). The cardiomyocyte phenotype is linked to homeodomain only protein (HOP) which interacts with HDAC2, and acts as a regulator of cardiomyocyte proliferation (Haberland et al, 2009b). GATA4 has also been implicated as it has been shown to be targeted by HDAC2 and this interaction is stabilised by HOP leading to regulation of cardiomyocyte proliferation during development (Reichert et al, 2012). Conversely, two other studies, both of which used

a gene-trap method to disrupt the HDAC2 gene, resulted in differing phenotypes, one exhibited partial perinatal lethality (50% died 25 days postnatal), the other study indicated mice survived to adulthood but with reduced tumour incidence rates (Trivedi et al, 2007; Zimmermann et al, 2007). HDAC3 knockout mice exhibit embryonic lethality at a similar time to HDAC1 null mice, with lethality occurring before E9.5, due to gastrulation defects, indicating HDAC3 is essential in early embryogenesis (Bhaskara et al, 2008; Montgomery et al, 2008). HDAC8 null mice, like HDAC2 deletions, results in perinatal lethality, due to inability to repress transcription factors in the cranial neural crest cells resulting in craniofacial defects and skull instability (Haberland et al, 2009a). Therefore, despite their overlapping expression and high level of similarity, class I HDACs have independent roles during the development of the mouse embryo.

Histone deacetylase	Lethality	Phenotype	Reference
HDAC1	E10.5	Growth retardation and proliferation defects	Lagger et al, 2002 Montgomery et al, 2007
HDAC2	Perinatal or viable	Cardiac defects	Montgomery et al, 2007 Trivedi et al, 2007 Zimmermann et al, 2007
HDAC3	E9.5	Gastrulation defects	Bhaskara et al 2008 Montgomery et al 2008
HDAC8	Perinatal	Craniofacial defects	Haberland et al 2009

Table 1-3 Summary of the effect of class I HDAC germline mutations in mice.

1.8.2 Tissue specific deletion of class I HDACs

Due to the lethality of germline deletion, conditional deletions of class I HDACs were generated to determine their role in specific tissues. Functional redundancy is often observed upon ablation of either HDAC1 or HDAC2, with deletion of both required to result in an aberrant phenotype in many cases including haematopoiesis and cardiac development (Montgomery et al, 2007; Wilting et al, 2010; Yamaguchi et al, 2010). For example, deletion of either HDAC1 or HDAC2 alone in the thymus of mice does not influence development, however double knockouts fail to develop mature T-cells due to a developmental block leading to neoplastic transformation of immature T-cells at approximately 15 weeks (Dovey et al, 2013). Additionally, despite the cardiac defects observed upon ablation of HDAC2 in the developing embryo, deletion of HDAC2 alone in a cardiac specific manner does not phenocopy this, whilst HDAC1/2 cardiac null mice show postnatal lethality after 14 days, suggesting multiple abnormalities are responsible for the HDAC2 germline deletion phenotype (Montgomery et al, 2007). HDAC3 has a unique role in cardiac development as cardiac specific deletion results in postnatal death of mice between 3-4 months due to cardiac hypertrophy and the upregulation of fatty acid uptake and oxidation genes (Montgomery et al, 2008).

HDAC1 null mouse embryonic stem (ES) cells, revealed reduced proliferation and increased cdk inhibitor p21 expression corresponding with increased acetylation of H3 and H4 at its promoter (Lagger et al, 2002). This defect in proliferation was compounded by double deletion of HDAC1 and HDAC2 in mouse embryonic fibroblasts (MEFs) (Yamaguchi et al, 2010). Ablation of p21 was shown to rescue the HDAC1 knockout ES cell phenotype yet was unable to rescue the germline deletion indicating lethality is not due to reduced proliferation (Zupkovitz et al, 2010). Indeed, deletion of either HDAC1 or HDAC2 in ES cells revealed normal proliferation but precocious differentiation upon ablation of HDAC1 indicated by increased cardiomyocyte and neural markers in embryoid bodies (EBs) (Dovey et al, 2010b). Moreover, a double knockout HDAC1/2 ES cell line implicated HDAC1 and HDAC2 in mitosis, particularly in chromosome separation, the lack of S phase deregulation could be due to the lack of a

G1 checkpoint in ES cells (Jamaladdin et al, 2014). HDAC3 has also been shown to play a role in cell cycle regulation as HDAC3 null MEFs show a S-phase delay and DNA damage due to defective double strand DNA repair resulting in apoptosis (Bhaskara et al, 2008).

Neuronal development is also perturbed by deletion of class I HDACs and their co-repressors. Deletion of HDAC1 and HDAC2 in the mouse central nervous system results in postnatal death at around day 7 due to severe brain abnormalities resulting from the inability of neuronal precursors to differentiate (Montgomery et al, 2009). Furthermore, ablation of HDAC1 and HDAC2 using an oligodendrocyte specific Cre-recombinase results in death 2 weeks postnatal, attributed to the stabilisation of β-catenin in the nucleus enabling activation of Wnt signalling leading to repression of Olig2 and prevention of differentiation (Ye et al, 2009). Moreover, Nodal an inhibitor of neural development is upregulated upon ablation of HDAC1, thereby indicating Nodal as a target of HDAC1 and neuronal regulation (Liu et al, 2015). The HDAC3 co-repressor SMRT has been shown to have a critical role in forebrain development through the prevention of retinoic-acid receptor dependent induction of differentiation in the absence of a ligand (Jepsen et al, 2007). It has since been shown through ChIP that in neural stem cells HDAC3 is found at the promoters of genes such as Pax6 and Sox8 which are transcription factor markers of neuronal development, thereby implicating HDAC3 in their regulation (Castelo-Branco et al, 2014).

Whilst HDAC1 and HDAC2 are not essential for liver homeostasis, HDAC3 has been shown to be critical in the regulation of liver metabolism. Liver specific deletion of HDAC3 in postnatal mice resulted in hypertrophy of hepatocytes leading to an enlarged liver (Knutson et al, 2008; Sun et al, 2012). The upregulation of carbohydrate and lipid metabolism genes was shown to be mediated through the recruitment of NCoR/HDAC3 via PPARγ orchestrated by the circadian rhythm (Feng et al, 2011). This combined with the role of HDAC3 in cardiac metabolism, indicates that HDAC3 is essential for normal metabolic homeostasis in multiple organs.

1.9 Inositol phosphates and class I HDACs

Inositol phosphate (IP) molecules are produced from the 6-carbon myo-inositol ring which can be phosphorylated at all 6 positions enabling the formation of many different molecules (Irvine & Schell, 2001). These various IPs act as signalling molecules which can regulate numerous cellular processes including; calcium release (via Inositol-1,4,5,-trisphosphate), chromatin remodelling (SWI/SNF regulation) and mRNA export through the binding of inositol hexaphosphate (IP_6) to Gle1 which stabilises and activates Dbp5 at the nuclear pore leading to mRNA export (Berridge & Irvine, 1989; Montpetit et al, 2011; Shen et al, 2003; Steger et al, 2003; York, 2006; York et al, 1999). More recently, Inostiol-1,4,5,6-tetraphosphate (Ins(1,4,5,6)P_4) has been identified at the interface of SMRT and HDAC3 (Figure 1-9), although initially believed to be a structural co-factor there is now *in vitro* evidence to suggest it is a bona-fide regulator of class I HDAC activity (Millard et al, 2013; Watson et al, 2012).

1.9.1 Regulation of class I HDACs by inositol phosphates

In 2012, Watson et al, resolved the X-ray crystallography structure of human HDAC3 bound to the deacetylase activation domain (DAD) of human SMRT (DAD:SMRT). This elucidated that Ins(1,4,5,6)P_4 can be detected at the interface of HDAC3 and DAD:SMRT in a highly basic pocket, and makes several interactions with HDAC3 (residues His17, Gly21, Lys25, Arg265, Arg301) and DAD:SMRT (residues Lys449, Tyr470, Tyr471, Lys474, Lys475) (Figure 1-10) (Watson et al, 2012). The presence of Ins(1,4,5,6)P_4 was believed to be essential for the formation of the HDAC3/SMRT complex. Previously mutagenesis of Lys449, Tyr470 and Tyr471, all of which interact with Ins(1,4,5,6)P_4 resulted in a failure of complex formation (Tyr470/471) or activation of the complex (Lys449) (Codina et al, 2005; Watson et al, 2012). Furthermore, Arg265 of HDAC3 is located in loop 6 and it is proposed that upon binding to DAD:SMRT with Ins(1,4,5,6)P_4 loop 6 is stabilised enhancing active site access, accordingly, mutation of Arg265 to proline abolishes HDAC3 activity (Watson et al, 2012).

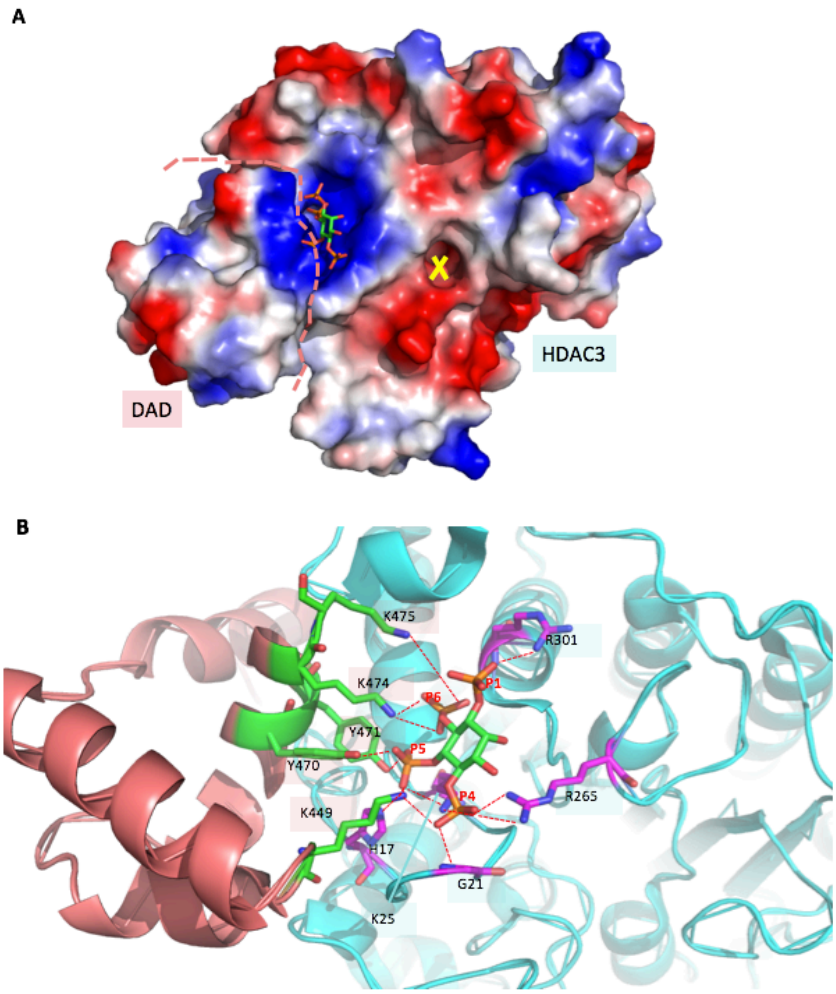

Figure 1-10 Inositol-1,4,5,6-phosphate forms extensive interactions with HDAC3 and DAD:SMRT. (A) *Electrostatic surface representation of Inositol-1,4,5,6-phosphate (IP_4) binding at the interface of DAD:SMRT/HDAC3 (denoted by salmon dotted line) in a basic pocket (blue). The active site of HDAC3 is shown by the yellow cross.* ***(B)*** *Detailed structure of interactions of IP_4 (stick model) with HDAC3 (cyan) bound to the DAD:SMRT (salmon). Interacting residues in HDAC3 are shown in magenta and those in DAD are shown in green, interactions are shown via red dotted lines. PDB ID: 4A69, Watson et al, 2012.*

Intriguingly, the residues involved in the interaction with Ins(1,4,5,6)P_4 in both HDAC3 and DAD:SMRT are conserved in HDAC1/2 and MTA1/2/3 and CoREST1/2/3. Thus suggesting that Ins(1,4,5,6)P_4 is a conserved binding partner of class I HDAC complexes (Watson et al, 2012). Indeed, the structure of HDAC1 in complex with the ELM2-SANT domain of MTA1 revealed that although Ins(1,4,5,6)P_4 was not isolated with the complex, a basic pocket is observed at the interface, similar to that of HDAC3/DAD:SMRT (Figure 1-11) (Millard et al, 2013; Watson et al, 2012).

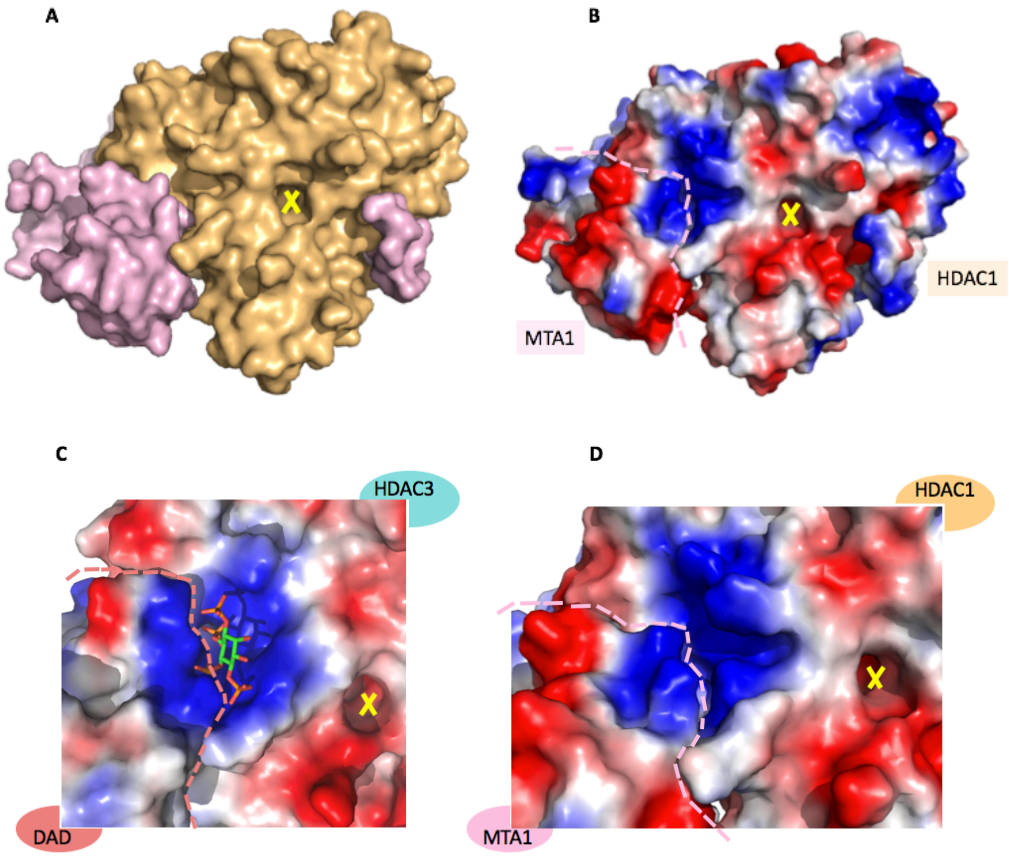

Figure 1-11 Crystal structure of MTA1/HDAC1 reveals a basic pocket characteristic of HDAC3/SMRTs Inositol-1,4,5,6-phosphate binding pocket. ***(A)*** *Surface representation of ELM2-SANT domain of MTA1 (light pink) bound to HDAC1 (light orange), active site denoted by yellow cross.* ***(B)*** *Electrostatic surface representation of MTA1 and HDAC1 showing the interface denoted by light pink dotted line.* ***(C)*** *Electrostatic surface representation of Inositol-1,4,5,6-phosphate binding at the interface of DAD-SMRT/HDAC3 (denoted by salmon dotted line) in a basic pocket (blue).* ***(D)*** *Electrostatic representation of MTA1 and HDAC1 shows an inositol phosphate binding pocket (blue basic pocket) like HDAC3/SMRT. PDB ID: 4BKX, Millard et al, 2013 and PDB ID: 4A69, Watson et al, 2012.*

As the ELM2-SANT domain of MTA1 and the extended DAD domain of SMRT are sufficient for complex formation without Ins(1,4,5,6)P_4, it is believed that binding of HDAC1/3 to their cognate co-repressors tethers but does not activate HDAC activity in the absence of Ins(1,4,5,6)P_4 (Millard et al, 2013). Accordingly, addition of Ins(1,4,5,6)P_4 to the purified MTA1/HDAC1 complex results in increased activity of HDAC1 with a K_d of 5μM, similar to the concentration of Ins(1,4,5,6)P_4 found in mammalian cells (Barker et al, 2004; Millard et al, 2013). Furthermore addition of exogenous Ins(1,4,5,6)P_4 to the SMRT/HDAC3 complex following high salt washes increases the activity of HDAC3, revealing a similar K_d of 6μM, thereby suggesting that

IPs activate class I HDAC complexes (Millard et al, 2013). This is further supported by the addition of Ins(1,4,5,6)P_4 to the novel HDAC1 complex, MIDEAS, leading to upregulated HDAC1 activity of the purified complex (Itoh et al, 2015). *In vivo* studies by Jamaladdin et al, 2014, also suggest a role for Ins(1,4,5,6)P_4 as a regulator of HDAC activity. Mutation of key binding residues in HDAC1 fail to rescue the lethal phenotype of HDAC1/2 double knockout ES cells, presumably due to decreased activity (Jamaladdin et al, 2014). Additionally, inositol pyrophosphates (PP-IP) have been shown to activate yeast Rpd3, a HDAC1 homolog, and mutation of the corresponding HDAC3 Ins(1,4,5,6)P_4 binding residues fails to result in transcriptional responses to stress signals (Worley et al, 2013).

The stereochemical requirements of IP binding were investigated to elucidate the requirements for activation and binding to HDACs. Multiple IP species were shown to activate the HDAC3/SMRT complex and revealed that activation of class I HDAC co-repressors requires the binding of three adjacent phosphate groups occupying binding sites A, B and C in the Ins(1,4,5,6)P_4 binding pocket (Figure 1-12) (Watson et al, 2016). Sites B and C are buried in the complex and have been shown to be important for binding whilst site A is adjacent to R265 in HDAC3 which has been shown to be essential for activation not binding (Watson et al, 2016). Site D interacts with the phosphate group on carbon 1 in the inositol ring and can tolerate a pyrophosphate inositol mimic on position 1 (1-PA-InsP_5) as activation of the complex remains similar to Ins(1,4,5,6)P_4 (Watson et al, 2016). Carbon 2 and 3 of the inositol ring are exposed and do not interact with the class I HDAC complexes, accordingly, it has been shown that these sites can tolerate additions without affecting the activation of the complex i.e. Ins(1,3,4,5,6)P_5 and Ins(1,2,3,4,5,6)P_6 are both able to activate to a substantial level (Watson et al, 2016). Interestingly, Ins(1,4,5)P_3 the well-known regulator of calcium release, is unable to activate the HDAC complexes due to its inability to occupy sites A,B and C thereby separating the activation of class I HDACs from calcium signalling (Berridge & Irvine, 1989; Watson et al, 2016).

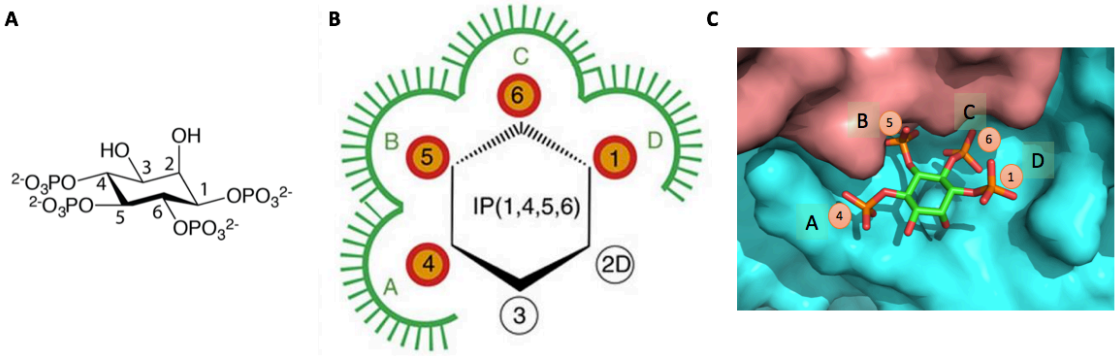

Figure 1-12 Stereochemistry of inositol phosphate binding. ***(A)*** *Structure of Ins(1,4,5,6)P_4* ***(B)*** *Schematic showing the four binding sites in the inositol phosphate binding pocket in green and phosphates in orange, taken from Watson et al 2016.* ***(C)*** *Surface structure of DAD (salmon) and HDAC3 (cyan) bound by Ins(1,4,5,6)P_4 with phosphates numbered in red circles and binding sites denoted by A,B,C,D in green boxes. (PDB ID: 4A69, Watson et al, 2012.)*

1.9.2 The inositol phosphate pathway

To elucidate the importance of IPs as physiological regulators of class I HDAC complexes, we need to understand the pathway leading to their synthesis. Inositol phosphate signalling pathways are instigated by the cleavage of phosphatidylinositol-4,5-bisphospahte (PIP_2) by phospholipase C (PLC) resulting in formation of diacylglycerol (DAG) and Ins(1,4,5)P_3 (Figure 1-13) (Berridge & Irvine, 1989). Inositol polyphosphate multikinase (IPMK) is a key regulator in the sequential production of inositol tetrakisphosphate (IP_4) and inositol pentakisphosphate (IP_5) in the IP synthesis pathway (Figure 1-13). Its homolog in *saccharomyces cerevisiae*, Arg82 was identified first in 1999, and has been implicated in transcriptional regulation (Odom et al, 2000; Saiardi et al, 1999). Whilst the method of IP synthesis in yeast via IPMK is well established, the mammalian system took longer to elucidate. Initially, *in vitro* studies indicated that IPMK could generate Ins(1,3,4,5)P_4 or Ins(1,4,5,6)P_4 and subsequently phosphorylate this to produce Ins(1,3,4,5,6)P_5 (Fujii & York, 2005; Nalaskowski et al, 2002; Saiardi et al, 2001). The mammalian 2-kinase IPPK then phosphorylates Ins(1,3,4,5,6)P_5 to produce Ins(1,2,3,4,5,6)P_6 (Saiardi *et al* 2001). However, in 2005 a study by Verbsky et al., outlining the pathway of inositol hexakisphosphate (IP_6) production in human cells via IPMK and IPPK changed this (Verbsky et al, 2005b). They suggested the pathway outlined in Figure 1-13 whereby IPMK generates

Ins(1,3,4,5,6)P_5 via Ins(1,3,4,5)P_4 but also generates Ins(1,3,4,5,6)P_5 via an extensive pathway of dephosphorylation and phosphorylation involving an inositol phosphate 5-phosphatase (INNP5) and an Ins(1,3,4)P_3 5/6Kinase (IP3 5/6-kinase) (Verbsky et al, 2005b). Despite the *in vitro* evidence Verbsky et al, 2005b, believed that IPMK is more active on Ins(1,3,4,6)P_4 than Ins(1,3,4,5)P_4 and therefore suggested that this is the primary intermediate of IP_5 production *in vivo*. This is further supported by efficiency studies which have since shown that IPMK has relatively poor 6-kinase activity in humans (Chang & Majerus, 2006). Therefore, phosphatase and tensin homolog (PTEN) is believed to produce Ins(1,4,5,6)P_4 through its ability to de-phosphorylate Ins(1,3,4,5,6)P_5 at the D3 position (Caffrey et al, 2001).

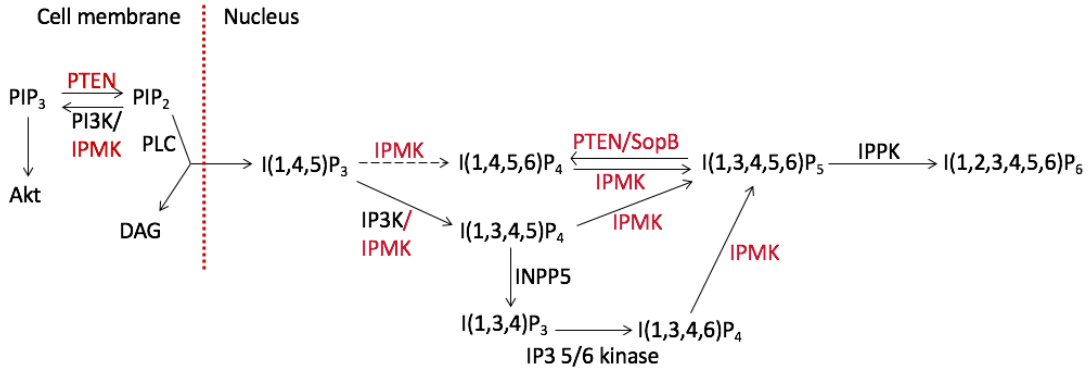

Figure 1-13 Inositol phosphate synthesis pathway. *Cleavage of PIP2 by PLC leads to generation of Ins(1,4,5)P3 which through the action of multiple enzymes including IPMK, IP3K (Inositol phosphate 3 kinase), INNP5 (5-phosphatase), IP3 5/6 kinase, IPPK, PTEN and external pathogen phosphatase SopB, results in the metabolism of various inositol phosphate molecules. Dotted line denotes in vitro evidence only.*

PTEN traditionally is a 3-phosphatase against phosphatidylinositiol 3,4,5-trisphosphate (PIP_3) which leads to the generation of PIP_2 thus counteracting the activity of PI3K kinase and preventing the activation of Akt (Maehama & Dixon, 1998). However, nuclear PTEN also has the ability to act as an IP 3-phosphatase. Although Ins(1,3,4,5)P_4 is not believed to a physiologically relevant substrate of PTEN, it has been shown that it can actively dephosphorylate Ins(1,3,4,5,6)P_5 when transfected into HEK-293Ts, with an affinity constant (Km) of 7.1μM (Caffrey et al, 2001; Maehama & Dixon, 1998). The dephosphorylation Ins(1,3,4,5,6)P_5 led to an increase in Ins(1,4,5,6)P_4, thus cementing its role in the pathway denoted in Figure 1-13 (Caffrey et al, 2001). Despite some evidence to suggest wildtype PTEN is not a physiologically relevant IP 3-phosphatase,

there is an assumption in the community that PTEN does de-phosphorylate IP_5 upon overexpression, thus PTEN was utilised in this thesis to alter the levels of IP (Orchiston et al, 2004).

The importance of both IPMK and IPPK is exhibited via the severe phenotype of the knockout mice. Mice deficient for IPMK and IPPK show embryonic lethality at E9.5 and E8.5 respectively (Frederick et al, 2005; Verbsky et al, 2005a). IPMK null mice show reduced levels of Ins(1,3,4,5,6)P_5 and Ins(1,2,3,4,5,6)P_6 and show morphological defects including abnormal neural tube folding (Frederick et al, 2005). IPPK ablation in mice results in a reduction of Ins(1,2,3,4,5,6)P_6 and its downstream metabolites, inositol pyrophosphates (Verbsky et al, 2005a). Accordingly, both IPMK and IPPK appear to be essential for life and a requirement for accurate embryogenesis.

The environmental pathogen *Salmonella Dublin (S.Dublin)* has also been shown to alter IP levels following invasion of epithelial cells resulting in an increase of Ins(1,4,5,6)P_4 via the de-phosphorylation of Ins(1,3,4,5,6)P_5 (Eckmann et al, 1997). The *S. Dublin* protein, SopB, was later identified as an IP phosphatase which resulted in the increase of Ins(1,4,5,6)P_4 levels (Norris et al, 1998). Its role was further validated using a Tetracycline (TET) dependent SopB expressing 293 cell line. IP_5 and IP_6 levels are almost completely depleted 4-6 hours after SopB induction, and a transient rise in IP_4 is observed overtime but gradually decreases below wildtype levels after prolonged expression (Figure 1-14) (Feng et al, 2001).

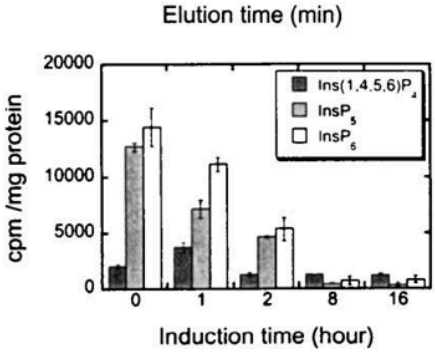

Figure 1-14 SopB induction in human 293 cells reduces the level of inositol phosphates. *Changes in inositol phosphate levels are shown at varying points after induction. The level of IP_5 and IP_6 decreases as the level of IP_4 increases but by 8 hours the levels of all inositol phosphates have dropped compared to wildtype levels. Taken from Feng et al, 2011*

1.9.3 Inositol phosphates and transcriptional regulation

The identification of IPMK as an orthologue of the yeast transcriptional repressor Arg82, led to the implication of IPs in transcriptional regulation. Arg82 is an essential member of the ArgR-Mcm1 transcription factor complex (Arg80, Arg81, Arg82(IPMK), Mcm1) where it enables formation of the complex and activates it through the production of Ins(1,4,5,6)P_4 (Odom et al, 2000). Deletion of Arg82 in yeast grown on arginine or ornithine prevents activation of the ArgR-Mcm1 target genes leading to inviable strains (El Alami et al, 2003; Odom et al, 2000). Conversely, other studies have suggested that the poly-aspartate region of IPMK, not its kinase activity is required for the activation of the ArgR-Mcm1 complex in yeast (Dubois et al, 2000; El Alami et al, 2003). However, *Arabidopsis thaliana* IPMK, which lacks the poly-aspartate region, can fully rescue IPMK knockout yeast strains, suggesting that this region is not essential for regulation (Endo-Streeter et al, 2012). More recently a cis-acting promoter element has been identified in yeast, which mediates IPMKs kinase dependent and independent regulation of gene expression through the binding of Mcm1 (Hatch et al, 2017). This element enables IPMK to act as a scaffold protein to recruit the ArgR-Mcm1 complex, and enables its production of IPs thus activating transcription, thereby suggesting that both activities are essential consequences of IPMK gene regulation (Hatch et al, 2017).

As well as activating transcription factor complexes, there is growing evidence that IPMK derived Ins(1,4,5,6)P_4 regulates chromatin remodelling. In yeast, upon phosphate starvation, the transcription factor Pho4 is activated and recruits SWI/SNF and INO80 to the PHO5 gene enabling chromatin remodelling and transcriptional activation (Steger et al, 2003). However, it was noted that in IPMK catalytically inactive strains transcription of PHO5 was reduced, this was linked to the reduced recruitment of SWI/SNF and INO80 to the promoter region thereby suggesting IP_4 or IP_5 may be required for their efficient recruitment (Steger et al, 2003). This is further supported by Shen et al, 2003 who showed that SWI/SNF is stimulated by Ins(1,4,5,6)P_4 and IP_5. Furthermore, INO80 appeared to be inhibited by IP_6 and this has since been reported for the human Ino80 complex (Shen et al, 2003; Willhoft et al, 2016). Despite, the overwhelming evidence to support Ins(1,4,5,6)P_4 as a cell signalling molecule and a regulator of transcription, there is some doubt over its physiological relevance. The concentrations of Ins(1,4,5,6)P_4 and IP_5 required (500μM) to stimulate the activity of SWI/SNF and the inhibition of INO80 by IP_6 (100-250μM) were much higher than the cellular levels of inositol phosphates (3-9μM, 40-90μM and 20-50μM respectively) (Barker et al, 2004; Shears et al, 2012; Shen et al, 2003; Willhoft et al, 2016). Despite these doubts, it is possible that cellular levels of inositol phosphates alter within individual cellular compartments, which could account for the differences in stimulatory levels and known whole cell level. Moreover, the calculated inhibitor constant (Ki) for the human INO80 complex inhibition by IP_6 is 37±4μM, which is in the range of cellular IP_6 levels (20-50μM), thus suggesting this could be a physiologically relevant phenomenon (Barker et al, 2004; Willhoft et al, 2016).

Additionally, IPMK has been shown to act as a co-activator of p53 mediated expression and the induction of immediate early genes (IEGs) through the recruitment of CBP (Xu et al, 2013a; Xu et al, 2013b). Furthermore, the interaction of IPMK with serum response factor has been shown to promote recruitment of SRF to serum response elements (SRE) thus stimulating IEF expression (Kim et al, 2013). The co-activator role of IPMK appears to be independent of its kinase activity, unlike its potential role as a

co-repressor via class I HDAC complexes, thereby theoretically allowing the separation of the two processes.

1.10 Mouse Embryonic stem cells

ES cells are derived from the inner cell mass (ICM) of the E3.5 day blastocyst formed during the pre-implantation stage of mouse embryogenesis. The ICM cells go on to form the primitive endoderm and the epiblast which gives rise to the three germ layers of the mouse, a process called gastrulation (Keller, 2005). ES cells were first isolated from the ICM of blastocysts in 1981, by two groups who explanted the ICM onto a feeder layer of mouse embryonic fibroblasts (Evans & Kaufman, 1981; Martin, 1981). Following their isolation, it was determined that ES cells have two properties which render them distinct to other cell types. Firstly, ES cells are capable of self-renewal indefinitely whilst retaining a normal karyotype, moreover, these cells can differentiate into any cell in the body, thus representing the cells they were originally derived from (Keller, 2005). Importantly, ES cells can recapitulate *in vitro* differentiation of the three germ layers (mesoderm, ectoderm and endoderm) of the developing mouse, thereby mimicking gastrulation and enabling recapitulation of the early developmental processes of the developing embryo (Doetschman et al, 1985; Tam & Behringer, 1997). Additionally, in 1984 it was shown that ES cells can be injected into the blastocyst enabling the formation of chimera mice (Bradley et al, 1984). Homologous recombination techniques established in ES cells enabled the generation of the first genetically modified mouse using this method, thus enabling in-depth studies of mouse genetics, development and physiology (Capecchi, 1989; Thompson et al, 1989).

1.10.1 Maintenance of pluripotency in ES cells

The self-renewal capacity of ES cells was initially maintained by culture on a layer of mouse embryonic fibroblasts, termed feeder cells (Evans & Kaufman, 1981; Martin, 1981).The identification of leukaemia inhibitory factor (LIF), led to the ability to culture ES cells independently of fibroblasts (Smith et al, 1988; Williams et al, 1988). The docking of LIF to its receptor, gp130, results in the activation of Janus-associated kinases (JAK) which phosphorylates signal-transducer and activator of transcription 3 (STAT3) (Figure 1-15) (Niwa et al, 1998). STAT3 has been shown to be essential for the maintenance of ES cell self-renewal as a dominant interfering STAT3 mutant promotes differentiation, whilst constitutively active STAT3 results in self-renewal (Matsuda et al, 1999; Niwa et al, 1998). LIF alone is not sufficient to promote self-renewal, bone morphogenic protein 4 (BMP4), usually present in serum, is also required. BMP4 acts through the activation of SMAD resulting in the induction of inhibitor of differentiation (Id) factors which inhibit neuronal differentiation and promote self-renewal (Figure 1-15) (Ying et al, 2003a). Overexpression of Id factors removes the requirement for BMP4 or serum and enables cells to be cultured in the presence of LIF alone (Ying et al, 2003a).

The autocrine secretion of fibroblast growth factor 4 (FGF4) and binding to its cognate receptor FGFR2 leads to the activation of MAPK/ERK kinase (MEK) and subsequently mitogen activated protein kinase (MAPK/ERK) (Figure 1-15) (Kunath et al, 2007). The deletion of FGF4 in ES cells resulted in decreased differentiation, compared to wildtype cells, thereby proposing a role of FGF4/MAPK signalling in the promotion of differentiation (Wilder et al, 1997). Stimulation of glycogen synthase kinase-3 (GSK3) targets β-catenin for degradation preventing association with the transcription factor Tcf3 (Sokol, 2011). Tcf3 represses pluripotency genes and its association with β-catenin in the absence of GSK3 dissociates Tcf3 from target DNA thus promoting self-renewal (Martello & Smith, 2014; Martello et al, 2012). Accordingly, a defined media containing 3 inhibitors (3i), which target FGF receptors (SU5402), MEK (PD184352), and GSK3 (CHIR99021), in the absence of LIF/BMP4, enabled serum free growth of ES cells (Ying

et al, 2008). Recently, a medium containing two inhibitors (PD0315901 (MEK) and CHIR99021 (GSK3)) and LIF has been defined and termed 2i media (Marks et al, 2012). ES cells grown in 2i conditions exhibit decreased expression of lineage specific genes, decreased bivalent domains and DNA methylation suggested to be more representative of naïve ground state pluripotency (Leitch et al, 2013; Marks et al, 2012).

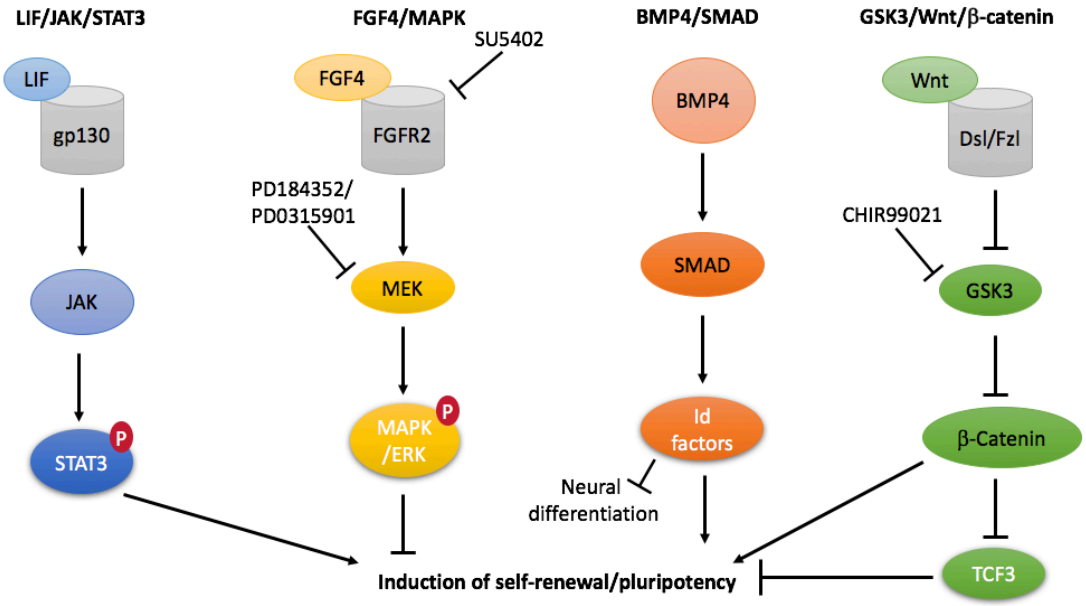

Figure 1-15 Schematic of signalling pathways involved in ES pluripotency maintenance. *LIF mediated activation of STAT3 via JAK results in upregulation of pluripotency genes. BMP4 signalling via Id factors prevents neural differentiation whist both activation of MAPK via FGF4 and TCF3 via GSK3 promote the differentiation of ES cells. Arrows denote activation and flat lines indicate repression.*

1.10.2 Transcriptional network of pluripotency factors

A core transcriptional regulatory network consisting of Oct4 (Pou5f1), Sox2 and Nanog, is also required for the maintenance of ES cell pluripotency. Oct4, is a POU containing transcription factor, whose expression is restricted to the inner cell mass (ICM) and epiblast (Nichols et al, 1998). Oct4 is essential for pluripotency as Oct4 deficient blastocysts produce an ICM incapable of pluripotency (Nichols et al, 1998). Furthermore, deletion of Oct4 in ES cells leads to formation of trophectoderm cells, whilst overexpression of Oct4 promotes differentiation towards the mesoderm and

primitive endoderm lineage (Niwa et al, 2000). These studies suggest that the level of Oct4 is carefully orchestrated to enable the establishment of pluripotency. Oct4 and the SRY-box HMG-like transcription factor, Sox2, are believed to work in concert to regulate pluripotency through the modulation of gene expression including FGF4 (Ambrosetti et al, 1997). Accordingly, deletion of Sox2, results in the formation of trophoblast cells and the inability to maintain the epiblast state (Avilion et al, 2003; Masui et al, 2007). Nanog is a homeodomain containing protein critical for the maintenance of stem cell self-renewal (Mitsui et al, 2003). ES cells deficient for Nanog exhibit differentiation into primitive endoderm, whilst the overexpression of Nanog enables self-renewal independently of LIF, thus indicating a clear role in the maintenance of the pluripotent state (Chambers et al, 2003; Mitsui et al, 2003).

Genome-wide ChIP experiments revealed the binding sites of Nanog, Oct4 and Sox2 in both human and mouse embryonic stem cells (Boyer et al, 2005; Loh et al, 2006). An auto-regulatory and feed-forward loop were observed as Nanog, Oct4 and Sox2 promote the expression of each other and other pluripotency regulators whilst inhibiting differentiation (Figure 1-16) (Boyer et al, 2005). In ES cells, Nanog and Oct4 bind to 3006 and 1083 sites respectively, and co-occupy 345 sites (Loh et al, 2006). Nanog and Oct4 regulate the expression of their target genes which primarily encode transcription factors such as STAT3, REST and Essrb all of which modulate the expression of pluripotency and differentiation genes (Loh et al, 2006). Pluripotency is also achieved through the activation of Wnt signalling components, whilst inhibiting Dkk1 a Wnt antagonist, thus promoting self-renewal (Boyer et al, 2005; Loh et al, 2006).

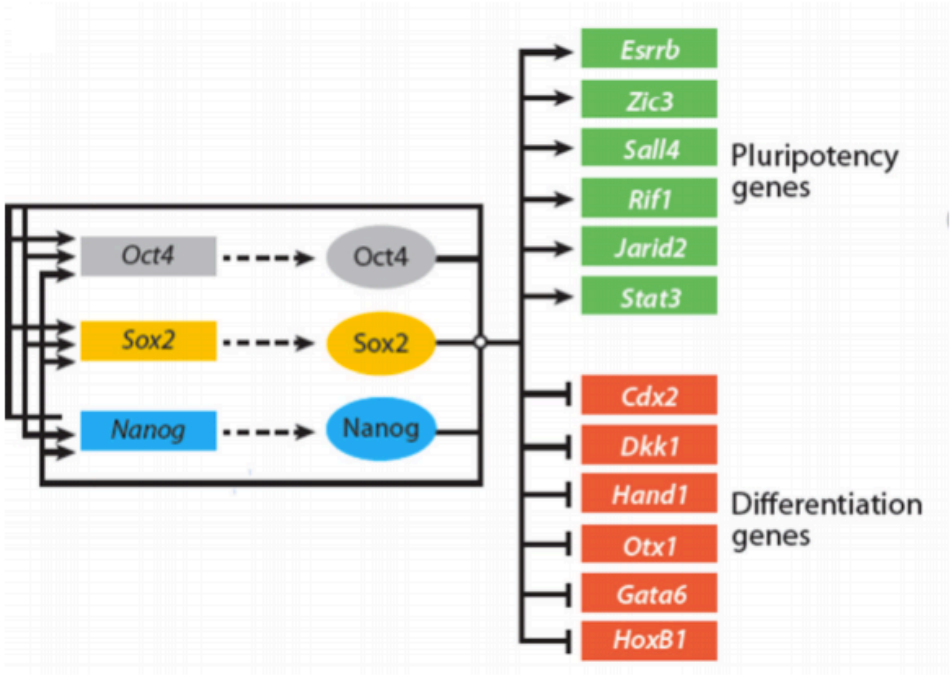

Figure 1-16 Oct4, Sox2 and Nanog maintain ES pluripotency. *Oct4, Sox2 and Nanog, work together to regulate each other through an auto-regulatory feed-forward loop, resulting in maintenance of pluripotency through the promotion of factors such as STAT3 and inhibition of differentiation through the regulation of factors such as GATA6. Taken from (Loh et al, 2011).*

1.10.3 Differentiation of ES cells

The ICM of a developing mouse embryo undergoes differentiation to form three primary germ layers during a process called gastrulation. These three layers go onto to form all elements of the developing embryo. Prior to gastrulation the cells of the ICM form a structure termed the primitive ectoderm which is characterised by expression of FGF5 and repression of Rex1 (Hebert et al, 1991; Keller, 2005). The primitive ectoderm later forms the epiblast which at the onset of gastrulation at E6.5 forms the three germ layers (Keller, 2005; Snow, 1977). The primitive streak arises at the posterior of the embryo from a subset of epiblast cells and coincides with the onset of gastrulation (Snow, 1977). The movement of epiblast cells through the primitive streak via epithelial to mesenchymal transition results in the formation of the mesoderm and definitive endoderm lineages through an intermediate mesendoderm layer characterised by brachyury and Gsc expression (Keller, 2005; Tada et al, 2005; Tam &

Behringer, 1997). The mesoderm maintains expression of brachyury and generates the bone, heart, vascular tissue, muscle and kidney (Figure 1-17) (Tada et al, 2005; Wang & Chen, 2016). Endoderm loses expression of brachyury and is characterised by expression of markers such as Sox17 and FoxA2, leading to the formation of the lungs, liver, pancreas, stomach and intestine (Figure 1-17) (Kubo et al, 2004; Wang & Chen, 2016). Cells at the most anterior region of the developing blastoctyst do not move through the primitive streak and from the definitive ectoderm lineage noted by the expression of markers including Nestin and Sox1 (Figure 1-17) (Li et al, 1998; Tam & Behringer, 1997). The ectoderm delineates into the neuroectoderm which gives rise to neurons and glial cells, whilst the epidermal ectoderm results in production of the skin epidermis (Okabe et al, 1996). The process of gastrulation is a tightly regulated process in which temporal and spatial expression of key transcription factors and modulation by extrinsic signals such as BMP, Wnt and Nodal designate lineage identity (Murry & Keller, 2008).

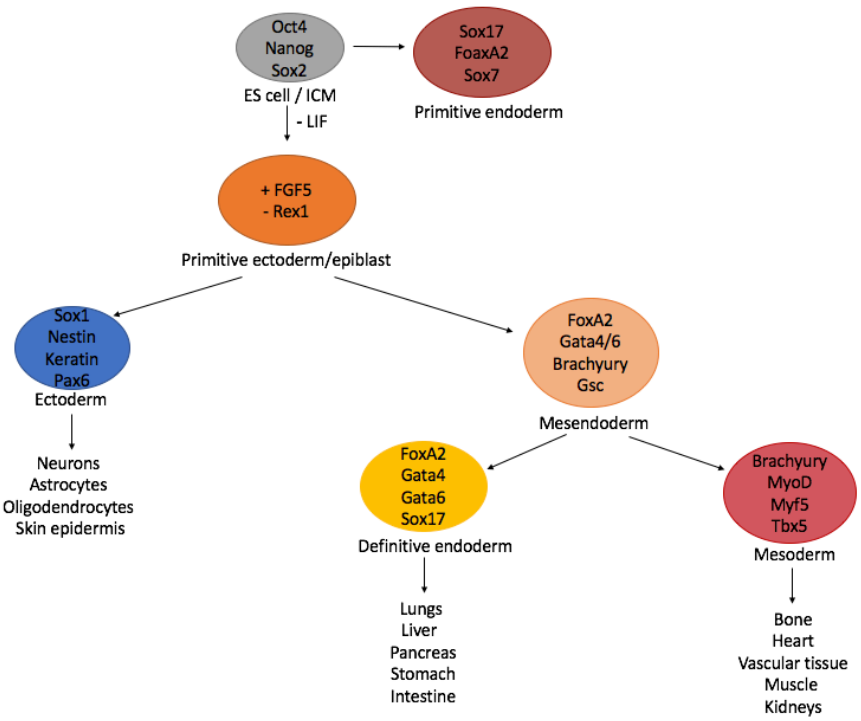

Figure 1-17 Differentiation of the inner cell mass/ mouse embryonic stem cells.
Differentiation of the inner cell mass cells results in the formation of the primitive ectoderm and subsequent epiblast leading to the formation of the primitive streak. ES cells form a primitive ectoderm/epiblast like structure without a primitive streak. From these various structures, the ectoderm lineage is produced and the mesendoderm differentiates into the definitive endoderm and the mesoderm lineage.

In vitro differentiation of ES cells to embryoid bodies (EBs) recapitulates the stages of gastrulation observed in the developing embryo (Doetschman et al, 1985). The differentiation of ES cells through mechanisms outlined below, leads to the formation of a primitive ectoderm like cell lineage which gives rise to the three germ layers reflecting the programmes seen in the gastrulating embryo (Keller, 2005; Murry & Keller, 2008; Smith, 2001). After three days of EB culture, they are believed to represent the point of gastrulation (E6.5) thus enabling the in-depth study of embryonic development (Doetschman et al, 1985; Snow, 1977).

The *in vitro* differentiation of ES cells into EBs can be stimulated through several different methods, one of which involves the culturing of ES cells in non-adherent conditions in the absence of LIF (Doetschman et al, 1985). The removal of LIF removes the inhibitory effect of STAT3 expression thus enabling formation of a 3D ES cell aggregate termed an embryoid body, in which the outer layer is made of primitive endoderm and the three germ layers are found in the core of the structure (Doetschman et al, 1985; Keller, 1995; Shen & Leder, 1992). A second method involves the culture of ES cells on an extracellular matrix such as collagen-coated dishes, thereby forming a 2D layer of differentiated cells (Nishikawa et al, 1998). A third method utilises the direct culture of ES on a layer of stromal cells, such as OP9, which promotes differentiation through cell-cell interactions (Nakano et al, 1994). Lineage determination of developing EBs can be manipulated through the addition and/or removal of signalling factors such as BMP4 and Activin A (Keller, 2005). For example, the addition of retinoic acid, results in enhanced neuroectodermal differentiation through the induction of Hox genes and neuronal lineage specific gene expression (Bain et al, 1995; Bain et al, 1996). Conversely, the addition of BMP4 inhibits neural differentiation through induction of Id factors (Figure 1-15), thereby promoting mesoderm differentiation(Finley et al, 1999). Furthermore, manipulation of Nodal signalling through the addition of Activin A can promote the formation of endoderm and mesodermal lineages and repress neuroectodermal differentiation (Kubo et al, 2004).

1.10.4 Modulation of chromatin structure in ES cells

Unlike differentiated cells which exhibit high levels of heterochromatin, ES cells display chromatin which is transcriptionally permissive and highly accessible (euchromatin) (Boyer et al, 2006). The chromatin of ES cells is vastly dynamic as demonstrated by the loose association with heterochromatin protein 1 (HP1) and histone linker H1. This is essential for the ability of ES cells to differentiate as replacement of H1 with an isoform which binds DNA with a greater affinity decreases the ability of ES cells to differentiate (Meshorer et al, 2006).

Whilst genes required for the maintenance of self-renewal and pluripotency of ES cells are actively expressed, lineage specific genes show minimal transcription in ES cells. Many of these developmental genes encode transcription factors such as the Sox family, and have been shown to been marked by both activating (H3K4Me3 and H3K9Ac) and repressive (H3K27Me3) histone marks, termed bivalent domains. It is postulated that the presence of the opposing marks enables the low-level transcription observed in ES cells to be rapidly upregulated during differentiation, thereby suggesting that bivalent marks poise these sites for transcription (Azuara et al, 2006; Bernstein et al, 2006). Upon differentiation, these bivalent domains are lost with genes showing either H3K27Me3 or H3K4Me3 depending on the lineage established (Bernstein et al, 2006). Oct4, Sox2 and Nanog have been shown to be bound at several bivalent domains indicating that they may be acting to either activate or repress transcription here (Bernstein et al, 2006). Interestingly, it has been reported that nearly all developmental genes bound by Oct4, Sox2 and Nanog co-occupy with the polycomb repressive complex 2 (PRC2) (Lee et al, 2006b). Furthermore, deletion of EED, a component of PRC2, results in abnormal differentiation in the presence of Oct4 due to the concomitant loss of H3K27Me3 at neuronal lineage genes, therefore indicating the importance of PRC2 in the repression of lineage specific genes (Azuara et al, 2006).

As well as regulating lineage specific genes, histone modifying complexes are also believed to be involved in the regulation of pluripotency. Sox2 has been shown to interact with the Sin3A/HDAC1 complex enabling the binding of mSin3A/HDAC1 to the Nanog promoter and ensuring positive regulation of Nanog (Baltus et al, 2009). The binding of Sin3A/HDAC1 to the Nanog promoter is lost during differentiation, accordingly, knockdown of the Sin3A complex results in decreased Nanog expression (Baltus et al, 2009). Moreover, as previously mentioned the alternative NuRD complex, NODE, interacts with Oct4 and Nanog and is believed to repress developmental genes as shown by the increased differentiation upon NODE knockdown (Liang et al, 2008). Additionally, HDAC3 has been shown to deacetylate MEF2 which inactivates it and prevents myogenesis, suggesting a crucial role for HDAC3 in the prevention of muscle differentiation (Gregoire et al, 2007).

Upon differentiation, mass gene expression changes are observed and histone modifying enzymes have been implicated in this process. The histone methyltransferase, G9a has been implicated in the silencing of Oct4 during differentiation, through the addition of H3K9 methyl marks leading to the recruitment of HP1 (Feldman et al, 2006). Furthermore, deletion of MBD3, a component of the NuRD complex, results in an inability to repress Oct4 expression thereby preventing differentiation occurring, even in the absence of LIF (Kaji et al, 2006). Initially, it was observed that inhibition of histone deacetylases by treatment with TSA prevents differentiation, there by implicating them in the process of differentiation (Lee et al, 2004b). Since then, deletion studies have indicated the role of HDACs in embryogenesis, for example, deletion of HDAC1 in ES cells results in aberrant differentiation including increased cardiomyocytes and neural markers (Dovey et al, 2010b). These results suggest that histone deacetylation is not only involved in the initialisation of differentiation but also in controlling lineage determination.

1.11 Project Aims

Numerous *in vitro* studies have indicated the activating role of IP on the activity of class I HDAC co-repressor complexes as discussed in section 1.9. A few studies have attempted to link inositol phosphates to the regulation of class 1 HDACs *in vivo*, with the primary study attempting to rescue the lethal phenotype of HDAC1/2 knockout ES cells with IP binding mutants (Jamaladdin et al, 2014). However, the physiological role of IP on the activity of class I HDACs remains unclear. Therefore, we aimed to elucidate the physiological role of IP *in vivo* using several systems. Initially, to manipulate the levels of IP present in ES cells by overexpression of SopB, PTEN and IPMK and measure the effect on HDAC activity (1.9.2). Latterly, we aimed to utilise the IPMK knockout ES cells generated by Frederick et al, 2005 to determine whether there is any difference in the level of HDAC activity when compared to wildtype cells (Frederick et al, 2005).

The second aim of this project was to explore the regulation of HDACs by IPs during the cell cycle. IPs alter throughout the cell cycle as does the level of histone acetylation, however, it has been reported that the level of HDAC3 does not (Barker et al, 2004; Bhaskara et al, 2010; Dangond et al, 2001; Unnikrishnan et al, 2010). Consequently, it is possible that the regulation of IP levels could be responsible for the changes in HDAC activity. Accordingly, by synchronising wildtype ES cells we aim to measure the activity of HDACs at various stages of the cell cycle and determine whether the level of IP are responsible for any changes observed.

The final aim of this project was to assess the effect of IPMK deletion during ES differentiation. Frederick et al, 2005, generated an IPMK knockout mouse line which showed embryonic lethality before E9.5 indicating that IPMK is essential for embryogenesis. Furthermore, HDAC1 and HDAC3 have also been shown to be essential for embryogenesis during this period (see section 1.8.1). Accordingly, we aimed to generate EB's from ES cells with and without IPMK and to determine the effect on the development, and to see whether any defects observed are related to those observed in the HDAC knockout systems.

Chapter 2 Materials and Methods

2.1 Culture of mouse embryonic stem cells

IPMK knockout mouse embryonic stem cells (ES) cells, kindly provided by John York, and E14 ES cells were used for experimental work outlined in this thesis. All ES cell culture and techniques used are described in the following section.

2.1.1 Thawing of ES cells

Corning® 100mm TC-Treated Culture dishes (Corning, 430167) were coated with 0.1% gelatin:PBS solution. 1.5ml Cryovials (Corning, 450487) were thawed rapidly and added to 9ml of warm ES culture medium (M15+LIF) before centrifugation at 200xg for 3 minutes to remove residual DMSO. Cells were resuspended in M15+LIF and plated onto tissue culture plates once excess gelatin was removed. ES cells were maintained by regular media changes and splitting every 2-3 days, and incubated in a 5% CO_2 incubator at 37°C.

ES cells frozen in a 96-well Clear Flat Bottom Polystyrene TC-Treated plate format (Corning, 3595) were revived from -80^{o}C by rapidly thawing and the addition of 100μl of pre-warmed M15+LIF and mixing by pipette. Each well was then transferred to a pre-gelatinised 96 well plate and a further 100μl of 1X M15+LIF (0.5X final volume) was added to each well before incubating in a 5% CO_2 incubator at 37°C.

2.1.2 Passaging of ES cells

After seeding, ES cells were split every 2-3 days once 75-90% confluent. Media was aspirated off before washing twice in 1X Dulbecco's Phosphate Buffered Saline (DPBS, Gibco, 14190). TrypLE solution was added to cells and incubated at 37^{o}C until cells had lifted off the plate. M15+LIF was added to neutralise the TrypLE solution and the cell suspension was spun for 3 minutes at 200xg. The supernatant was aspirated off and

the cell pellet was resuspended in fresh M15+LIF and split onto new pre-gelatinised plates. The plates were placed in the 5% CO_2 incubator at 37°C.

Cells in 96 well plates were split by washing twice with 100μl !X DPBS, 50μl of !X TrypLE was added, which after incubation, was neutralised with 150μl of fresh M15+LIF. 150μl of fresh M15+LIF was added to pre-gelatinised plates and the cell suspension was split 1:3 between three 96 well plates to allow for replica plating.

2.1.3 Generation of PiggyBAC TET IPMK Inducible ES cell lines

The PiggyBAC system utilises a naturally occurring transposon to enable stable transgene incorporation into TTAA sites within the host genome in the presence of a transposase (Ding et al, 2005; Wilson et al, 2007). To generate stable PiggyBAC TET IPMK inducible cell lines 5x10^5 cells were seeded onto a 6 well plate 24 hours prior to transfection. The following day 2.5μg of transposase (Systems, Bioscience, PB210PA-1) and 2.5μg of the PiggyBAC TET IPMK Inducible plasmid (see section 2.6.1) (Glover et al, 2013) were transfected into cells with 10μl of Lipofectamine2000 as outlined in 2.4.1. 24 hours post transfection cells were plated at low density (5000 or 10,000 cells per 10cm plate) and treated with 1μg/ml Puromycin + M15 + LIF (Sigma, P8833-10MG) for 10 days. Following formation of single cell colonies, 50μl of 1X TrypLE (0.25X final volume) was added to each well of a 96 well round bottom plate (Nunc, 163320) and single cell colonies were isolated from a 10cm low density plate. The 10cm plate was washed twice in 1X DPBS and 10ml of 1X DPBS was added to the plate which was transferred to a microscope. Single cell colonies were isolated with a P20 Gilson pipette and added to a well containing TrypLE. After 5-10 minutes in TrypLE, 150μl of 1X M15+LIF (0.75X final volume) was added to each well and the cell suspension was transferred to a pre-gelatinised 96 well flat bottom plate (Corning, 2595) for long term expansion. Following isolation cells were treated with 1μg/ml Doxycycline hyclate (Dox) (Sigma, D9891-1G) to induce expression of the transgene.

2.1.4 Freezing ES cells

ES cells were dissociated from the plate using TrypLE as described in 2.1.2. Once spun, the cell pellet was resuspended in 1X freezing media, 1ml was added to a cryovial (Corning, 450487) and placed in the -80^{o}C in a cryopreservation freezing container, after 24-48 hours the vials were transferred to liquid nitrogen for long term storage. 96 well plates were frozen through the addition of TrypLE as described in 2.1.2, and neutralised in 50µl of 2X freezing media. The plates were sealed with autoclave tape and wrapped in several layers of blue roll before being placed in the -80^{o}C freezer.

2.1.5 Population doubling assay

The population doubling time of IPMK knockout cells and control cells was analysed by plating 5x10^4 cells in triplicate onto a 6 well plate (VWR, 734-2323). Total and live cell counts were taken daily in triplicate for 4 days using an automated cell counter (BioRad TC-10). The proliferation time was calculated using the following equation:

$$Population\ doubling = (T \times log2)/[log(Total) - \log(Initial)]$$

$$T = Time\ (hours) since\ plated$$

$$Total = Total\ or\ Live\ cell\ count\ on\ given\ day$$

$$Initial = Initial\ number\ of\ cells\ seeded$$

2.1.6 *In Vitro* Differentiation of ES cells

ES cell lines were assessed for differences in *in vitro* differentiation potential and gene expression alterations using two different methods outlined below.

2.1.6.1 Differentiation into Embryoid Bodies (EBs)

ES cells were differentiated into Embryoid Bodies in the absence of LIF using DMEM:F12 differentiation media. ES cells were detached from the plate using TrypLE and neutralised in M15+LIF. Cells were spun and then resuspended in DMEM:F12 media. The cell suspension was counted and 5x10^4 cells were resuspended in 10ml of DMEM:F12 differentiation media. From this diluted stock of cells, 100µl (500 cells) were plated per well of a 96 well low attachment round bottom plate (Corning, 7007).

The cells were incubated in 5% CO_2 at 37°C for 10 days with daily imaging and measured using GNU image manipulation program (GIMP, version 2.8.18). EBs were measured along the x and y axis, this value was normalised to a scaling factor and these measurements were then averaged to determine the size of the EBs. Cells were fed with 50μl of DMEM:F12 differentiation media on days 5 and 7. If EBs were cultured in the presence of Dox, they were fed with fresh media + 1ug/ml Dox on days 3 and 6.

2.1.6.2 Retinoic acid induced differentiation of ES cells

ES cells were induced to exit pluripotency with the presence of retinoic acid (RA) in the absence of LIF using DMEM:F12 differentiation media. ES cells were detached from the plate as outlined in 2.1.6.1 and plated down at 1x10^6 on a 10cm plate in DMEM:F12 + 1μM Retinoic acid. Media was changed every 2-3 days before harvesting on day 5.

2.1.7 Cell cycle Synchronisation of ES cells

To determine differences in inositol phosphate levels and HDAC activity during the cell cycle, cells were synchronised using a Cdk1 inhibitor Ro3306 (Merk Millipore, Calbiochem, 217699). This inhibitor synchronised cells at the G2/M border, by blocking cells in G2 through Cdk1 inhibition. Cells were plated down at 3x10$^{\wedge 5}$ for a 60mm plate and 2x10$^{\wedge 6}$ for a 100mm plate. The following day cells were treated with 10μM Ro3306 for 14 hours overnight. After treatment, cells were washed 3 times in 1x PBS and then treated with 30ng/ml Nocodazole (Sigma, M1404) for 2 hours. After 2 hours the cells were released by washing 3 times in PBS and samples were collected every 1-2 hours for analysis.

2.1.8 Media and reagents used for culture of ES cells

Standard ES cell culture medium (M15 + LIF)

1X Knockout Dulbecco's Modified Eagle Media (GIBCO,10829-018)	500ml (83%)
1X Foetal Bovine Serum (Seralab, EU 000F)	90ml (15%)
100X Glutamine/Penicillin/Streptomycin (GIBCO, 10378-016)	6ml (1X)
50mM β- mercaptoethanol (Fischer Scientific, 125472500)	600μl (0.05mM)
Leukaemia Inhibitory Factor (LIF, Synthesised In House)	25μl (1000U/ml)

2i media

1X Knockout Dulbecco's Modified Eagle Media (GIBCO,10829-018)	500ml (99%)
100X Glutamine/Penicillin/Streptomycin (GIBCO, 10378-016)	6ml (1X)
50mM β- mercaptoethanol (Fischer Scientific, 125472500)	600μl (0.05mM)
Leukaemia Inhibitory Factor (LIF, Synthesised In House)	25μl (1000U/ml)

Per 50 ml of stock 2i media the following were added:

- 1μM MEK inhibitor (PD0325901) (Sigma, A3734) 5μl
- 3μM GSK inhibitor (CHIR99021) (Sigma, P20162) 6μl
- B-27 Supplement (Thermo Fischer Scientific, 17504044) 1 ml
- N2 Supplement (Thermo Fischer Scientific, 17502048) 500μl

Differentiation media (DMEM:F12)

1X Dulbecco's Modified Eagle Medium: F-12 (GIBCO, 11320-033)	500ml (89%)
1X Foetal Bovine Serum (Seralab, EU 000F)	56.2ml (10%)
100X Glutamine/Penicillin/Streptomycin (GIBCO, 10378-016)	6ml (1X)
50mM β- mercaptoethanol (Fischer Scientific, 125472500)	600μl (0.05mM)

Retinoic acid differentiation (DMEM:F12 + RA)

1X Dulbecco's Modified Eagle Medium: F-12 (GIBCO, 11320-033)	500ml (89%)
1X Foetal Bovine Serum (Seralab, EU 000F)	56.2ml (10%)
100X Glutamine/Penicillin/Streptomycin (GIBCO, 10378-016)	6ml
50mM β- mercaptoethanol (Fischer Scientific, 125472500)	600µl (0.05mM)
100mM Retinoic acid	600µl (10µM)

TrypLE

1X TrypLE Express (GIBCO, 12604021)	500ml

0.1% gelatin

1X Dulbecco's Phosphate Buffered Saline (GIBCO,14190144)	475ml
2% Gelatin from Porcine Skin (Sigma, G1890)	25ml

1X Freezing media

1X Knockout Dulbecco's Modified Eagle Media (GIBCO,10829-018)	40%
1X Foetal Bovine Serum (Seralab, EU 000F)	50%
1X DMSO hybri-max (Sigma, D2650)	10%

2X Freezing media

1X Knockout Dulbecco's Modified Eagle Media (GIBCO,10829-01)	60%
1X Foetal Bovine Serum (Seralab, EU 000F)	20%
1X DMSO hybri-max (Sigma, D2650)	20%

2.2 Culture of Human Embryonic Kidney-293T cells

The Human Embryonic Kidney-293T (HEK-293T) cell line was used in several of the experiments outlined in this thesis. All HEK-293T culture techniques and reagents are described below.

2.2.1 Thawing and maintenance of HEK-293T cells

HEK-293T cells were thawed from 1.5ml cyrovials by rapidly warming and adding to 9ml of warm HEK-293T culture medium (M10) before being centrifuged at 200xg for 3 minutes. Cells were resuspended in M10 and plated onto a Corning® 100mm TC-Treated Culture dishes (Corning, 430167) coated with 0.1% gelatin:PBS with excess removed. Cells were grown in a 5% CO_2 incubator at 37°C and passaged every 2-3 days.

2.2.2 Passaging of HEK-293T cells

HEK-293T cells were passaged at 75-90% confluency. M10 media was removed from the cells and they were gently washed twice in DPBS. After the addition of TrypLE to the cells, M10 was used to neutralise and the cell suspension was spun at 200xg for 3 minutes. After pelleting, cells were resuspended in fresh M10 and split onto new pre-gelatinised plates and incubated at 37^{o}C with 5% $CO_{2.}$

2.2.3 Freezing HEK-293T cells

HEK-293T cells were frozen from an 80% confluent 10cm plate through the addition of TrypLE as outlined in 2.2.2. Cells were resuspended in freezing media and 1ml was aliquoted into 1.5ml cyrovials. These were placed in a cryopreservation freezing container and placed in the -80^{o}C. After 1-2 days the cyrovials were transferred into liquid nitrogen.

2.2.4 Media and reagents used for culture of HEK-293T cells

Standard HEK-293T culture medium (M10)	
1X Dulbecco's Modified Eagle Media (GIBCO, 41965-039)	500ml (89%)
1X Foetal Bovine Serum (Seralab, EU-000F)	54ml (10%)
100X Glutamine/Penicillin/Streptomycin (GIBCO, 10378-016)	6ml (1X)

TrypLE	
1X TrypLE Express (GIBCO, 12604021)	500ml

0.1% gelatin	
1X Dulbecco's Phosphate Buffered Saline (GIBCO,14190144)	475ml
2% Gelatin from Porcine Skin (Sigma, G1890)	25ml

Freezing media	
1X Dulbecco's Modified Eagle Media (GIBCO, 41965-039)	40%
1X Foetal Bovine Serum (Seralab, EU-000F)	50%
1X DMSO hybri-max (Sigma, D2650)	10%

2.3 Culture of Human Embryonic Kidney-293F cells

The Human Embryonic Kidney-293F (HEK-293F) cell line was used in several of the experiments outlined in this thesis, and were kindly provided by John Schwabe.

2.3.1 Passage of HEK-293F cells

HEK-293F cells were cultured in 60ml cultures in 250ml conical tissue culture flasks. Cell density was counted using a glass haemocytometer, once a density of approximately 1.5-2x10^6 cells/ml was reached, cells were split to $0.35x10^6$ cells/ml and made up to a final volume of 60ml using standard HEK-293F culture media. Cells were cultured in a humidified shaking incubator at 37°C, 5% CO_2 at 120 rpm.

2.3.2 Media used for the culture of HEK-293F cells

Standard HEK-293F culture medium

FreeStyle™ HEK-293F Expression Medium (Gibco, 12338-018) 1L

2.4 Plasmid transfection

2.4.1 Lipofectamine2000 transfection

Transfection of ES cells and HEK-293T cells with plasmids was carried out on various plate sizes using Lipofectamine 2000 (Invitrogen, 11668-019). The day prior to transfection, cells were seeded according to plate size as outlined in Table 2-1. 24 hours after seeding, Lipofectamine2000 was added at a 1:2/1:3 ratio of DNA:Lipofectamine2000 to Opti-MEM® Reduced Serum Medium (Thermo Fisher, 31985062), this was incubated at room temperature for 5 minutes. Meanwhile DNA was added to Opti-MEM® Reduced Serum Medium depending on plate size (Table 2-1) and incubated at room temperature. After 5 minutes, the diluted DNA and lipofectamine2000 were combined and incubated for 20 minutes after gently mixing. Following incubation, the mixture was added to the culture media dropwise and the plate was gently swirled to allow maximum coverage of cells.

Plate size	Number of cells seeded	Amount of Opti-MEM® Reduced Serum Medium	Amount of DNA added	Amount of Lipofectamine2000 added
10cm	3x10^6	2x 500µl	10µg	20µl
6cm	5x10^5	2x 300µl	4µg	12µl
6 well	2.5x10^5	2x 250µl	3µg	9µl
48 well	5x10^4	2x 25µl	0.5µg	1µl

Table 2-1. Transfection conditions for Lipofectamine2000

2.4.2 Polyethylenimine (PEI) transfection

HEK-293F cells were transfected with PEI in the following way for a 30ml culture. 30μg of DNA was added to a 15ml falcon tube and diluted in 3ml of PBS. 120ul of PEI (0.5mg/ml, pH7.5) was added to the DNA:PBS and lightly vortexed before incubation at room temperature for 20 minutes. During the incubation period HEK-293F cells were counted using a haemocytometer and cells were seeded at 1x10^6/ml, the 3ml transfection reagent was added and the culture was made up to 30ml with fresh FreeStyle™ HEK-293F Expression Medium before being incubated for 48 hours in a humidified shaking incubator at 37°C, 5% CO_2 at 120 rpm.

2.5 Protein and Enzyme analysis

2.5.1 Protein extraction from ES cells and HEK-293T cells

24 hours after transgene transfection, media was removed from the plate and cells were washed in PBS. 1ml of PBS was then added directly to the cells to allow removal via a plastic cell scraper (Fisher Scientific, 08-100-240). The cell suspension was transferred to a 1.5ml eppendorf and spun for 3 minutes at 200xg. Cells were re-suspended in 2-3X packed cell volume of cell lysis buffer or HDAC assay lysis buffer depending on downstream applications. The lysates were incubated at 4°C with rotation for 30 minutes, and centrifuged at 14000xg at 4°C for 20 minutes. The supernatant was transferred to a new eppendorf. Protein concentration was determined using a Bradford assay as follows. 1ml of 1X Bradford reagent (diluted ¼ from stock) (BioRad 500-0006) was used per sample to obtain an absorbance at λ595. The absorbance of the standards 0μg/ul, 1.25μg/ul, 2.5μg/ul, 5μg/ul, 10μg/ul with BSA diluted in lysis buffer was used to generate a standard curve from which protein concentration of samples were interpolated.

Cell Lysis Buffer:

- 50mM Tris HCl pH 8.0
- 250mM NaCl
- 0.5% Igepal
- 0.5% Triton-X
- Protease Inhibitor Cocktail (Sigma, p8340-1ml)

HDAC Assay Lysis Buffer:

- 50mM NaCl
- 50mM Tris HCl pH7.5
- 0.3% Triton-X
- 5% Glycerol
- Protease inhibitor tablet EDTA Free (Roche, 05 892791001)

2.5.2 Protein extraction from HEK-293F cells

48 hours post transfection cells were harvested into a 50ml falcon tube and centrifuged for 10 minutes at 2755xg. The pellet was resuspended in 1ml of 293F cell lysis buffer and pipetted up and down 10-12 times. The cell suspension was sonicated for 10 seconds on 10 seconds off for 3 cycles and spun at 25,000xg at 4^{o}C for 20 minutes. The supernatant was used in a flag resin pull down as outlined in 2.5.5.2.

293F Cell Lysis Buffer:

- 100mM KAc
- 50mM Tris pH 7.5
- 5% Glycerol
- 0.3% Triton X
- Protease Inhibitor tablet EDTA Free (Roche, 11873580001)

2.5.3 Histone extraction

Cells were harvested and whole cell extract was made as outlined in 2.5.1 or 2.5.2. Pellets were then resuspended in 2-3X packed cell volume of 0.4N H_2SO_4 and incubated overnight at 4^{o}C with rotation. The following day, samples were spun for 20 minutes at 14,000rpm at 4^{o}C. The supernatant was transferred to a fresh 1.5ml

eppendorf and used to analyse histone acetylation marks by western blotting as outlined in 2.5.4.

2.5.4 Immunoblotting

30μg of protein extract or an equal volume of histone extract were prepared for gel electrophoresis by adding an equal volume of 2x protein loading buffer and boiling at 100^{o}C for 5 minutes. Samples were loaded onto a 4-12% Bis-Tris-PAGE gel (Invitrogen, NP0323) and run at 140V for approximately 1 hour in running buffer. The protein was then transferred to a PVDF membrane (Merk Millipore, Immobilon-FL IP FL00010) by transferring for 1 hour at 30V in a transfer tank filled with transfer buffer.
After transferring, the membrane was blocked for an hour at room temperature in 1:1 odyssey blocking buffer:PBS (Li-CoR, 927-40000) with rotation. The membrane was then probed with a primary antibody in 3ml of odyssey blocking buffer at an appropriate dilution (Table A1 1) for 1 hour at room temperature with rotation. The membrane was then washed 3 times for 10 minutes with rotation in PBST (PBS + 0.1% Tween). Following washing, the membrane was probed with a IRDye conjugated secondary antibody in blocking buffer + 0.1% Tween + 0.01% SDS (Table A1 1) for 1 hour and then washed twice with PBST and once with PBS alone. The membrane was then scanned using the Odyssey Infrared Imaging System (Li-COR Biosciences) and quantitation of relative protein level was performed.

Running Buffer (Invitrogen, NP0002-02):

- 50mM MES (2-(N-morpholino)ethanesulfonic acid)
- 50mM Tris Base
- 0.1% SDS
- 1mM EDTA, pH7.3

Transfer Buffer (Biorad, 161-0771)

- 25mM Tris
- 192mM Glycine pH8.3
- 20% Methanol

2X protein loading buffer

- 240mM Tris HCl pH 6.8
- 6% SDS
- 30% Glycerol
- 16% β-Mercaptoethanol
- 0.0075% bromophenol blue

2.5.5 Immunoprecipitation

Two different types of Immunoprecipitation assays were used to perform different experiments outlined in this thesis and are detailed below.

2.5.5.1 Dynabead Immunoprecipitation

Protein G Dynabead (Thermo Fisher, 10003D) Immunoprecipitations (ImPs) were carried out in ES cells. Protein extract was made from a full 100mm plate as outlined in 2.5.1 using ImP lysis buffer. Whilst the protein extract was incubating 40μl of Protein G Dynabeads were washed three times in 500μl of ImP lysis buffer and incubated with 1μg of antibody with rotation at 4^{o}C for 30 minutes. After incubation, the beads were washed three times in 500μl of ImP lysis buffer. Protein samples were normalised to 5mg/ml and 300μl was added to each ImP and incubated overnight at 4^{o}C with rotation. The following day the beads were washed with 500μl of ImP lysis buffer three times, and resuspended in 100ul of ImP lysis buffer. 20μl of the bead suspension was used in immunoblotting to check the pull down and the remaining 80μl was used in a HDAC assay as outlined in 2.5.6.

ImP Lysis Buffer:

- 250mM NaCl
- 20mM HEPES pH 8.0
- 0.5% Igepal
- 1mM EDTA
- Protease inhibitor tablet (Roche, 05 892791001)

2.5.5.2 Flag resin Immunoprecipitation

Post transfection of HEK-293Fs protein extract was made as outlined in 2.5.2 and quantified using a standard Bradford assay, at this point some of the lysate was set aside for a whole cell extract HDAC assay (described in 2.5.6). The remainder of the protein was added to 40µl of Anti-Flag M2 affinity resin (Sigma, A220) washed 3 times with 1ml of 293F Cell Lysis Buffer and spun for 1 minute at 6000xg. The protein-resin mix was incubated with rotation at 4^{o}C for 30 minutes, before being washed 3 times in 1ml of 293F Cell Lysis Buffer and spinning for 2 minutes at 6000xg at 4^{o}C. The beads were then washed twice in 1ml of Cleavage Buffer with centrifugation at 4^{0}C for 2 minutes at 6000xg. An equal volume of cleavage buffer was added to the resin and 15µl of the mix was removed as a control. The remainder of the resin was incubated overnight at 4^{o}C with 1µl of 0.1mg/ml TEV protease (Tobacco Etch Virus nuclear-inclusion-a endopeptidase).

Following overnight incubation, the TEV treated resin samples were spun at 6000xg, 4^{o}C for 2 minutes. The supernatant was collected and used for a coomassie blue gel and a HDAC assay as outlined in 2.5.6. 15µl of TEV treated resin was collected in the same way as the pre-TEV treated beads to act as a control for cleavage.
The coomassie blue gel was run by loading 10µl pre-TEV treated resin, TEV treated resin and the supernatant on a 4-12% Bis-Tris-PAGE gel and running at 125mA for 35minutes. The gels were then stained with Instant Blue (Expedeon, ISBIL) for an hour and pull down was analysed by densitometry using ImageJ (version 1.49v).

Cleavage Buffer:

- 50mM Tris HCl pH 7.5
- 50mM KAc
- 5% Glycerol
- 0.5mM TCEP

2.5.6 Histone deacetylase assay

The activity of histone deacetylases was analysed via a BOC-(Ac)Lys-AMC based assay. This relies on HDACs to remove the Acetyl group from the Lysine residue allowing the fluorescent AMC molecule to be cleaved off by the addition of trypsin. The AMC can then be detected with an excitation wavelength of 353nm and emission wavelength of 448nm in a plate reader.

The amount of sample used in the assay depended on the upstream application, 30μg of protein from whole cell extract (2.5.1 and 2.5.2) , or 20μl of resuspended Dynabeads (2.5.5.1) or 1μl of flag resin supernatant or 5μl of a 1 in 5 dilution of the supernatant depending on amount of protein pulled down (2.5.5.2). The protein sample was made up to a total of 40μl with deacetylase buffer and 10μl of 50μM BOC-(Ac)Lys-AMC (Sigma, SCP0168) was added, this was then incubated at 37^{o}C for 30 minutes with gently shaking in the dark. The reaction was stopped by addition of 50μl of developing solution, incubated for 10 minutes at room temperature and analysed using a plate reader (Perkins Elmer 2030 Victor^{TM} X5).

Deacetylase buffer:

- 50mM Tris HCl pH 7.5
- 50mM NaCl

Developing solution

- 2μM Trichostatin A (TSA) (Sigma, T8525)
- 10μg/μl Trypsin from Porcine Pancreas (Sigma, T0303-1G)
- 50mM Tris pH7.5
- 50mM NaCl

2.6 Plasmid Generation and Preparation

2.6.1 Generation of PiggyBAC TET inducible plasmids

A PiggyBAC TET inducible plasmid was kindly provided by the McGrew lab at The Roslin Institute, University of Edinburgh (Glover et al, 2013). IPMK was cloned into the plasmid by first cleaving 1-2μg of the plasmid with the restriction enzyme HpaI (NEB, R0105S) for three hours at 37°C. The cleaved plasmid was run on a 1% agarose gel at 100 volts for 30 minutes and purified using the QIAquick gel extraction kit (Qiagen, 28704).

At the same time as the digest and purification of the plasmid, IPMK cDNA was PCR amplified with primers designed to add homology arms to the fragment (Table A3 6) using KOD Hot Start DNA Polymerase (Merk Millipore, 71086-3) as described in 2.6.2. After the PCR reaction was complete, the reaction was run on a 1% agarose gel and the band was purified from the gel using Qiagen Gel Extraction kit (Qiagen, 28604).

The purified plasmid and PCR product were then taken forward into an infusion reaction kindly provided by The University of Leicester, Protein Expression Laboratory, PROTEX, run by Dr. Xiaowen Yang. The reaction required 2μl of the PCR fragment and cleaved plasmid combined with 3μl of the infusion reaction. The reaction mix was incubated at 37°C for 20 minutes followed by incubation for a further 20 minutes at 50°C before transformation into α- Select Chemically Competent Bronze Cells (Bioline, BIO-85025) as outlined in 2.6.3.

2.6.2 KOD Hot Start DNA Polymerase

KOD HOT Start DNA Polymerase (Merk Millipore, 71086-3) was used to generate PCR fragments used in cloning due to its high-fidelity and proof-reading capabilities. The reaction mix is shown in Table 2-2. The PCR parameters used for the BioRad T100^{TM} Thermocycler are described in Table 2-3.

Reaction Component	Amount required for a 50µl Reaction
10X KOD Hot Start Buffer	5µl
25mM $MgSO_4$	3µl
2mM dNTPs	5µl
10µM Forward Primer	1.5µl
10µM Reverse Primer	1.5µl
Template DNA	Up to 500ng
KOD Hot Start DNA Polymerase	1µl
Betaine	13µl
DMSO	0.5µl
Water	Up to 50µl

Table 2-2 KOD Hot Start Polymerase Standard Reaction Mixture

Temperature (^{o}C)	Time (Minutes)	
95	2:00	
95	0:10	35 cycles
Primer Tm	0:30	
70	0:45	
75	7:00	
4	Hold	

Table 2-3 KOD Hot Start PCR Thermocycler reaction parameters

2.6.3 Transformation and DNA plasmid preps of alpha- Select Chemically Competent Bronze cells

α- Select Chemically Competent Bronze Cells (Bioline, BIO-85025) were transformed with 1-2μg of DNA or 5μl of a ligation reaction according to the manufacturer's instructions. Once the cells were plated onto LB-AGAR plates with antibiotic (100μg/ml Ampicillin (Sigma) or 15μg/ml Kanamycin (Sigma)) they were incubated at 37°C overnight. The following day colonies were picked and placed in 5ml of LB for mini-preps and 200ml of LB for maxi-preps, both with antibiotics (100μg/ml Ampicillin or 15μg/ml Kanamycin) and were incubated at 37°C with shaking overnight. Cells were then harvested and glycerol stocks (used for subsequent preps) were made with 500μl of culture and 500μl of 50% glycerol and stored at -80°C, the remaining culture was used for mini-preps or maxi-preps. Mini-preps and Maxi-preps were carried out using Qiagen kits according to the manufacturer's instructions (Qiagen, 27106 & Qiagen, 12362).

2.7 Flow Cytometry

2.7.1 GFP expression analysis

For analysis of transfection levels by GFP, HEK-293F cells were harvested by spinning for 10 minutes at 2755xg. All other cells analysed were harvested by trypsinisation as outlined in 2.1.2 and 2.2.2. Cell pellets were washed once in PBS before being resuspended in 500-1000μl of PBS and transferred to FACS analysis tubes (Falcon, 352054). Cells were immediately analysed on the BD FACSCanto® for GFP analysis in the FITC-A channel, cells were gated based on Forward SCatter (FSC) and Side SCatter (SSC).

2.7.2 Analysis of Cell Cycle Phases by Propidium Iodide (PI) staining

For analysis of cell cycle synchronisation ES cells were collected by addition of TrypLE as outlined in 2.1.2. Cells were washed once in PBS before being resuspended in 500-1000μl of -20°C 70% ethanol to fix the cells. Cells were stored in the -20°C until FACS

analysis could be carried out. Upon analysis an equal volume of PBS was added to the cells before spinning for 5 minutes at 200xg. Cells were then washed in 500μl of PBS to remove any excess ethanol. The cell pellet was resuspended in 500μl of Propidium Iodide (PI) stain (500μl PBS, 50μg/ml PI (Invitrogen, P3566), 10μg/ml RNaseA (Sigma, R4642)) and incubated in the dark at room temperature for 30 minutes. FACS analysis was then carried out on the BD FACSCanto® using FSC and SSC to gate cells and analyse PI staining in the PE-A laser channel.

2.8 Reporter assays

2.8.1 Reporter assay transfection

24 hours prior to transfection, HEK-293T cells were plated out onto a 48 well plate with 50,000 cells per well as outlined in 2.2.2. Reporter assay transfections were carried out using Lipofectamine2000 at a 1:2 ratio according to the manufacturer's instructions. The concentrations of each plasmid used in the reporter assay is outlined in Table 2-4. The β-galactosidase construct and the Thymidine Kinase-Luciferase construct were kindly provided by Peter Watson from the Schwabe lab. A full list of all plasmids used in the reporter assay transfections can be found in the appendix (Table A3 7).

Plasmid concentration (μg /well)		
β-galactosidase	Thymidine Kinase-Luciferase	All other plasmids
0.18	0.23	0.1

Table 2-4. Concentrations (μg) of plasmids transfected per well for a reporter assay.

After transfection cells were incubated in the 5% CO_2 incubator at 37°C for 48 hours after which they were harvested. The cells were washed in PBS once and then 140μl of 1X Reporter assay lysis buffer was added per well. The plate was incubated for 2 hours at room temperature on a plate shaker before being placed in the -80^{o}C for a minimum of half an hour before proceeding to downstream analysis.

5X Reporter Assay Lysis Buffer

- 6.25mM Tris HCl pH 7.8
- 0.01M DTT
- 0.01M EDTA
- 50% Glycerol
- 5% Triton-X

2.8.2 β-galactosidase and Luciferase Luminescence assays

Analysis of the reporter assays is a two-step process with analysis of the β-galactosidase taking place first to act as a transfection control between the samples. Then the Luciferase assay is carried out to determine the level of transcriptional repression occurring in each condition.

The cell lysates were removed from the -80^{o}C and thawed on ice, 80μl of lysate was aliquoted into a 96 well clear plate and 100μl of β-galactosidase Substrate (made from β-galactosidase Stock Solution) was added per well. The plate was incubated at 37^{o}C until a yellow colour began to appear in the wells. The absorbance at 420nm was then measured using the Perkins Elmer 2030 Victor^{TM} X5 plate reader. Following the β-galactosidase assay, Luciferase expression was analysed using a Luciferase Reporter Assay Kit (BioVision K801-200) according to the manufacturer's instructions with the Perkins Elmer 2030 Victor^{TM} X5 plate reader.

β-galactosidase Stock Solution

- 0.06M Na_2HPO_4
- 0.01M KCl
- 1mM $MgCl_2$
- 0.04mM NaH_2PO_4

β-galactosidase Substrate

- 10ml β-galactosidase Stock solution
- 20mg ONPG
- 35μl β-Mercaptoethanol

Luciferase assay absorbance values were normalised to the β-galactosidase absorbance values and data was plotted relative to the Thymidine kinase-Luciferase

control sample (see equation below) to determine percentage changes in gene expression.

$$\frac{Lucifase\ absorbance}{\beta\ \text{galactosidase absorbance}} = Normalised\ Luciferase$$

$$Transform\ normalised\ luciferase:$$

$$Y = \frac{Y}{K}$$

$$Y = normalised\ lucifase\ value$$

$$K = Averaged\ Thymidine\ Kinase\ Luciferase\ values$$

$$Transform\ Transformed\ normalised\ luciferase\ values:$$

$$Y = K\ x\ Y$$

$$Y = Transformed\ lucifase\ value$$

$$k = 100\ \%$$

2.9 RNA extraction and quantitative real time-PCR analysis

Prior to RNA extraction and analysis by quantitative real time-PCR analysis (qRT-PCR) all surfaces, centrifuges and pipettes were cleaned with RNaseZap (Sigma, R2020) to remove any trace amount of RNase and prevent any inadvertent digestion of RNA.

2.9.1 RNA extraction from ES cells and EBs

RNA was extracted from ES cells on a 100mm plate by washing cells twice in 1X DPBS and lifting cells of the plate in TrypLE solution. The cells were neutralized in M15+LIF and spun down at 1100rpm for three minutes. RNA was extracted from EB's by harvesting them from a 96 well plate and washing the plate in PBS before spinning at 1100rpm for three minutes. The cell/EB pellet was stored at -80^{o}C or RNA was extracted immediately. To the pellet 500-1000µl of TRI reagent (Zymo Research, R2050-1-200) was added and the Direct-Zol^{TM} RNA MiniPrep Kit (Zymo Research,

R2052) was used to isolate the RNA according to the manufacturer's instructions. After isolation, RNA was quantified using a nanodrop.

2.9.2 cDNA generation

A reverse transcriptase reaction was carried out to generate complementary DNA (cDNA) using q-script (Quanta, 84034). cDNA was made using 500ng of RNA, 4μl q-script and made up to a 20μl reaction with water, the reaction was incubated in a PCR thermocyler (BioRad, T100^{TM} Thermocycler) as outlined below in Table 2-5. After incubation cDNA was diluted 1:5 with RNase/DNase free water and quantified.

Temperature (^{o}C)	Time (Minutes)
25	5:00
42	30:00
85	5:00
12	Hold

Table 2-5 Parameters used for cDNA generation in BioRad PCR thermocycler.

2.9.3 qRT-PCR analysis of cDNA

cDNA was analysed by qRT-PCR using a BioRad CFX Connect™ Real-Time PCR Detection System. Samples were analysed using SensiFAST™ SYBR as outlined in Table 2-6 and the parameters used were outlined in Table 2-7. Primers used for each gene (Table A2 1) were used from the Harvard primer bank (Wang et al, 2012).

Reagent	Volume
SensiFAST™ SYBR	5μl
20μM Forward/Reverse primer mix	0.5μl
cDNA	2μl
H_2O	2.5μl

Table 2-6. Reaction mix used for qRT-PCR

Temperature (°C)	Time (Minutes)	
95	15:00	
95	0:10	40 cycles
50-60	0:30	
72	1 minute + plate read	
Melt curve 65 →95 in 1°C increments	Plate read every 0.05 seconds	

Table 2-7. Parameters used for qRT-PCR run on BioRad CFX Connect™ Real-Time PCR Detection System

qRT-PCR data was analysed by normalising the threshold cycle (Ct) value against the reference gene B-actin Ct value, these normalised values are termed ΔCt values. The ΔCt values were used to generate the ΔΔCt values by comparing the sample to a calibrator sample, such as a control sample. The change in gene expression was calculated using the following equation:

$$Change\ in\ gene\ expression = 2^{-\Delta\Delta Ct} = Relative\ Quantity\ (RQ)$$

2.10 Measurement of Inositol Phosphate levels

2.10.1 Inositol phosphate extraction

Inositol phosphates were isolated from cells using the method outlined in (Barker et al, 2010). Adherent cells were washed once in PBS and then 1ml of Ice cold 5% Trichloroacetic acid (TCA) was added to the plate. The plate was incubated on ice for 20 minutes, after which cells were scrapped off. The plate was washed in 0.5ml of 5% TCA to ensure maximum recovery of cells. Suspension cells were pelleted and 1ml of ice cold 5% Trichloroacetic was added and the cells were incubated for 20 minutes on ice. After incubation, all samples were centrifuged at 6000xg for 10 minutes at 4°C. The supernatant was transferred to a 15ml tube and the sample was washed 4x with 1ml of water saturated diethylether. 50µl of 0.1M EDTA pH 7.4 was added to the sample brought to neutrality using trimethylamine. The samples were freeze dried

overnight and sent to Dr Andrew Bottrill in the Protein and Nucleic Acid Chemistry Laboratory (PNACL) for analysis by HPLC-mass spectrometry the following day.

2.10.2 Analysis of Inositol Phosphates by Anion Exchange Chromatography/ Tandem Mass Spectrometry

Inositol phosphates were identified at PNACL using anion exchange chromatography with tandem mass spectrometry as described in (Liu et al, 2009) using an Agilent 1100 HPLC system (Agilent, Santa Clara, CA) and a 4000 Q-Trap mass spectrometer (Sciex, Framingham, MA). Following isolation of IPs as described in 2.10.1 the freeze-dried sample was re-suspended in 110µl of 5% methanol (Solvent A). 55µl of this solution was then transferred to an HPLC vial and 50µl was injected into a 150 x 1mm BioBasic anion exchange column (ThermoFisher Scientific, Waltham, MA) maintained in a column heater at 25^{o}C. The IPs were eluted at a flow rate of 0.1mL/min using a gradient (%B) of 200mM ammonium bicarbonate (Solvent B) thus changing the ionic strength as shown in Table 2-8.

Phase of separation	Time (minutes)	% Solvent A	% Solvent B
Sample Loading	0	100	0
	3	100	0
Sample Separation	8	55	45
	28	25	75
Sample Elution	29	10	90
	32	10	90
Column Wash & Equilibration	33	100	0
	50	100	0

Table 2-8 Conditions used for separation by HPLC. *This table shows the phase of separation in the HPLC and the time at which the solvent gradient was altered with 200mM ammonium bicarbonate to elute the inositol phosphates from the anion exchange column.*

Following HPLC separation the output was directly sprayed into the TurboV electrospray ion source of the 4000 Q-Trap mass spectrometer. The ion spray voltage was -4200V, temperature (TEM) 300 °C and declustering potential -30V. The 4000 Q-Trap was used as a triple quadrupole to collect selected reaction monitoring (SRM) data with both Q1 and Q3 tuned for unit resolution as shown in Table 2-9. Data recorded from the 4000 Q-Trap was analysed by Andrew Bottrill at PNACL by integrating the area under the peak using Skyline (64-bit) 3.6.0.10493 (MacLean et al, 2010).

Inositol Phosphate detected	Q1 Precursor size	Q3 Product size	Detection Time (msec)	Collision Energy applied in Q2 (V)
Inositol Phosphate 3	419.0	321.0	100	-20
	419.0	223.0	100	-20
Inositol Phosphate 4	499.0	401.0	100	-30
	499.0	321.0	100	-30
Inositol Phosphate 5	579.0	481.0	100	-35
	579.0	401.0	100	-35
Inositol Phosphate 6	659.0	579.0	100	-40
	659.0	561.0	100	-40

Table 2-9 Selected Reaction Monitoring transitions used. *This table outlines the SRM transitions used for each inositol phosphate species, were Q1 indicates the size of analyte ion isolated in Quadrupole 1, Q3 denotes the size of analyte ion isolated and measured in Quadrupole 3 following collision energy being applied in Q2 (Quadrupole 2). Detection time denotes the time between each iterative detection of each fragment pair.*

Chapter 3 Investigating the effect of SopB, PTEN and IPMK on HDAC activity

3.1 Chapter aims

In this chapter, I aimed to establish a link between IP levels and the deacetylase activity of class 1 HDAC complexes *in vivo*. Inositol-1,4,5,6-tetrakisphosphate (Ins(1,4,5,6)P_4) was first co-purified in complex with the deacetylate activation domain (DAD) of SMRT and HDAC3 and was later shown to activate the complex *in vitro* (Millard et al, 2013; Watson et al, 2012; Watson et al, 2016). Bioinformatic studies indicated that residues important for the interaction between Ins(1,4,5,6)P_4 and class I HDAC complexes are conserved, suggesting Ins(1,4,5,6)P_4 is a conserved activator. Indeed, the structure of MTA1 bound to HDAC1 revealed an inositol phosphate binding pocket and exogenous addition of Ins(1,4,5,6)P_4 to MTA1/HDAC1 and HDAC1/MIDEAS/DNTTP1 robustly activates the complexes (Itoh et al, 2015; Millard et al, 2013).

To corroborate the role of Ins(1,4,5,6)P_4 as a regulator of HDAC activity *in vivo*, a method was required to alter the levels of IP. This was done by overexpressing the phosphatases SopB, PTEN and the kinase IPMK (see section 1.9.2), and measuring the effect on HDAC activity in HEK-293 cells. These enzymes are all involved in the regulation of IP as outlined in Figure 1-13. Recent research by (Watson et al, 2016) suggest that several isoforms of IP can activate the SMRT/HDAC3 complex providing there are three contiguous phosphates. Consequently, due to the action of SopB, PTEN and IPMK, their manipulation should alter the quantities and ratios of IP_4, IP_5 and IP_6 present, and potentially HDAC activity. As HDAC1 and HDAC2 represent approximately 50% of the total HDAC activity in mammalian ES cells (Jamaladdin et al, 2014). I expected to observe an alteration in HDAC activity and subsequently establish a link with IP and HDAC activity *in vivo*.

It is important to note that when the experiments outlined in this chapter were carried out, our laboratory did not have a method to measure inositol phosphate levels in cells. As a result, the data presented below, was interpreted and new experiments planned based on experimental data previously published on the effect of these enzymes. Since these experiments have been carried out we have developed a method to measure inositol phosphates from cells which is described at the end of this chapter.

3.2 Overexpression of SopB, PTEN and IPMK alone does not affect global HDAC activity in HEK-293F cells

Inositol phosphates have been shown to regulate HDAC activity *in vitro*, however, *in vivo* evidence is relatively limited. To understand the contribution of IPs in the regulation of global HDAC activity in cells, we examined the effect of addition of exogenous SopB, PTEN and IPMK in HEK-293F cells. We hypothesised that HDAC activity should decrease with transfection of SopB due to its ability to decrease the level of IPs in cells over time (Feng et al, 2001). The effect of PTEN is more complex due to its potential ability to de-phosphorylate both IP_5 and IP_4 therefore, an increase or decrease in HDAC activity might be expected due to the ability of IP_5 to activate HDAC3/SMRT *in vitro* (Caffrey et al, 2001; Maehama & Dixon, 1998; Watson et al, 2016). It was theorized that overexpression of IPMK would increase HDAC activity through its ability to generate IPs as outlined in Figure 1-13. This is further supported by overexpression of rat IPMK in rat-1 cells resulting in an increase in IP_5 (Fujii & York, 2005). Protein expression and transfection rate was analysed 48 hours post transfection of SopB, PTEN and IPMK using western blotting and FACS analysis respectively (Figure 3-1a+b). SopB exhibited a lower transfection rate potentially due to its relative toxicity to cells as an environmental pathogen, through its action to modulate endoplasmic reticulum to golgi transport, modulation of endosome to lysosome trafficking and causing wide spread actin rearrangements in host cells (Bakowski et al, 2010; Dukes et al, 2006; Perrett & Zhou, 2013). The transfection rate

of IPMK could not be assayed due to a lack of GFP tagged protein, however, it is clearly expressed at a detectable level in the cells (Figure 3-1a). Following conformation of expression, HDAC activity was analysed using a standard HDAC assay, no significant change in global HDAC activity was observed (Figure 3-1c). The result suggests that manipulation of inositol phosphate levels (based on previously published data, see section 1.9.2) does not alter the activity of HDACs at a global level. However, the transfection rate of SopB, PTEN and IPMK was not 100%, accordingly, IP levels may remain sufficiently high enough to maintain HDAC activity at the control level. A further explanation for the lack of change in global HDAC activity is that the changes occur at the level of the complex e.g. SMRT/HDAC3. Accordingly, these changes might be masked by compensatory effects of other HDAC complexes believed not to be regulated by IPs such as Sin3A which lacks an identifiable ELM2-SANT domain (Millard et al, 2013).

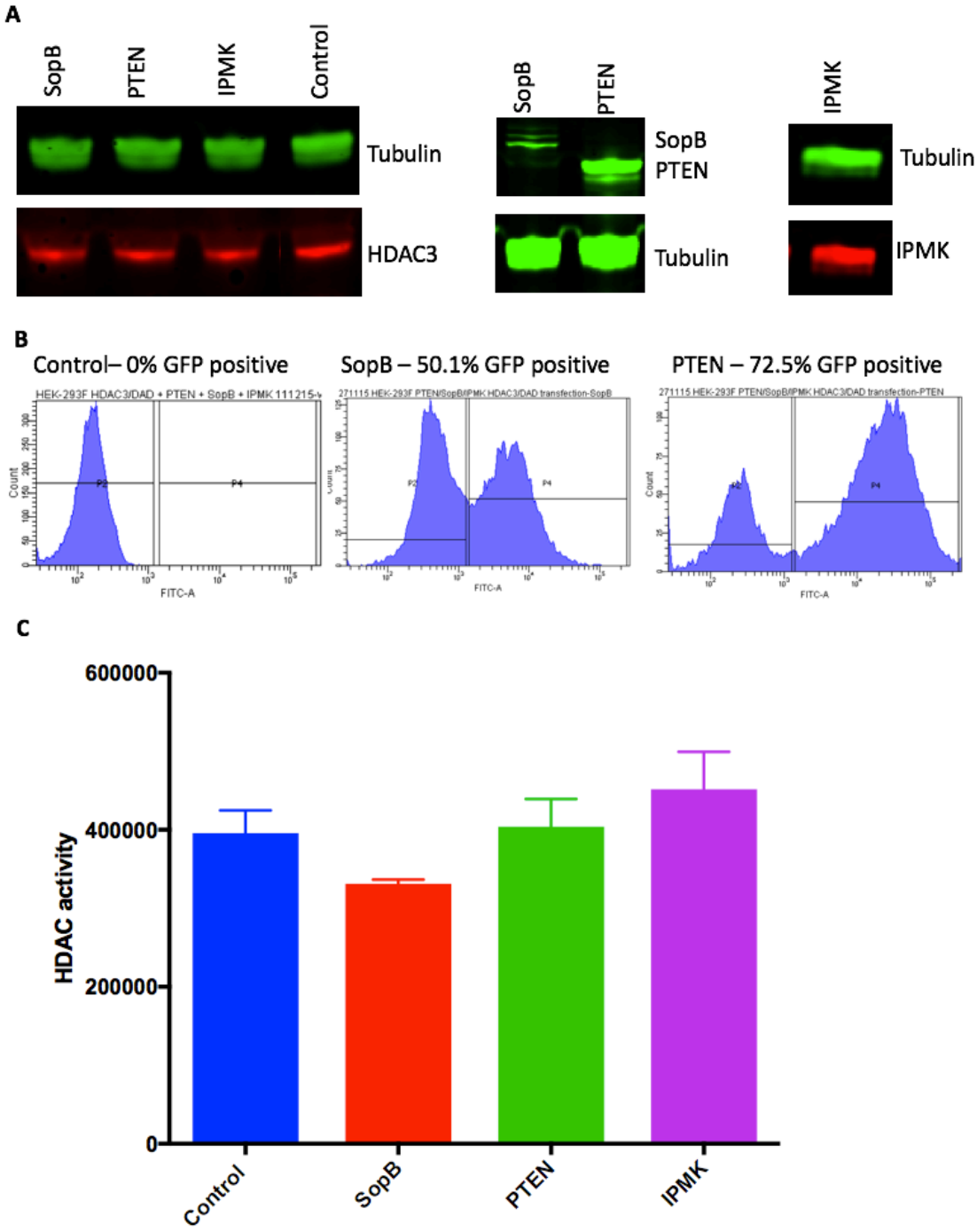

Figure 3-1 SopB, PTEN and IPMK expression have no effect on global HDAC activity
SopB, PTEN and IPMK expressing plasmids were transfected into HEK-293F cells, 48 hours following transfection whole cell extract was harvested to determine deacetyalse activity. Prior to whole cell extract, some cells <10% were isolated for FACS analysis of GFP-tagged proteins SopB and PTEN. ***(A)*** *Western blots of whole cell extract were carried out to determine expression of SopB, PTEN and IPMK as well as HDAC3. Tubulin was used as a loading control and used to normalise the HDAC assay.* ***(B)*** *Fluorescently activated cell sorting data in the FITC-A channel shown for control cells and IRES GFP SopB and PTEN transfected cells to determine the level of transfection of SopB and PTEN.* ***(C)*** *Deacetylase activity was assayed using whole cell extract and a standard deacetylase activity assay (see methods) Mean deacetylase activity where n=3 ±SD shown.*

3.3 Changes in HDAC activity become apparent upon overexpression of SMRT/HDAC3 in parallel with SopB, PTEN or IPMK.

Since global HDAC activity was not affected by addition of exogenous SopB, PTEN or IPMK we next looked at the effect of overexpressing these enzymes in conjunction with SMRT/HDAC3. The SMRT/HDAC3 complex was chosen as it is reported to be more sensitive to addition of IPs in HDAC assays than MTA1/HDAC1 (Watson et al, 2016). The original structure was solved using the DAD domain of SMRT consisting of residues 389-450, however, this can only form a complex with HDAC3 in the presence of Ins(1,4,5,6)P_4. As a result throughout this thesis an extended DAD domain of SMRT (called Xt-DAD) comprising of residues 350-480 was utilised as this construct is able to mediate interaction with HDAC3 in the absence of Ins(1,4,5,6)P_4 (Millard et al, 2013).

Xt-DAD SMRT (here on out termed SMRT) and full length HDAC3 were overexpressed in conjunction with the inositol phosphate perturbing enzymes (SopB, PTEN and IPMK) in HEK-293F cells. 48 hours post transfection expression was analysed by FACS analysis and western blotting (Figure 3-2b + c). Enhanced expression of HDAC3 was observed (48 fold) compared to the wild type cells (Figure 3-2b). FACS analysis indicated transfection and expression of both SopB and PTEN, although SopB was expressing at a lower rate than in previous experiments (Figure 3-2c). An HDAC assay of the lysate revealed a significant reduction in HDAC activity upon expression with either SopB (p-value = 0.0196) or PTEN (p-value = 0.0388) (Figure 3-2a). This suggests that IP may become limiting upon overexpression of HDAC3. Surprisingly, IPMK doesn't have an effect on global HDAC activity, despite good levels of protein expression (Figure 3-2c). Nonetheless, this is not confirmation of altered IP levels. Although overexpression of IPMK has been reported to increase IP_5 levels in rat cells, and some isoforms of IP_5 have been shown to activate HDAC3/SMRT *in vitro*, we did not know whether we are altering inositol phosphate levels to a high enough degree to detect a change in HDAC activity (Fujii & York, 2005; Watson et al, 2016).

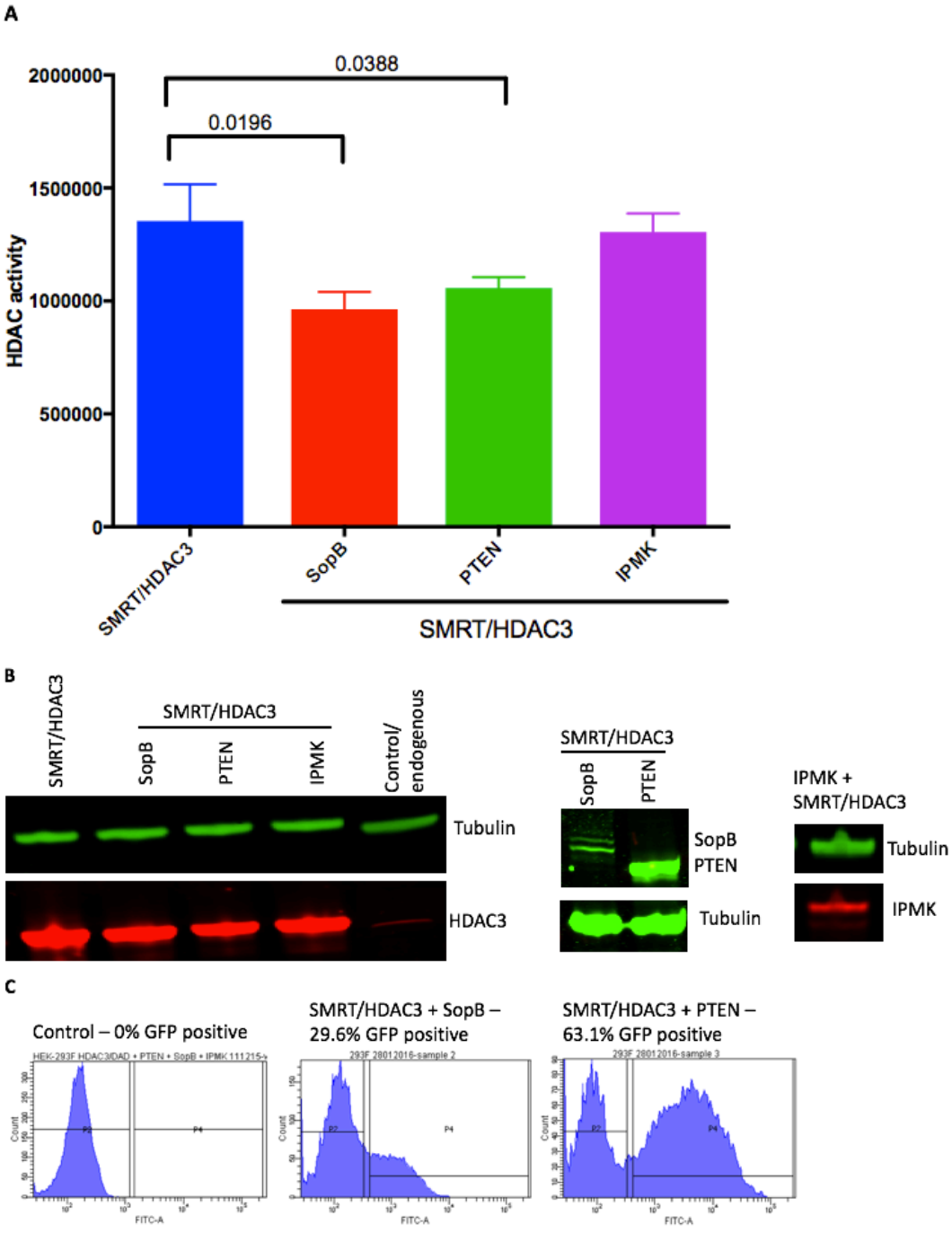

Figure 3-2 Overexpression of SopB and PTEN but not IPMK with SMRT/HDAC3 changes global HDAC activity. ***(A)*** *Deacetylase activity was measured 48hours post transfection. Statistical significance (p-value) was calculated using Two-tailed T-test. Mean Deacetylase activity values are shown where n=3 ±SD* ***(B)*** *Western blots were carried out to check expression of the constructs and tubulin and HDAC3 were assayed to normalise the HDAC assay****. (C)*** *FACS analysis in the FITC-A channel to determine transfection rate of IRES GFP SopB and PTEN containing cells.*

3.3.1 Changes in HDAC activity are not reflected in histone acetylation levels

The changes in HDAC activity prompted us to examine global histone acetylation levels in cells co-expressing SopB, PTEN or IPMK with SMRT/HDAC3. However, quantitative western blotting revealed minimal changes in H3 or H4 acetylation levels (Figure 3-3). Interestingly we observed a slight decrease in H3K56Ac (0.6 fold) and H3K27Ac (0.7 fold) and H4K5Ac (0.6 fold) when SMRT/HDAC3 was overexpressed alone, rationalised by its enhanced expression compared to the wildtype cells (Figure 3-2b). Simultaneous expression of SMRT/HDAC3 and IPMK results in a slight decrease (0.5 fold) in H3K56Ac similar to that of the SMRT/HDAC3 alone sample. Class I and Class II HDACs have previously been implicated in the deacetylation of H3K56Ac thus explaining why we see a change (0.6 fold) upon overexpression of SMRT/HDAC3 (Das et al, 2009a; Vempati et al, 2010). Moreover, significant alterations in H3K56Ac levels are known to occur in HDAC1 and HDAC1/HDAC2 knockout cell lines with a fold change of 1.6 and 4 respectively (Dovey et al, 2010b; Jamaladdin et al, 2014).

The other histone mark which appears to show a minor change is H3K27Ac (0.7 fold decrease upon overexpression of HDAC3/SMRT), this mark is associated with the region surrounding the transcriptional start site and enhancer regions of active genes (Creyghton et al, 2010; Wang et al, 2008). There is evidence for local increase of H3K27Ac upon deletion of HDAC3 in embryonic stem cells at retinoic acid target genes suggesting that we are potentially seeing a more global effect (Urvalek & Gudas, 2014). H4K5Ac also appears to show a slight decrease upon HDAC3/SMRT overexpression. This mark is involved in epigenetic memory of transcription activation post mitosis (Zhao et al, 2011). H4K5Ac has been shown to be perturbed when SMRT or NCoR are impaired by siRNA targeting, implying it is a target of HDAC3 deacetylation (Bhaskara et al, 2010).

Overall, simultaneous expression with either SopB, PTEN or IPMK appears to result in little to no change in histone acetylation levels relative to the wildtype sample. Since

we only see limited changes in HDAC activity at a global level (Figure 3-1a) this is perhaps unsurprising. In addition, multiple studies suggest knockdown or knockout of various HDACs including HDAC1/2 and HDAC3 do not result in widespread global histone acetylation changes; rather it yields local changes (Bradner et al, 2010; Montgomery et al, 2008; Oehme et al, 2009). This would therefore go some way to explain why we do not see a reduction when IP manipulating enzymes are co-expressed with SMRT/HDAC3.

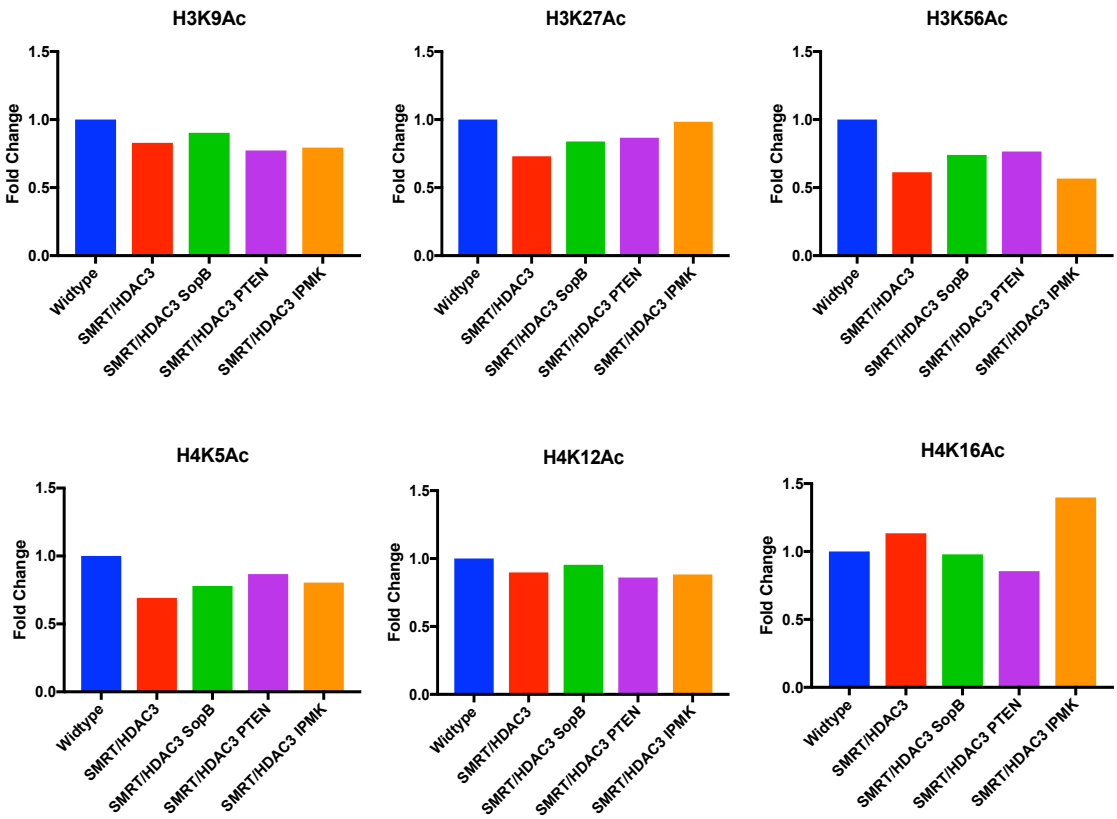

Figure 3-3 Effect of inositol phosphate manipulation of histone acetylation levels
Quantitative western blotting was used to determine the level of global H3 and H4 acetylation levels. Histones were extracted from wildtype cells and those transfected with SMRT/HDAC3 ± SopB, PTEN or IPMK 48 hours post transfection. Acetylation levels were normalised to the total amount of H3/H4 quantified using an Odyssey scanner relative to the wildtype control.

3.4 Isolation of a SMRT/HDAC3 complex reveals differences in HDAC3 activity upon co-expression with SopB, PTEN and IPMK

The slight changes observed in global HDAC activity upon overexpression of Xt-DAD SMRT/HDAC3, compelled us to isolate the complex through a flag resin pull down of the flag tagged Xt-DAD SMRT protein. This enabled isolation of HDAC3 and the removal of any confounding effects of other HDAC complexes.

Flag tagged Xt-DAD SMRT (residues 350-480) and full length HDAC3 were co-expressed with SopB, PTEN and IPMK (flag tag removed) in HEK-293F cells for 48 hours. Following transfection (48 hours), a sample of cells were isolated and used to determine the level of transfection efficiency of GFP tagged protein (SopB and PTEN) (Figure 3-4a). The GFP levels revealed relatively low expression levels of SopB (30%) potentially due to its role as a virulence factor in *Salmonella dublinI.* PTEN revealed a transfection rate of 75%, indicating a high level of transfection and suggesting the majority of cells in the sample will have perturbed IP levels. Upon confirmation of transfection, whole cell lysate was extracted from the remaining cells co-expressing Xt-DAD SMRT, HDAC3 and SopB/PTEN or IPMK. Western blots were run to check expression of the proteins prior to flag resin pull down (Figure 3-4b). As can be observed, all conditions were expressing HDAC3 at a high level, similar to the SMRT/HDAC3 alone condition. Furthermore, IPMK, SopB and PTEN were all detectable by western blotting suggesting a good level of transfection.

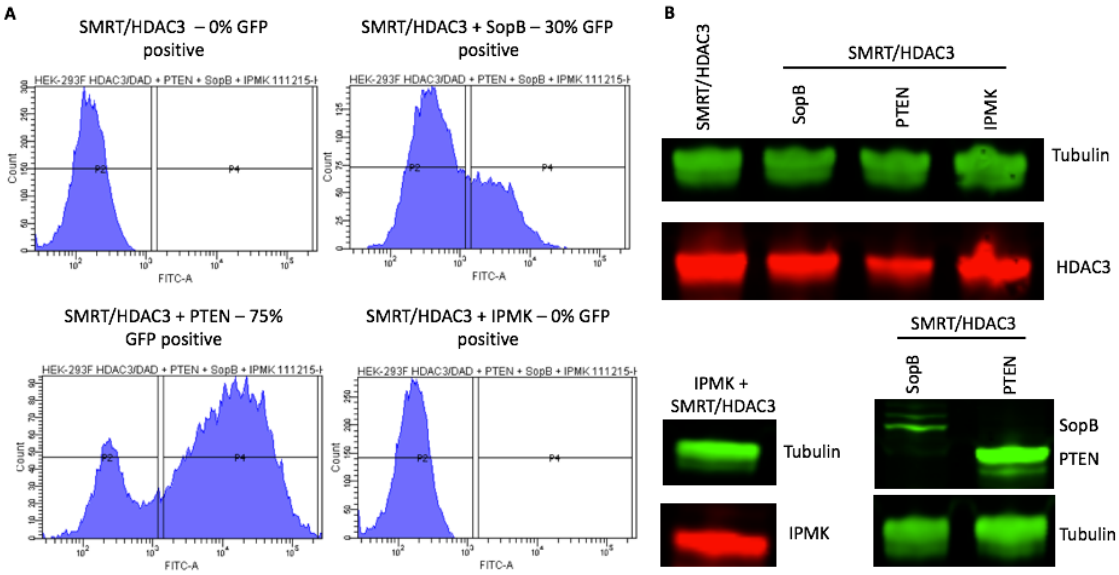

Figure 3-4 Confirmation of transfection in HEK-293F cells *Xt-DAD SMRT and full length HDAC3 were co-expressed with SopB/PTEN or IPMK for 48 hours in HEK-292F cells to determine the effect of these phosphatases and kinases on HDAC3 activity.* ***(A)*** *After 48 hours some cells were isolated for FACS analysis in the FITC-A channel to determine transfection rate of the transfected cells which were expressing GFP tagged proteins (SopB and PTEN)* ***(B)*** *Whole cell extract was also generated 48 hours after transfection to enable western blot analysis to confirm expression of HDAC3 and the inositol phosphate manipulating enzymes, Tubulin was used as a loading control.*

Meanwhile the remaining whole cell lysate was immediately incubated with flag resin beads for half an hour, Tobacco Etch Virus protease (TEV) was added to the beads overnight and supernatant was isolated the following day. A coomassie blue gel was run to check pull-down of both the Xt-DAD SMRT and HDAC3 (Figure 3-5a). The purified complex was then used in an HDAC assay to determine any differences between samples (Figure 3-5b). The HDAC assay was then normalised to the amount of HDAC3 in each sample relative to the SMRT/HDAC3, calculated by densitometry analysis of the coomassie blue gel (Figure 3-5a).

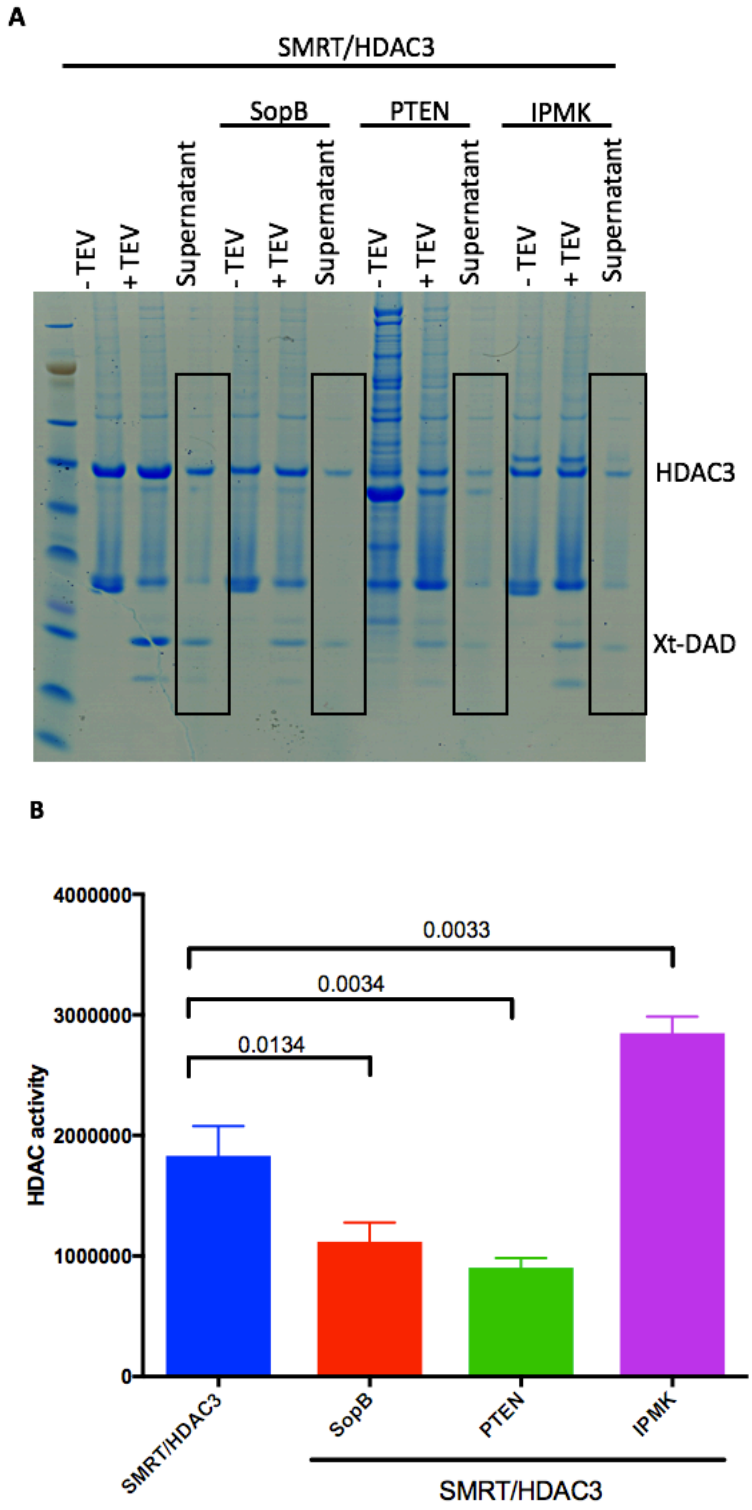

Figure 3-5 Isolation of Flag tagged SMRT/HDAC3 complex reveals differences in HDAC3 activity with expression of SopB/PTEN/IPMK. *Xt-DAD SMRT and full length HDAC3 were co-transfected with SopB/PTEN or IPMK for 48 hours in HEK-292F cells to measure HDAC activity in relation to perturbed IP levels* ***(A)*** *Flag tagged Xt-DAD domain of the SMRT/HDAC3 complex was isolated using whole cell extract passed through a flag resin and the purified complex (shown in black boxes)* ***(B)*** *Deacetylase activity was analysed using the isolated complex flag. Activity levels were normalised to the HDAC3 band on the coomassie blue gel. P values were generated using Two-tailed T test where n=3 ±SD.*

Previously in the global HDAC assay we saw a decrease in activity with SopB (p-value = 0.0196) and PTEN (p-value = 0.0388), but no change in IPMK (Figure 3-3a). Upon isolation of the SMRT/HDAC3 complex we also observed a decrease in HDAC activity in cells transfected with SopB (p-value = 0.0134) (Figure 3-5b); further indicating that a reduction of inositol phosphate levels reduces SMRT/HDAC3 activity (Feng et al, 2001; Norris et al, 1998). PTEN has a more significant p-value of 0.0034 (Figure 3-5b), suggesting that the effect of PTEN on the global HDAC assay was perhaps due to its influence on HDAC3 activity. Interestingly, isolation of HDAC3 enables us to see an increase in SMRT/HDAC3 activity upon co-expression with IPMK (p-value = 0.0033) (Figure 3-5a). This suggested that the increased HDAC3 activity observed is due to an increase in IP, potentially IP_4 or IP_5 as has previously been witnessed (Fujii & York, 2005).

3.4.1 Effects of manipulating inositol phosphates are altered by catalytically dead enzymes

As previously stated, although we know these enzymes are expressed in cells, at this stage we had no way of determining whether the levels of IP were being altered. Consequently, a literature search was carried out to identify catalytically inactivating mutations in SopB, PTEN and IPMK. The aim of this was to reverse the effects seen by the enzymes and therefore go some way to confirming that we were affecting IP levels. The IP phosphatases, SopB and PTEN both contain the consensus sequence Cysteine-$(X)_5$-Arginine where X denotes any amino acid. Mutation of the critical cysteine residue in SopB (C460) and PTEN (C124) to alanine renders the enzymes catalytically inactive (Caffrey et al, 2001; Communi & Erneux, 1996; Weng et al, 2001). IPMK also contains a consensus sequence in its catalytic core (proline(P)-xxx-aspartate(D)-x-lysine(K)-x-glycine(G)) (Shears et al 2004). Mutation of the key aspartate residue in human IPMK (D144) to alanine renders the enzyme inactive due to an inability to position ATP (Gonzalez et al, 2004; Nalaskowski et al, 2002).

Flag-tagged Xt-DAD SMRT and HDAC3 were co-expressed with SopB, SopB C460A, PTEN, PTEN C124A, IPMK (flag tag removed) or IPMK D144A in HEK-293F cells. 48 hours post transfection cells were harvested and transfection efficiency was analysed by FACS (Figure 3-6a). Whole cell extract was made to confirm expression of the mutant proteins via western blotting, no change in expression between wildtype or mutant versions of all IP manipulating proteins was observed (Figure 3-6b).

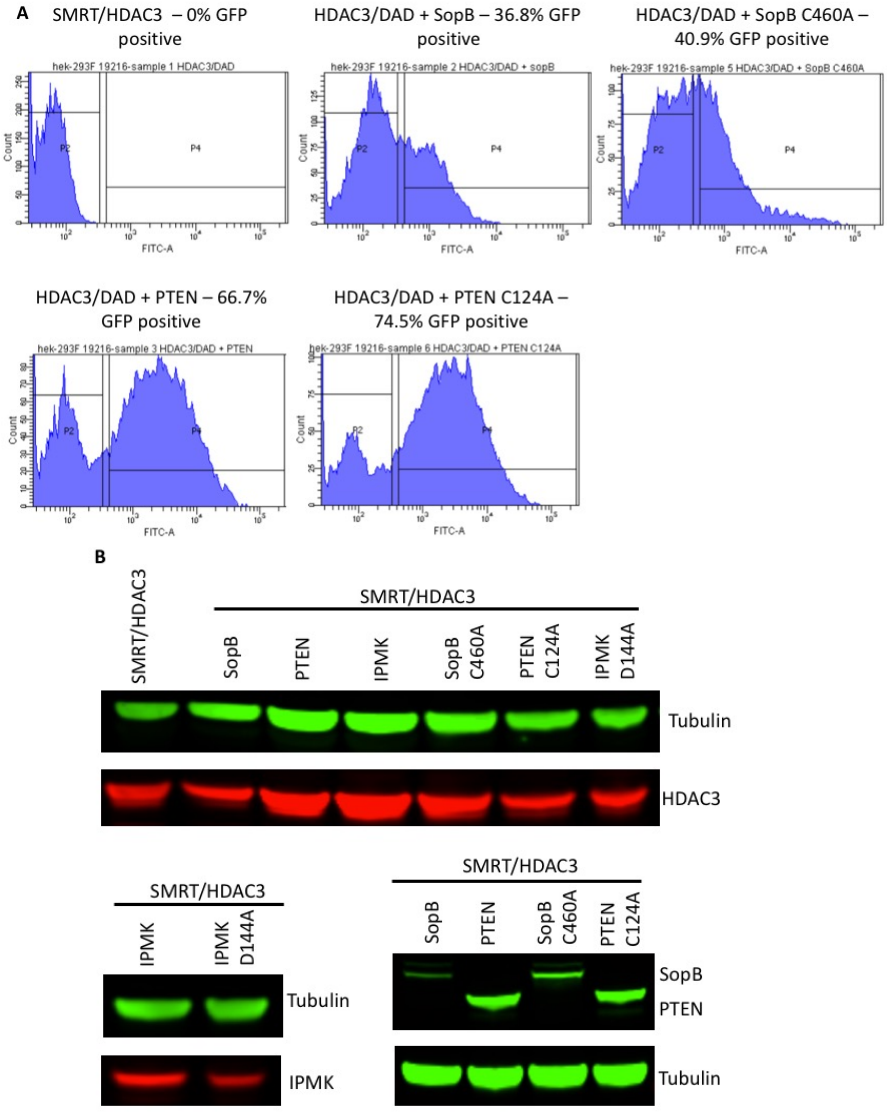

Figure 3-6 FACS analysis and western blotting of SopB, PTEN, IPMK wildtype and mutant protein expression *Xt-DAD SMRT and full length HDAC3 were co-transfected with wildtype or catalytically dead SopB/PTEN or IPMK for 48 hours in HEK-292F cells to deterimine if changes in HDAC activity are related to catalytic activity.* ***(A)*** *48 hours post transfection, cells were analysed for GFP tagged protein expression (SopB and PTEN proteins) to determine transfection levels.* ***(B)*** *Whole cell extract was generated from remaining transfected cells to determine expression of all proteins. Mutation of key catalytic residues appears to have minimal impact on protein expression.*

Isolation of the HDAC3/SMRT complex and analysis of HDAC activity revealed a reduction in complex activity from cells expressing SopB and SMRT/HDAC3 (p-value = 0.0273) (Figure 3-7b). This decrease in activity is not observed upon expression of the SopB C460A mutant, indicating that the phosphatase activity of SopB is responsible for the decrease in HDAC activity. Interestingly, wildtype (WT) PTEN produces a small reduction in HDAC activity (although p-value=0.1571), while the C124A mutant decreases HDAC activity even further (p-value=0.0394) (Figure 3-7b). This is surprising and suggests that the mutant had some residual activity remaining, or that the phosphatase activity was not responsible for the change. Overexpression of IPMK failed to increase HDAC activity, yet the mutant significantly decreased complex activity compared to both the SMRT/HDAC3 and IPMK/SMRT/HDAC3 samples (p-value=0.0306 and 0.0007 respectively). This was unanticipated as a catalytically inactive IPMK should have no effect on the levels of inositol phosphates if endogenous IPMK is still present. One possible reason for this reduction is that the D144 residue is involved in ATP binding, not inositol phosphate binding (Gonzalez et al, 2004). Therefore, it is possible that IP_3 is binding to the IPMK D144A mutant but not being released by the enzyme due to a lack of phosphorylation; leading to the mutant acting like a 'sponge' for IP_3 thus causing an overall reduction in inositol phosphate levels.

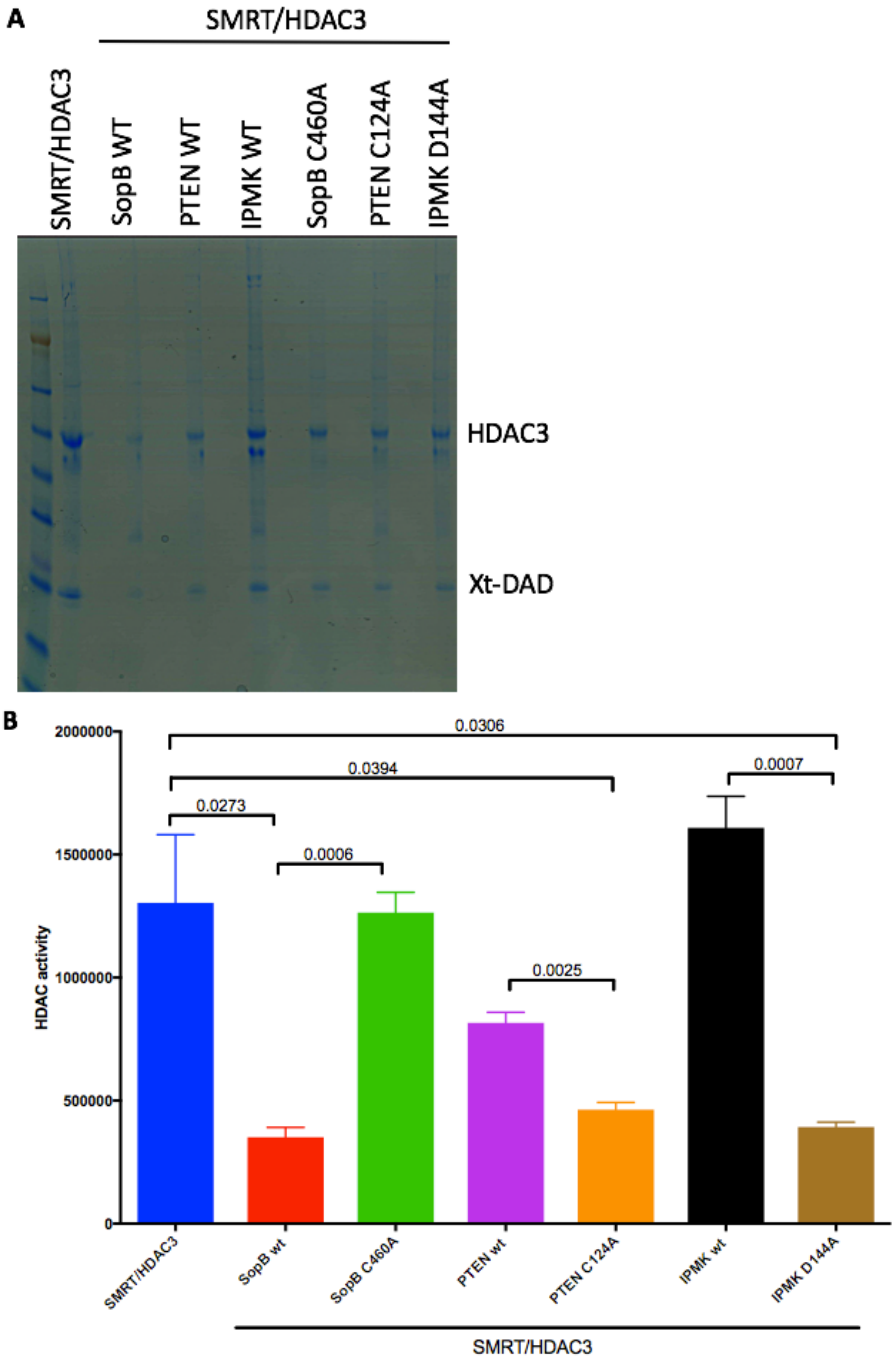

Figure 3-7 Catalytically dead enzymes alter the effect on SMRT/HDAC3 activity in a deacetylase assay. *Xt-DAD SMRT and full length HDAC3 were co-expressed with wildtype or catalytically dead SopB/PTEN or IPMK for 48 hours in HEK-292F cells to determine if changes in HDAC activity are related to catalytic activity.* ***(A)*** *Whole cell extract was isolated from co-transfected cells and passed through a flag resin to isolate the HDAC3 complex. TEV-treatment of the flag resin released the HDAC3 complex from the resin and is shown in the coomassie blue gel.* ***(B)*** *The purified HDAC3 complex was used in a standard deacetylase assay to determine HDAC activity of the purified complex from samples expressing wildtype or catalytically dead IP manipulating proteins. Deacetylase activity was normalized to the HDAC3 band on the coomassie gel by densitometry. Statistical significance was calculated using Two-tailed T test (p-value) where n=3 ±SD.*

3.4.2 Altering the method of normalisation alters the effect observed on HDAC3 activity.

In general, it was observed that samples containing SopB and occasionally IPMK, isolated less HDAC3 than controls. Concerns about the normalisation technique led us to alter the method to examine whether the results were affected. Subsequently, the coomassie blue gel was run and the ratio of HDAC3 pulled down relative to the SMRT/HDAC3 was calculated and then this normalized amount of protein was added to the HDAC assay (Figure 3-8). The results observed using this new method of normalisation differed from those previously witnessed.

Previously, expression of WT SopB with SMRT/HDAC3 resulted in a decrease in HDAC3 activity (Figure 3-5b). However, using the modified normalisation method, SopB no longer caused an effect (Figure 3-8b). Furthermore, expression of SopB C460A resulted in an increase in HDAC3 activity compared to the SMRT/HDAC3 alone. These results suggest that either SopB is not influencing IP levels, or that it is not affecting the activity of HDAC3. Additionally, PTEN revealed an increase in HDAC3 activity compared to the SMRT/HDAC3 control, (p-value = 0.0136). Mutation of PTEN (C124A) abolished this effect, bringing down complex activity to that of the SMRT/HDAC3 control (Figure 3-8b). This suggests that PTEN is de-phosphorylating IP_5 to generate IP_4 but not IP_4 as previously believed. IPMK consistently increased the level of complex activity observed, (p-value = 0.0003), however, the mutant failed to remove the effect of the enzyme, suggesting a more stringent mutant involving K146 may be required (Figure 3-8b). The differences in the two sets of results (Figure 3-5 and Figure 3-8) indicate that alterations in normalisation techniques can greatly alter the results. Since at this stage in the project we still had no way of measuring IP levels, it was difficult to interpret the results accurately. Therefore, we could not determine which way of normalising the assay was appropriate, thus highlighting further, the need for an effective method to measure inositol phosphate levels.

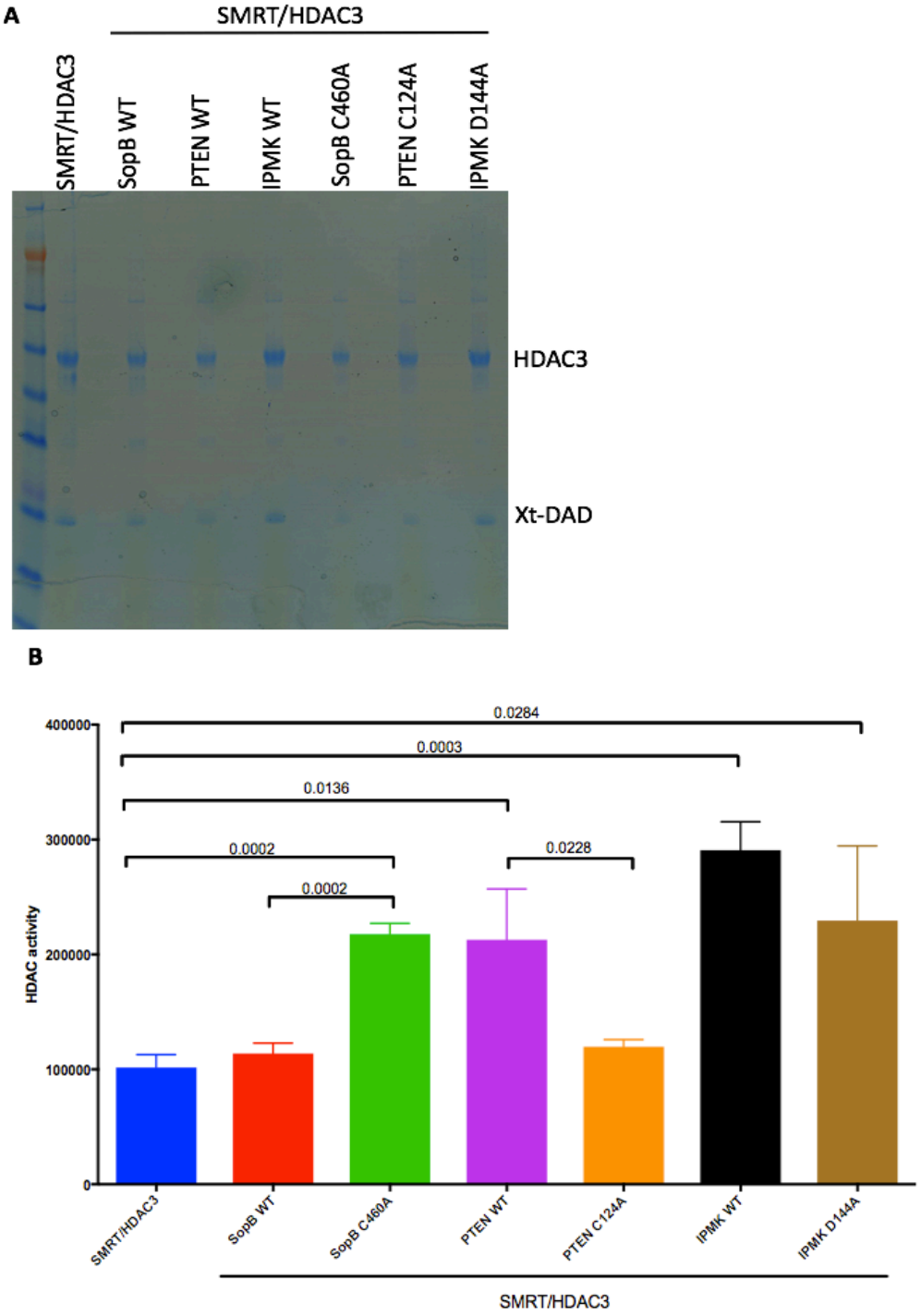

Figure 3-8 Effect on HDAC3 activity is affected by normalisation technique used. *Xt-DAD SMRT and full length HDAC3 were co-expressed with wildtype or catalytically dead SopB/PTEN or IPMK for 48 hours in HEK-292F cells to determine if changes in HDAC activity are related to catalytic activity* ***(A)*** *Following flag-resin isolation of the HDAC3 complex, purified complex was run on a Coomassie blue gel to determine the level of HDAC3 in each sample. Densitometry was carried out on the HDAC3 band to determine the ratio of HDAC3 compared to the SMRT/HDAC3 sample. This ratio was then used in the HDAC assay.* ***(B)*** *Deacetylase activity was assayed following isolation of the HDAC3/SMRT complex from the flag resin. All p-values were calculated using a Two-tailed T test, where n=3 ±SD.*

3.5 The effect of IPMK on the ability of SMRT/HDAC3 to repress transcription

HDAC3 is inactive until it forms a multi-component complex with SMRT, or its homolog NCoR (Guenther et al, 2001). Activation of HDAC3 was previously believed to be enabled by the DAD of SMRT, later studies revealed that Ins(1,4,5,6)P_4 also has an activating role on the complex *in vitro* (Codina et al, 2005; Guenther et al, 2001; Millard et al, 2013; Watson et al, 2012; Watson et al, 2016). HDAC3 has a repressive effect on gene expression, we therefore aimed to use a conventional luciferase assay in conjunction with IPMK expression to identify whether this activity is IP dependent. As Ins(1,4,5,6)P_4 is believed to be an activator of the HDAC3/SMRT complex; overexpression of HDAC3/SMRT in combination with IPMK should result in increased repression of the luciferase gene due to an increase in IP levels (Fujii & York, 2005). IPMK was selected over PTEN and SopB to analyse the repressive effects of HDAC3/SMRT due to its endogenous role as an inositol phosphate kinase. Furthermore, SopB is known to have pathogenic effects on host cells during *Salmonella dublin* invasion, through its ability to alter many cellular processes such as inhibition of nuclear mRNA export (Feng et al, 2001).

3.5.1 IPMK enhances HDAC3/SMRT mediated transcriptional repression

To ascertain the effects of IPMK on HDAC3/SMRT mediated transcriptional repression, HEK-293T cells were transfected with luciferase assay constructs (Table A3 7). Following transfection, it is assumed that the luciferase construct is chromatinised enabling PTMs to take place. Luciferase expression is driven by a thymidine kinase promoter (TK) with multiple Gal4-upstream activating sequences (GAL4-UAS) enabling high levels of basal transcription to be modulated by GAL4-DNA binding domain (GAL4-DBD) fusion proteins (Figure 3-9a).

The well-known repressor GAL4-MadN35 was used as a control and effectively reduced luciferase expression 2.7 fold (p-value 0.0157) (Figure 3-9b), indicating that the system is an effective way of measuring HDAC induced repression. GAL4-DBD tagged Xt-DAD SMRT (GAL4-SMRT, SMRT in figure) alone is unable to inhibit expression, but in the presence of untagged HDAC3 (unHDAC3) transcription is repressed 2.5 fold (p-value = 0.0181), indicating recruitment of HDAC3 to the TK promoter (Figure 3-9b). Recruitment to the promoter is essential as expression of unHDAC3 alone results in no change (Figure 3-9b). Addition of IPMK to the system increases SMRT/HDAC3 facilitated repression of the luciferase construct 1.8 fold (p-value = 0.0150) (Figure 3-9b). IPMK with GAL4-SMRT does not alter luciferase expression, indicating that IPMK mediates its effects through increased activation of the HDAC3/SMRT complex, presumably due to increased IP production (Fujii & York, 2005) (Figure 3-9b).

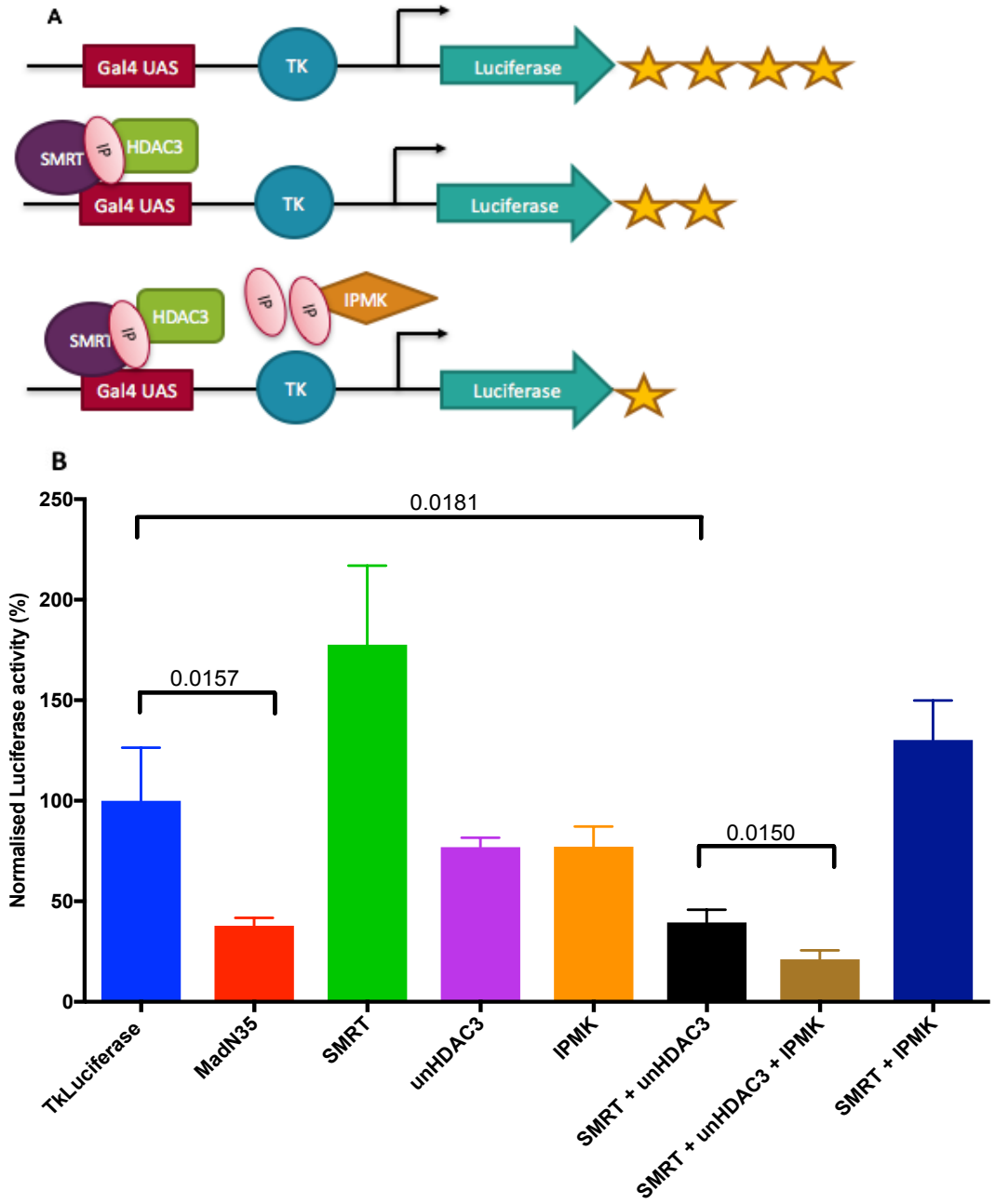

Figure 3-9 IPMK increases SMRT/HDAC3 repression of Tk-Luciferase (A) *Schematic showing principle of Luciferase assay with stars indicating level of luciferase expression. Tk-Luciferase construct has high basal expression alone, with recruitment of SMRT/HDAC3 expression decreases, this repression increases further upon addition of IPMK through increased IP_4 available to activate the complex.* ***(B)*** *HEK-293T cells were transfected with TKLuc, β-gal and various other constructs as denoted on axis. 48 hours following transfection, cells were harvested and luciferase expression was analysed. Normalised luciferase expression (relative to TKluc sample) is shown where n=3 ±SD, p-values were calculated using a Two-tailed T-test. Addition of IPMK to the system causes a 1.8 fold increase in repression of Tk-Luciferase by the SMRT/HDAC3 complex (p value = 0.0150) indicating enhanced IP levels increase activity of the SMRT/HDAC3 complex.*

3.5.2 IPMK does not affect repression by HDAC3 inositol phosphate binding mutants

HDAC3 and the SMRT-DAD form five hydrogen bonds and salt bridges with phosphate groups on Ins(1,4,5,6)P_4 in the basic pocket between their interface (His17, Gly21, Lys25, Arg265, Arg301 of HDAC3 and Lys449, Tyr470, Tyr471, Lys474 and Lys475 of SMRT) (Watson et al, 2012). Mutation of Tyr470, Tyr471 of SMRT reduces HDAC3 binding to the DAD and activation of HDAC activity, presumably due to decreased Ins(1,4,5,6)P_4 binding (Codina et al, 2005; Guenther et al, 2001). Further to this, mutation of Lys449 in SMRT to Ala allows the complex to form but activation of HDAC3 is abolished indicating an activating role for Ins(1,4,5,6)P_4 (Codina et al, 2005). Moreover, mice containing Ala mutations in SMRT Tyr470 and the corresponding residue in NCoR Tyr478, show increased local acetylation and reduced genomic recruitment of HDAC3 (You et al, 2013). These data suggest that these Ins(1,4,5,6)P_4 binding residues are essential to both recruitment and activation of the HDAC3/SMRT complex.

To try and demonstrate that IPMK is exerting its effect on SMRT/HDAC3 mediated transcriptional repression through IP, it was decided to utilise mutations in HDAC3 at key IP binding residues. Arginine 265 in HDAC3 is believed to form a key interaction with Ins(1,4,5,6)P_4, as loop 6 is important for active site access and in the absence of Ins(1,4,5,6)P_4 would likely be highly mobile (Watson et al, 2012). Mutation to R265A has been shown to decrease activity of HDAC3/SMRT via a luciferase assay and is believed to be important in the activation of the complex (Watson et al, 2016). As well as the R265A mutant, an HDAC3 enzyme which had all the inositol phosphate binding residues mutated to its HDAC8 counterpart was also utilised. This HDAC3:5m contained the following mutations in residues H17C, G21A, K25I, R265P and R301A as shown in Figure 3-10a+c. HDAC8 residues were utilised as this enzyme is the only class 1 HDAC which is active outside of a corepressor complex and therefore is believed not to require IP for its activation.

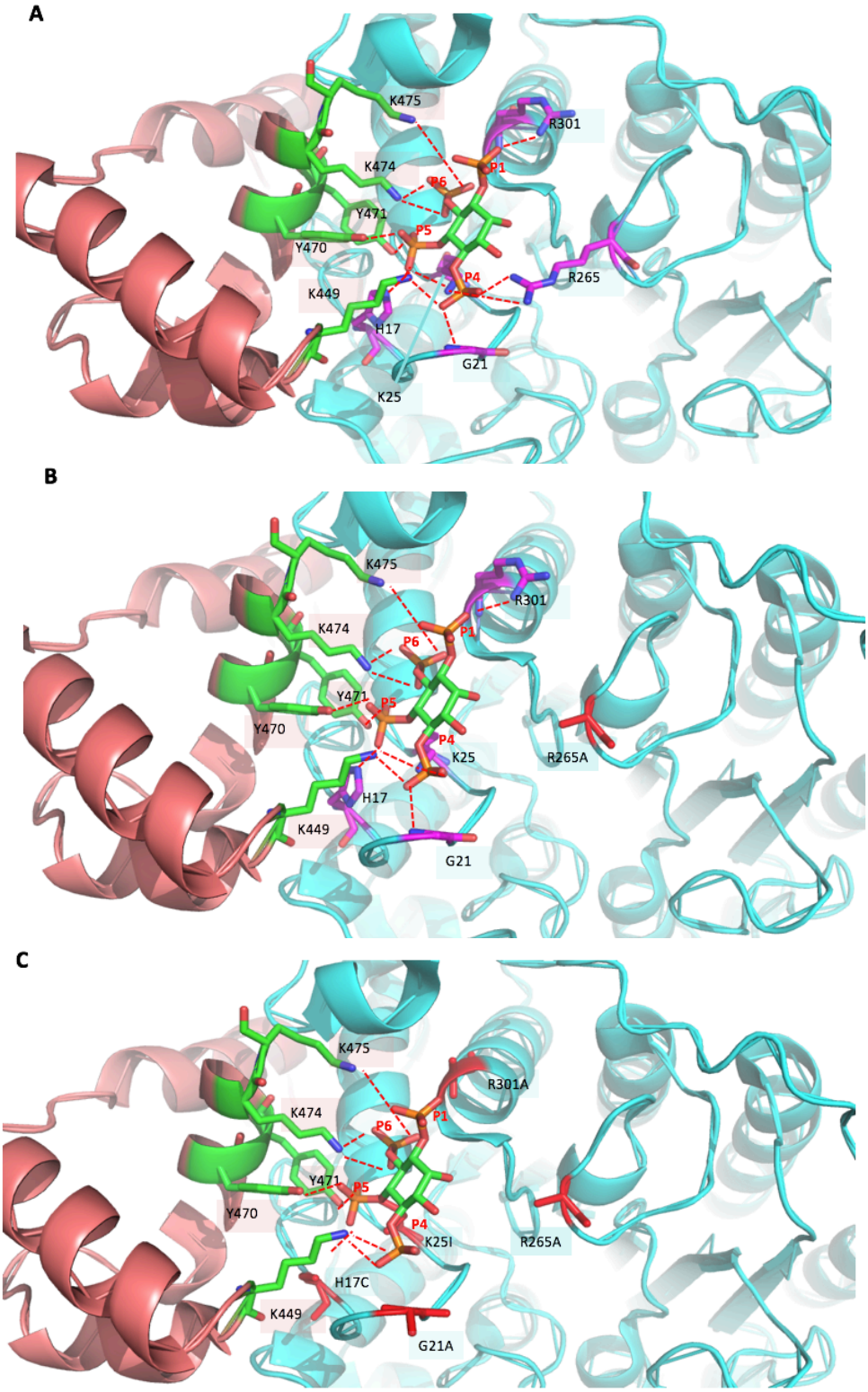

Figure 3-10 Structure of Inositol-1,4,5,6-tetrakisphosphate binding to SMRT/HDAC3. ***(A)*** *Structure of WT HDAC3 (cyan) bound to the DAD domain of SMRT (salmon) with Ins(1,4,5,6)P_4 at the interface (stick model). Interacting residues in HDAC3 (magenta) and DAD (green) are shown.* ***(B)*** *Structure showing HDAC3:R265A* ***(C)*** *All IP_4 interacting residues in HDAC3 have been mutated to the corresponding residues in HDAC8 (HDAC3:5m). Mutations are shown in red. PDB ID: 4A69, (Watson et al, 2012).*

As can be seen in Figure 3-11 GAL4-SMRT and unHDAC3 are unable to repress luciferase alone, but co-expression represses transcription 2.5 fold (p-value = 0.0181). Upon expression of GAL4-SMRT and HDAC3:R265A we observe a decrease in repression of luciferase activity by 1.8 fold compared to SMRT and wildtype unHDAC3 (p-value = 0.0055) (Figure 3-11). Interestingly the R265A mutation although not significantly different to basal luciferase expression does show a slight decrease to 71% transcription. This implies that SMRT and HDAC3:R265A are still able to bind, perhaps to a lesser extent, and still exert some of their repressive abilities. This indicates that with reduced inositol phosphate binding complete activation of the SMRT/HDAC3 complex is not detected. This corresponds with the evidence that the interaction of SMRT/HDAC3 with some phosphate groups on IP are more important in binding of IP whilst others are important in activation of the complex (Watson et al, 2016). Addition of IPMK in this case had no effect on the ability of HDAC3:R265A and GAL4-SMRT to repress luciferase expression (Figure 3-11). This further indicates that R265 is important in activating HDAC3, as mutation of this residue even in an environment with increased IP fails to fully activate the complex.

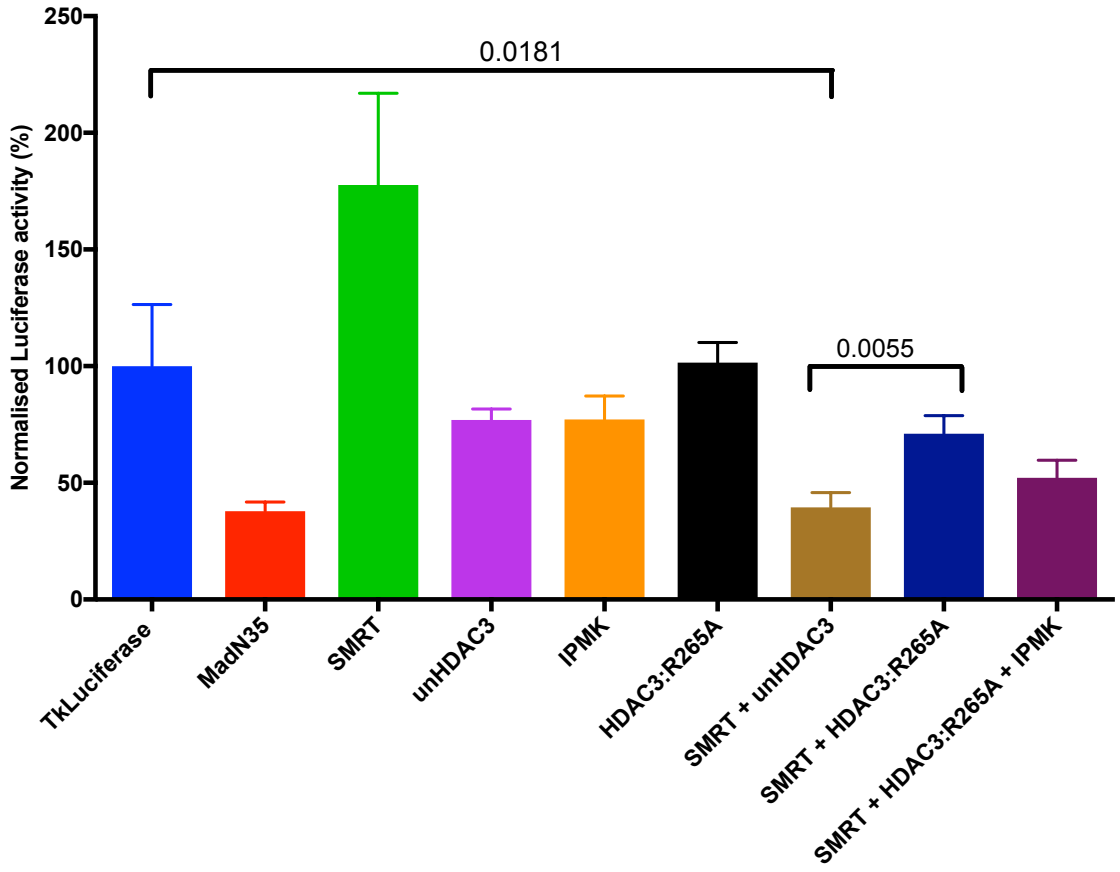

Figure 3-11 The R265A HDAC3 mutation fails to allow repression of Tk-Luciferase expression. *HEK-293T cells were transfected with TKLuc, β-gal and various other constructs including mutant HDAC3 as denoted on axis. 48 hours following transfection, cells were harvested and luciferase expression was analysed. Normalised luciferase expression (relative to TKluc sample) is shown. The SMRT/HDAC3:R265A mutation shows a 1.8 fold relief in repression of Tk-Luciferase compared to the wildtype SMRT/HDAC3 complex. IPMK has no effect on this relief in repression, indicating that activation by IP binding is lost. The significance value (p value = 0.0055) was calculated using a Two-tailed T-test. Mean luciferase activity shown (n=3, ±SD)*

The HDAC3:5m is mutated such that Ins(1,4,5,6)P_4 should be unable to bind and therefore have reduced repressive activity, if IP is regulating activity. As with previous experiments, GAL4-SMRT and unHDAC3 are unable to exert their repressive effects until expressed together (Figure 3-12). Co-expression of GAL4-SMRT and the HDAC3:5m mutant however, completely removes the ability of the complex to repress transcription compared to wild-type unHDAC3 (p-value = 0.0008) (Figure 3-12). This inability to enable repression of transcription indicates IP binding is required for activation of the complex. This is further supported by the lack of change observed when IPMK is co-expressed with HDAC3:5m and GAL4-SMRT.

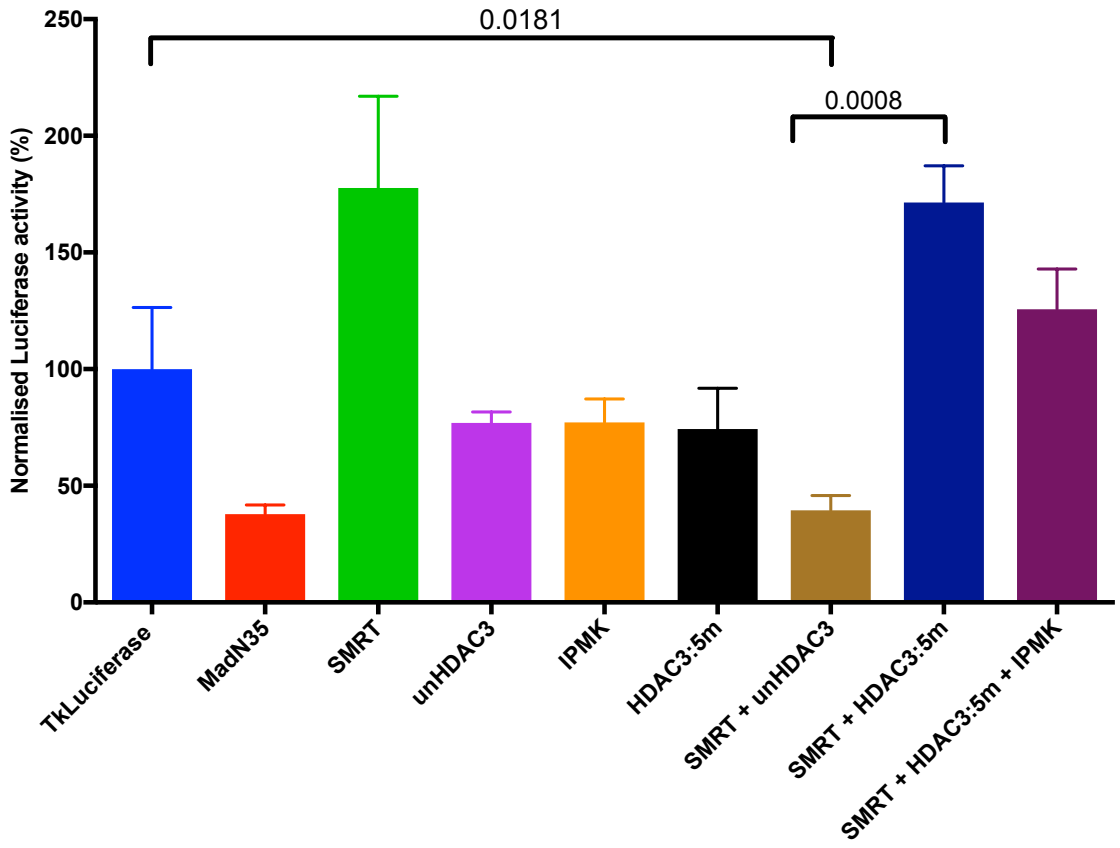

Figure 3-12 The all IP HDAC3 mutation relieves repression of Tk-Luciferase expression. *HEK-293T cells were transfected with TKLuc, β-gal and various other constructs as denoted on axis. 48 hours following transfection, cells were harvested and luciferase expression was analysed. Normalised luciferase expression (relative to TKLuc sample) is shown above. The SMRT/HDAC3:5m shows a 4.3 fold relief in repression of Tk-Luciferase compared to the wildtype SMRT/HDAC3 complex. IPMK has no effect on this relief in repression, indicating IP binding is lost. The significance value (p value = 0.0008) was calculated using a Two-tailed T-test. Mean luciferase activity shown (n=3, ±SD)*

3.6 Anion exchange Chromatography-Mass Spectrometry can be used for the determination of Inositol Phosphate levels

Throughout this chapter, we aimed to manipulate the levels of IP in cells and measure the effect on HDAC activity. The conclusions reached and the experiments planned have so far been based on previous experimental data. Thus, without a method to determine IP levels in cells it is difficult, if not impossible, to reach any confident conclusions on the effect on HDAC activity. Consequently, we aimed to establish a

method to measure IP levels, in collaboration with Peter Watson from the Schwabe laboratory.

Several methods have been used to measure IP levels to understand the role of inositol phosphate kinases and their products in cellular processes. Perhaps the most well used method is labelling cells with tritiated inositol ([^{3}H]Inositol), thus enabling labelling of cellular IP (Azevedo & Saiardi, 2006). The [^{3}H]Inositol labelled cells are then harvested and the IPs extracted and the composition of IP is measured via high-performance liquid chromatography (HPLC) (Azevedo & Saiardi, 2006; Stevenson-Paulik et al, 2006). The issue with this method is that it requires tritium to be added to the cells which whilst an effective method, the radioactive isotype is unable to be detected using traditional methods. A second method which has been used to determine the levels of IPs is the use of polyacrylamide gel electrophoresis (PAGE) coupled to toluidine blue or 49,6-diamidino-2-phenylindole (DAPI) staining (Losito et al, 2009). This method has a caveat in that it can only detect IP present at high levels making it unamenable to mammalian cells (Losito et al, 2009; Wilson et al, 2015). A new extraction method using a titanium dioxide bead extraction of IP claimed to overcome this (Wilson et al, 2015). However, although this method purified lower order inositol phosphates they were not able to be quantified using PAGE and toluidine blue staining (Wilson et al, 2015). The advent of mass spectrometry coupled detection of IP enabled highly selective measurements of inositol phosphate mixtures and is the protocol which we aimed to establish in our collaboration with the Schwabe group.

The anion exchange chromatography-mass spectrometry method used to measure IP was set up by Peter Watson and Andrew Bottrill from Leicester's Protein Nucleic Acid Chemistry Laboratory (PNACL). The method of extraction was adapted from a previously published method in (Barker et al, 2010). This extraction method involves a trichloroacetic acid (TCA) extraction rather than a more common acetic acid extraction so as to reduce the overall acidity of extraction which can hydrolyze IP (Barker et al, 2010; Liu et al, 2009). Following TCA extraction, the sample is washed in water saturated diethlyether which acts as an organic solvent, leaving behind the IP. The

sample is then brought to neutrality with triethylamine to prevent any adverse effects occurring on the column (Barker et al, 2010). Following extraction, the samples were run on an anion exchange column as outlined in (Liu et al, 2009) (details can be found in section 2.10.2). A gradient involving 200mM ammonium bicarbonate and 5% methanol was used to isolate the IPs and remove them from the column. Ammonium bicarbonate is used as although a phosphate ion would produce a better separation if a stronger anion was utilised such as potassium chloride it cannot be ionized in the mass spectrometry machine. As the ionic strength of ammonium bicarbonate is increased IPs come off the column and enter the mass spectrometry machine and are ionized by electrospray ionisation (ESI). The inositol phosphate molecule fragments are then detected as outlined in section 2.10.2 as recommended by (Liu et al, 2009). The chromatograms produced by the mass spectrometry analysis as seen in Figure 3-13a are then analyzed by integrating the area under the peak to determine relative levels of inositol phosphate species in the samples. We are unable to accurately quantify these levels due to a lack of an internal control, as such, we can compare IP_3 across different samples, but we are unable to compare the levels of IP_3 and IP_4 due to their different charge properties.

Initially, we attempted to determine the sensitivity of the assay by sending varying numbers of HEK-293F cells for analysis. As shown in Figure 3-13b, we observe a clear increase in the yield and detection of inositol phosphates with increased cell number as measured by integrated peak area increasing over background levels. Based on this, in all subsequent experiments utilizing the anion exchange chromatography-mass spectrometry method we aimed to send between 1x10^7 to 2x10^7 cells per sample.

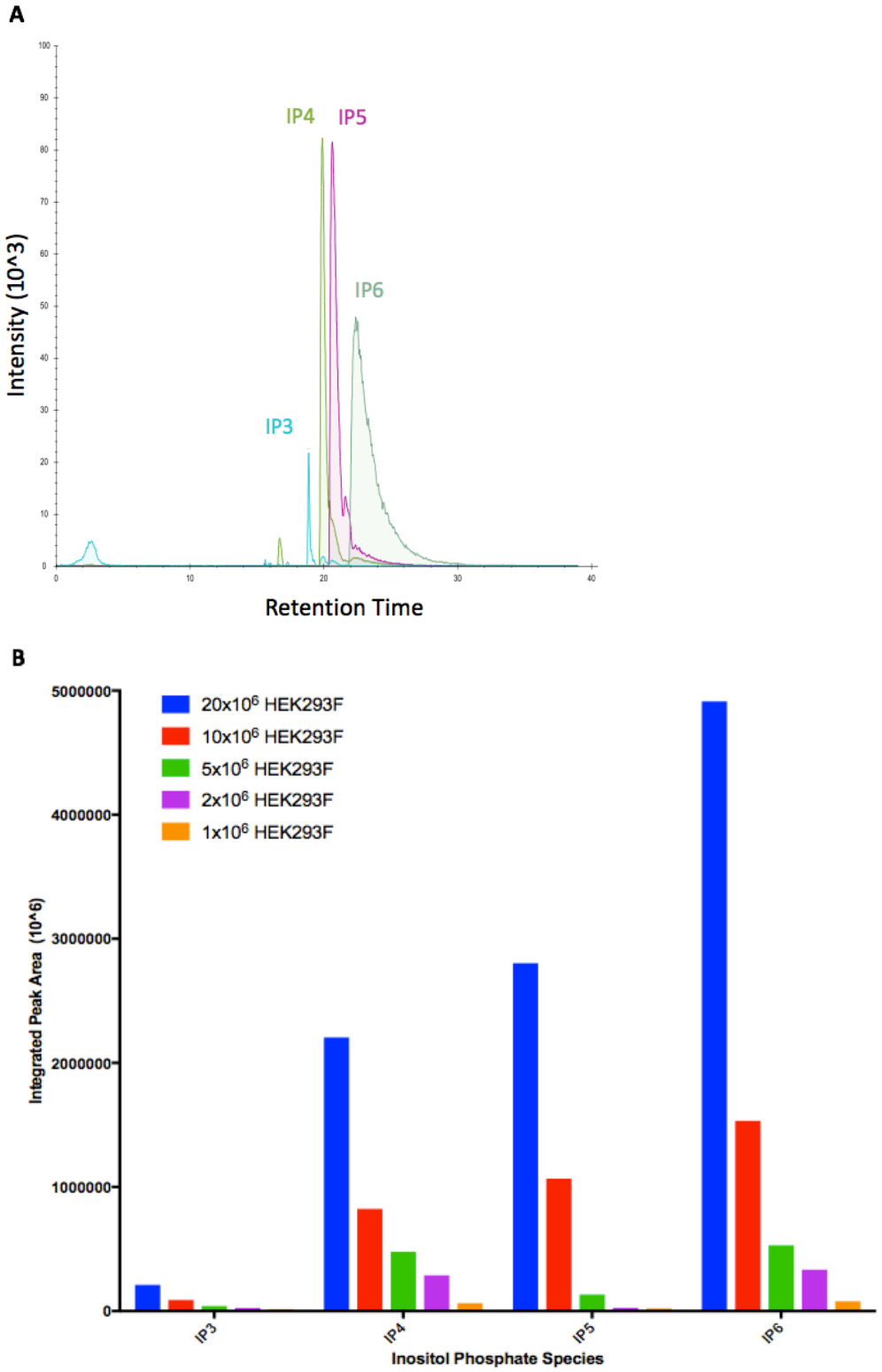

Figure 3-13 Determining the cell number required for effective detection of Inositol Phosphates by Mass Spectrometry (A) *Example chromatogram produced by the method is shown, for each peak the area underneath is integrated to determine the relative quantity of IPs in the sample.* ***(B)*** *A HEK-293F cell number titration was carried out from 1-20x10^6, it is clear to see that larger cell numbers result in more IP detected.*

After identification of the optimal cell number, we aimed to repeat transfections carried out previously and determine how SopB, PTEN and IPMK affected IP levels. We intended to establish a link between the composition of IPs present in each sample and the HDAC activity observed. FACS analysis was carried out to ensure that relatively similar transfection rates were observed compared to previous experiments. As can be seen in Figure 3-14, all transfection rates are comparable to previous experiments, apart from the PTEN transfected sample which has a slight reduction in transfection level.

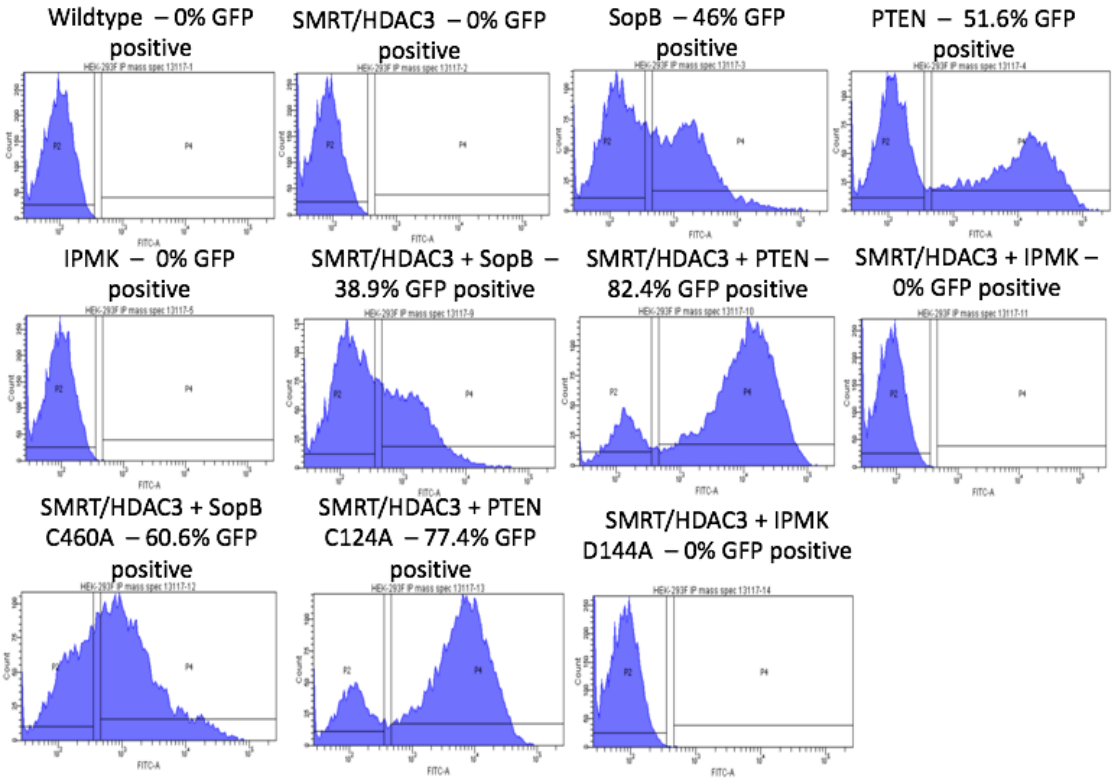

Figure 3-14 FACS analysis of samples sent for anion exchange chromatography mass spectrometry. *Samples sent for mass spectrometry were analysed 48 hours post transfection of HDAC3/SMRT with PTEN/SopB and IPMK (wildtype and catalytically dead) by FACS to ensure relatively similar transfection rates as compared to previous experiments. All levels appear to be like those previously observed, apart from the PTEN alone transfection rate which is slightly lower than previously observed. Accordingly samples were taken forward for mass spectrometry analysis.*

The cells were then harvested and live cell number counted for normalisation of the mass spectrometry results. Inositol phosphates were extracted and analysed by anion exchange chromatography-mass spectrometry. Integrated peak areas of IP peaks were

provided by PNACL and were normalised to the live cell number of the sample and plotted as shown in Figure 3-15.

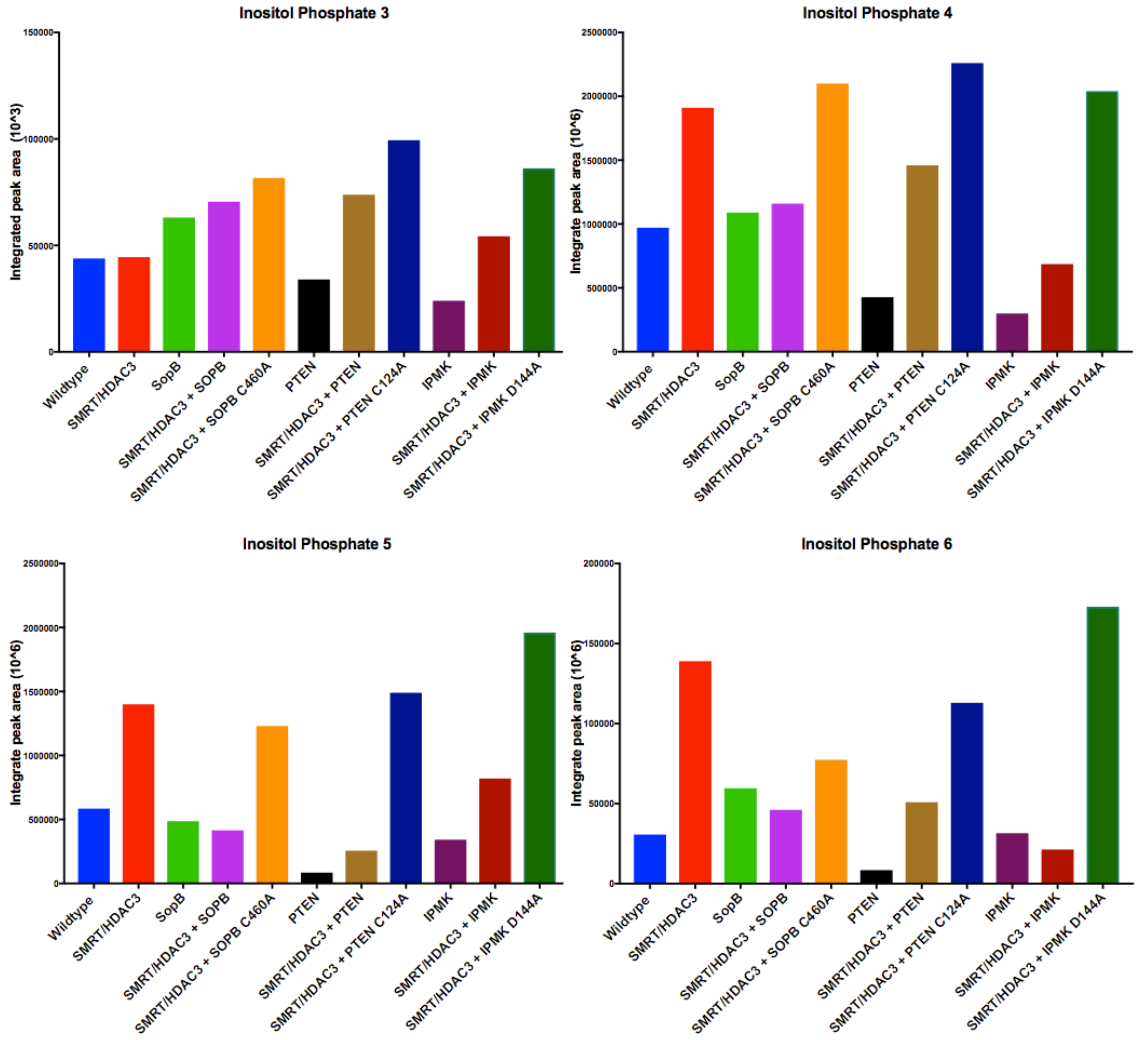

Figure 3-15 Effect of SopB/PTEN/IPMK on Inositol Phosphate levels. *HEK-293F cells were transfected with SMRT/HDAC3 and either wildtype of mutant SopB, PTEN or IPMK. 48 hours following transfection, inositol phosphates were extracted and sent for mass spectrometry analysis at PNACL. Andrew Bottrill calculated the integrated peak areas for all inositol phosphates measured. The integrated peak areas of IP_3, IP_4, IP_5 and IP_6 chromatograms were normalised to cell number and are shown above. Fluctuations are seen depending on the conditions of the cells indicating IP levels are being altered by expression of SopB, PTEN and IPMK.*

The level of IP_3 doesn't alter greatly with overexpression of the various constructs, apart from in PTEN and IPMK alone samples we see a slight decrease compared to the wildtype sample. The more interesting results come from the IP_4, IP_5 and IP_6 data. Upon overexpression of SMRT/HDAC3 we see a substantial increase in IP_4, IP_5 and IP_6

(Figure 3-15). Although there is currently no evidence for a pool of HDAC3 waiting for IP_4 to bind to it, this data does suggest that if the level of SMRT/HDAC3 increases then the level of inositol phosphate in the cells could compensate for this (Millard et al, 2013).

Overexpression of SopB does not cause a decrease in IP_4 or IP_5 and in fact we witness a slight increase in IP_6 levels compared to the wildtype sample (Figure 3-15). This supports the result of the global HDAC assay where we saw no change in HDAC activity upon SopB expression (Figure 3-1a). Nonetheless, this is surprising when compared to previous data showing a rapid decrease of inositol phosphates with SopB expression (Feng et al, 2001). The lack of change could in part be due to our low transfection rates (ranging from 30-50%). Additionally, the previous data used an inducible SopB cell line, meaning that all cells experience the same change in inositol phosphate levels. However, if only 30-50% of our cells are undergoing the effects of SopB then this may not be enough of a change within the whole sample to detect changes by mass spectrometry.

PTEN is believed to de-phosphorylate IP_5 and IP_4 by its 3-phosphatase activity *in vitro* (Caffrey et al, 2001; Maehama & Dixon, 1998). It is perhaps not surprising that PTEN results in a decrease in IP_4, IP_5 and IP_6 upon expression (Figure 3-15). The fold changes of this decrease, 2 fold, 6 fold and 3 fold for $IP_4/_5/_6$ respectively, (fold changes should be approached with caution due to quantitation issues), would suggest a decrease in HDAC activity, however, this is not the case in the global HDAC assay (Figure 3-1a). The expression of IPMK yields another unexpected result. Previous studies have shown that overexpression of IPMK results in an increase in IP_5 levels (Fujii & York, 2005). Yet, Figure 3-15 indicates that the levels of IP_4 and IP_5 decrease 2 fold and 1.6 fold respectively, which again contradicts the lack of change in the global HDAC assay (Figure 3-1a). It is somewhat counterintuitive that overexpression of IPMK results in a reduction of inositol phosphate level compared to wildtype cells, as IPMK catalyses the conversion of IP_3 to IP_5 via IP_4 (Figure 1-13) (Frederick et al, 2005). It is possible that overexpression of IPMK results in an up-regulation of IPs but this activates endogenous

phosphatases to enable the maintenance of IP ratios, thereby leading to an overall reduction in IP levels.

As has previously been stated in this chapter we may be detecting changes in IP levels but not HDAC activity at a global level due to the compensation. Accordingly, we examined the SMRT/HDAC3 assays to try and gain a more rational understanding of the role of IP in HDAC3 activation. Transfection of SMRT/HDAC3 with SopB leads to a decrease in IP_4, IP_5 and IP_6 levels compared to the SMRT/HDAC3 sample, the same occurs with PTEN and IPMK (Figure 3-15). These results can be rationalised in terms of SopB and PTEN being known phosphatases. Both Figure 3-2a and Figure 3-5b show a decrease in HDAC activity upon SopB and PTEN transfection thus indicating that reducing the level of IP is directly linked to HDAC activity. However, it is not clear why a decrease in IP upon IPMK expression is observed. The confusion is further compounded by both Figure 3-2a and Figure 3-5b where the consequence of IPMK overexpression is either no change or an increase in HDAC activity respectively. One possible reason for this increase in HDAC activity despite decreasing levels of IP is the normalisation method. The coomassie blue gel in Figure 3-5a indicates that less HDAC3 was pulled down in the flag resin isolation compared to the SMRT/HDAC3 sample, thus any potential errors in normalisation could have skewed the result. However, when we tried to compensate for this potential normalisation error by altering the normalisation technique (3.4.2) we observed no change in HDAC activity upon addition of SopB, whereas, PTEN and IPMK resulted in an increase in HDAC activity (Figure 3-8b).

The catalytically inactivate enzymes generated to confirm that we were affecting IP levels and therefore HDAC activity, do in fact result in very little changes in the levels of IP5 and IP6 (Figure 3-15). Interestingly, they do appear to result in an increase in IP4, however, this increase only appears to be a roughly 2 fold increase in all cases. It is possible that a fold change of 2 is due to issues quantitating the IP mass spec rather than an effect potentiated by the mutant enzymes themselves. This would in turn explain why we detect a lack of change in HDAC activity compared to HDAC3/DAD for SopB C460A but not the decrease in PTEN C124A or IPMK D144A HDAC activity (Figure

3-7b). As with the catalytically active proteins, we see differences when the errors of normalisation were attempted to be compensated for in Figure 3-8b. We no longer observe decreased HDAC activity with PTEN C124A expression rather no change at all. Similarly, upon overexpression of SopB C460A and IPMK D144A we detect an increase in HDAC activity compared to the HDAC3/DAD control, perhaps due to the 2 fold increases in IP_4 levels.

3.7 Summary

In this chapter, we have demonstrated that overexpression of SopB, PTEN and IPMK does not affect global HDAC activity (Figure 3-1b) despite bringing about changes to IP levels (Figure 3-15). Furthermore, overexpression and isolation of the SMRT/HDAC3 complex in the presence of IP manipulating enzymes alters the activity of the HDAC complex (Figure 3-2b and Figure 3-5b). In conjunction with previous evidence that the composition of IP is altered in the cells, this suggests that IPs do affect HDAC activity (Caffrey et al, 2001; Feng et al, 2001; Fujii & York, 2005). This is further supported in the case of SopB where the WT SopB reduces HDAC activity yet the catalytically inactive C460A mutant level is analogous to the control (Figure 3-7b). However, our analysis of the composition of IPs in cells following overexpression of SopB, PTEN and IPMK brings this into doubt, due to the inability to align differences in HDAC activity to alterations in IP levels observed (Figure 3-15).

Inositol phosphates appear to be important in the mediation of SMRT/HDAC3 repression of luciferase, with IPMK increasing the level of repression and having no effect on IP binding HDAC3 mutants (Figure 3-9, Figure 3-11 and Figure 3-12). This was believed to be due to its ability to increase IP levels in the HEK-293T cells. However, data from HEK-293F (Figure 3-15) suggests that IPMK alone decreases IP levels bringing into question our conclusions.

There are several caveats to the experiments outlined above including transfection efficiencies and quantitation issues. Together, with the difficulties in aligning what is known about the effects of these enzymes, and our own mass spectrometry data has made for an arduous task. This is compounded by the inconsistencies in relating IP levels back to the results of HDAC activity and luciferase assays. As such in the remaining chapters of this thesis a different system for investigating the effect of IP on HDAC activity was utilized.

Chapter 4 Understanding the role of inositol polyphosphate multikinase in HDAC activity in mouse embryonic stem cells

4.1 Chapter aims

As discussed previously, Ins(1,4,5,6)P_4 is believed to be a regulator of class 1 HDAC complexes (Itoh et al, 2015; Millard et al, 2013; Watson et al, 2012; Watson et al, 2016). However, upon overexpression of SopB, PTEN and IPMK we were unable to conclusively confirm the role of Ins(1,4,5,6)P_4 as a regulator of HDAC activity. There were several caveats to this series of the experiments resulting in difficulties to align our results with the IP mass spectrometry data. In 2005, an inositol polyphosphate multikinase (IPMK) knockout (KO) mouse model was generated which exhibited embryonic lethality at embryonic day 9.5 (E9.5) (Frederick et al, 2005). ES cells were isolated and shown to have attenuated levels of IP (Frederick et al, 2005). Consequently, these cells provide a model system in which to investigate the effect of IP on class-1 HDAC activity. Therefore, using the IPMK KO ES cells, kindly provided by John York's group, I aimed to assess the biochemical and proliferative properties of ES cells lacking IPMK and its involvement in the regulation of HDAC activity.

4.2 Characterisation of IPMK knockout and rescue ES cells

IPMK consists of three lobes, the N-lobe and C-lobe, involved in ATP binding, and the IP-lobe, responsible for IP binding and contains the catalytic consensus sequence PxxxDxKxG (Figure 4-1a) (Gonzalez et al, 2004; Shears, 2004). In 2005, IPMK KO mice were generated through targeted removal of exon 4 and replacement with a Neo cassette which removed the catalytic consensus site rendering the enzyme catalytically inert (Figure 4-1b) (Frederick et al, 2005). ES cells were isolated from the blastocyst at

E3.5 and grown in feeder-free conditions, labelling with [^{3}H] inositol indicated a 90% decrease in IP_5 and IP_6 compared to wildtype cells (Frederick et al, 2005) (Figure 4-1c). The level of IP_4 remained relatively constant but the peak observed is not believed to be $Ins(1,3,4,5)P_4$ or $Ins(1,4,5,6)P_4$ (Frederick et al, 2005).

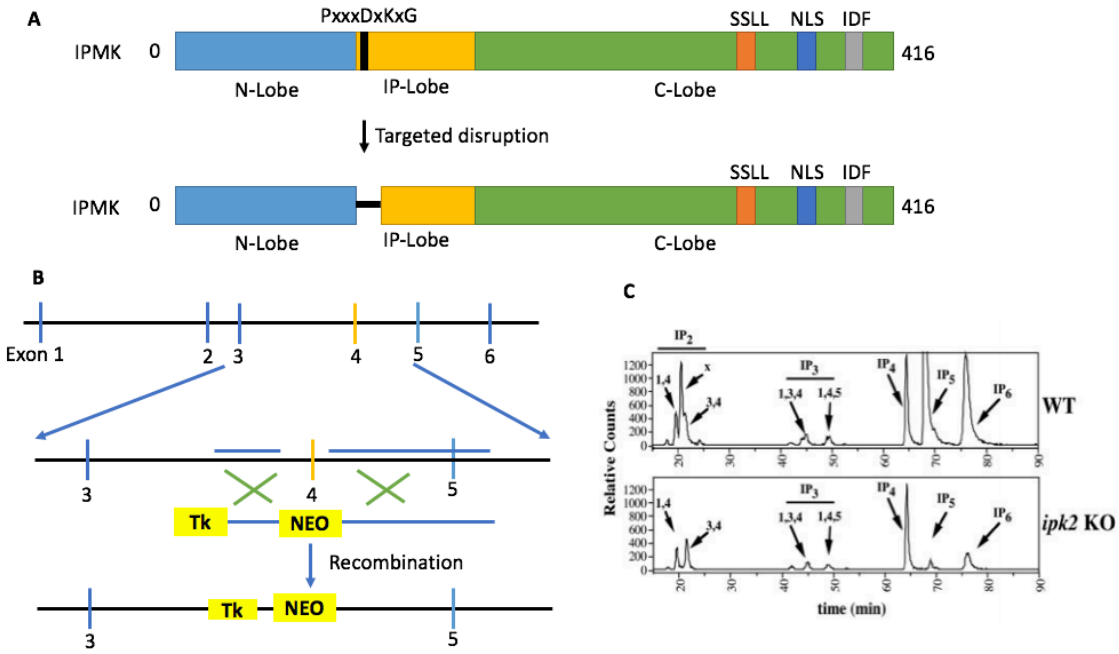

Figure 4-1 Deletion of IPMK exon 4 reduces levels of inositol phosphates. (A) *Schematic diagram of IPMK. The N and C –lobe are involved in ATP binding and positioning of the magnesium co-factor. The IP domain binds the inositol phosphate and contains the catalytically active PxxxDxKxG motif. The SSLL domain is conserved in all IP_6-kinases and is important for catalysis. The NLS ensures nuclear localisation and the IDF motif is involved in ATP binding. Targeted disruption by Frederick et al 2005 as shown in* ***(B)*** *deletes exon 4 which contains the catalytic core as well as intronic regions surrounding exon 4. A Tk-Neo selection cassette was inserted in place of exon 4.* ***(C)*** *Deletion of the active domain of IPMK (Ipk2) reduces the level of IP_5 and IP_6 by ~90% compared to the wildtype cells, IP_2, IP_3 and IP_4 levels were slightly reduced. The IP_4 peak was not believed to be either $Ins(1,3,4,5)P_4$ or $Ins(1,4,6,6)P_4$. Taken from Frederick et al 2005.*

4.2.1 Analysis of inositol phosphate levels in IPMK knockout ES cells

Inositol phosphate levels of IPMK KO (KO(5) and KO(2)) and wildtype (WT(10)) cells, kindly provided by the York group, were measured via anion exchange chromatography with tandem mass spectrometry. This was for two reasons, the first was to ensure that our method produced similar results to those seen in Frederick *et al*, 2005 and the second was to determine if the level of IP in the two knockout clones were comparable. To analyse the IP levels, cells were cultured on 100mm plates for 48 hours, after which cell numbers were calculated and the pellet was sent for analysis after IP extraction.

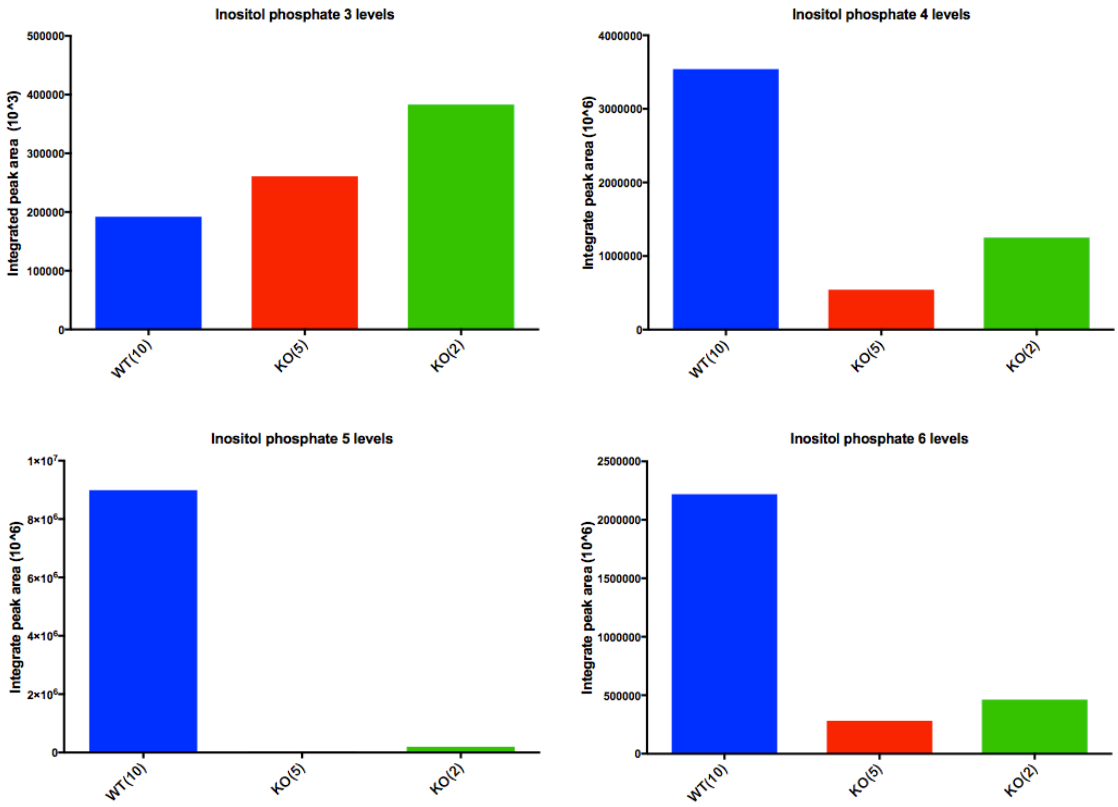

Figure 4-2 Analysis of inositol phosphate levels of IPMK KO ES cells. *IPMK clones were grown to confluency to obtain 2*10^7 cells per sample and inositol phosphates were extracted as outlined in methods and analysed by mass spectrometry. Integrated peak areas calculated by Andrew Bottrill in PNACL were normalised to cell number and are shown above. IP_3 shows a slight increase in KO(5) and KO(2)) compared to the WT(10). IP_4, IP_5 and IP_6 all show a decrease in levels in the knockouts compared to the wildtype clone.*

A large accumulation of IP_3 is not observed (slight increase in KO(2) compared to WT(10)), despite the anticipated block in the pathway (Figure 4-2). IP_4 levels differ to those reported in Frederick *et al*, 2005, whereby they observed no change in levels. We detected a decrease in IP_4 production in the IPMK KO(5) and KO(2) cells compared to the WT(10) (Figure 4-2). This is not surprising as IPMK is involved in the production of several IP_4 isoforms (Figure 1-13). The level of IP_5 and IP_6 observed in both the knockouts is in agreement with the 90% reduction observed in the Frederick *et al*, 2005 paper. These results indicate that our method of IP analysis can reproduce previously published data and is therefore an effective way of measuring IP levels.

4.2.2 Generation of PiggyBac (PB) TET IPMK stable rescue cell lines

We aimed to generate tetracycline inducible IPMK rescue cell lines which would enable direct comparison of KO(5) and KO(2) with and without IPMK thus removing any potential clonal variation. Inducible IPMK rescue clones were generated using a tetracycline inducible PiggyBac vector in conjunction with a transposase (Figure 4-3b). This vector was kindly provided by the McGrew laboratory at the Roslin Institute at the University of Edinburgh (Glover et al, 2013). The adapted construct can be observed in Figure 4-3a and shows that a CAG promoter drives expression of a 3rd generation reverse tetracycline transactivator (rtTA3) which in the presence of tetracycline (TET) or doxycycline (Dox) activates the minimal tetracycline response element (TRE) thus driving the expression of IPMK in a TET dependent manner (Glover et al, 2013).

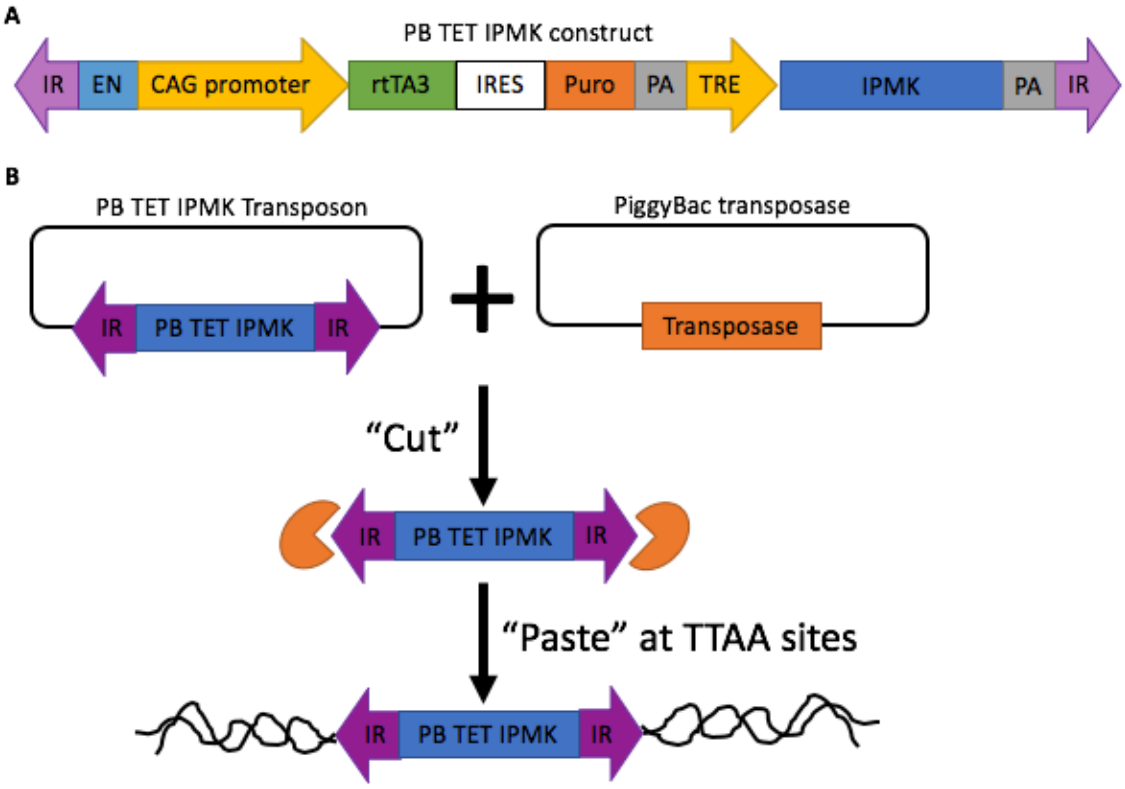

Figure 4-3 Generation of the PB TET IPMK rescue cell lines. ***(A)*** *Schematic representation of the PB TET IPMK vector, inverted repeats are represented by IR containing arrows, EN denotes the enhancer upstream of the CAG promoter which drives the expression of the 3rd generation reverse tetracycline transactivator (rtTA3) coupled to an IRES puromycin cassette. Downstream is the minimal tetracycline response element (TRE) promoter that drives expression of IPMK-polyA in the presence of tetracycline/doxycycline. Adapted from Glover et al, 2013.* ***(B)*** *Schematic showing the insertion of the PB TET IPMK construct into the genome of clone 5 and 2. Co-transfection of PB TET IPMK transposon with a transposase allows removal ("cut") of the construct from the plasmid. The transposase then "pastes" the transposon containing the IPMK construct in the genome at random at any TTAA sites.*

To generate the PB TET IPMK cells the construct was co-transfected with a transposase (Systems Bioscience) into KO(5) and KO(2) as outlined in section 2.1.3 (Figure 4-3b). They were then treated with puromycin for 10 days before isolation of 12 single cell colonies per parental clone. The colonies were expanded and treated with doxycycline (Dox) for 24 hours prior to whole cell lysate extraction to enable screening of IPMK induction by western blotting. All isolated clones contained the IPMK transgene and expressed IPMK after addition of Dox (Figure 4-4a). The fold change of IPMK induction was calculated by quantitative western blotting and enabled the selection of two TET-IPMK clones per parental cell line (Figure 4-4b). The chosen clones were KO(5) TET-

IPMK clone B4 (C5-B4), KO(5) TET-IPMK clone C3 (C5-C3), KO(2) TET-IPMK clone A6 (C2-A6) and KO(2) TET-IPMK clone C3 (C2-C3) due to their differences in IPMK induction (19-fold, 41-fold, 38-fold and 12-fold respectively).

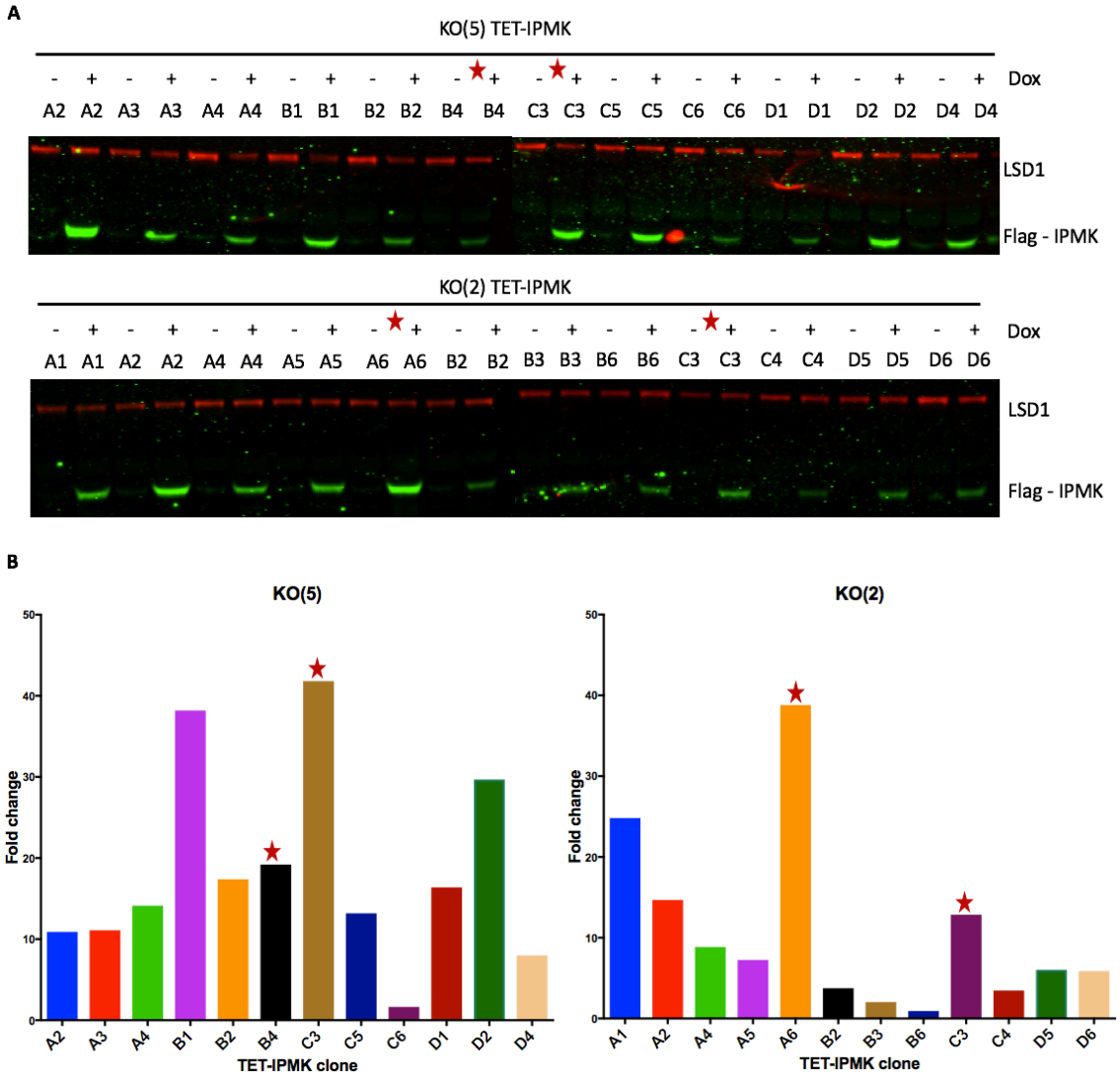

Figure 4-4 Screening PB TET IPMK stable rescues. *PB TET IPMK stable cell lines were grown up to a 48 well plate size and treated with or without 1ug/ml Doxycycline for 24 hours to measure induction of IPMK expression. Whole cell extract was generated as outlined in methods and IPMK expression was analysed by quantitative western blotting.* ***(A)*** *Western blots indicate the absence or presence of flag tagged IPMK upon addition of doxycycline, LSD1 was used as a loading control.* ***(B)*** *Fold changes were calculated using quantitative western blotting and normalising to the level of LSD1 present in the cells****.*** *Red starts denote clones taken forward for analysis of HDAC activity.*

4.2.2.1 Induction of IPMK restored inositol phosphate levels

Previously it had been shown that the generation of mouse IPMK rescue cell lines restores the level of IP (Frederick et al, 2005). The clones chosen (C5-B4, C5-C3, C2-A6 and C2-C3) showed a range of IPMK induction enabling us to determine whether the level of IPMK expression was important. The clones were grown on two 100mm plates, one was induced with Dox for 24 hours, prior to IP extraction and anion exchange chromatography with tandem mass spectrometry.

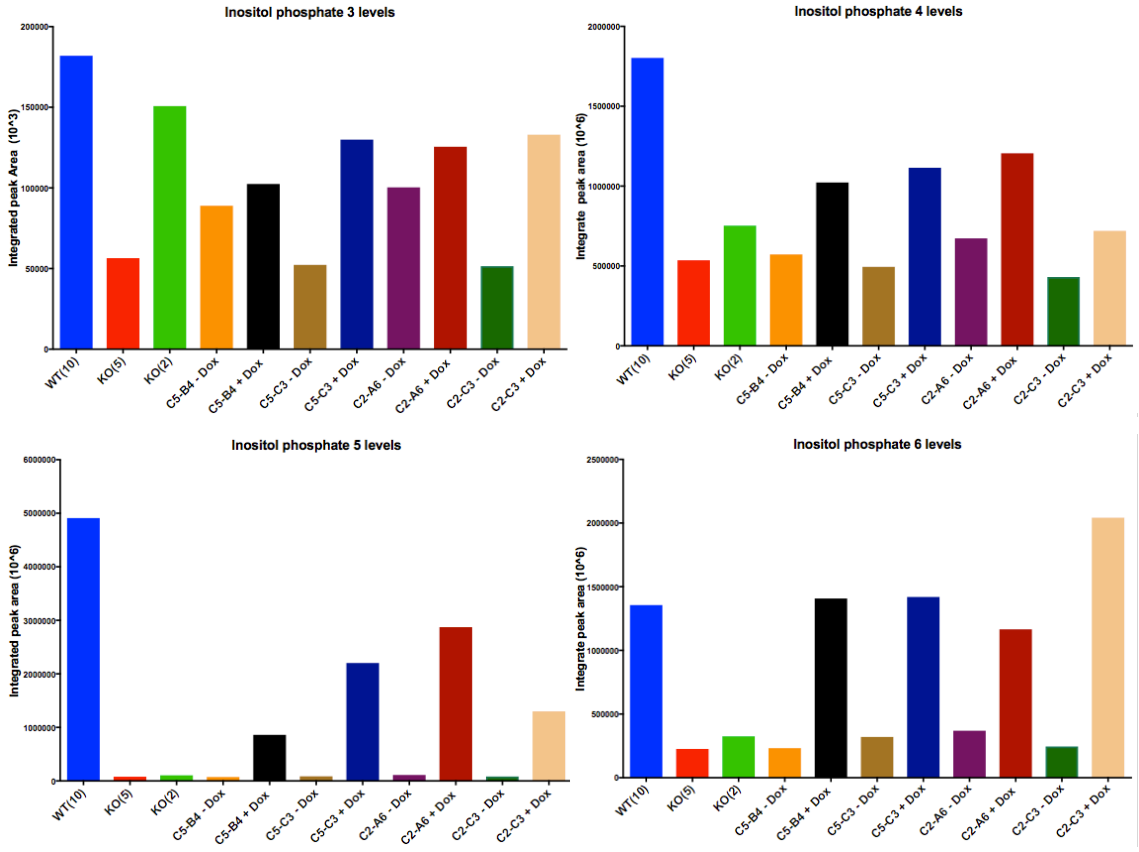

Figure 4-5 Analysis of inositol phosphate levels of IPMK rescue ES cells. *Parental IPMK clones and TET IPMK clones were grown to 2*10^7 cells with and without doxycycline and inositol phosphates were extracted and sent for mass spectrometry analysis. Integrated peak areas calculated by Andrew Bottrill, normalised to cell number are shown above. IP_3 shows slight changes in levels upon addition of Dox and therefore activation of IPMK. IP_4 also shows increases in quantities present in the cell upon addition of Dox but to a lower extent compared to IP_5 and IP_6. This data indicates that we see a clear increase in IP levels upon induction of IPMK in the conditional cell line and suggests the system is not "leaky" due to low levels of IP production without doxycycline.*

As seen in Figure 4-5 the level of IP_3 shows a reduction in KO(5) compared to WT(10) and KO(2). This contrasts with Figure 4-2 where we observed no change in IP_3 levels, suggesting that perhaps we lost some of the sample in KO(5). The lack of significant difference in IP levels between the parental cell line levels and 'no dox' TET-IPMK cell lines (Figure 4-5), suggests that IPMK is not being expressed at low levels in the absence of Dox, thus the inducible system is not 'leaky'. The addition of doxycycline to the TET-IPMK cells results in a slight increase in IP_3 levels compared to the 'no dox' samples. The level of IP_4, IP_5 and IP_6 present in the IPMK KO clones appears to be comparable to the levels witnessed previously, with IP_4 slightly higher, most likely due to the lack of internal control. We see an effective increase in IP levels upon addition of Dox, however, the level of induction of IP_4 and IP_5 is approximately 50-60% of endogenous levels. This could potentially be that despite the 82% homology between human IPMK and mouse IPMK, human IPMK could be less active or a longer incubation with Dox may be required to see saturation of IP levels. However, the level of IP_6 induction is similar to endogenous and therefore suggests that the former is not the case. Overall, this data suggests that we are able to induce IPMK and this results in an increase in IP levels in the cells, thus providing a good model system to investigate the effect of IP levels on HDAC activity in ES cells.

4.3 Deletion of IPMK does not impact global HDAC activity

To determine whether altering the levels of IP affects global HDAC activity levels, wildtype, knockout and TET-IPMK cells were cultured for 48 hours with the addition of doxycycline for 24 hours. Whole cell extract was generated and HDAC activity was assayed and normalised to the level of tubulin present, as assayed by western blotting. Deletion of IPMK, or induction with Dox had no effect on global HDAC activity Figure 4-6a & b. This is not altogether surprising as overexpression of IPMK itself did not affect global HDAC activity (Figure 3-1).

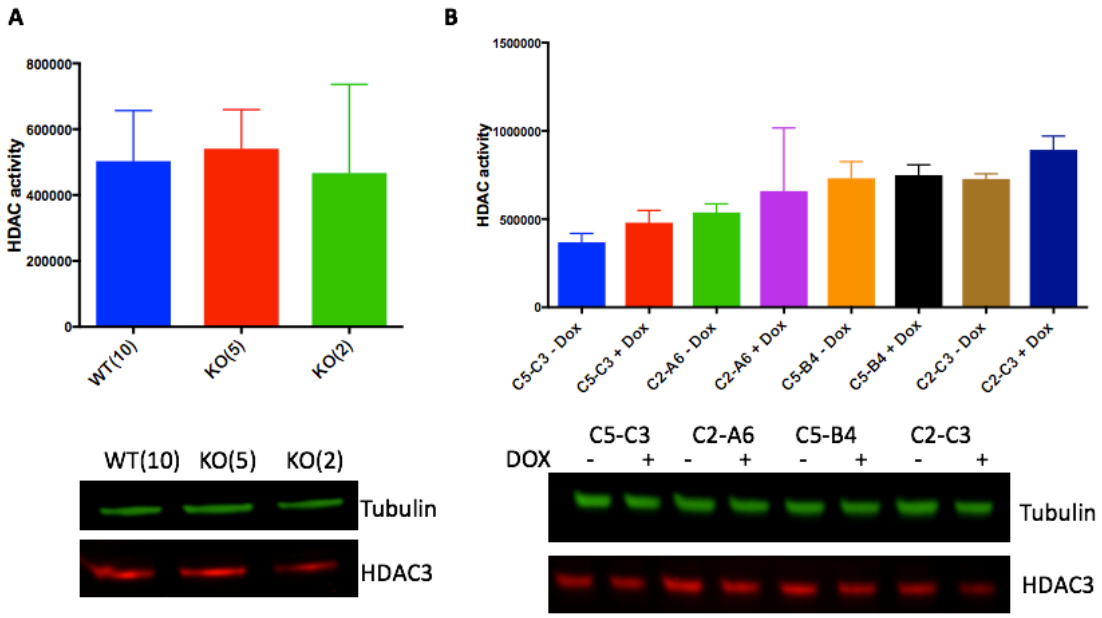

Figure 4-6 Deletion of IPMK has no effect on global HDAC activity. *IPMK parental cells and TET-IPMK cells were grown with and without Doxycycline for 24 hours and whole cell extract was extracted for histone deacetylase activity analysis and western blotting.* ***(A)*** *HDAC deacetylase activity was assayed from whole cell lysate of WT(10) and KO(5) and (KO(2) clones. Mean activity is shown where n=3 ±SD shown.* ***(B)*** *IPMK expression was induced by addition of doxycycline (Dox) for 24 hours before analysis of deacetylase activity on whole cell lysate was carried out.*

4.4 Global histone acetylation levels are not influenced by IPMK expression

Given the large induction in IPs between the IPMK KO cells and the rescue clones we believed it might have been possible to detect a change in histone acetylation levels. Specifically, we expected to observe changes at, H4K5Ac, H3K27Ac and H3K56Ac which all showed slight reductions upon addition of SMRT/HDAC3 previously in HEK-293 cells. All three of these marks have been previously been associated with class 1 HDACs. Indeed deletion of HDAC1 and HDAC2 results in an increase in H3K56Ac, whilst deletion of HDAC3 results in elevation of H3K27Ac marks at retinoic acid responsive genes and knockdown of SMRT/NCoR results in enhanced levels of H4K5Ac (Bhaskara et al, 2010; Dovey et al, 2010b; Jamaladdin et al, 2014; Urvalek & Gudas, 2014).

Consequently, depending on the level of regulation by IP, deletion of IPMK may reduce the level of acetylation at these sites through the reduction of HDAC activity. Alternatively, H3K9Ac and H3K18Ac levels have been shown to remain unchanged following deletion of HDAC1/2 (Jamaladdin et al, 2014). Accordingly, it would be expected that if IP's are regulating class I HDAC activity, then these marks should not alter, thus acting as a control. To ascertain whether IPMK deletions and rescue cells have differing levels of histone acetylation, cells were grown for 24 hours with Dox and histone was harvested via a standard acid extraction.

Analysis of several histone marks by quantitative western blotting (H3K9Ac, H3K14Ac, H3K18Ac, H3K27Ac, H3K56Ac and H4K5Ac) indicated limited changes in acetylation levels upon perturbation of IP levels (H3K56Ac increases 1.2-fold only in IPMK KO clones) (Figure 4-7). Previously, deletion of HDAC1/2 or 3 has been shown to result in alterations in histone acetylation levels in ES cells, for example increases in the H3K56Ac and H3K14Ac are observed upon loss of HDAC1/2 whilst H3K27Ac reveals alterations upon ablation of HDAC3 (Dovey et al, 2010b; Jamaladdin et al, 2014; Urvalek & Gudas, 2014). However, upon ablation or induction of IPMK we observe no significant changes in these marks (Figure 4-7). Although we see a 2-fold decrease in H3K56Ac levels in C5-C3 and C2-C3 upon addition of Dox, this effect is not consistent between TET-IPMK or KO clones (Figure 4-7). Consequently, histone acetylation doesn't appear to be influenced by IP levels suggesting that HDAC activity is unaffected by deletion of IPMK. Alternatively, it is possible that loci specific changes which cannot be detected using global analysis are taking place, as previously reported for H3K9Ac in HDAC3 ablated hearts (Montgomery et al, 2008).

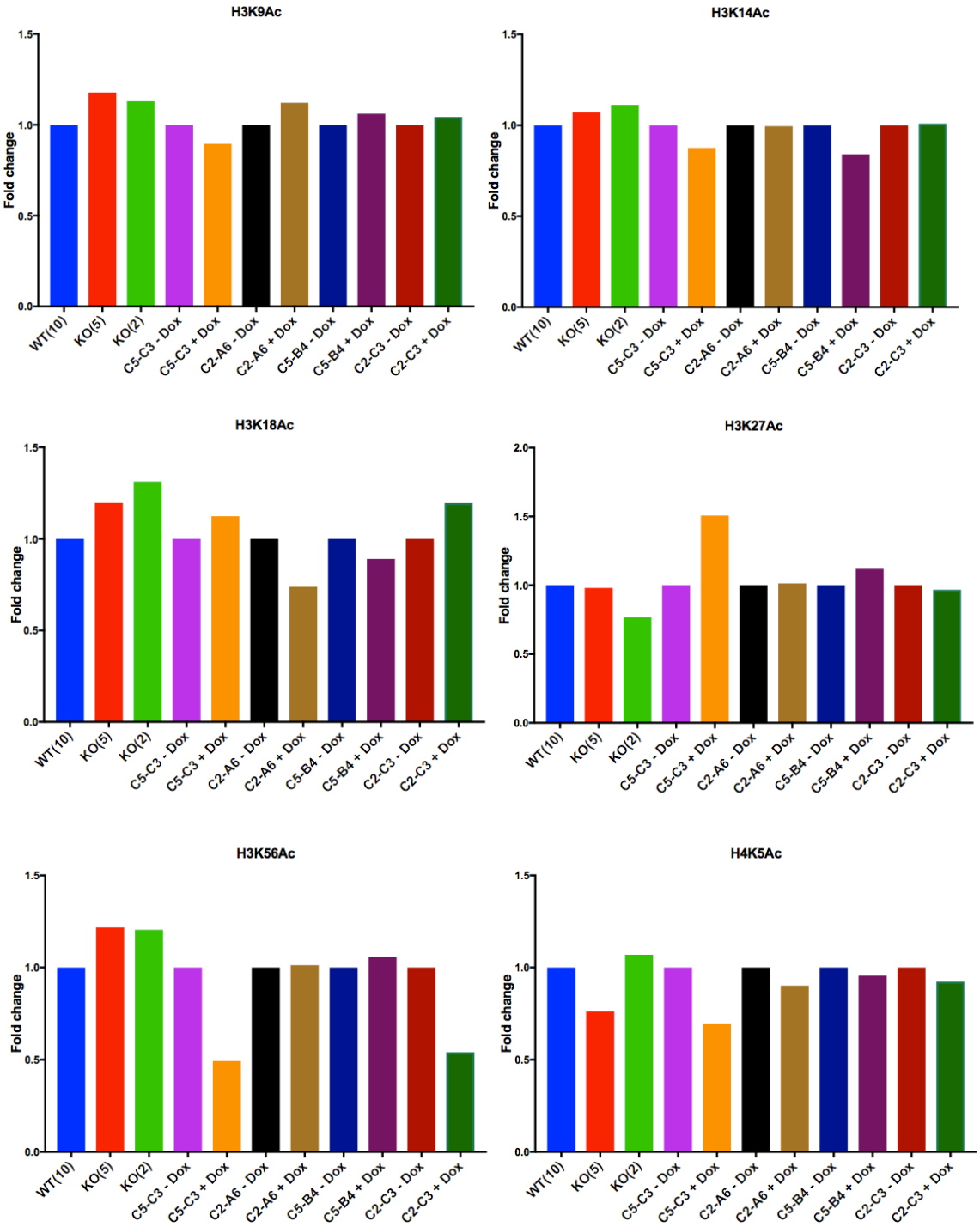

Figure 4-7 IPMK has limited effects on global histone acetylation levels. *Quantitative western blotting was carried out on TET-IPMK and parental IPMK KO clones following addition of dox for 24 hours. Cells were harvested and histones extracted using a standard acid extraction to enable analysis of histone H3 and H4 acetylation marks. Histones were extracted from wildtype, knockout and TET-IPMK cells 24 hours after induction of IPMK expression. Histone acetylation levels were normalised to the level of H3 or H4 relative to the wildtype or un-induced clone.*

4.5 Isolation of endogenous class 1 HDACs in IPMK KO cells indicates limited changes in HDAC activity

Due to the lack of change in global HDAC activity upon deletion of IPMK, we next isolated endogenous HDACs via Immunoprecipitation assays. This enabled the analysis of specific co-repressor complexes and removed any not regulated by IP, such as Sin3A. Previously, isolation of overexpressed SMRT/HDAC3 enabled us to detect changes in HDAC3 activity due to overexpression of IP pathway enzymes (chapter 3). Consequently, isolation of endogenous complexes should allow us to determine whether class 1 HDACs are regulated by inositol phosphates *in vivo*.

Initially, endogenous HDAC3 was isolated via a HDAC3 Immunoprecipitation assay using dyna beads. Following isolation, activity was assayed using a HDAC assay, normalised to the level of HDAC3 present as determined by western blotting (Figure 4-8b). Isolation of HDAC3 enabled us to detect a decrease in activity between the WT(10) and KO(2) ES cells (p-value = 0.0065) (Figure 4-8a). Conversely, no change in HDAC activity is observed between WT(10) and KO(5) (Figure 4-8a). The reason for this difference in HDAC3 activity between the two KO clones is not clear, especially since the level of IPs present in the cells are relatively consistent (Figure 4-2).

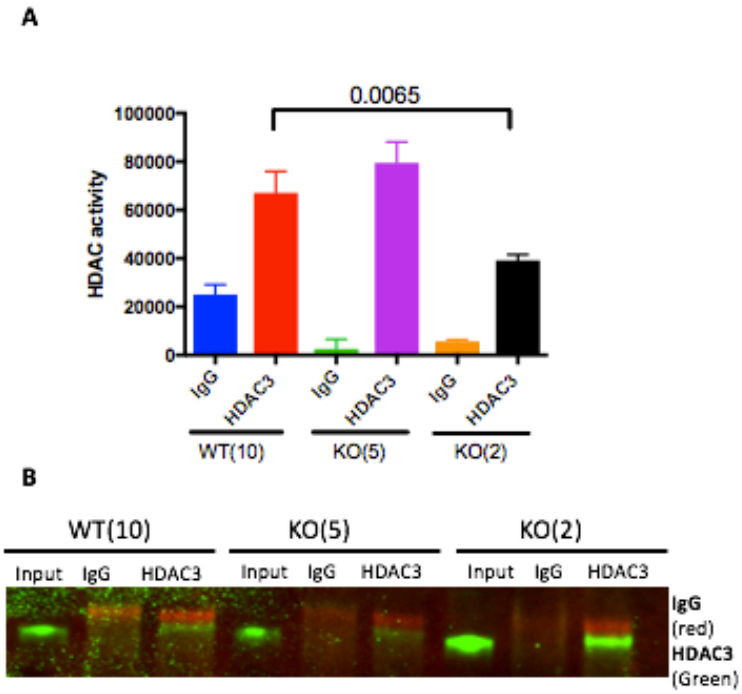

Figure 4-8 Isolation of the endogenous HDAC3 complex shows a reduction in HDAC activity. *TET-IPMK cells were cultured to confluency and whole cell extract was generated. Immunoprecipitation enabled isolation of HDAC3 which was assayed for deacetylase activity to determine the effect of IPMK.* ***(A)*** *Deacetylase activity was assayed by a HDAC assay following isolation of the endogenous HDAC3. Deacetylase activity is shown as n=3±SD where statistical significance (p-value) was calculated using a standard Two-tailed test.* ***(B)*** *Western blotting ensured isolation of HDAC3 and was used to normalise the HDAC assay.*

Following isolation of HDAC3 it was decided to isolate HDAC1/2. The antisera used is effective in Immunoprecipitation, however in theory, it isolates all HDAC1/2 complexes including; Sin3, CoREST, NuRD and MiDAC. Both MiDAC and NuRD have been shown to have increased activity upon addition of Ins(1,4,5,6)P_4 (Itoh et al, 2015; Millard et al, 2013). Whilst there is no published evidence for the activation of the CoREST complex by Ins(1,4,5,6)P_4; the fact that CoREST contains an ELM2-SANT domain which interacts with HDAC1/2 and contains the residues required for Ins(1,4,5,6)P_4 interaction, suggests that this corepressor complex would also be activated by Ins(1,4,5,6)P_4 (Watson et al, 2012; You et al, 2001). The Sin3 complex on the other hand does not encompass any proteins which contain a ELM2-SANT domain, consequently, it is not believed to be activated by Ins(1,4,5,6)P_4 and therefore may compensate for a decrease in IP levels (Millard et al, 2013). The activity of HDAC1/2 isolated via a

HDAC2 Immunoprecipitation was assessed via a HDAC assay and normalised to the level of HDAC2 present as quantified via western blotting (Figure 4-9b). As can be seen in Figure 4-9a, no significant difference was observed in endogenous HDAC activity between the WT or IPMK KO clones. As previously discussed this could be due to the Sin3 complex also being isolated in the Immunoprecipitation.

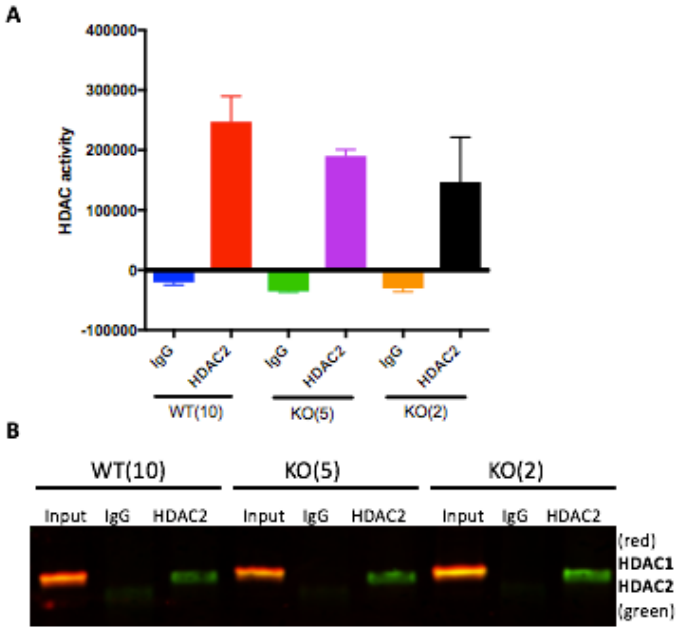

Figure 4-9 Isolation of the endogenous HDAC2 complexes has no effect on HDAC activity *Whole cell extract was generated from TET-IPMK cells and used in a HDAC2 immunoprecipitation to isolate HDAC1 and HDAC2 enabling analysis of their HDAC activity and determination of the effect of IPMK.* ***(A)*** *Deacetylase activity was assayed by a HDAC assay following to isolation of the endogenous HDAC2 complexes. Deacetylase activity is shown as n=3±SD.* ***(B)*** *Western blotting ensured isolation of HDAC1 and HDAC2. HDAC2 was used to normalise the HDAC assay.*

In an attempt to remove the effect of potential compensation via Sin3, LSD1 was used to isolate the CoREST complex (HDAC1/2, LSD1, CoREST, BHC80, CtBP and BRAF35) (Hakimi et al, 2002; Lee et al, 2005; Shi et al, 2003; You et al, 2001). Complex activity was analysed by a HDAC assay and normalised to the level of HDAC2 pull down (Figure 4-10b). However, we do not observe a significant change in the HDAC activity of the CoREST complex upon deletion of IPMK when compared to the WT ES cell line (Figure 4-10a). The overarching issue with this experimental method, and possible explanation

for the lack of observed changes in HDAC activity, is that we are uncertain whether inositol phosphates remain bound to the HDAC complexes at the salt concentrations required for this experiment. Loss of IP from the complex would render any changes in HDAC activity undetectable due to the purification process, and as such could explain the lack of change.

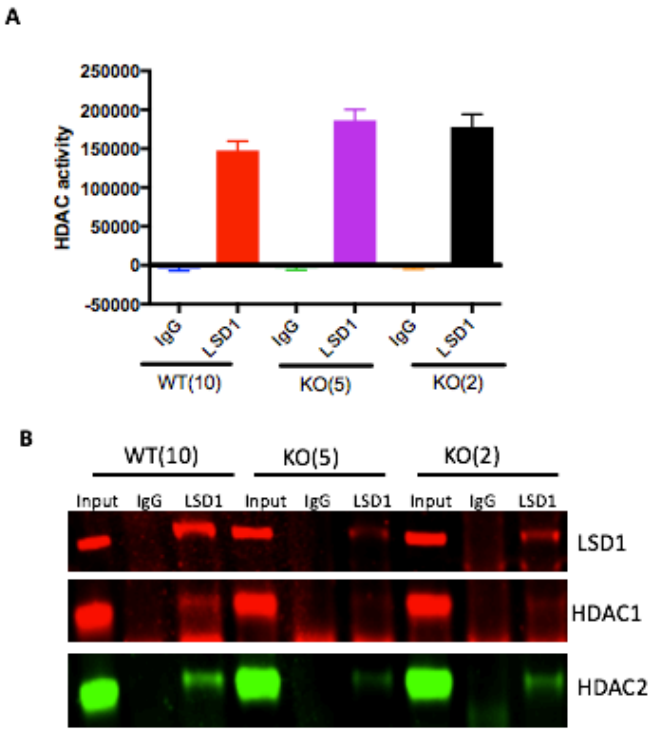

Figure 4-10 Isolation of the endogenous CoREST:LSD1:HDAC1/HDAC2 complex has no effect on HDAC activity *An LSD1 antibody was used to immunoprecipitate the CoREST complex from whole cell extract generated from TET-IPMK cells to enable deacetylase activity to be assayed.* ***(A)*** *Deacetylase activity was assayed by a HDAC assay following to isolation of the endogenous CoREST complex via an LSD1 Immunoprecipitation. Deacetylase activity is shown as n=3±SD.* ***(B)*** *Western blotting ensured isolation of LSD1, HDAC1 and HDAC2. HDAC2 was used to normalise the HDAC assay.*

4.6 IPMK deletion has a partial effect on HDAC3 target gene expression

To identify the effect of manipulating IP levels in cells we next examined potential HDAC3 target genes in ES cells. HDAC3 target genes have been identified previously via tissue specific deletions such as in the liver (Sun et al, 2012). However, as our IPMK knockout cells are ES cells, we needed to identify HDAC3 target genes in pluripotent cells. Recently, in our laboratory, Lyndsey Wright has generated conditional HDAC3 knockout ES cells on which she carried out a microarray comparing the cells with and without HDAC3. This enabled us to identify genes with increased expression upon deletion of HDAC3 and therefore should in theory increase upon deletion of IPMK. Upon ablation of HDAC3 the following genes showed increased expression levels for Hnf4α, HoxB2, CD68, Hist1h2bq, Tbx30s2 and Rpgrip, of 3.4, 3.9, 5.6, 6, 6.9 and 10-fold respectively.

TET-IPMK ES cells (grown in 2i media to replicate HDAC3-KO conditions) were induced for 24h with Dox and the RNA extracted for qRT-PCR analysis. Three genes analysed, Tbx30s2, CD68 and Rpgrip exhibited increased expression upon deletion of HDAC3 consistent with the HDAC3 KO microarray. However, no changes were detected between WT(10) or KO(5) and KO(2), indicating alterations in IP levels are not sufficient to alter their expression (Figure 4-11). In contrast, all remaining genes tested (Hnf4α, HoxB2 and Hist1h2bq) exhibited increased expression upon ablation of HDAC3 and alterations in expression upon manipulation of IPMK (Figure 4-11). These changes in expression however are not consistent across genes or clones. For example, both Hnf4α and Hist1h2bq result in increased expression in KO(2) but not KO(5) when compared to WT(10). Additionally, in both Hnf4α and Hist1h2bq, upon addition of Dox two TET-IPMK clones (C5-C3 and C2-C3 respectively) show decreased expression, suggesting potentially increased HDAC3 activity. HoxB2 induction increases over 2-fold in both KO(5) and KO(2) compared to WT(10) (Figure 4-11). This indicates that deletion of IPMK may be altering HDAC3 activity due to a decrease in IP resulting in a less active HDAC3 akin to the effect of the HDAC3 KO. This is further supported by decreased

expression of HoxB2 upon addition of Dox to C5-C3. Conversely, an increase in HoxB2 expression is detected in clones C5-B4 and C2-A6 (1.6-fold and 4.5-fold respectively) (Figure 4-11). This enhanced expression is unanticipated as an increase in IP levels, brought on by IPMK induction, should decrease expression of HoxB2 due to the increasing activity of the SMRT/HDAC3 complex.

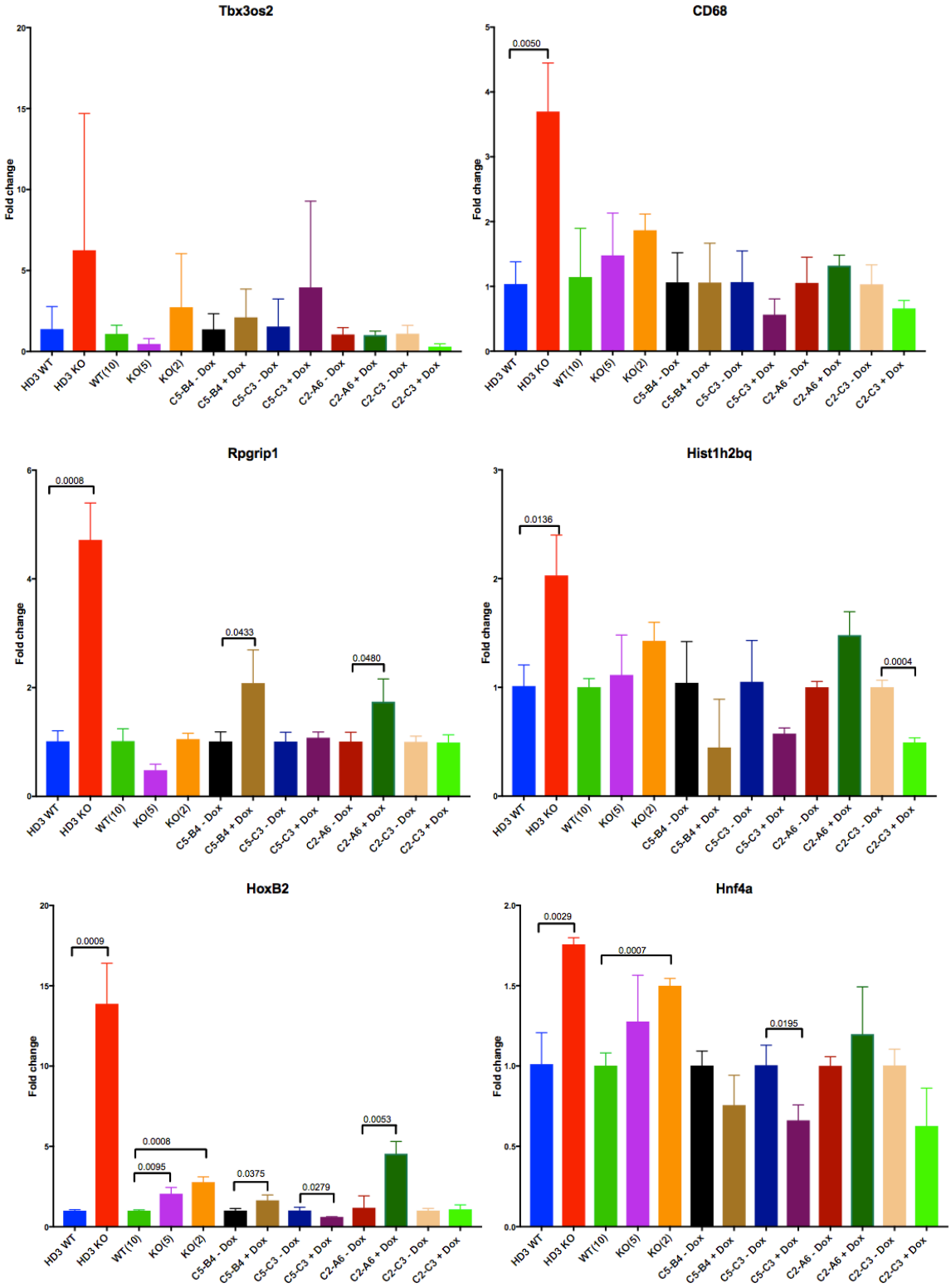

Figure 4-11 IPMK has minimal effects on ES cell HDAC3 target genes. IPMK parental cells and TET-IPMK cells were grown in 2i media for two weeks and treated with Doxycycline for 24 hours prior to RNA extraction. *Quantitative RT-PCR of HDAC3 target genes (taken from L. Wright 2017 microarray) was carried out in HDAC3 conditional KO ES cells as a control and compared to IPMK cells. All values are represented as mean fold change where n=3 ±SD. Values represent expression of the gene relative to B-actin reference gene.*

Due to the inconsistencies in results across clones, two genes were chosen from the HDAC3 KO microarray to act as controls. Controls (CDS2 and Fam35a) were chosen based on an absence of change in expression levels (1-fold change) upon HDAC3 deletion. Analysis of qRT-PCR data revealed, analogous to the HDAC3 KO microarray, a 1.2-1.4-fold change between HDAC3 WT and KO cells for both control genes, indicating an absence of change in expression (Figure 4-12). Consistent with this, alterations in expression of CDS2 and Fam35a between cells expressing and not expressing IPMK were all within a 1.5-fold change range, indicating that they are within the tolerance of the assay and show non-significant changes (Figure 4-12). A 60% reduction in Fam35a expression was detected for one clone, C5-C3, upon addition of Dox (Figure 4-12). This is just above the threshold for the assay and indicates that alterations detected in HDAC3 target genes for this clone may be due to clonal differences rather than the effects of IP.

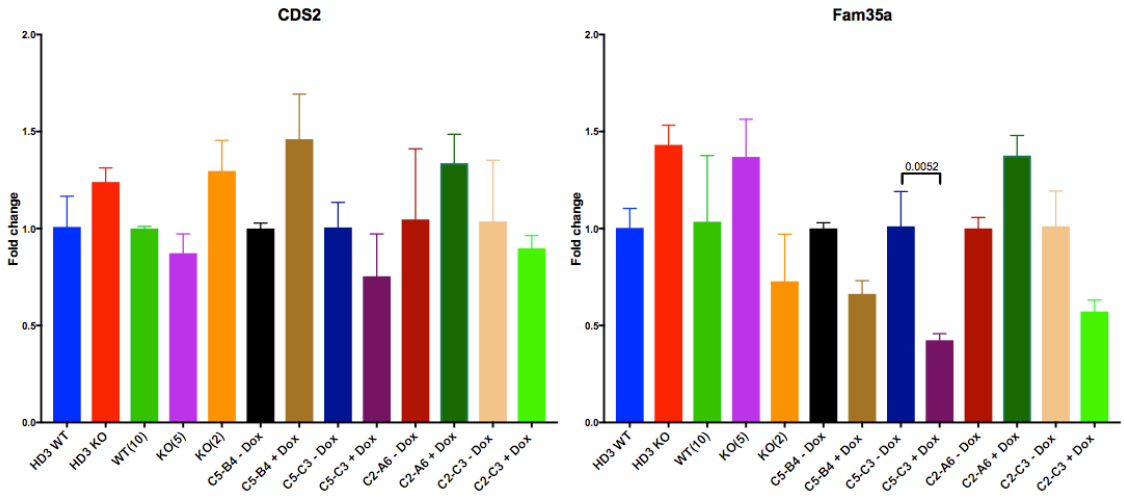

Figure 4-12 Deletion of IPMK does not affect Non-HDAC3 target genes *Quantitative RT-PCR data of genes identified as unchanged in HDAC3-/- conditional knockout ES cells is shown. qRT-PCR was performed on cDNA of 2i treated IPMK wildtype, knockout and rescue cell lines. All values are represented as mean fold change where n=3 ±SD. Values represent expression of the gene relative to B-actin reference gene.*

In summary, the fold changes in gene expression observed upon manipulation of IPMK expression are generally less than 2-fold, which is around the cut-off of many microarrays. Despite hints that IPMK may be altering expression of HDAC3 target genes, without larger fold changes consistent between clones, it is hard to draw definitive conclusions on whether alterations in IP levels are altering the level of expression of HDAC3 target genes or whether changes observed are due to clonal variation.

4.7 Cell cycle progression of ES cells is not affected by deletion of IPMK

A double knockout HDAC1/2 ES cell line implicated HDAC1 and HDAC2 in chromosome segregation in M phase (Jamaladdin et al, 2014). Furthermore, deletion of HDAC3 in MEFs and silencing of HDAC3 in human colon cancer reveals a delay in cell cycle progression (Bhaskara et al, 2008; Wilson et al, 2006). Consequently, we aimed to establish whether deletion of IPMK results in a similar delay in cell cycle progression through a reduction in HDAC activity via decreased IP levels. As can be seen in Figure 4-13 neither deletion of IPMK or induction of IPMK via dox resulted in a difference in population doubling time suggesting that deletion of IPMK does not abolish the ability to regulate progression through the cell cycle.

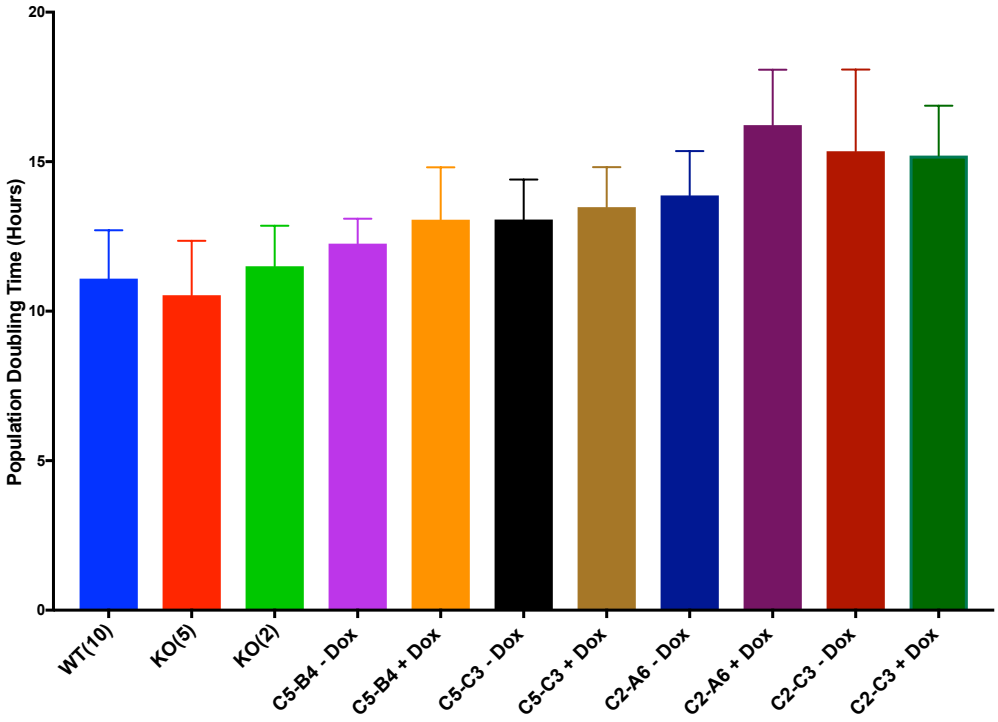

Figure 4-13 No difference is observed in population doubling time between wildtype, IPMK knockout or IPMK rescue cell lines. *Equal number of IPMK parental and TET-IPMK cells were plated out on day 0 in triplicated and counted in triplicate every 24 hours for a period of 4 days. Mean population doubling time shown where n=12±SD.*

4.8 Investigating the effect of inositol phosphates and cell cycle on HDAC activity

Despite the lack of change in population doubling time there is evidence that IP levels change during the cell cycle in rat mammary tumour cells (WRK-1 cells) (Barker et al, 2004). The levels of histone deacetylases do not appear to alter at the protein level during the cell cycle (Bhaskara et al, 2010; Dangond et al, 2001). However, there are several studies which suggest that acetylation levels do change during the cell cycle (Li et al, 2008; Ma et al, 2015; Unnikrishnan et al, 2010). To examine IP levels throughout the cell cycle, WT(10) ES cells were synchronised with consecutive treatments of the Cdk1 inhibitor (Ro3306), followed by Nocodazole. Treatment with Ro3306 enables the generation of a sample representative of G2, subsequent release and treatment with Nocodazole forms a population of M phase cells (Vassilev, 2006) (Figure 4-14). Following removal of Nocodazole, cells were cultured for a further 2 hours to generate

a G1 sample, an S phase sample was collected 5 hours post Nocodazole treatment as analysed by propidium iodide (PI) staining (Figure 4-14). A natural G2/M sample was harvested at 10 hours to ensure any differences in IP levels or HDAC activity were due to the cell cycle and not the inhibitor.

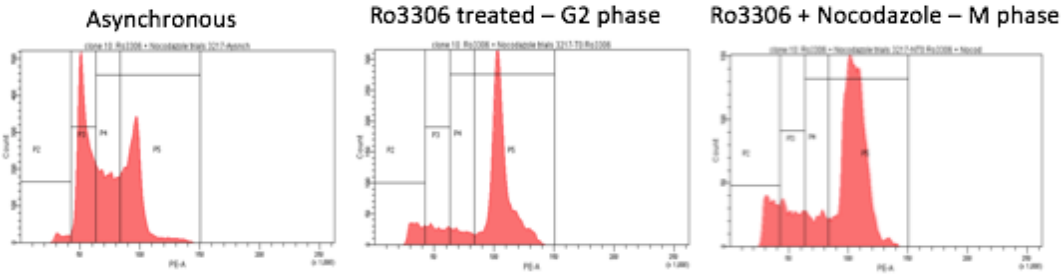

Gate	Phase	Cells (%)
P2	<G1	1.8
P3	G1	37.2
P4	S	24.8
P5	G2/M	36.2

Gate	Phase	Cells (%)
P2	<G1	8.1
P3	G1	9.9
P4	S	7.7
P5	G2/M	74.2

Gate	Phase	Cells (%)
P2	<G1	10.4
P3	G1	11.8
P4	S	10.0
P5	G2/M	67.8

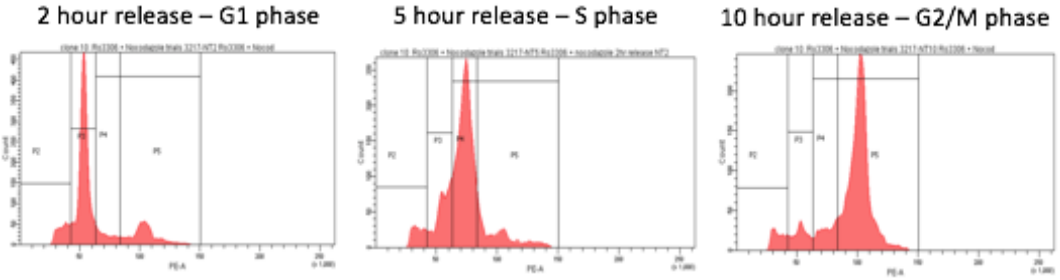

Gate	Phase	Cells (%)
P2	<G1	10.2
P3	G1	62.5
P4	S	8.4
P5	G2/M	18.9

Gate	Phase	Cells (%)
P2	<G1	6.4
P3	G1	19
P4	S	59.1
P5	G2/M	15.6

Gate	Phase	Cells (%)
P2	<G1	6.2
P3	G1	9.1
P4	S	10.3
P5	G2/M	74.4

Figure 4-14 Propidium iodide staining of synchronised WT(10) ES cells. *Cells were synchronised using Ro3306 and Nocodazole and harvested in 70% ethanol and stored at -20^{o}C. Propidium iodide staining was carried out and samples were analysed in the PE-A channel on the BD FACS Canto. FACS plots are shown as well as tables indicating the percentage of cells in each phase of the cell cycle.*

Following synchronisation, IP levels were analysed by anion exchange chromatography with tandem mass spectrometry. All the samples bar G2 were sent for analysis because a minimum of $2x10^6$ cells were required for analysis. Previously, it has been shown that the level of IP_4, IP_5 and IP_6 is highest in G1 and declines in S phase, followed by a slight increase in M phase (Barker et al, 2004). Our results concur in that we observe an increase in IP_4, IP_5 and IP_6 levels from S phase to M phase (Figure 4-15). However, for all IP species Barker et al,. report the highest levels during G1, we on the other hand, do not detect this effect. Furthermore, we observe only a minimal change between G1 to S phase (Figure 4-15). The difference in results may be due to differing cell types and analytical methods used.

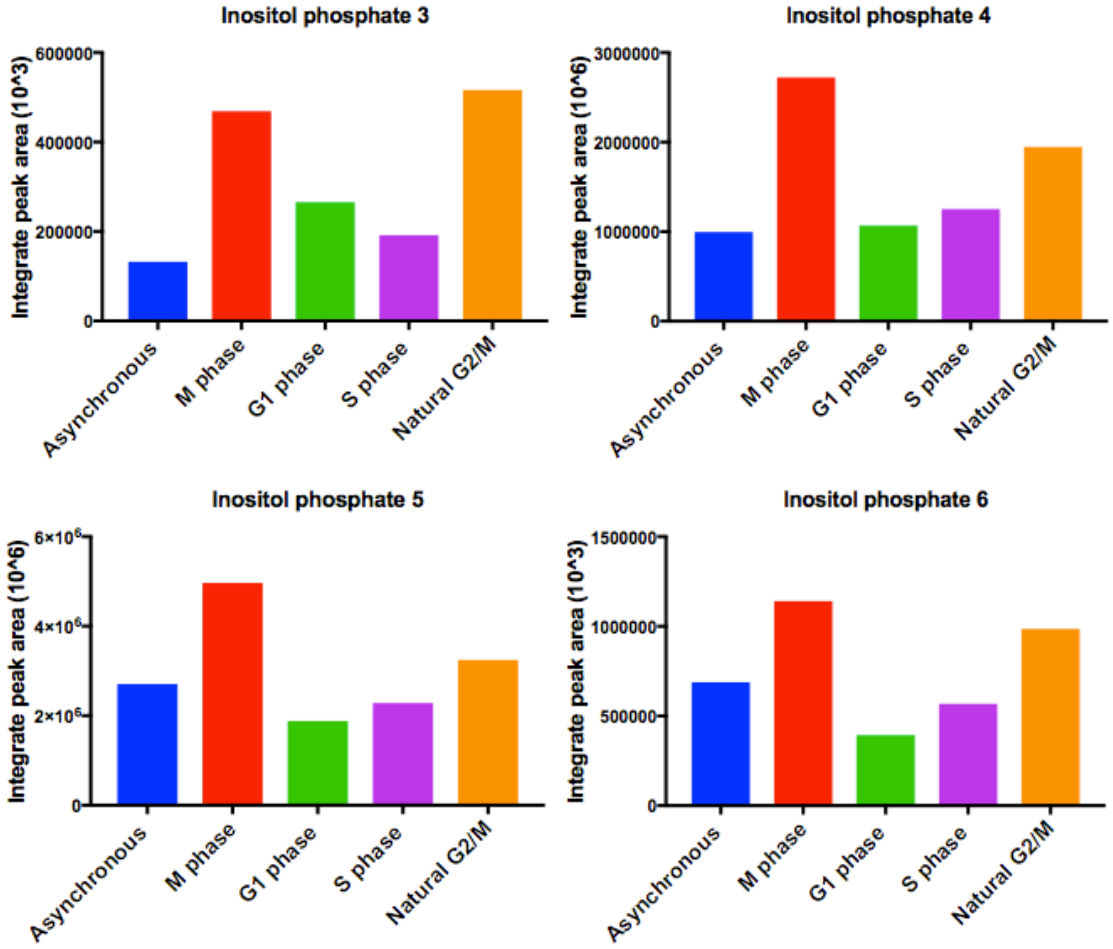

Figure 4-15 Inositol phosphate levels fluctuate during the cell cycle. *Analogous samples to those seen in figure 4-14 were harvested for IP mass spectrometry analysis. Integrated peak areas were provided by Andrew Bottril in PNACL and were normalised to live cell number ($2x10^7$ for each sample). (Ro3306 treated sample is not shown due to low cell numbers). Natural G2/M refers to 10 hours following removal of inhibitors.*

As we detected changes in IP levels, we next analysed the level of histone acetylation and HDACs at various stages of the cell cycle. Cells were synchronised as shown in Figure 4-14 and whole cell extract and histone extract was generated. To ensure M and G2/M phase samples were representative of M phase, Histone 3 Serine10-phosphorylation (H3S10P) was analysed. The M phase sample shows a 33-fold increase in H3S10P compared to the asynchronous sample and a 7-fold increase is observed in the G2 sample suggesting that some cells are entering M phase (Figure 4-16). Surprisingly, an increase in H3S10P is not observed in the natural G2/M sample indicating that the cells are still in G2, rather than M, as indicated by PI staining (Figure 4-14).

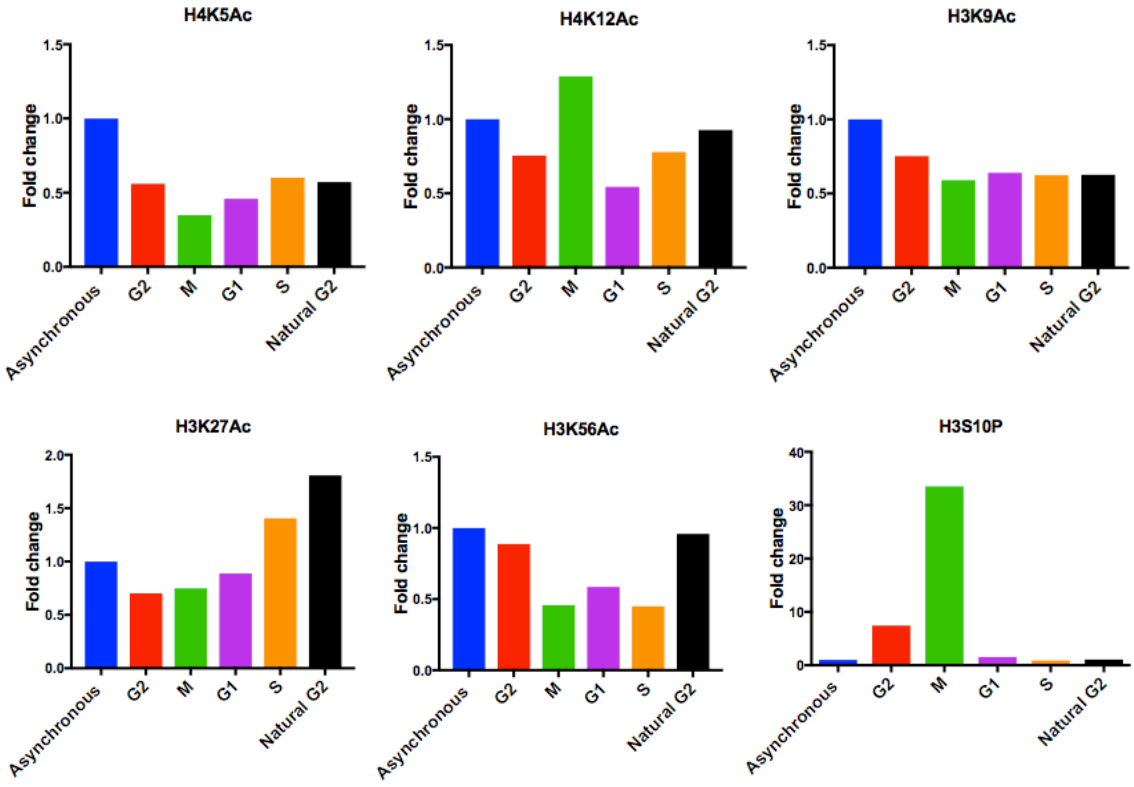

Figure 4-16 Histone acetylation marks show minor changes during the cell cycle in mouse embryonic stem cells. *Quantitative western blot analysis was carried out on synchronised acid extract. Histone acetylation marks were normalised to H3 or H4 histone relative to the asynchronous sample. Natural G2/M refers to 10 hours following removal of inhibitors.*

Overall acetylation appears to be lowest during M phase for all marks bar H4K12Ac, this is consistent with the formation of compacted chromatin during mitosis (Figure 4-16). Although not significant, H4K5Ac and H3K27Ac show slight elevations in levels

during S phase, consistent with the suggestions that H4K5Ac levels increase during S phase (Figure 4-16) (Ma et al, 2015; Sobel et al, 1995). Furthermore, H3K56Ac shows the highest level of acetylation during G2 and the lowest levels during M, G1 and S phase, despite previously being reported to be at its highest level in S phase (Figure 4-16) (Li et al, 2008). The reason for the lack of significant increase during S phase could be due to the fact that often increases are only observed at origins of replications not globally (Unnikrishnan et al, 2010). Overall changes appear to be non-significant suggesting that histone acetylation levels are not altering as much as previously proposed, perhaps due to the high levels of basal acetylation levels found in ES cells (Boyer et al, 2006).

Analysis of protein expression revealed that cyclin A, which facilitates progression through the cell cycle, shows low levels of expression in G1 and S phase with higher levels in G2 (Figure 4-17) (Mateo et al, 2010). The level of fold change is relatively small and correlates with the 2-3-fold changes previously observed in embryonic stem cells compared to the 10-30-fold changes observed in somatic cells (Ballabeni et al, 2011). Consistent with previous results, HDAC3 protein level does not appear to significantly alter through the cell cycle (Bhaskara et al, 2010). In contrast, alterations in protein level of HDAC1 and HDAC2 are detected throughout the cell cycle, with highest protein levels occurring during S phase (Figure 4-17). Despite reports that HDAC1 levels do not change in MEFs, it has been reported that HDAC1 expression increases at G1/S in L929 cells (Dangond et al, 2001).

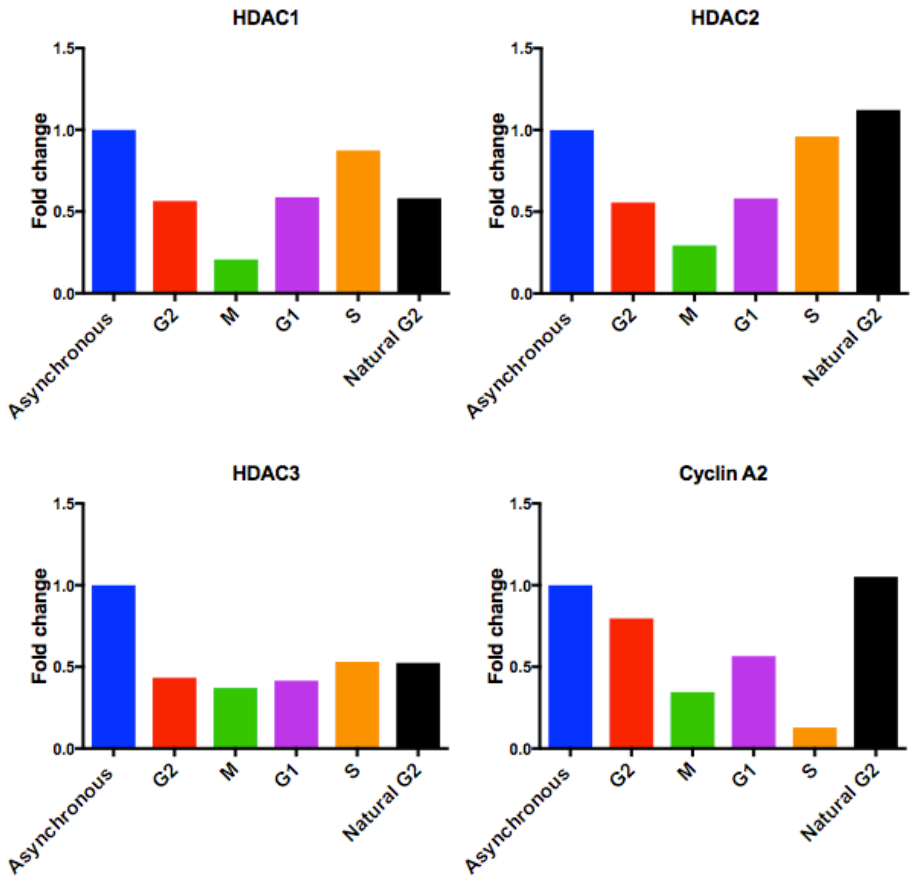

Figure 4-17 Protein levels of HDAC1/2 and Cyclin A2 fluctuate during the cell cycle. *Quantitative western blot analysis was carried out on synchronised whole cell lysate. HDAC1/2/3 and cyclin A2 levels were normalised to tubulin levels relative to the asynchronous sample.*

4.8.1 Changes in HDAC activity correlate with HDAC1/2 expression, but not inositol phosphate levels

To determine whether the change in IP and lack of change in HDAC3 protein was affecting HDAC activity in ES cells cell cycle, a global HDAC assay was carried out on synchronised cells. Analysis of global HDAC activity revealed alterations throughout the cell cycle (Figure 4-18). The level of HDAC activity significantly increases from G2 to S phase (p-value = 0.0011), this effect is also observed upon progression from M to S phase (p-value = 0.0088) and G1 to S phase (p-value = 0.0009) (Figure 4-18). Consequently, it appears that HDACs are most active during S phase, however, all samples are significantly decreased when compared to the natural G2 sample.

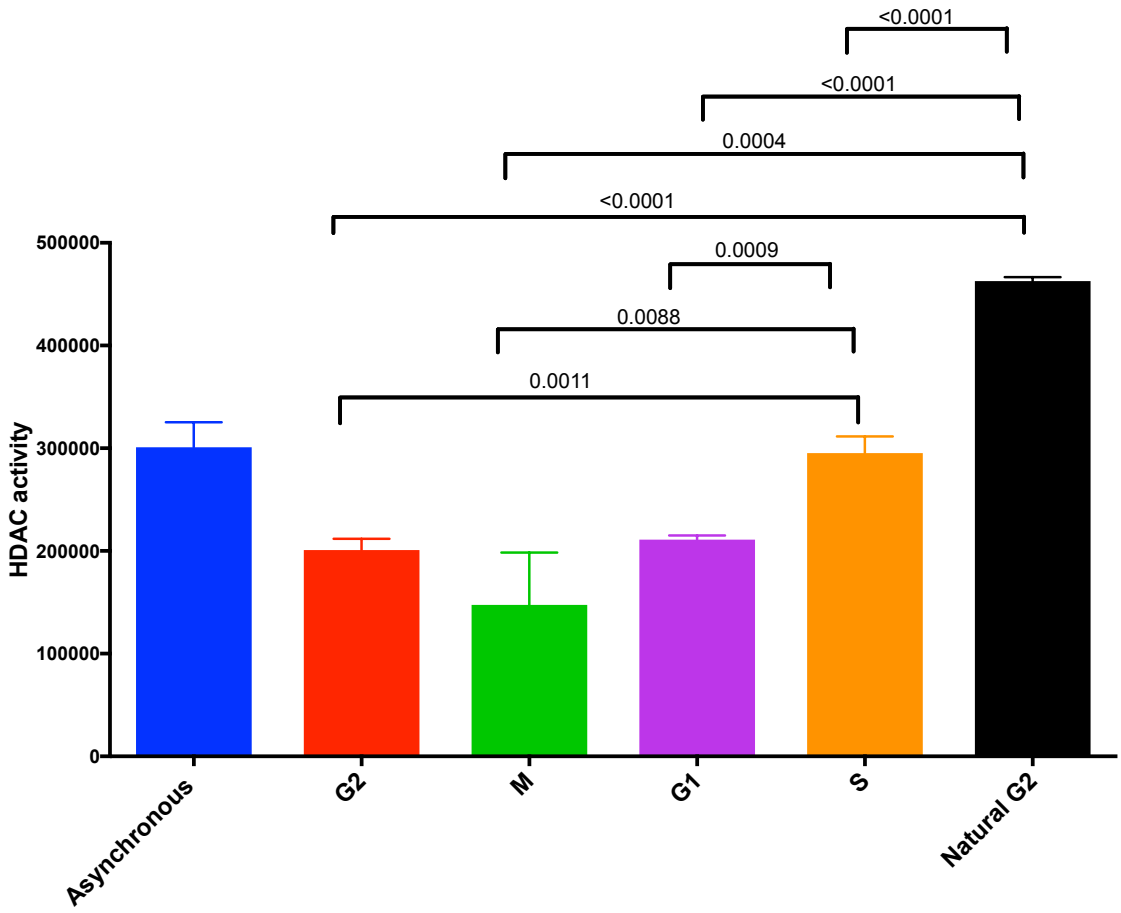

Figure 4-18 Global HDAC activity alters during the cell cycle. *Whole cell extract of synchronised samples was harvested and global HDAC activity analysed by a global deacetylase assay. Mean deacetylase activity is shown were n=3±SD. Statistical significance (p-value) was calculated using a two-tailed T test. A western blot was run to normalise the HDAC assay to tubulin (not shown).*

Although alterations in HDAC activity are observed, these do not correlate with the changes in IP levels as indicated in Figure 4-15. When the level of HDAC activity is highest (S phase) the level of IP appears to be at its lowest. Furthermore, when the highest level of IPs are present in M phase we detect the lowest level of HDAC activity. Consequently, these data suggest that *in vivo*, the level of IP present in the cell is not indicative of HDAC activity. Moreover, the protein level of HDAC1/2 fluctuate during the cell cycle, and increased activity detected in the HDAC assay corresponds with increased protein level (Figure 4-17 and Figure 4-18). Accordingly, this suggests that the adjustment in protein level and not inositol phosphates may be responsible for the altered activity observed during the cell cycle.

4.9 Summary

In this chapter I have shown that deletion of IPMK reduces IP levels compared to WT cells comparable to Frederick et al, 2005, and this can be rescued to almost endogenous levels with the addition of IPMK in a tetracycline inducible cell line (Figure 4-1 & Figure 4-5). However, despite this large-scale ablation of IP levels, HDAC activity is not altered at a global level (Figure 4-6). Furthermore, whilst one of the knockout clones, KO(2) indicated a decrease in HDAC3/SMRT activity was not replicated with a second KO clone, KO(5), or HDAC1/2 complexes (Figure 4-8, Figure 4-9 and Figure 4-10). Moreover, qRT-PCR analysis of HDAC3 target genes and respective controls with and without IPMK revealed conflicting results surrounding the effect of IPMK deletion and induction (Figure 4-11, Figure 4-12). Additionally, although changes in HDAC activity can be detected during the cell cycle, this cannot be related to the level of inositol phosphates present. Accordingly, we are unable to provide conclusive evidence that IPMK or IP levels affect the activity of class I HDACs *in vivo.*

Chapter 5 Understanding the role of IPMK in embryonic development

5.1 Chapter aims

In chapter 4, I described a Dox inducible IPMK rescue cell line generated from IPMK knockout ES cells from the York group (Frederick et al, 2005). These cells indicated that IP levels were not regulating global HDAC activity in ES cells. However, it is possible that the regulation of HDACs by IPMK may only become important during differentiation or upon differentiation into a somatic cell line. HDACs have been implicated in early embryogenesis with mouse models often resulting in prenatal or perinatal embryonic lethality (Bhaskara et al, 2008; Lagger et al, 2002; Montgomery et al, 2007; Montgomery et al, 2008; Trivedi et al, 2007; Zimmermann et al, 2007). The lethality of the histone deacetylase deletion, indicates a role for these enzymes in embryogenesis in distinct ways. Additionally, the parental ES cells from which the inducible IPMK rescues were generated, were isolated from a knockout mouse model which exhibited embryonic lethality at embryonic day 9.5 (E9.5) (Frederick et al, 2005). The relatively early embryonic lethality suggests a potential role for IPMK in gastrulation. A similar phenotype was described for the IPK1 knockout mouse model which displayed embryonic lethality at E8.5, indicating an essential role for IPs during embryogenesis (Verbsky et al, 2005a).

Consequently, in this chapter I aimed to establish whether a difference in global HDAC activity could be detected in TET-IPMK ES cells differentiated with retinoic acid. Furthermore, I aimed to examine the role of IPMK during embryonic development through the differentiation of ES cells into embryoid bodies (EBs) and establish phenotypic and genetic similarities with the role of HDACs in embryogenesis.

5.2 Investigating the effect of differentiation on HDAC activity in IPMK knockout cells

To ascertain whether the regulation of HDAC complexes by IP becomes more important in non-pluripotent cells, TET-IPMK cells were treated with retinoic acid (RA) for 5 days in DMEM:F12 media. RA treatment results in differentiation towards a neuronal fate, enabling us to determine whether HDAC activity is altered in somatic cells upon deletion of IPMK. Following addition of RA to TET-IPMK cells in the presence or absence of Dox, cells were harvested and whole cell extract generated. Western blot analysis revealed that RA treated cells were not expressing key pluripotency markers, Oct4 and Nanog, thereby indicating they were no longer pluripotent cells (Figure 5-1).

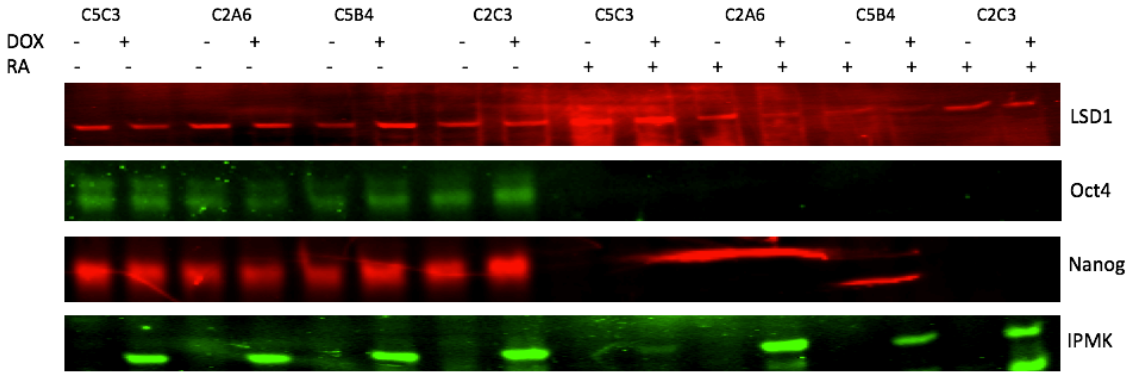

Figure 5-1 Retinoic acid treatment induces loss of pluripotency in ES cells after 5 days. *Quantitative western blot analysis shows the absence of Oct 4 and Nanog protein in whole cell extract from RA treated TET-IPMK cells vs pluripotent TET-IPMK ES cells. Cells were cultured for 5 days with or without IPMK in the presence or absence of Doxycycline. LSD1 was used to normalise protein loading, IPMK is present only in cells treated with doxycycline indicating induction was successful.*

5.2.1 RA mediated differentiation of IPMK KO cells has a limited effect on HDAC activity

After establishing that the RA treated cells have exited the pluripotent state (Figure 5-1) a global HDAC assay was carried out. As previously observed in chapter 4, we observed no change in HDAC activity in the control ES cells (Figure 5-2a). However, upon RA mediated differentiation we begin to discern alterations in global HDAC activity (Figure 5-2a). Addition of doxycycline to C2-A6 in the presence of RA results in a statistical increase in HDAC activity (p-value = <0.0001). Although the other clones assayed do not result in a statistical increase in HDAC activity, we do observe hints of increase upon addition of doxycycline in clone C2-C3 treated with RA. However, C5-C3 reveals an absence of change in the RA treated cells upon addition of Dox (Figure 5-2a). C5-B4 was not included in the global HDAC assay once treated with RA due to the relatively low abundance of tubulin present, thus rendering normalisation of its HDAC activity difficult (Figure 5-2b). Due to the differential responses to RA ± Dox between the clones it's difficult to conclude that IPs impact HDAC activity in non-pluripotent cells more than ES cells. Any changes detected are likely to be clonal variation rather than a direct effect of IP regulation.

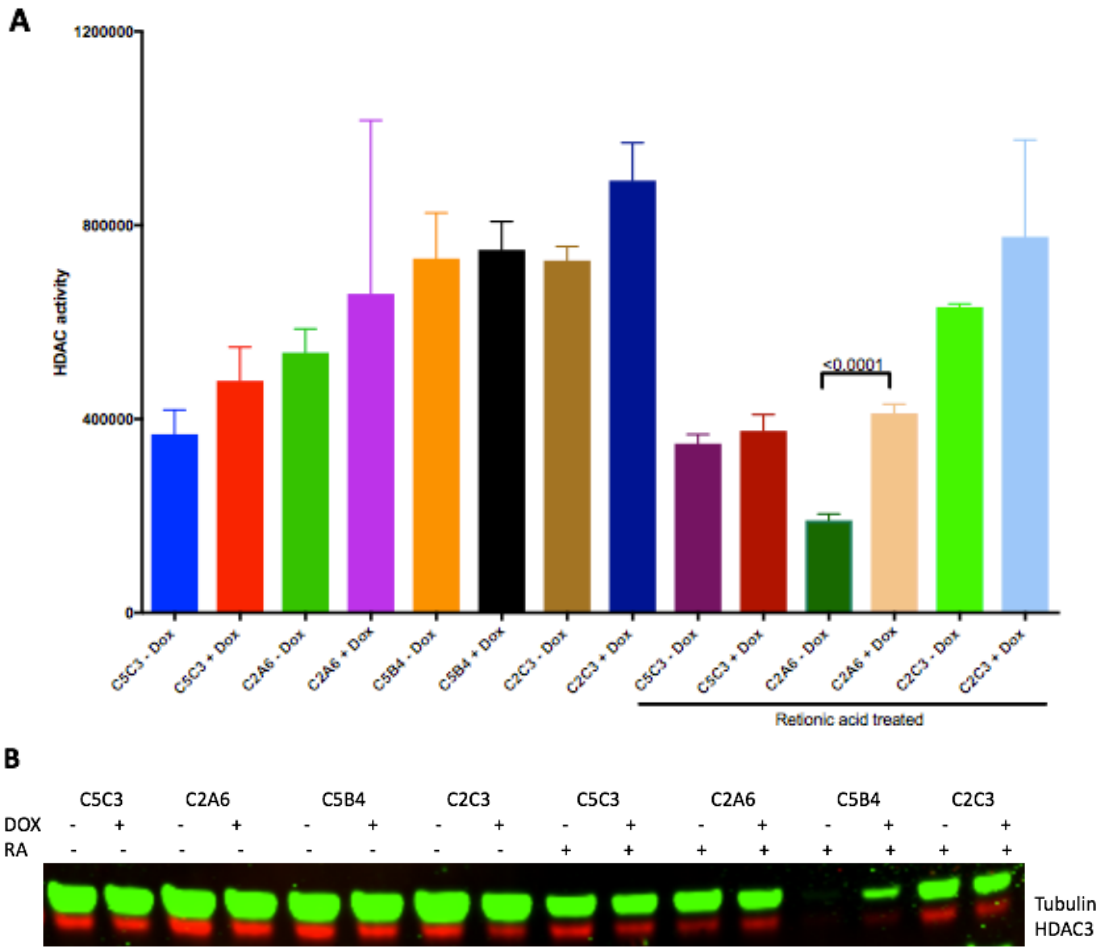

Figure 5-2 Deletion of IPMK has limited effect on global HDAC activity in retinoic acid treatment cells. *TET-IPMK cells were treated with or without retinoic acid for 5 days ± Doxycycline to induce loss of pluripotency in the presence or absence of IPMK* ***(A)*** *Mean deacetylase activity was measured in whole-cell extracts after 5 days of treatment ±RA. Deacetylase activity is shown for 30ug of whole cell extract where n=3 ±SD, the statistical significance (p-values) were calculated using a Standard Two-tailed T-test* ***(B)*** *Quantitative western blot analysis of 30ug of whole-cell extract was used to normalise the HDAC assay relative to the level of tubulin expression a house-keeping gene.*

5.2.2 Deletion of IPMK has minimal effect on global histone acetylation in differentiated ES cells

Previously, analysis of global histone acetylation levels failed to reveal significant changes upon deletion of IPMK, potentially due to the high basal level of histone acetylation in ES cells (Figure 4-7) (Boyer et al, 2006; Das et al, 2009a). Following differentiation, it is reported that the level of histone acetylation marks such as H3K56Ac and H3K9Ac decrease, accordingly it is possible that a reduction in HDAC

activity may be more readily observed (Das et al, 2009a; Qiao et al, 2015). Consequently, the level of histone acetylation at key lysine residues in H3 and H4 were analysed in TET-IPMK cells upon RA treatment ± Dox.

Quantitative western blotting of histone acetylation levels revealed minimal alterations in levels, although these were not consistent between samples. Both H4K5Ac and H3K9Ac exhibit a lack of change in acetylation between clones after treatment with RA (Figure 5-3). Unlike H4K5Ac, H3K9Ac does not result in a decrease in acetylation levels following RA treatment (Figure 5-3). This is unexpected as studies have indicated that H3K9Ac levels decrease during the initial stages of neuronal differentiation in human ES cells (Qiao et al, 2015). Although this study utilised an EB stage and we used serum containing media which blocks neuronal differentiation, it has been suggested that somatic cells have decreased acetylation levels and increased heterochromatin compared to ES cells (Boyer et al, 2006). Consequently, we would expect to detect decreases in acetylation levels compared to ES cells if H3K9Ac levels are altering during differentiation. The remaining histone acetylation marks assayed indicated changes in levels upon addition of RA and Dox, however, these were inconsistent between clones. For example, H3K14Ac and H3K27Ac indicated a 1.5 fold decrease in acetylation levels in differentiated clone C2-C3 in the presence of Dox, however, no other clones exhibited this effect (Figure 5-3). Moreover, whilst H3K18Ac and H3K56Ac levels decrease in some clones following addition of Dox to RA treated clones (C5-C3 and C2-A6 & C5-B4 respectively), other RA treated clones counterintuitively indicate increases in acetylation following addition of Dox (C2-A6 & C2-C3 and C5-C3 respectively) (Figure 5-3).

Consequently, although changes are observed they are not consistent with the perceived effect of IP levels on HDAC activity, rendering it difficult to conclude that IPMK is regulating HDAC activity. Furthermore, the method used to determine these changes is unlikely to be sensitive enough to detect minor changes. As previously stated, to ascertain a link between the regulation of HDAC activity and IPMK via histone acetylation levels, isolation of site specific histone acetylation sites may enable more profound changes to be observed and a regulatory mechanism established.

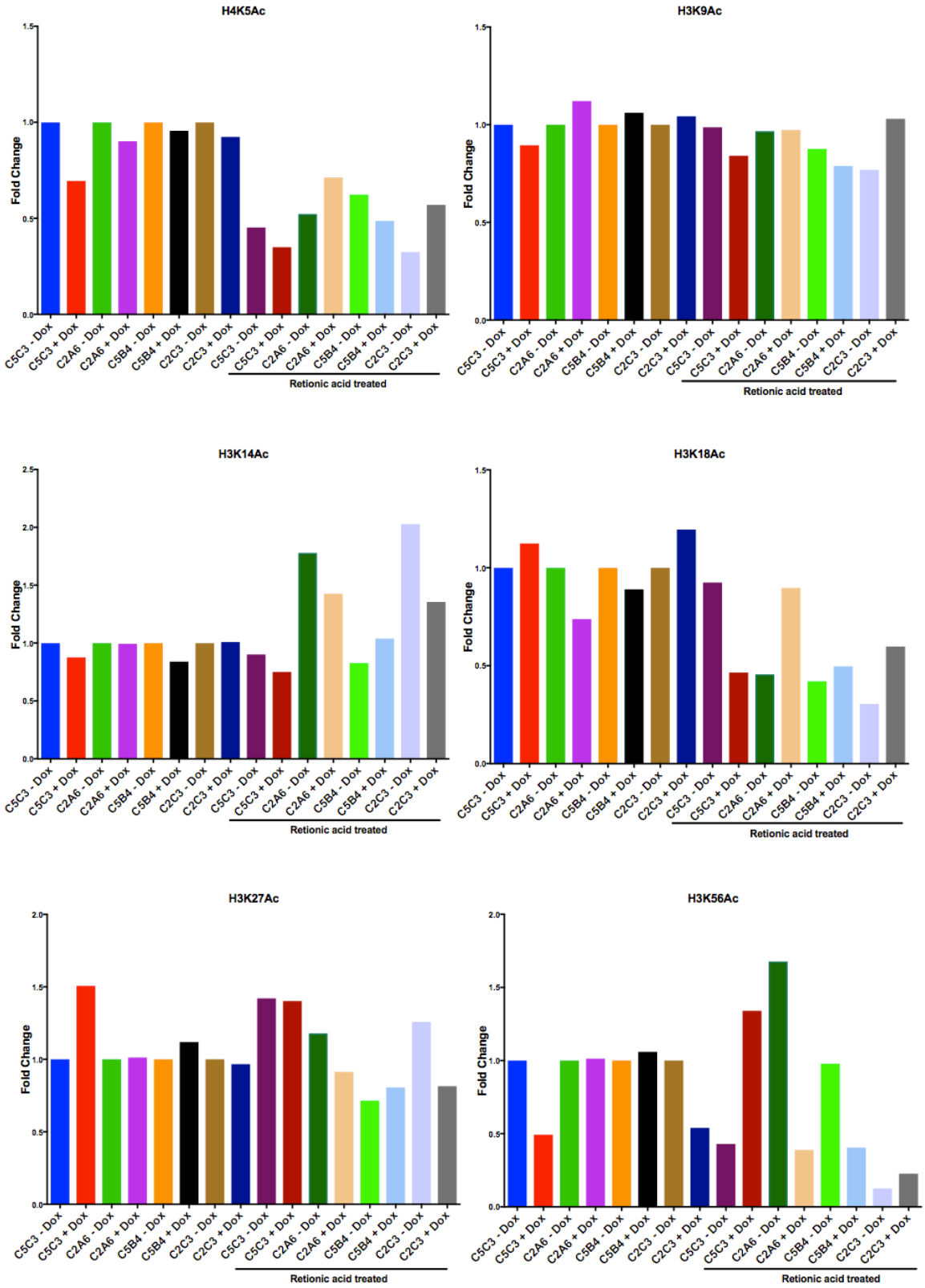

Figure 5-3 Inconsistent changes in histone acetylation levels are detected in differentiated TET-IPMK cells. *TET-IPMK cells were treated ± RA for 5 days ± Dox to induce loss of pluripotency with or without IPMK. Following whole-cell extract an acid extract was carried out to isolate histone proteins. Quantitative western blotting was carried out to determine the acetylation status of specific acetylated lysine's on H3 and H4 and normalised to the total amount of H3 or H4 present.*

5.2.3 Isolation of HDAC3 from differentiated TET-IPMK cells indicates variable HDAC activity

Due to the inconsistent differences observed in global HDAC activity upon RA treatment, we next isolated the endogenous HDAC3/SMRT complex from two clones via ImP assays. The two chosen clones, C2-A6 and C5-C3, initially showed the highest level of IPMK during screening of the clones and resulted in the highest restoration of IP levels (see chapter 4). Accordingly, it was believed that they may exhibit the largest differences in HDAC3 activity between conditions.

Isolation of HDAC3 in untreated C5-C3 cells indicated a lack of change in HDAC activity (Figure 5-4a), consistent with previous results (chapter 4), and thus acts as an internal control. Upon addition of RA differences in HDAC3 activity are exposed. Addition of Dox to the RA treated C5-C3 cells triggered an increase in HDAC activity (p-value = 0.0033) (Figure 5-4a). This suggests that despite a lack of change at the global level, IPMK is affecting HDAC3 activity in somatic cells, in this clone.

Isolation of the HDAC3 complex in C2-A6 samples indicates a change in both ES cells and RA treated cells (Figure 5-4a). Again, this change in HDAC3 activity was observed in the KO(2) parental cell line (chapter 4). The increase in global HDAC activity (Figure 5-2) is thus supported by the increase in HDAC3 activity upon addition of doxycycline to RA treated cells.

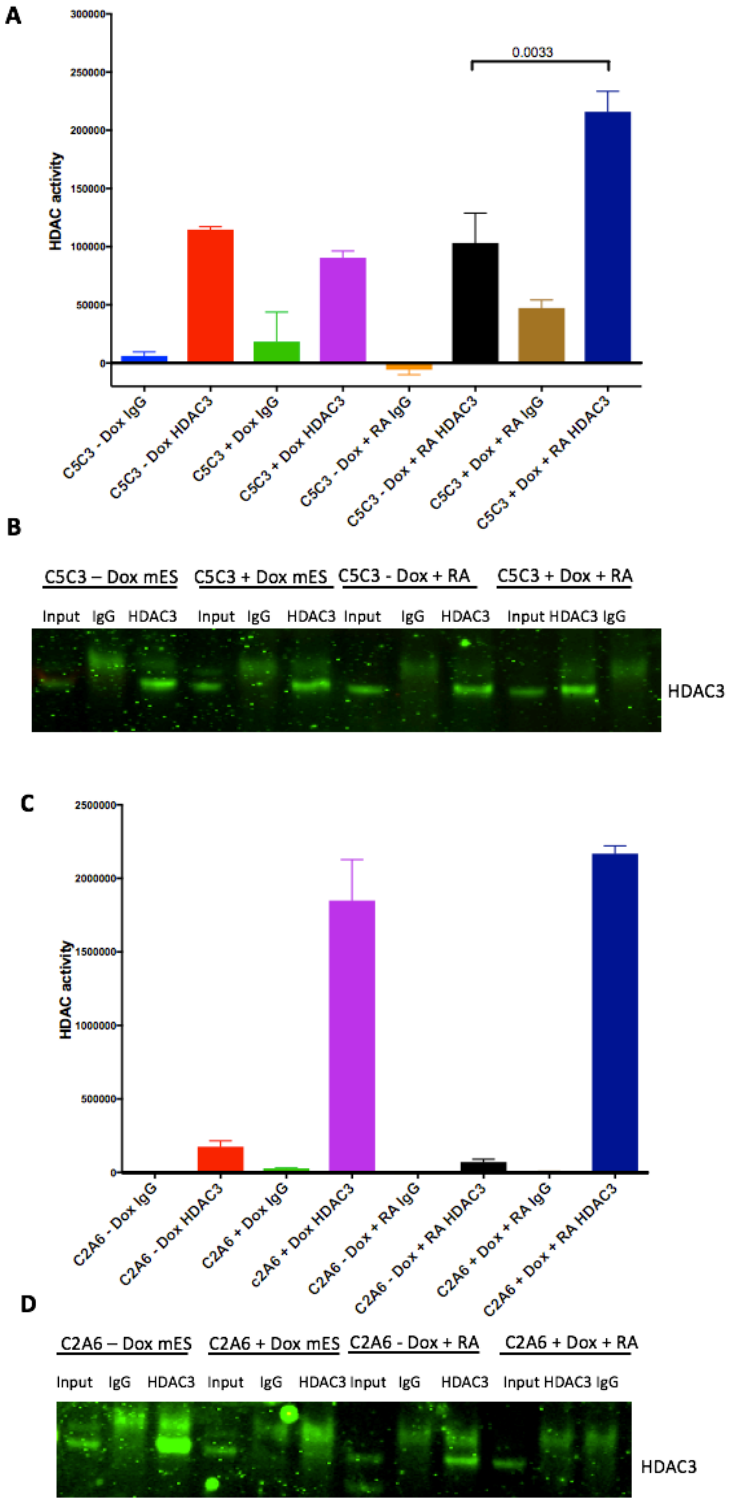

Figure 5-4 Isolation of HDAC3 reveals an increase in HDAC activity in the presence of IPMK in RA treated cells. *TET-IPMK cell lines C5-C3 and C2-A6 ± Dox were treated with RA for 5 days to induce loss of pluripotency. After 5 days whole-cell extract was generated and a HDAC3 antisera was used to isolate HDAC3.* ***(A+C)*** *After isolation of HDAC3 from C5-C3 and C2-A6 ±Dox ±RA samples, deacetylase activity was measured. Mean deacetylase activity (n=3±SD) is shown, statistical significance (p-value) were calculated using a Standard Two-tailed T-test.* ***(B+D)*** *Quantitative western blotting was used to determine HDAC3 pulldown compared to the IgG control, he level of HDAC3 pulldown was used to normalise the HDAC assay.*

The differences between the global HDAC (Figure 5-2) and the HDAC3 ImP HDAC assays (Figure 5-4) suggest that IP may be altering HDAC activity at a non-global level. However, this is confounded by the limited HDAC3 pull down in C2-A6 (Figure 5-4d) which makes normalisation difficult in this experiment, and consequently could be responsible for the large-scale changes observed. Furthermore, clonal differences are observed as C2-A6 indicates that HDAC activity is increased in the presence of RA following IPMK induction in both global assays (Figure 5-2) and the HDAC3 specific assays (Figure 5-4), yet this is not replicated in C5-C3, whereby changes are only detected following isolation of HDAC3. Additionally, a caveat of these experiments is that we are unsure whether IPs remain bound to the complexes during the ImP. Accordingly, it is difficult to draw any definitive conclusions from these experiments as they may not be a true representation of the effect of IP on HDAC activity.

5.3 Insights into the role of IPMK during gastrulation

Manipulation of IPMK in ES cells and during RA stimulated differentiation revealed minimal differences in measurable HDAC activity suggesting that it is unaffected. However, mouse studies have implicated the importance of IPMK during embryogenesis (Frederick et al, 2005). IPMK KO mice models exhibit embryonic lethality at E9.5, primarily due to developmental defects in the neuroectoderm. Although minimal somite production occurs, development of the mesoderm appears relatively normal (Frederick et al, 2005). Accordingly, TET-IPMK cells were differentiated into embryoid bodies to elucidate a role for IPMK in gastrulation and embryonic development.

Embryoid bodies (EBs) arise upon the removal of LIF from ES cells which form aggregates of cells in which spontaneous differentiation occurs (Keller, 2005). Through the formation of primitive ectoderm like cells, EBs give rise to the three germ layers, definitive endoderm, mesoderm and ectoderm (Figure 5-5) (Doetschman et al, 1985;

Keller, 2005; Keller, 1995; Smith, 2001). After 3 days of propagation EB's are believed to represent the morphological and genetic expression profiles of mouse embryos at the onset of gastrulation at around E6.5 (Doetschman et al, 1985; Keller, 2005; Snow, 1977; Tam & Behringer, 1997). Consequently, they are an ideal model system for understanding the role of IPMK in embryogenesis and gastrulation.

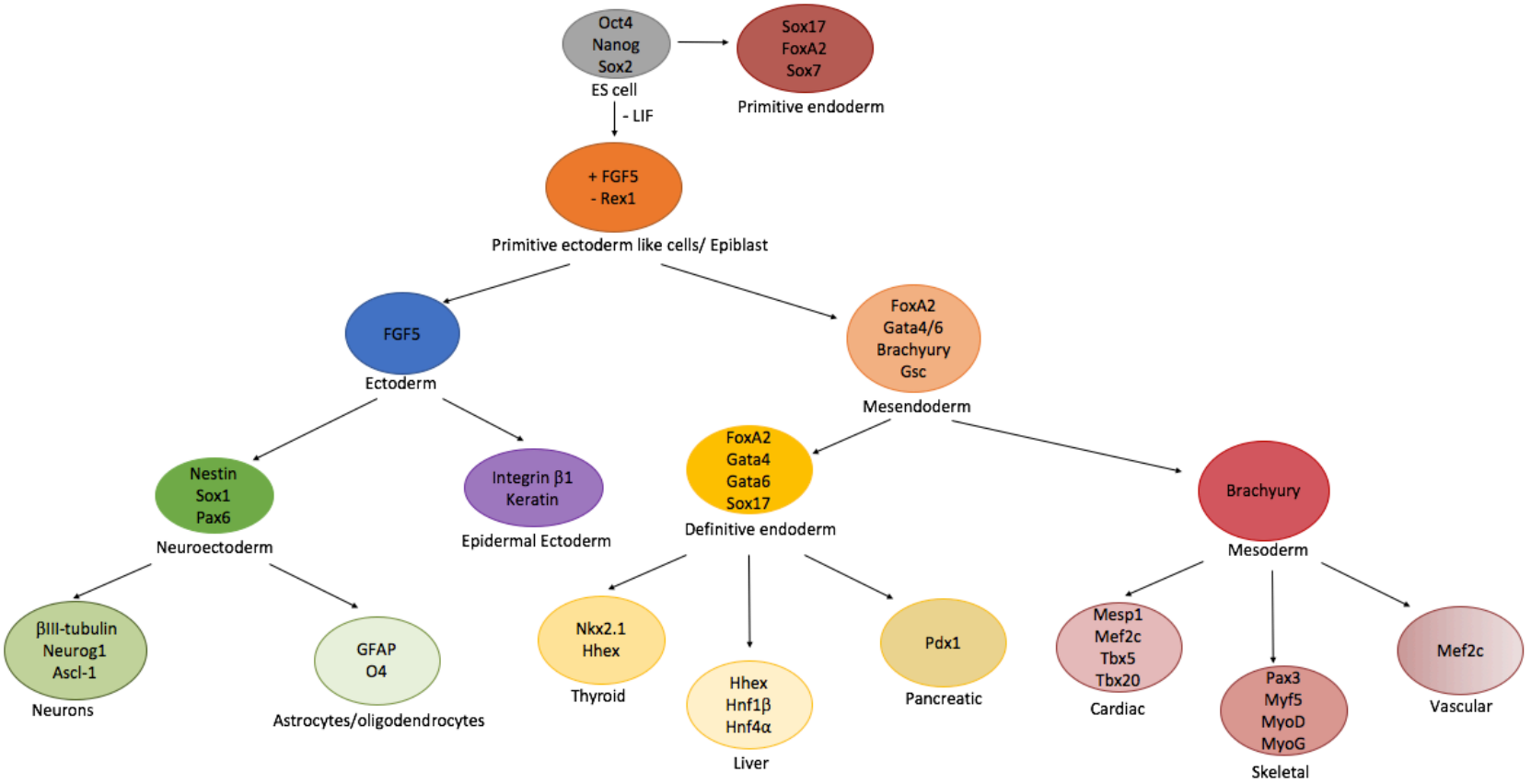

Figure 5-5 Schematic denoting the generation of the three germ layers in embryoid bodies (EB) and their corresponding markers. *Prior to differentiation ES cells express pluripotency factors such as Oct4, Nanog, Sox2. Embryoid formation results in a primitive endoderm surrounding the EB, expressing Sox17, FoxA2 and Sox7.The primitive ectoderm expresses FGF5 and is negative for Rex1.This layer goes on to produce the ectoderm which differentiates into the neuroectoderm (Nestin, Pax6 and Sox1) and the epidermal ectoderm (Keratin). The neuroectoderm delineates into neurons and astrocytes. The mesoderm originates (Gsc, Brachyury) from the primitive ectoderm and forms the definitive endoderm (FoxA2, GATA4/6) leading to the production of the thyroid, liver and pancreas etc. The mesoderm is formed by continued expression of Brachyury leading to production of cardiac, skeletal and vascular lineages.*

Control IPMK cells, IPMK knockouts and TET-IPMK cell lines were all cultured on ultra-low attachment plates in DMEM:F12 differentiation media for 9 days. To ascertain the longevity of Dox in media prior to EB differentiation, a time course was carried out to determine how long it remains active in cells. As shown in Figure 5-6, Dox remains active at a high level until day 3, when the level of IPMK induction decreases. Accordingly, all EBs were fed on day 3 and day 6 to enable supplementation of Dox and therefore consistent IPMK expression.

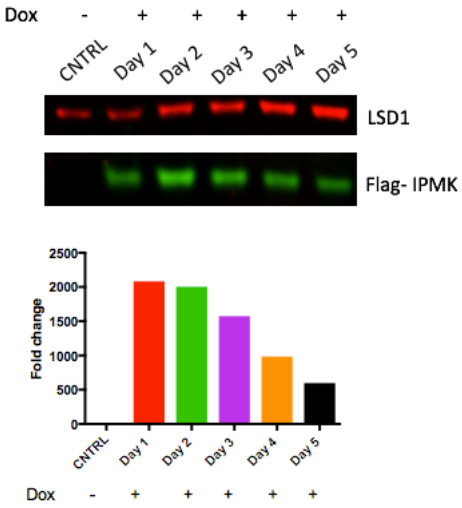

Figure 5-6 Doxycycline induced expression of IPMK time course. *Equal number of TET-IPMK ES cells were plated and Dox was added on Day 0 and media was left for up to 5 days. Cells were harvested daily and whole-cell extract was generated. Quantitative western blotting for IPMK relative to LSD1 expression revealed IPMK expression remains relatively constant for 3 days after addition of doxycycline. Following 3 days without subsequent addition of dox, the lecel of IPMK expression diminishes.*

5.3.1 Ablation of IPMK does not alter embryoid body morphology

Previously, it has been observed that upon deletion of HDAC1 and the HDAC1/2 complex component, LSD1, defective EB differentiation and a change in morphology occurs (Dovey et al, 2010b; Foster et al, 2010). EBs were therefore visualised and measured from day 3 onwards (see methods) (Figure 5-7). Initial comparison of the IPMK wildtype and IPMK knockouts KO(5) and KO(2) indicated a significant increase in the size of KO(5) compared to WT(10) or KO(2) (Figure 5-7 a + c). However, analysis of two of the TET-IPMK clones C5 C3 and C2 A6 revealed an absence of morphological difference upon the addition of Dox (Figure 5-7 b + d). Consequently, it appears that IPMK is not impacting the size of EB formed and the initial difference observed is more likely to be due to clonal differences rather than the absence of IPMK. Accordingly, only TET-IPMK clones were taken forward for analysis.

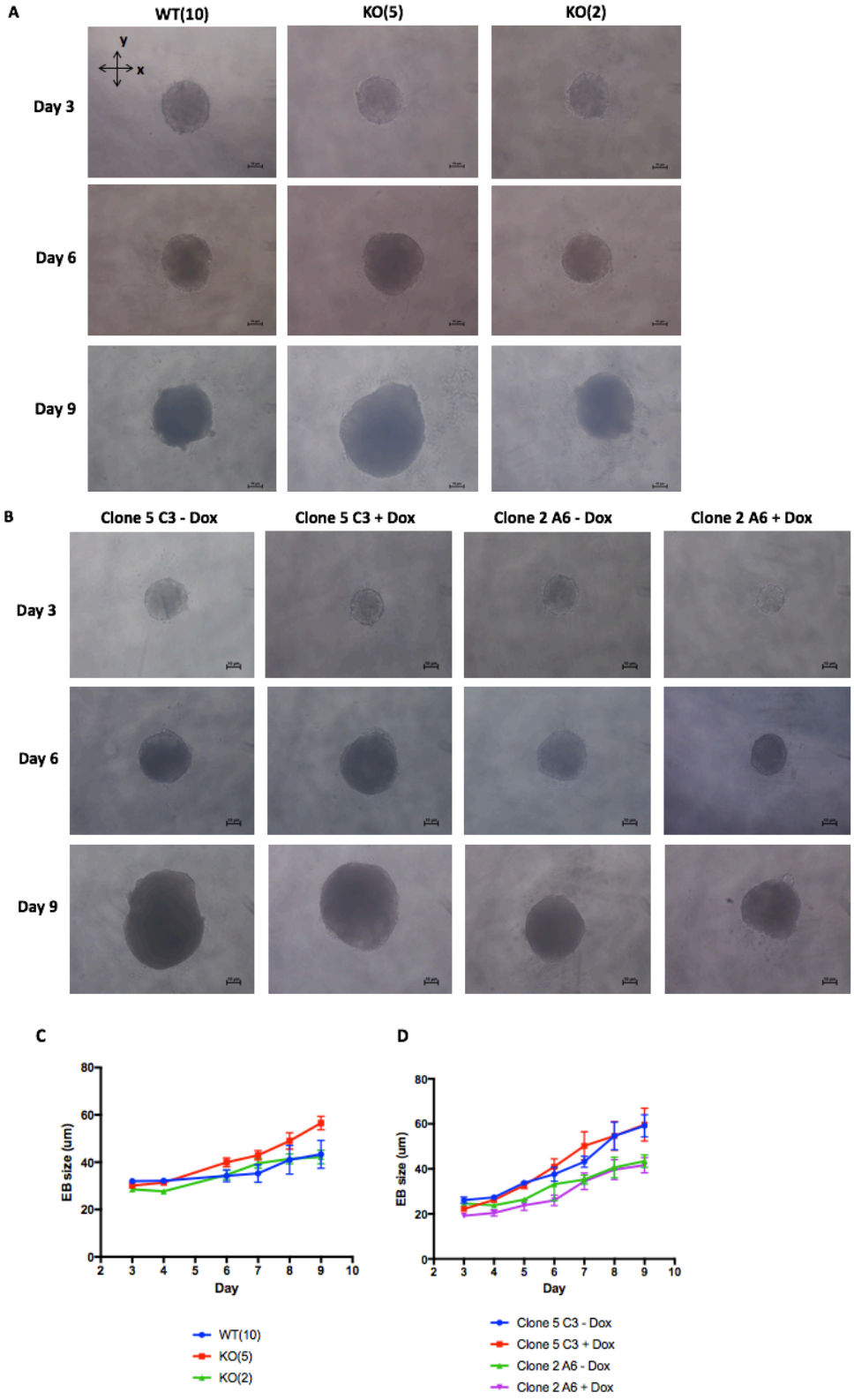

Figure 5-7 IPMK knockout embryoid bodies show a uniform size *TET-IPMK ES cells were plated onto low attachment plates in the absence of LIF and resultant EBs were sized daily from day 3, 10 EBs were sized per day.* ***(A+B)*** *Images shown are representative of EBs at indicated time points of WT, KO(5), KO(2) and TET-IPMK clones C5-C3 and C2-A6 ± Dox.* ***(C+D)****.* ***(C)*** *10 EBs were sized per day as described in methods 2.1.6.1, the mean size of WT, KO and TET-IPMK clones are shown all values are n=10±SD.*

5.3.2 Initial stages of differentiation are affected by IPMK loss

During EB formation, RNA was extracted on day 0, 3, 6 and 9 to examine potential alterations in gene expression by qRT-PCR. Key pluripotency markers, Oct4 (Pou5F1), Sox2 and Nanog are unaffected by loss of IPMK and were significantly depleted by day 9 in all cell lines, indicating they had successfully exited pluripotency (Figure 5-8).

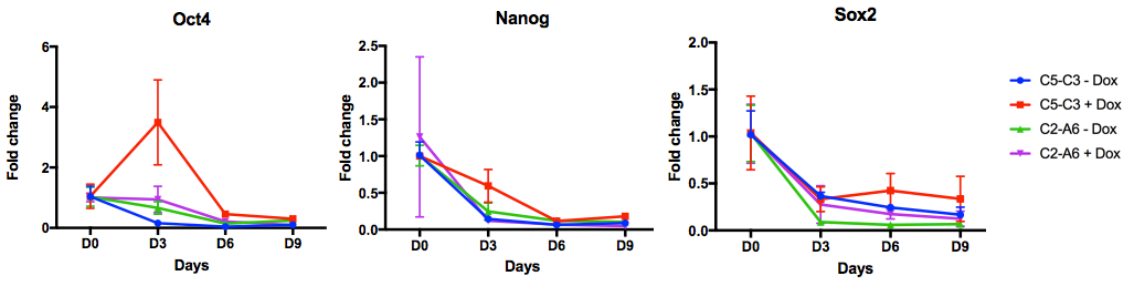

Figure 5-8 Deletion of IPMK does not affect ability to exit pluripotency. *TET-IPMK ES cells were plated onto low attachment plates in the absence of LIF, EBs were harvested on day 0, 3, 6 and 9 and RNA extracted. qRT-PCR analysis was carried out to determine the expression of key pluripotency genes. Oct4, Nanog and Sox2 all indicated a reduction in levels during the time course in all samples suggesting they exited pluripotency. C5-C3 + Dox, shows an unusual increase in Oct4 expression on day 3 but this decreased back to a similar level to wildtype cells by day 6. The key on the right shows the cell type and corresponding colour. All values are mean fold change where n=3±SD, values indicate expression relative to the B-Actin reference gene.*

As previously mentioned, EBs mimic the process of gastrulation culminating in the formation of the three germ layers, definitive endoderm, mesoderm and ectoderm (Figure 5-5) (Doetschman et al, 1985; Keller, 2005; Keller, 1995; Smith, 2001). To enable formation of the three germ layers, expression of key regulatory drivers which mark the formation of the definitive ectoderm and mesendoderm from the epiblast are required (Figure 5-5) (Keller, 2005; Kubo et al, 2004; Lolas et al, 2014; Tam & Behringer, 1997). The formation of the primitive ectoderm is marked by the isolated increase in expression of fibroblast growth factor 5 (FGF5) at E6.5 and loss of expression by E7.5 (Haub & Goldfarb, 1991; Hebert et al, 1991). Likewise, the mesendoderm is characterised by the expression of Brachyury (T) throughout the primitive streak at E7.5-8.5 (Evans et al, 2012; Herrmann et al, 1990).

qRT-PCR analysis of these key factors in TET-IPMK EBs ±Dox, revealed that the pattern of FGF5 induction (day 3) and repression (day 6) is similar between TET-IPMK clones (Figure 5-9). However, the level of induction is decreased in TET-IPMK EBs without Dox, indicating decreased primitive ectoderm formation. Furthermore, the pattern of Brachyury expression also indicates consistent induction and repression, however, C5-C3 shows enhanced expression in EBs expressing IPMK (Figure 5-9). The difference in this induction compared to C2-A6 could be due to the lower levels of IPMK induction in C2-A6 or clonal differences (Figure 5-9). Consequently, these results suggest that loss of IPMK results in potentially decreased initial differentiation of the primitive ectoderm.

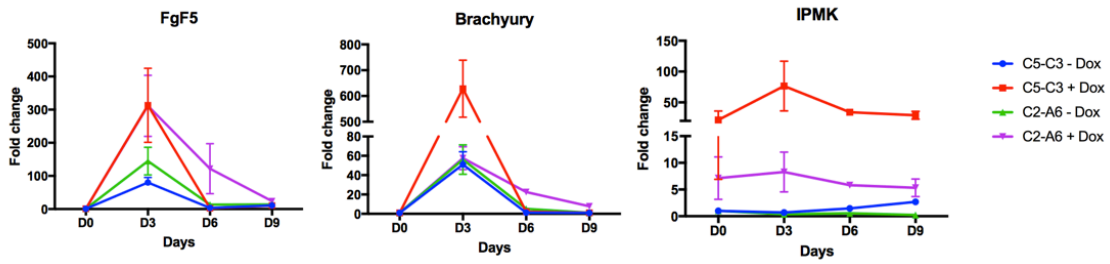

Figure 5-9 Initial differentiation of the mesendoderm and ectoderm are altered by IPMK deletion. *RNA extracted from TET-IPMK EBs harvested on day 0, 3, 6 and 9 was used in qRT-PCR to analyse early differentiation markers FGF5 and Brachyury. qRT-PCR revealed FGF5 expression decreases upon loss of IPMK (-Dox) whereas analysis of brachyury RNA levels indicates increased expression in C5-C3 following addition of Dox but not C2-A6. IPMK analysis indicates increased expression levels in EBs treated with Dox. The key on the right shows the cell type and corresponding colour. All values are mean fold change where n=3±SD, values indicate expression relative to the B-Actin reference gene.*

5.3.3 Loss of IPMK leads to increased mesoderm formation and decreased ectoderm differentiation

Following initial differentiation, the three germ layers, definitive ectoderm, mesoderm and definitive endoderm are generated. Since analysis of initial differentiation markers indicated decreased expression of FGF5 and Brachyury upon deletion of IPMK, germ line specific markers were analysed.

The definitive endoderm germ layer give rise to the lungs, liver, pancreas, stomach and intestine of the developing embryo and is generated following the divergence of the mesendoderm layer (Figure 5-5) (Tada et al, 2005; Wang & Chen, 2016). The definitive endoderm is marked by the expression of several factors including; sry-related HMG-box family member 17 (Sox17), forkhead transcription factor A2 (FoxA2), GATA4, GATA6, Hnf4α and Hnf1β (Figure 5-5) (Ang et al, 1993; Dufort et al, 1998; Gordillo et al, 2015; Holtzinger et al, 2010; Kanai-Azuma et al, 2002; Kubo et al, 2004; Morrisey et al, 1998; Qu et al, 2008). qRT-PCR analysis of the markers GATA4, FoxA2 and Hnf1β reveals no significant changes between samples, indicating that IPMK does not impact their induction (Figure 5-10). On the other hand, GATA6, a driver of hepatic development, exhibits increased expression in the absence of IPMK, suggesting that IPMK maybe involved in its expression (Figure 5-10). GATA6 is known to activate Hnf4α, however, in contrast to GATA6, Hnf4α indicates a decrease in expression upon deletion of IPMK in C2-A6, but not C5-C3 (Figure 5-10). These clonal differences are also observed with Sox17 which also exhibits decreased expression in the absence of IPMK in C2-A6 but not C5-C3. Since the addition of Dox does not cause consistent changes in expression of endoderm markers; these data suggest that IPMK is not regulating their induction.

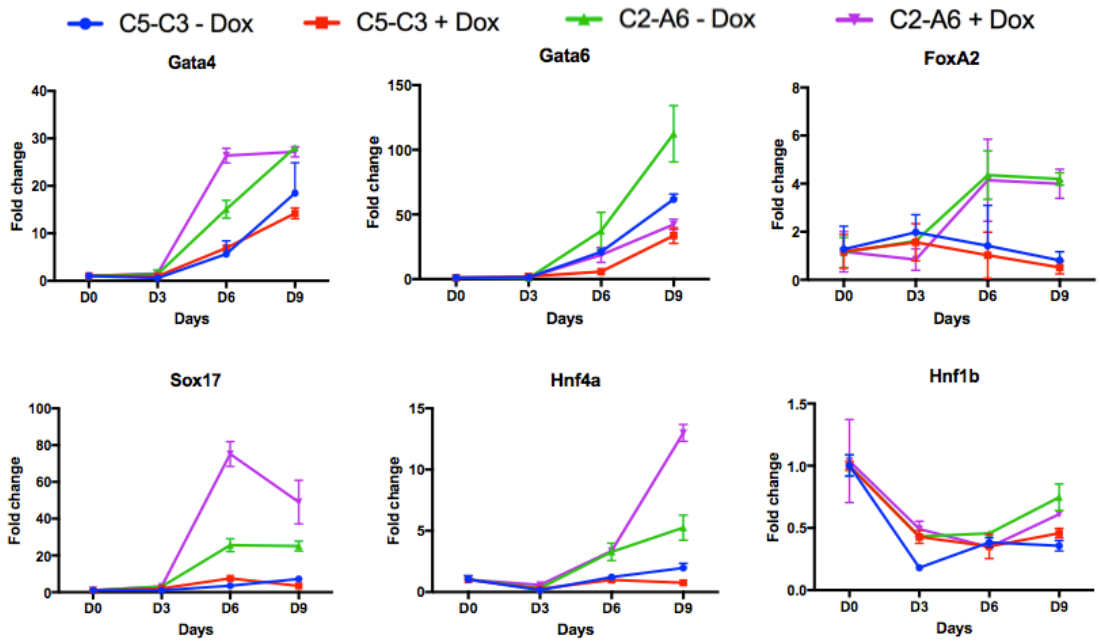

Figure 5-10 IPMK deletion results in minor changes in endoderm lineage differentiation. *RNA from day 0, 3, 6 and 9 TET-IPMK EBs was analysed by qRT-PCR for expression of endodermal gene markers. Markers show minimal changes upon deletion of IPMK. All values are mean fold change where n=3±SD, values indicate expression relative to the B-Actin reference gene. A key is shown at the top denoting the sample and corresponding colour.*

The mesoderm, formed through the mesendoderm precursor, maintains the expression of Brachyury upon distinction from the endoderm and goes onto generate the bone, heart, vascular tissue, muscle and kidney of the developing embryo through expression of tissue specific factors (Figure 5-5) (Tada et al, 2005; Wang & Chen, 2016). Cardiac mesoderm formation is characterised by the expression of T-box transcription factors 5 and 20 (Tbx5 and Tbx20) and myocyte enhancer factor-2c (Mef2c) (Chakraborty & Yutzey, 2012; Olson, 2006; Pon & Marra, 2016). Skeletal muscle differentiation is marked by induction of myogenic regulatory factor (MRF) Myf5 which leads to the activation of MyoD, Myf6 and MyoG (Kodaka et al, 2017; Rohwedel et al, 1994).

Analysis of cardiomyocyte marker expression in TET-IPMK EB's indicated increased expression of Mef2c in all clones upon ablation of IPMK, despite no induction of Tbx5 (Figure 5-11). This result correlates with Tbx20 (increased expression by day 9 without IPMK) suggesting that IPMK and therefore presumably IP levels may potentially be

regulating cardiac muscle differentiation (Figure 5-11). Analysis of skeletal muscle markers revealed that Myf5 is unaffected by deletion of IPMK, although C5-C3 shows increased expression in the presence of Dox, this may be an outlier due to clonal differences in brachyury expression (Figure 5-11). This lack of change is continued in MyoD and MyoG which show minimal induction suggesting that IPMK is not likely to be affecting skeletal muscle differentiation.

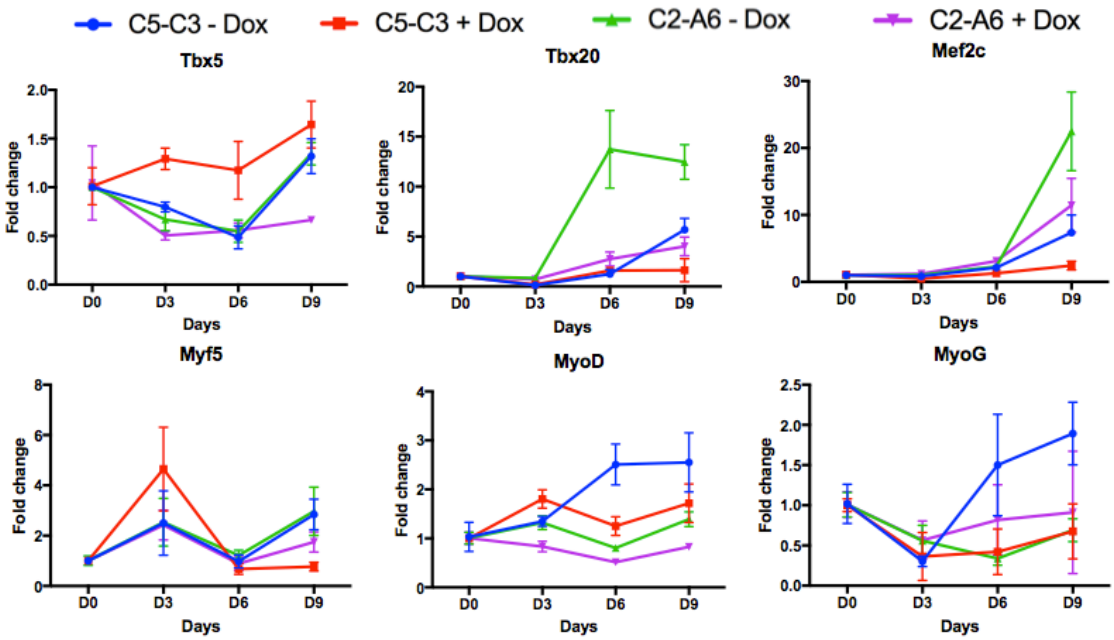

Figure 5-11 Absence of IPMK increases mesoderm differentiation. *qRT-PCR analysis of mesoderm differentiation markers from RNA isolated from TET-IPMK EBs at day 0, 3, 6 and 9 indicate increases in cardiomyocyte marker expression (Mef2c and Tbx20) but not skeletal markers (Myf5 and MyoD). All values are mean fold change where n=3±SD, values indicate expression relative to the B-Actin reference gene. The key at the top indicates samples and their corresponding colour.*

The primitive ectoderm cells gives rise to the ectoderm following expression of FGF5 and goes onto generate the neuroectoderm and epidermis leading to formation of the central nervous system and skin epidermis (Figure 5-5) (Hebert et al, 1991; Keller, 2005; Okabe et al, 1996). Sox1 is an early marker of the neuroectoderm expressed in early progenitor cells, followed by the expression of Nestin and Pax6 (Abranches et al, 2009; Lendahl et al, 1990; Suter et al, 2009; Walther & Gruss, 1991; Ying et al, 2003b). Later markers of neuroectoderm include; Achaete scute-like 1 (Ascl-1), Neurogenin 1

(Neurog1) and β-III tubulin (Lee et al, 1990; Wilkinson et al, 2013). In the absence of Dox, TET-IPMK EBs exhibit downregulation of early markers Sox1 and Nestin compared to control cells (with Dox) (Figure 5-12). Several other markers of the neuroectoderm, Pax6, Ascl-1, Neurog1, β-III tubulin show limited induction during EB formation. These data suggest that IPMK deletion results in decreased early neuroectoderm formation, suggesting that IPMK and IP levels are regulating neuroectoderm differentiation.

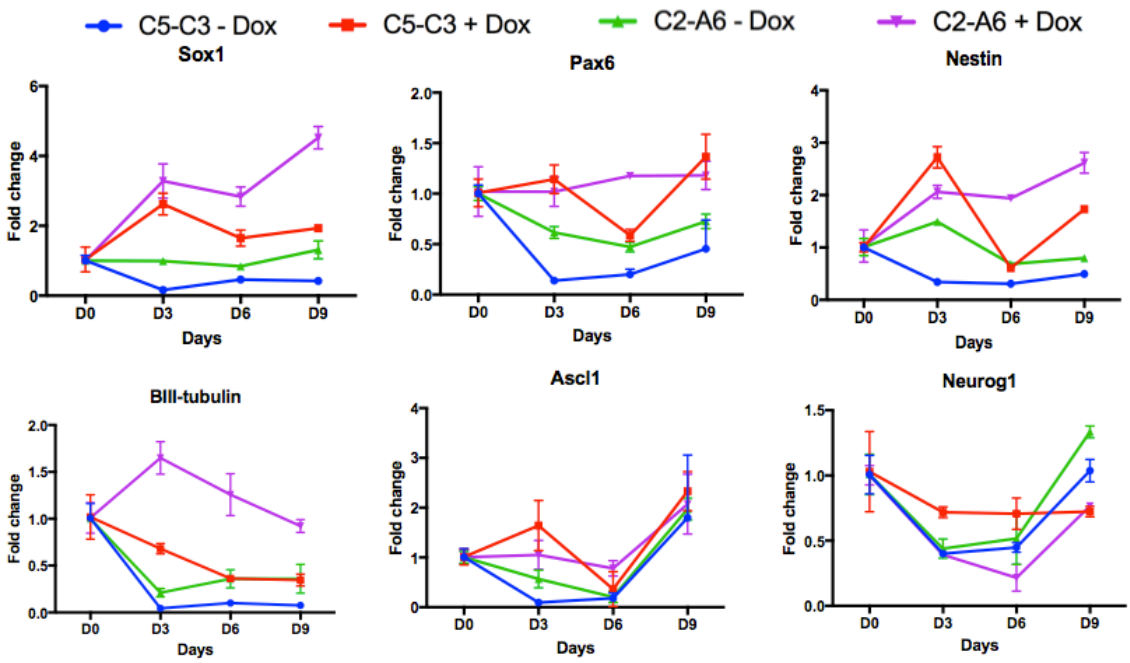

Figure 5-12 Deletion of IPMK reduces ectoderm differentiation. *qRT-PCR analysis of neuroectoderm markers reveals decreased expression in early markers in IPMK null cells. All values are mean fold change where n=3±SD, values indicate expression relative to the B-Actin reference gene.*

5.3.3.1 Brief analysis of intrinsic and extrinsic signalling pathways in TET-IPMK EBs

Extrinsic and intrinsic signalling is essential for accurate patterning of the germ layers and organogenesis in the developing embryo. The balance of these signalling pathways and the interaction with transcription factors can determine the germ layer formed in certain areas of the developing embryo. Activation of Nodal and Wnt/β-catenin signalling inhibits neuroectoderm formation whilst promoting mesoderm and

endoderm formation (Gordillo et al, 2015; Wang & Chen, 2016). IPMK has been implicated in the regulation of Wnt/β-catenin, as blocking IP_5 production blocks β-catenin accumulation and promotion of the endoderm (Gao & Wang, 2007). Additionally, Hes1, inhibits Notch, thus promoting mesodermal differentiation (Kobayashi & Kageyama, 2010). The expression of Hes1 is inhibited by Sox1, suggesting that it may be upregulated in the TET-IPMK knockout EBs (Kan et al, 2004). Despite alterations in neuroectoderm formation, neither Nodal, β-catenin or Hes1 signalling was attenuated by deletion of IPMK (Figure 5-13), thereby indicating that IPMK signalling does not alter their induction. Other signalling pathways which can determine lineage differentiation include Noggin, an antagonist of BMP4 which promotes neuroectoderm formation (McMahon et al, 1998; Tropepe et al, 2001). qRT-PCR analysis indicated that Noggin expression is elevated in C2-A6 in the presence of Dox (Figure 5-13), correlating with the increased level of neuroectoderm markers observed. However, this is not consistent across the clones, rendering it difficult to conclude that Noggin is regulated by IPMK.

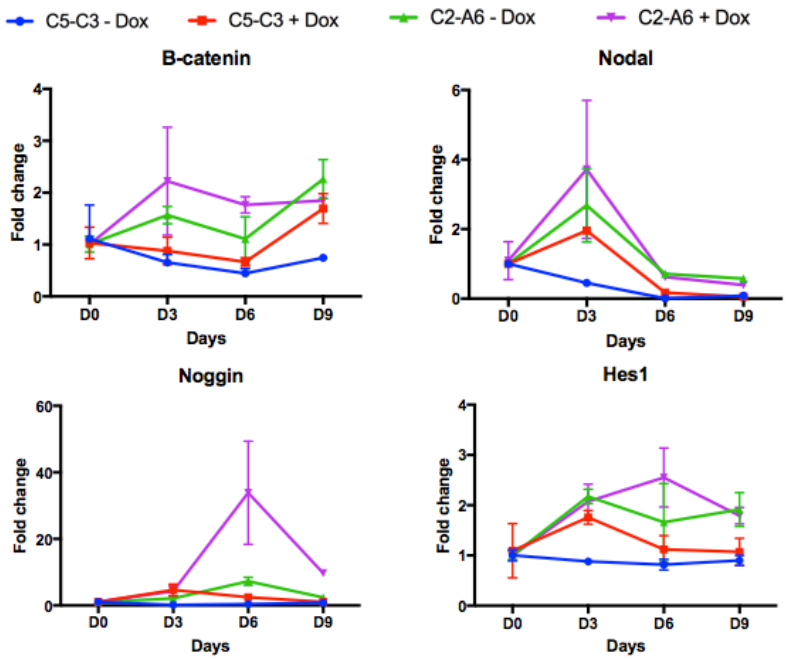

Figure 5-13 Analysis of extrinsic and intrinsic pathways which inhibit neuroectoderm formation are not affected by IPMK. *RNA isolated from TET-IPMK EBs on day 0, 3, 6 and 9 was subject to qRT-PCR analysis. Analysis of RNA levels of β-catenin, Nodal and Hes1 show no significant difference upon deletion of IPMK. qRT-PCR analysis of Noggin indicates elevated expression upon addition of Dox to C2-A6. All values are mean fold change where n=3±SD, values indicate expression relative to the B-Actin reference gene.*

5.4 Summary

Initial measurements of HDAC activity in ES cells have resulted in limited changes, consequently, RA treatment was utilised to generate cells which had exited pluripotency. Global HDAC activity was altered in C2-A6 but not in other clones. These discrepancies were further compounded upon isolation of HDAC3 revealing differences in activity depending on the clone. Consequently, we are still unable to conclusively show that IP levels regulate HDAC activity *in vivo*. Differentiation of IPMK KO and rescue cells into EBs revealed an absence of morphological abnormalities when compared to the wildtype cells or rescue cell lines, contrasting with previous HDAC studies (Figure 5-7). Analysis of the transcriptome indicated that IPMK deletion does not affect exit from pluripotency (Figure 5-8), whilst FGF5 RNA levels are decreased upon deletion of IPMK (Figure 5-9). These changes lead to minimal alterations in endoderm upon deletion of IPMK and potential increases in cardiomyocyte markers in the mesoderm (Figure 5-11). In addition, IPMK null cells exhibited decreased expression of early neuroectoderm markers (Figure 5-12). Taken together, these data, suggest that IPMK knockout EBs may show a predisposition to differentiate towards the mesoderm, potentially at the expense of the neuroectoderm.

Chapter 6 Discussion

6.1 HDAC activity is unaffected by alterations in IP levels

The identification of Ins(1,4,5,6)P_4 at the interface of HDAC3/SMRT prompted research into its role as a structural co-factor or regulator of HDAC activity (Watson et al, 2012). Addition of exogenous Ins(1,4,5,6)P_4 to class I HDAC complexes, SMRT, NuRD and MiDAC resulted in enhanced complex activity *in vitro* indicating IPs are conserved regulators of HDAC activity (Itoh et al, 2015; Millard et al, 2013; Watson et al, 2016). Indeed, HDAC1/2 knockout ES cell rescue experiments indicate IP binding HDAC1 mutants are unable to rescue the cell lethal phenotype (Jamaladdin et al, 2014). Collectively, these data suggested that IPs are involved in the regulation of class I HDAC activity. To further understand the consequence of IP binding to class I HDAC complexes, we perturbed the IP pathway through deletion or overexpression of IPMK, or overexpression of SopB and PTEN and measured resultant HDAC activity (Caffrey et al, 2001; Feng et al, 2001; Frederick et al, 2005). Together, the results presented in this thesis suggest that HDAC activity may not be regulated by IPs.

Overexpression of SopB, PTEN and IPMK in HEK-293F cells was unable to bring about an alteration in global HDAC activity or histone acetylation levels despite changes in IP levels (Figure 3-1, Figure 3-3, Figure 3-15). Furthermore, isolation of the HDAC3/SMRT complex revealed changes in HDAC activity which do not correlate with perturbations in IP levels brought about by SopB, PTEN and IPMK overexpression (Figure 3-2, Figure 3-5, Figure 3-7, Figure 3-8, Figure 3-15). These results consequently suggest that IPs may not regulate HDAC activity. This was further supported by a lack of change in global HDAC activity or histone acetylation levels and inconsistencies in HDAC3 ImPs in IPMK KO cells (Figure 4-6, Figure 4-7, Figure 4-8, Figure 4-9, Figure 4-10). If Ins(1,4,5,6)P_4 is a physiological regulator of class I HDAC complexes, then changes in IP concentrations would be expected to exhibit a measurable change in HDAC activity. However, our results indicate that this biological response does not occur as

perturbations in HDAC activity are not observed upon large scale alteration of IP levels, thereby suggesting IP levels may not be regulating HDAC activity *in vivo*. In isolation HDAC1,2 and 3 are believed to be inactive, incorporation into their respective corepressor complexes, through interaction with key domains, enables their enzymatic activity (Guenther et al, 2001; Kelly & Cowley, 2013; Zhang et al, 1999). It was later suggested that IPs were essential for this elevated activity (Millard et al, 2013; Watson et al, 2012). However, *in vitro* T7-transcirption and translation of HDAC3, SMRT/NCoR and TBL1 in the absence of IP, followed by enzymatic analysis, reveals that SMRT/NCoR is sufficient to enable HDAC3 activity, suggesting that IP may not be required for basal HDAC activity (Guenther et al, 2001). This is further supported by the lack of evidence of a free pool of HDAC3 waiting for Ins(1,4,5,6)P_4 to mediate interaction with SMRT/NCoR and activate the complex (Millard et al, 2013). Furthermore, although HDAC activity is greatly enhanced through the addition of IP to HDAC3/SMRT or HDAC1/MTA1 as indicated via HDAC assays, they do reveal a basal level of activity in the absence of IP_4 (Figure 6-1) (Millard et al, 2013; Watson et al, 2012). This suggests that although IP may increase HDAC activity *in vitro*, it may not be required to regulate basal activity, hence why we do not observe alterations in HDAC activity *in vivo.*

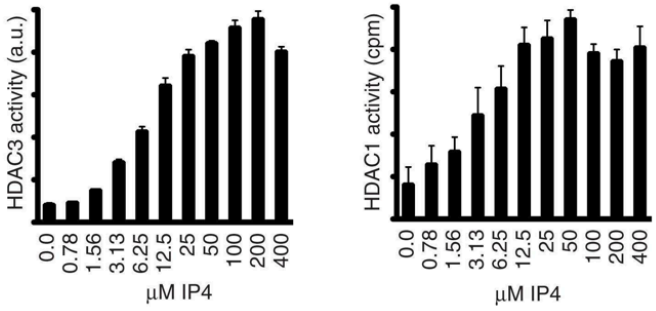

Figure 6-1 Addition of IP_4 to HDAC3/SMRT or MTA1/HDAC1 elevates HDAC activity
HDAC3/SMRT and HDAC1/MTA1 activity assays. Taken from Millard et al, 2013.

6.1.1 Potential limitations of our experiments for detecting IP regulation of HDACs

If IPs are regulating HDAC activity as proposed in *in vitro* studies, it is possible that we are not detecting global changes in HDAC activity due to compensation from other HDAC complexes (Itoh et al, 2015; Millard et al, 2013; Watson et al, 2016). Whilst the class I HDAC co-repressor complexes, SMRT, NuRD and MiDAC have all been shown to be activated by addition of exogenous Ins(1,4,5,6)P_4, there is currently no experimental evidence to show that CoREST and Sin3 are regulated by Ins(1,4,5,6)P_4 (Itoh et al, 2015; Millard et al, 2013; Watson et al, 2016). However, CoREST1, 2 and 3 all contain an ELM2-SANT domain which interacts with HDAC1 and HDAC2 (You et al, 2001). The CoREST1-3 ELM2-SANT domains contain the conserved IP binding residues found in the SANT domain of SMRT and the ELM2-SANT domain of MTA, suggesting that CoREST may be similarly activated by IPs (Watson et al, 2012). Sin3 on the other hand, does not contain a SANT domain, but interacts with HDAC1 and HDAC2 via a HDAC interaction domain (HID) which is sufficient for Sin3 mediated repression (Hassig et al, 1997; Laherty et al, 1997; Zhang et al, 1997). Consequently, due to the differences in HDAC recruitment, it is believed that the Sin3-HDAC1/2 complex is not regulated by IPs. Consequently, it remains possible that Sin3 may be upregulated to compensate for the lack of IPs present in the cells.

Immunoprecipitation of endogenous HDAC complexes may exhibit no change in activity if inositol phosphates are not remaining bound during purification. Whilst it remains possible that IPs remain tightly bound, a salt concentration of 50mM KCl was required to isolate SMRT/HDAC3 in complex with Ins(1,4,5,6)P_4 (Watson et al, 2012). The salt concentration of the extraction buffers used in this thesis ranged from 50mM to 250mM, depending on the experiment. Accordingly, it is possible that any Ins(1,4,5,6)P_4 bound, dissociated from the class I HDAC complexes during extraction, thus removing any of the potential effects of IP on HDAC activity. We attempted to overcome this through the examination of HDAC3 target gene expression in TET-IPMK cells, with the expectation that gene expression would decrease in the presence of

Dox due to increased HDAC3 activity (Figure 4-11). Whilst all genes analysed revealed increased expression upon deletion of HDAC3, the expression of CD68, Tbx30s2 and Rpgrip did not alter upon ablation of IPMK, indicating that IPMK does not regulate their activity. Furthermore, whilst Hnf4α, Hist1h2bq and HoxB2 exhibited the expected alterations in gene expression, the results were not consistent across different clones. Therefore, we are unable to conclusively say that IPMK ablation results in an increase in HDAC3 target gene expression. The expected changes in HDAC3 target gene expression may not be observed due to sufficient basal HDAC activity remaining upon loss of IPMK (Figure 6-1). Additionally, ES cells have relatively high levels of histone acetylation which coupled with histone methylation acts to maintain the tightly regulated ES cell transcriptome (Boyer et al, 2006). Indeed, deletion of HDAC1 or HDAC2 in ES cells result in minimal changes in histone methylation marks, indicating the methylome remains largely unaffected (Dovey et al, 2010b; Jamaladdin et al, 2014). Consequently, it is possible that the remaining activity of HDACs coupled with the tightly regulated ES cell transcriptome is sufficient to maintain appropriate gene regulation of the HDAC3 target genes.

It is also possible that the chromatin characteristics of ES cells may be responsible for the lack of measurable change in HDAC activity. ES cells are transcriptionally permissive with high levels of euchromatin and basal histone acetylation (Boyer et al, 2006). The high level of histone acetylation found in ES cells could account for the lack of changes upon perturbation of IP levels (Figure 4-8, Figure 4-9, Figure 4-10). Indeed, treatment of ES cells with TSA, a HDAC inhibitor, results in a limited effect on histone acetylation levels, particularly H3K9/K14Ac, suggesting that modulation of IP dependent HDAC activity would have no effect (Dovey et al, 2010b). Nevertheless, deletion of HDAC1 alone or in conjunction with HDAC2 results in a small increase of H3K56Ac 1.6-fold or 4-fold, respectively (Dovey et al, 2010b; Jamaladdin et al, 2014). This effect was not witnessed upon attenuation of IP levels, perhaps due to residual HDAC activity and the maintenance of corepressor complex integrity. It is widely accepted that following differentiation, acetylation levels decrease, indeed treatment of MEFs with TSA enables changes in H3K9/K14Ac to be observed, consequently alterations may be detectable upon perturbation of IP levels (Boyer et al, 2006; Das et

al, 2009b; Dovey et al, 2010b). Accordingly, TET-IPMK cells were treated with retinoic acid in the absence of LIF to induce differentiation. However, histone acetylation levels remained unchanged in the absence or presence of IPMK suggesting that HDAC activity was unaffected (Figure 5-5). The occurrence of gene specific alterations cannot be discounted, this has been observed upon ablation of HDAC3 where global acetylation levels remain unchanged but increases are detected at PPAR responsive genes (Montgomery et al, 2008). Accordingly, it may be prudent to examine specific loci previously shown to have altered histone acetylation levels upon perturbation of the class I HDACs. If these sites indicate altered histone acetylation via ChIP-qPCR analysis, it would provide a convincing link between IPs and class I HDAC activity.

Finally, it is possible that we are not altering the levels of IPs enough to detect a change in HDAC activity. The apparent Kd (Kd_{app}) of HDAC3/SMRT and HDAC1/MTA1 for Ins(1,4,5,6)P_4 has been reported to range between 5-10μM (Millard et al, 2013; Watson et al, 2016). It was proposed by Millard et al, 2013, that the variation of Ins(1,4,5,6)P_4 throughout the cell cycle of 3.6-10.5μM (as calculated by Barker et al, 2004), would result in a 2-fold change. Accordingly, we believed that alteration of IPs levels, especially at the level observed in the IPMK knockout cells where IP_5 and IP_6 decrease by 90% (Frederick et al, 2005), would enable us to detect a change in HDAC activity. However, our results suggest that the remaining basal activity of HDACs or levels of IPs may be sufficient. To try to determine whether this is the reason for the lack of observed change it is reasonable to further decrease IP levels. This could potentially be achieved through the addition of a TET inducible SopB construct to the IPMK knockout cell lines. The IPMK knockout cells already have low levels of IPs, however the addition of SopB to these cells may decrease levels further as observed in Feng et al, 2001 (Figure 1-14). Subsequently, if IPs are regulating HDAC activity *in vivo,* the potentially undetectable levels of IP could lead to a detectable change in HDAC activity. Without further investigation, it is implausible to conclusively say that IPs are regulating class I HDAC corepressor complex activity *in vivo*.

6.2 Characterization of inositol phosphates through the cell cycle

As the levels of IPs have been shown to fluctuate during the different phases of the cell cycle, it is plausible that IPs could be regulating HDAC activity in a cell cycle dependent manner (Barker et al, 2004). Consistent with Barker et al, 2004., we observed an increase in IP levels from S phase to G2/M. However, in contrast the highest level of IPs detected was during G2/M phase and not G1 phase (Figure 4-15). A potential explanation for this discrepancy is that ES cells lack the normal G1/S checkpoint due to a constant hyper-phosphorylated-retinoblastoma protein (Rb) (Burdon et al, 2002; Savatier et al, 1994). Barker et al, proposed that as IP_6 and IP_5 inhibit protein phosphatase 1 and 2A (PP1/2A), which dephosphorylate Rb, their levels may be elevated in G1 phase to enable progression into S phase (Barker et al, 2004; Kolupaeva & Janssens, 2013; Larsson et al, 1997). Consequently, the presence of hyper-phosphorylated Rb and constitutively active Cdk2 in ES cells may mean it is not necessary to increase the levels of Ins(1,2,3,4,5,6)P_6 or Ins(1,3,4,5,6)P_5 in G1. Analysis of histone acetylation levels also resulted in conflicting data compared to the literature, where an increase in acetylation during S phase is reported (Figure 4-16) (Li et al, 2008; Ma et al, 2015). The lack of change we observe might be due to the relatively high levels of acetylation found in ES cells prior to differentiation, making changes harder to detect (Boyer et al, 2006; Das et al, 2009b). Moreover, it has previously been shown that bulk acetylation levels do not change during the cell cycle, alterations can only be detected at the origins of replication (Unnikrishnan et al, 2010). Consequently, it may be possible to detect global or loci specific changes upon synchronisation of differentiated cells such as MEFs. Our results, also indicate that the levels of HDAC1/2 change during the cell cycle, but HDAC3 levels do not (Figure 4-17). The lack of change in HDAC3 correlates with what has been previously reported in Bhaskara et al, 2010. Furthermore, the changes in HDAC1/2 protein levels appear to correlate with the changes in HDAC activity with the highest level of protein and activity both observed during S phase (Figure 4-18). In contrast, the level of IP levels detected is lowest during S phase suggesting that the alterations in HDAC activity are dependent on adjustment of protein levels, not IP levels. Barker et al 2004, reports

alterations of Ins(1,4,5,6)P_4/Ins(3,4,5,6)P_4 between 3.6-10.5μM, however, we are unable to calculate our exact changes in IP levels, thus it remains possible that the levels of IP are not changing enough to influence HDAC activity. Indeed, the apparent Kd of HDAC3 for Ins(1,4,5,6)P_4 has been reported between 5-10μM, suggesting that alterations in IP levels may only result in minor changes, if any, which are not detectable (Millard et al, 2013; Watson et al, 2012; Watson et al, 2016). This would account for our inability to align alterations in HDAC activity with IP levels during the cell cycle.

6.3 The role of IPMK in gene regulation and development

There is a large body of evidence to support the role of IPMK and inositol phosphates in the regulation of gene expression through the activation, recruitment and stabilisation of transcription complexes such as Mcm1-Arg80 in yeast (Dubois et al, 2000; El Alami et al, 2003; Endo-Streeter et al, 2012; Hatch et al, 2017; Odom et al, 2000). IPMK and IPs also play a role in the regulation of chromatin remodelling via SWI/SNF and INO80 and as co-activators of transcription through CBP/p300 and SRF recruitment (Kim et al, 2013; Shen et al, 2003; Steger et al, 2003; Willhoft et al, 2016; Xu et al, 2013a; Xu et al, 2013b). Consequently, it is plausible that IPMK and therefore IPs could control gene expression through the regulation of class I HDAC activity.

6.3.1 Wildtype HDAC3, but not IP binding mutant HDAC3, mediated gene repression is enriched with IPMK expression

To determine the effect of IP on HDAC3 mediated repression, a luciferase reporter assay was utilised in HEK-293T cells. GAL4-SMRT and HDAC3 together repressed luciferase assay expression and this was further increased following expression of IPMK (Figure 3-9). Since IPMK is involved in the production of IP_4 and IP_5, it suggests increased repression was due to elevated amounts of IP being incorporated into the complex enabling activation of HDAC3/SMRT. Furthermore, HDAC3 IP binding mutants

previously shown to have reduced activity, alleviated the ability of HDAC3 to repress transcription even in the presence of IPMK (Figure 3-11, Figure 3-12) (Watson et al, 2016). This therefore suggests that increased IP levels increase the repressive abilities of HDAC3 and mutation of key binding sites, which alter activation and binding of IP, reduce the activity of HDAC3 mediated repression. Consequently, it appears that the ability to make essential interactions with IP is crucial for repression of gene expression by HDAC3. However, IP levels in HEK-293F cells where IPMK is overexpressed show slightly reduced levels of IP_4 and IP_5 (Figure 3-15). Whilst it is possible that the level of IPs increase in HEK-293T cells upon overexpression of IPMK as previously reported by other groups, it seems prudent to extrapolate our data from the HEK-293F cells (Fujii & York, 2005). Accordingly, this leads us to question the above conclusions as a decrease in IP levels would be expected to alleviate HDAC3 mediated repression due to decreased activation of the complex. It is possible that the HDAC3 mediated repression is independent of its deacetylase function as has been reported by Sun et al 2013. This would mean that complex activation is not required for HDAC3 mediated repression and as such a decrease in IP levels would have minimal effects on luciferase repression. It is possible to test this hypothesis by carrying out the luciferase assay with a deacetylase dead version of HDAC3. If the same results are observed as to those in this thesis it would suggest that the repression being observed is mediated independently of the catalytic activity of HDAC3.

6.3.2 IPMK ablation increases cardiomyocyte gene expression and reduces neuroectoderm formation in EBs

During embryogenesis, wide spread changes in gene expression occur as lineages are defined through the process of gastrulation and differentiation. HDAC1, HDAC3 and IPMK KO mice all have early embryonic lethal phenotypes at a point just after gastrulation (E10.5, E9.5 and E9.5 respectively) (Bhaskara et al, 2008; Frederick et al, 2005; Lagger et al, 2002; Montgomery et al, 2007; Montgomery et al, 2008). This led us to investigate the gene expression changes which occur in IPMK KO cells during differentiation via EB formation.

Consistent with the IPMK KO mouse phenotype, TET-IPMK cells maintain the ability to repress pluripotency markers (Oct4, Sox2 and Nanog) during EB formation (Figure 5-8) suggesting that IPMK is not important for their regulation (Frederick et al, 2005). Frederick et al., 2005, also stated that initial stages of gastrulation were unaffected due to the presence of all three germ layers in the KO model. However, the TET-IPMK EBs reveal decreased expression of FGF5 and potentially Brachyury upon loss of IPMK indicating reduced primitive ectoderm and mesendoderm formation (Figure 5-9). This suggests that in TET-IPMK EBs, unlike the mouse model, the initial stages of ES the initial stages of differentiation are affected and that IPMK may be involved in the regulation of primitive ectoderm formation. Analysis of key definitive endoderm markers (Figure 5-10), revealed minimal alterations in expression indicating that IPMK does not impact the generation of the definitive endoderm. This is in agreement with the IPMK KO mouse model where a layer of definitive endoderm was present in the embryo (Frederick et al, 2005). Loss of IPMK during mouse embryogenesis has been shown to result in the development of mesoderm but with delayed formation of the somites, suggesting abnormalities in its formation (Frederick et al, 2005). Nevertheless, the development of the heart appeared to be normal, this contrasts with the upregulation of cardiomyocyte markers (Tbx20 and Mef2c) observed in TET-IPMK EBs in the absence of IPMK (Figure 5-11). This upregulation of cardiomyocyte markers suggests that IPMK or IPs regulate their expression. Indeed, analysis of IPPK expression in mice revealed a high level of expression in the developing heart indicating that either IPPK or IP_6, of which the latter is downregulated in the IPMK KO mouse, may be important for proper development of the heart (Frederick et al, 2005; Verbsky et al, 2005a). In addition to the alterations in cardiomyocyte formation, loss of IPMK resulted in decreased expression of early ectoderm markers (Sox1 and Nestin) (Figure 5-12) suggesting that IPMK or IPs may positively regulate their expression and control the formation of the neuroectoderm. Both IPMK and IPPK are highly expressed in the neural tube of the developing mouse, thus supporting their role in the regulation of neuroectoderm formation and neural tube patterning (Frederick et al, 2005; Verbsky et al, 2005a). Furthermore, it has previously been observed that IPPK is induced in differentiating PC12 cells and loss of IPPK and therefore decreased IP_6,

reduces neuronal differentiation of PC12 cells (Loss et al, 2013). This highlights the essential role of IPs and their kinases in the development of the neuroectoderm. However, our TET-IPMK EB results contrast with the mass accumulation of neuroectoderm and kinking of the neural tube detected in the IPMK KO mice model (Frederick et al, 2005). It is possible that the less defined conditions of EB formation are affecting the outcome of IPMK ablation. Indeed, our EBs are formed in the presence of serum which contains BMP4 an inhibitor of neuroectoderm formation, which could account for the decreased formation (Finley et al, 1999). Consequently, it may be more effective to induce *in vitro* differentiation of TET-IPMK cells using defined (serum-free) media and the addition of specific factors to promote differentiation towards certain lineages.

The alterations in gene expression during EB formation indicates that IPMK is affecting gene regulation during differentiation. It is possible that this is through the modulation of HDAC activity, if IPs are regulating complex activity as shown *in vitro* (Millard et al, 2013; Watson et al, 2012; Watson et al, 2016). In accordance with the loss of IPMK, deletion of HDAC1 also upregulates key cardiomyocyte markers Nkx2.5 and Mef2c during EB formation, suggesting potential overlapping functions (Dovey et al, 2010b). However, whilst HDAC1 KO EB's display increased expression of neuroectoderm markers (Nestin and βIII-tubulin) and HDAC3 KO models indicate an absence of change in expression, TET-IPMK EBs exhibit decreased expression of Sox1 and Nestin, thus highlighting independent roles (Dovey et al, 2010, Wright et al, 2017, manuscript in progress). This is further supported by the lack of change in endoderm formation unlike the enhanced expression observed upon ablation of HDAC3 (Wright et al, 2017, manuscript in progress). Accordingly, the differences in gene expression profiles and the results presented earlier in this thesis, suggest that it is unlikely that IPMK is regulating differentiation through the activity of class I HDACs.

Alternative mechanisms of gene regulation by IPMK must also be considered. Indeed, yeast IPMK has been implicated in the transcriptional activation of arginine-response genes through stabilisation, recruitment and activation of the ArgR-Mcm1 transcription factor complex via kinase independent and dependent mechanisms

(Dubois et al, 2000; Hatch et al, 2017; Odom et al, 2000). Likewise in mammals, the mcm1 homolog, serum response factor (SRF) is bound by IPMK which promotes its recruitment to serum response elements (SREs) in immediate early genes (IEGs) enabling their transcription (Kim et al, 2013). Depletion of IPMK reduces SRF binding and activation of its target genes, indicating IPMK plays a positive role in gene expression. Accordingly, it is possible that IPMK acts as a co-activator of transcription factors involved in gene regulation during differentiation and depletion of IPMK reduces the ability of these genes to be activated. IPMK has also been observed to stimulate the recruitment p300 and CBP to p53 target genes and IEGs respectively (Xu et al, 2013a; Xu et al, 2013b). Deletion of IPMK results in reduced acetylation of histones and recruitment of p300/CBP, leading to reduced expression of target genes (Xu et al, 2013a; Xu et al, 2013b). Ablation of IPMK, which is expressed highly in the neural fold of the developing mouse, may result in decreased recruitment of p300/CBP to neuronal differentiation genes, resulting in decreased acetylation and gene expression. Conformation of p300/CBP binding to these neuronal markers (Sox1, Nestin etc.) during embryonic differentiation via ChIP and histone acetylation analysis; as well as comparison to levels of histone acetylation and binding in the IPMK knockout system, would be required to investigate this hypothesis further.

Inositol phosphates have also been implicated in the regulation of gene expression through indirect methods including chromatin remodelling and mRNA export (Shen et al, 2003; Steger et al, 2003; Wickramasinghe et al, 2013). Indeed, the nucleosome remodelling complex SWI/SNF has been shown to be activated by IP_4 and IP_5 whilst IP_6 inhibits the action of INO80 in human and yeast (Shen et al, 2003; Willhoft et al, 2016). As chromatin remodelling complexes can act as transcriptional activators or repressors, it is compelling to speculate that the developmental defects observed in the TET-IPMK EBs may be due to modulated activity of SWI/SNF and INO80 complexes. Indeed, depletion of BAF250a, a subunit of a mammalian SWI/SNF complex, results in the upregulation of cardiac genes such as Nkx2.5 and GATA4/6 indicating that BAF250a negatively regulates their expression (Singh & Archer, 2014). Therefore, it is possible that the reduction of IP_4 and IP_5 in the TET-IPMK EBs leads to an upregulation of cardiac markers through a reduction in activity of BAF250a. Conformation of

BAF250a binding to the promoters or enhancers of these genes and comparison to binding in the TET-IPMK EBs would enable this hypothesis to be investigated further. Human IPMK has recently been implicated in selective mRNA export through the requirement of PIP_3 binding to ALY, an RNA-binding adaptor protein, enabling its binding to sequence motifs in mRNAs involved in genome maintenance such as RAD51 (Wickramasinghe et al, 2013). Depletion of IPMK resulted in a reduction of ALY binding and subsequently reduced export of RAD51 mRNA (Wickramasinghe et al, 2013). It is possible that during differentiation, IPMK is required for the binding of proteins involved in mRNA export of a subset of developmental genes, and that loss of IPMK alters their export which in turn could alter the level of their expression.

6.4 Alternative roles for inositol phosphate in class I HDAC co-repressor complexes

Biophysical data demonstrates that Ins(1,4,5,6)P_4 is an important molecule in the regulation of class I HDAC complexes (Itoh et al, 2015; Millard et al, 2013; Watson et al, 2012; Watson et al, 2016). Despite these convincing results, the contents of this thesis implies that IPs are not physiological regulators of class I HDAC complexes. In 2012, Shears et al, discussed the role of IPs as signalling molecules whereby IPs must elicit a biological effect following an alteration in their concentration. The only IPs which he deemed to satisfy this requirement were Ins(1,4,5)P_3 a well-known regulator of calcium release and Ins(3,4,5,6)P_4 an inhibitor of chloride channel conductance (Shears et al, 2012). If Ins(1,4,5,6)P_4 is a physiological regulator of class I HDAC complexes, then changes in its concentrations should exhibit a measurable change in HDAC activity. However, this biological response is not observed by us upon large scale alteration of IP levels, suggesting that it is not a regulatory signal.

The presence of IP_6 at the interface of class I HDACs and their co-repressors results in a stabilising effect as measured by circular dichroism studies (Watson et al, 2016). Consequently, it is possible that Ins(1,4,5,6)P_4 is acting as a structural co-factor.

Indeed, simulations carried out on the structure of HDAC3 indicated that DAD stabilised HDAC3, but its intrinsic flexibility was further stabilised by the binding of Ins(1,4,5,6)P_4 (Arrar et al, 2013b). The interaction of Ins(1,4,5,6)P_4 with R265 in HDAC3 is believed to stabilise the highly mobile loop 6 therefore enhancing active site access, mutation of this residue to proline or alanine renders the complex inactive (Watson et al, 2012; Watson et al, 2016). Furthermore, mutagenesis studies of IP binding residues in either HDAC3 or SMRT, often render the complex unable to form as well as inactive (Codina et al, 2005; Watson et al, 2012). This therefore suggests that Ins(1,4,5,6)P_4 is required for formation of the complex (preventing charge repulsion) as well as its activity. The lack of activity observed could be due to the inability of complex assembly, which is known to be required for the activation of HDAC1/2 and 3. However, later studies have indicated that Ins(1,4,5,6)P_4 is not required for the interaction of HDAC1/MTA1 or HDAC3/SMRT (Millard et al, 2013). The co-repressors instead bind through the extended SANT domain of SMRT or the ELM2-SANT domain of MTA1 enabling extensive interactions with a nonpolar groove in HDAC3 or HDAC1 without the need for Ins(1,4,5,6)P_4 (Millard et al, 2013). This led to the suggestion that Ins(1,4,5,6)P_4 is not a structural co-factor and in fact activates the complex by engaging the SANT domain with the HDAC catalytic domain (Millard et al, 2013). However, my *in vivo* data argues against this proposal suggesting that maybe Ins(1,4,5,6)P_4 is required for, but does not regulate, the activity of class I HDACs. Alternatively, the binding of Ins(1,4,5,6)P_4 at the interface of SMRT/HDAC3 and MTA1/HDAC1 could have unconventional roles not yet considered. One possible function for Ins(1,4,5,6)P_4 is control of cellular localisation. Whilst HDAC1 and HDAC2 are predominantly nuclear proteins due to a C-terminal nuclear localisation signal (NLS), HDAC3 is both a cytoplasmic and nuclear protein due to the presence of a nuclear export signal (NES) in the N-terminus in addition to its C-terminal NLS (Taplick et al, 2001; Yang et al, 2002). Computational analysis indicates Ins(1,4,5,6)P_4 binding to HDAC3/DAD stabilises loop 6 in HDAC3, but also stabilises helix 6 and the C-terminal domain of HDAC3 (Arrar et al, 2013b; Watson et al, 2012). Accordingly, it is possible that this stabilisation of the C-terminal region promotes nuclear translocation of HDAC3 through the stabilisation of the NLS (Arrar et al, 2013a). This hypothesis could be tested by studying the cellular localisation of GFP tagged HDAC3 in IP depleted cells

compared to wildtype cells by fluorescence microscopy. Furthermore, it is possible that the genomic localisation of class I HDAC complexes could be regulated by Ins(1,4,5,6)P_4 binding. Indeed, mice harbouring Y470A and Y478A mutations in SMRT and NCoR respectively (NS-DADm), show reduced genomic recruitment of HDAC3 compared to wildtype mice (600 sites vs 5799) (You et al, 2013). Interestingly, Y470 in SMRT (corresponding to Y478 in NCoR) was shown to interact with Ins(1,4,5,6)P_4 in the 2012 structure and mutation of these residue reduces HDAC3 activity (Codina et al, 2005; Guenther et al, 2001; Watson et al, 2012). Accordingly it is plausible that the reduced ability to bind Ins(1,4,5,6)P_4 in the mutant mice, decreases HDAC3 recruitment to the genome through an unknown mechanism. Analysis of HDAC1/2/3 binding in the presence or absence of IPs by ChIP-Seq would enable us to determine whether the presence of IPs influence the recruitment of HDACs to the genome.

The basic interface between HDAC3/SMRT where Ins(1,4,5,6)P_4 was shown to bind, could also target the complex to specific substrates. Phosphoinositide's (PIPs) have previously been shown to regulate nuclear processes such as activation of transcription. For example, the nuclear receptor, steroidogenic factor 1 (SF-1) binds the free fatty acid chains of phosphatidylinositol 4,5-bisphosphate (PI(4,5,)P_2) which enables IPMK to phosphorylate it to phosphatidylinositol (3,4,5)-trisphosphate (PI(3,4,5)P_3) promoting transcriptional activation of target genes (Blind et al, 2012). Nuclear phosphoinositide's are present in both the nuclear envelope and the interior of the nucleus and can be bound through multiple domains including plekstrin homology domains as well as regions rich in lysine and arginine, like the HDAC3/SMRT interface (Shah et al, 2013). It is possible that PI(3,4,5)P_3 binds to the lys/arg rich interface between HDAC3/SMRT as although the fatty acid chains are bound at position P1 in the inositol ring, Ins(1,3,4,5)P_4 is capable of activating the complex without site D being occupied (Watson et al, 2016). The idea that PIPs can regulate HDAC complexes has previously been proposed. For example, the SAP30-like protein (SAP30L) which can bind the Sin3/HDAC complexes has the ability to bind DNA via a N-terminal Zinc finger but can also bind phosphatidylinositol-(5)-monophosphate (PI(5)P) (Viiri et al, 2009). The binding of SAP30L to PI(5)P, dissociates the complex from the DNA as PI(5)P binds in the same area as chromatin, thus decreasing the repressive

effects of the Sin3/HDAC complex (Viiri et al, 2009). Recruitment of HDAC3/SMRT to $PI(3,4,5)P_3$ at the nuclear membrane would result in the active site of HDAC3 facing towards the membrane (Figure 6-2). This could potentially enable deacetylation of membrane bound proteins such as lamins. Clusters of silenced genes have been shown to associate at the nuclear periphery with lamins, depletion of lamins results in decreased silencing and increased acetylation at these regions as does downregulation of HDAC1 and HDAC3 (Milon et al, 2012). It was proposed that lamin associated proteins recruit HDAC1/3 to promote gene silencing, however it is possible that HDAC3/SMRT binding to PIPs adjacent to lamins helps establish these transcriptionally silent regions (Milon et al, 2012). This hypothesis could be tested, following confirmation of PIP binding, by confocal microscopy to determine if HDAC1/2/3 co-localise with lamins at the nuclear membrane and whether this is altered upon disruption of PIP production. It is clear from the contents of this thesis that more research is required to understand the physiological role of IPs or indeed PIPs at the HDAC/co-repressor interface.

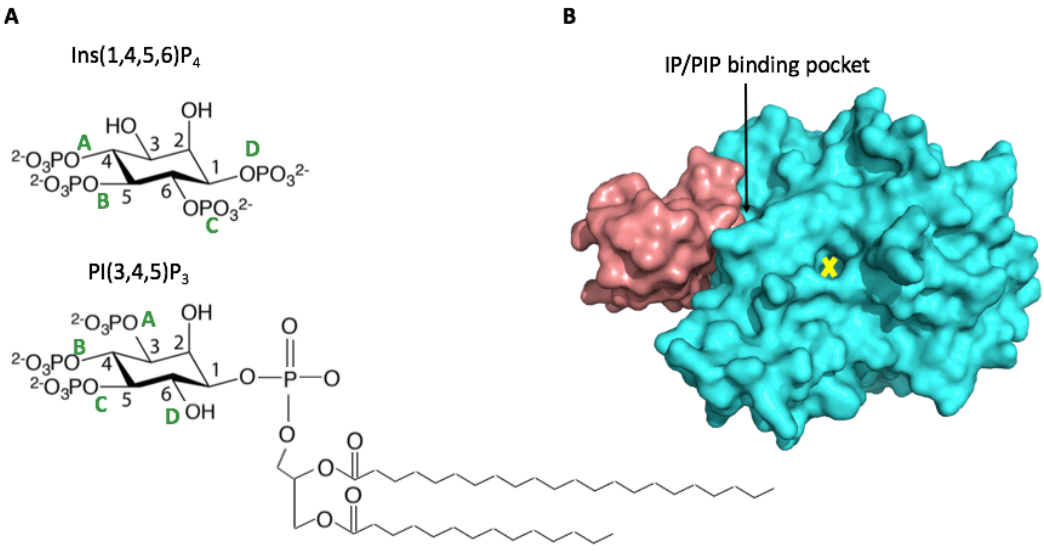

Figure 6-2 PIP binding to HDAC3/SMRT orientates the active site towards the nuclear membrane (A) *Structure of Ins(1,4,5,6)P_4 and PI(3,4,5)P_3 are shown with A,B,C and D denoting phosphate group binding sites in HDAC3 (fatty acid chains not to scale).* ***(B)*** *Surface structure of DAD (salmon) and HDAC3 (cyan) rotated to show orientation when PIP bound at the membrane (shown by arrow). Active site (yellow cross) faces towards the membrane. (PDB ID: 4A69, Watson et al, 2012.)*

6.5 Summary

In this thesis, contrary to *in vitro* data, we have shown that manipulation of inositol phosphate levels does not significantly affect the activity of class I HDACs. Overexpression of IPMK, PTEN or SopB has no obvious effect on HDAC activity which can be correlated with alterations in the levels of IP present. Furthermore, loss of IPMK does not reduce the level of global histone acetylation levels or HDAC activity in ES cells or upon RA mediated differentiation. Alterations in HDAC activity did not correlate with alterations in IP levels during the cell cycle. Consequently, it appears that inositol phosphates may not regulate class I HDACs *in vivo*. Unlike deletion of HDAC1/2/3, IPMK knockout ES cells are able to differentiate into EBs without any morphological differences observed. Q-PCR analysis indicates that mesodermal markers are potentially over-expressed whilst early neuroectodermal markers are underrepresented. The embryonic lethality of IPMK indicates it has important function in embryogenesis in agreement with our EB analysis. If, as our data suggests, this function is not directly regulating class I HDAC complex activity then the essential nuclear role of IPMK during embryogenesis remains to be discovered.

Appendices 1 Antibodies

Table A1 1 Antibodies

Target protein	Source	Clonality	Dilution	Origin	Application
HDAC1	Rabbit	Monoclonal	1:2500	Abcam – ab109411	WB
HDAC2	Mouse	Monoclonal	1:2000	Millipore – 05-814	WB & IP
HDAC3	Rabbit	Monoclonal	1:2500	Abcam – ab32369	WB & IP
HDAC3	Mouse	Monoclonal	1:2500	Cell Signaling7G6C5	WB & IP
LSD1	Rabbit	Monoclonal	1:10,000	Abcam – ab129195	WB & IP
GFP (B2)	Mouse	Monoclonal	1:1000	Santa-Cruz Sc-9996	WB
anti-Flag M2	Mouse	Monoclonal	1: 2500	Sigma – F1804	WB
IPMK	Rabbit	Polyclonal	1:1000	Abcam – ab 96753	WB
α-Tubulin	Mouse	Monoclonal	1:10,000	Sigma – T5168	WB
Cyclin A2	Rabbit	Polyclonal	1:1000	Abcam – ab137769	WB
Oct4	Mouse	Monoclonal	1:500	Santa Cruz– Sc5279	WB
Nanog	Rabbit	Polyclonal	1:2500	Bethyl –A300-397A	WB
H3	Mouse	Monoclonal	1:1000	Upstate – 05-499	WB
H3K9Ac	Rabbit	Polyclonal	1:1000	Active Motif 39917	WB
H3K14Ac	Rabbit	Polyclonal	1:1000	Active Motif 39599	WB
H3K18Ac	Rabbit	Polyclonal	1:1000	Upstate 07-354	WB
H3K27Ac	Rabbit	Polyclonal	1:1000	Active Motif 39135	WB
H3K56Ac	Rabbit	Polyclonal	1:1000	Active motif 39281	WB
H3S10P	Rabbit	Polyclonal	1:1000	Active motif 39253	WB
H4	Mouse	Monoclonal	1:8000	Active Motif 61521	WB
H4K5Ac	Rabbit	Polyclonal	1:1000	Active Motif 39699	WB
H4K12Ac	Rabbit	Polyclonal	1:1000	Active Motif 39927	WB
H4K16Ac	Rabbit	Polyclonal	1:1000	Active Motif 39167	WB
IRDye 800Cw	Goat anti-mouse		1:10,000	LiCoR – 926 32210	WB
IRDye 680Cw	Donkey anti-Rabbit		1:10,000	LiCoR – 926 68023	WB
Normal mouse IgG	Mouse		1ug	Santa Cruz – Sc-2025	IP
Normal Rabbit IgG	Rabbit		1ug	Millipore – 12-370	IP

Appendices 2 qRT-PCR Primers Sequences

Table A2 1 qRT-PCR primer sequences

Target	Primer name	Sequence 5' → 3'	Tm (°C)
β-Actin	B-ACTIN F	GGCTCCTAGCACCATGAAGA	60
	B-ACTIN R	AGCTCAGTAACAGTCCGCCT	
HNF4a	HNF4aF2	GCAAGTGAGCCTGGAGGATT	60
	HNF4aR2	CTCCGAGAAGCATCTCCTGC	
Rpgrip	Rpgrip F3	TGCCTTCTCCCTAGCAGACC	60
	Rpgrip R3	CACATCTTCTCTGAATCGGCTTT	
HoxB2	HoxB2 F3	ATTCGCCTTTTCTACCGGACC	60
	HoxB2 R3	GGGCTATCGAGAGAACCCTG	
Cds2	Cds2 F1	ATGACCGAACTACGGCAGAG	60
	Cds2 R1	GAGGTTGGTAGGGGAGCTG	
Fam35a	Fam35a F1	CCACTGAAAACGACAGTATCACA	60
	Fam35a R1	CCTTTGGGGACTTGACAGTCTT	
Athl1	Athl1 F1	GGGAACAAACCCATCACAGT	55
	Athl1 R1	CTCAGGGTTAAGTACGTGGC	
CD68	CD68 F1	GCCATGTTTCTCTTGCAACC	55
	CD68 R1	GCTGGTAGGTTGATTGTCGT	
TbX3os2	TbX30S2 F1	CTGCAGTTTAAGCCGAGCTA	55
	TbX30S2 R1	GAGTGCTTAAGGGGACATGG	
Hist1h2bq	Hist1h2bqF2	CTAGGGTACCTTCCTCAGCA	55
	Hist1h2bqR2	GCATCTTACTAGAGTCGGC	
Oct4	Oct4 F	AGTATGAGGCTACAGGGACA	60
	Oct4 R	CAAAGCTCCAGGTTCTCTTG	
Sox2	Sox2 F	TAGAGCTAGACTCCGGGCGATGA	60
	Sox2 R	TTGCCTTAAACAAGACCACGAAA	
Nanog	Nanog F	AGGGTCTGCTACTGAGATGCTCTG	60
	Nanog R	CAACCACTGGTTTTTCTGCCACCG	
hIPMK	hIPMK F1	TGACGCGCATACATCTTGGAC	60
	hIMPK R1	AGGACAACTGTCAGACACAGA	
Brachyury	Brachyury_F	GCTTCAAGGAGCTAACTAACGAG	55
	Brachyury_R	CCAGCAAGAAAGAGTACATGGC	
Fgf5	Fgf5_F	AAGTAGCGCGACGTTTTCTTC	60
	Fgf5_R	CTGGAAACTGCTATGTTCCGAG	
Gata4	Gata4_F	CTGGAAGACACCCCAATCTC	60
	Gata4_R	CCATCTCGCCTCCAGAGT	
Gata6	Gata6_F	TGGCTCCGGTAACAGCAGTG	60
	Gata6_R	GTGGTCGCTTGTGTAGAAGGA	
Foxa2	Foxa2_F	CCCTACGCCAACATGAACTCG	55
	Foxa2_R	GTTCTGCCGGTAGAAAGGGA	
Sox17	Sox17_F	GATGCGGGATACGCCAGTG	60
	Sox17_R	CCACCACCTCGCCTTTCAC	
Hnf1β	Hnf1β F	AGGAGTGTAATAGGGCGGAGT	55
	Hnf1β R	GAGGTCCGTTATAGGTGTCCA	
Tbx5	Tbx5_F	ATGGCCGATACAGATGAGGG	57
	Tbx5_R	TTCGTGGAACTTCAGCCACAG	

Tbx20	Tbx20_F	AAACCCCTGGAACAATTTGTGG	60
	Tbx20_R	CATCTCTTCGCTGGGGATGAT	
Mef2C	Mef2C_F	ATCCCGATGCAGACGATTCAG	60
	Mef2C_R	AACAGCACACAATCTTTGCCT	
Myf5	Myf5_F	AAGGCTCCTGTATCCCCTCAC	60
	Myf5_R	TGACCTTCTTCAGGCGTCTAC	
MyoD	MyoD_F	CCACTCCGGGACATAGACTTG	60
	MyoD_R	AAAAGCGCAGGTCTGGTGAG	
MyoG	MyoG F	GAGACATCCCCCTATTTCTACCA	60
	MyoG R	GCTCAGTCCGCTCATAGCC	
Sox1	Sox1_F	GATGCCACCAACGCTAAAGC	60
	Sox1_R	TTGCGGTTGAAGTCCAGGC	
Pax6	Pax6_F	TACCAGTGTCTACCAGCCAAT	60
	Pax6_R	TGCACGAGTATGAGGAGGTCT	
Pax6	Pax6_F	TACCAGTGTCTACCAGCCAAT	60
	Pax6_R	TGCACGAGTATGAGGAGGTCT	
Nestin	Nestin_F	CCCTGAAGTCGAGGAGCTG	60
	Nestin_R	CTGCTGCACCTCTAAGCGA	
BIII-Tubulin	BIII-Tubulin_F	TAGACCCCAGCGGCAACTAT	60
	BIII-Tubulin_R	GTTCCAGGTTCCAAGTCCACC	
Ascl1	Ascl1_F	GCAACCGGGTCAAGTTGGT	60
	Ascl1_R	GTCGTTGGAGTAGTTGGGGG	
Neurog1	Neurog1 F1	CCAGCGACACTGAGTCCTG	57
	Neurog1 R1	CGGGCCATAGGTGAAGTCTT	
B-Catenin	B-Catenin F	ATGGAGCCGGACAGAAAAGC	60
	B-Catenin R	CTTGCCACTCAGGGAAGGA	
Nodal	Nodal_F4	TTCAAGCCTGTTGGGCTCTAC	60
	Nodal_R4	TCCGGTCACGTCCACATCTT	
Noggin	Noggin_F	GCCAGCACTATCTACACATCC	60
	Noggin_R	GCGTCTCGTTCAGATCCTTCTC	
Hes1	Hes1 F1	CCAGCCAGTGTCAACACGA	60
	Hes1 R1	AATGCCGGGAGCTATCTTTCT	

Appendices 3 Plasmids and Constructs

Table A3 1 Salmonella Dublin SopB constructs

Plasmid	Vector	Protein	Domain	Mutation	Tag	Resistance
pL21 SopB	pLeics21	SopB	Full length	None	eGFP	Kanamycin
pL21 SopB C460A	pLeics21	SopB	Full Length	C460A	eGFP	Kanamycin

Table A3 2 SopB cloning primer sequences

Plasmid	Primers used	Sequence
pL21 SopB	SopB-21-5	GTATTTTCAGGGCGCCCCAAAGAAGAAGCGTAAGGTCATGCAAAT ACAGAGCTTCTATCAC
	SopB-21-3	GTCGACTGCAGAATTtcaTTACTTTTTCTTTTTTGCCTGGCCGGCCTT TTTCGTGGCCGCCGGCCTTTTAGATGTGATTAATGAAGAAATGCC
pL21 SopB C460A	Pl21 SopB 5’	GTATTTTCAGGGCGCCCCAAAGAAGAAGCGTAAGGTCATGCAAAT ACAGAGCTTCTATCAC
	SopB C460A F	TACCCGCCTGGAATGCTAAAAGCGGCAAAG
	SopB C460A R	CTTTGCCGCTTTTAGCATTCCAGGCGGGTA
	Pl21 SopB 3’	CATCATTTTGGCAAAGAATTCATGgattacaaggatcatgacattgactacaa agacgatgacgacaagcacgacggcCCAAAGAAGAAGCGTAAGGTCATGC AAATACAGAGCTTCTATCAC

pL21 SopB wildtype and C460A plasmid map:

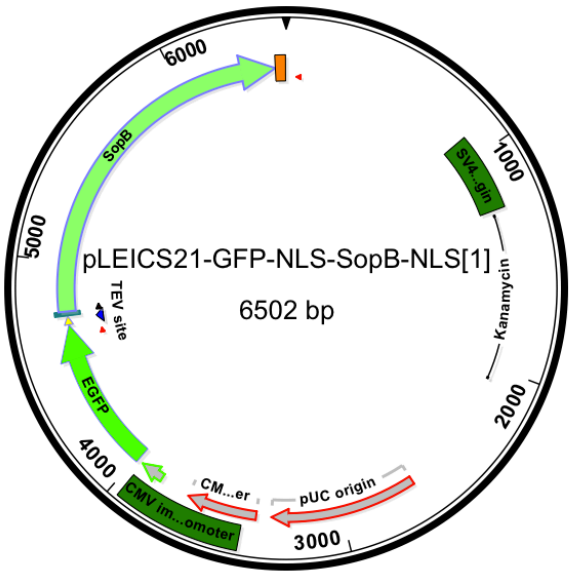

Sequencing results for pL21 SopB wildtype:

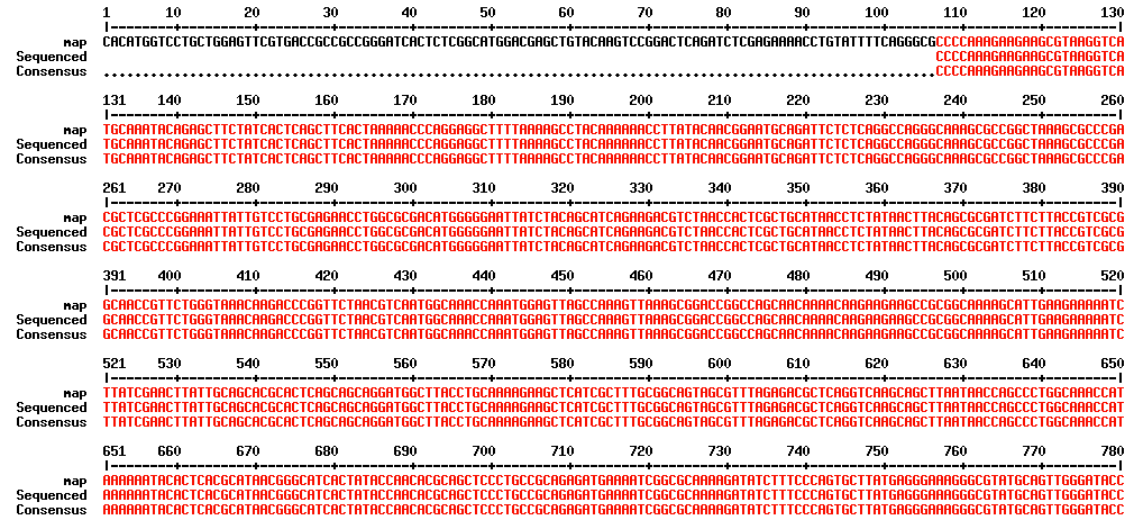

Sequencing results for pL21 SopB C460A:

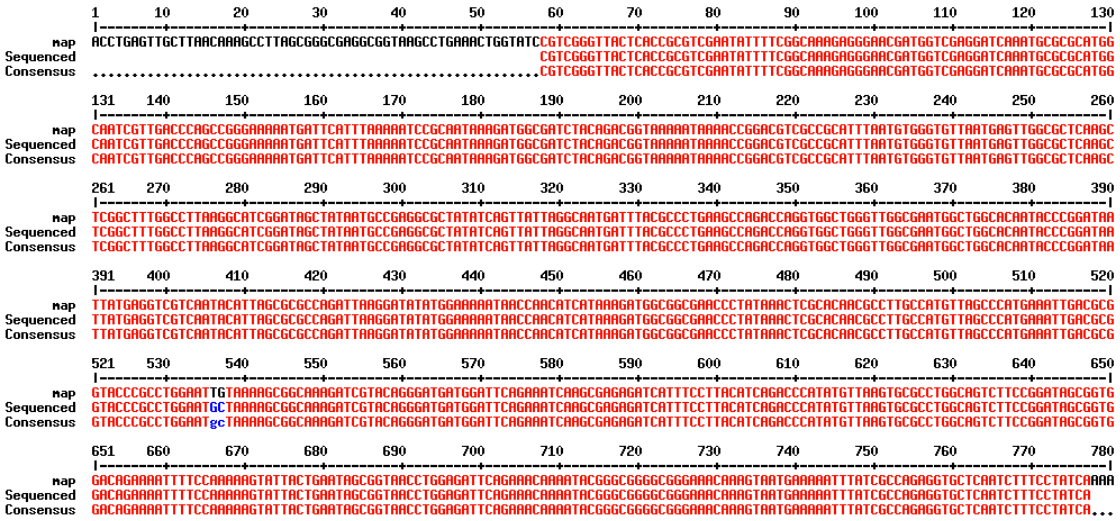

Table A3 3 Human PTEN plasmids

Plasmid	Vector	Protein	Domain	Mutation	Tag	Resistance
pL21 PTEN	pLeics21	PTEN	Full length	None	eGFP	Kanamycin
pL21 PTEN C124A	pLeics21	PTEN	Full length	C124A	eGFP	Kanamycin

Table A3 4 PTEN cloning primer sequences

Plasmid	Primers used	Sequence
pL21 PTEN	pL21 PTEN 5	ctactctagagctagcgaattcCAACCATGgattacaaggatca tgacattgactacaaagacgatgacgacaagcacgacggcATGAC AGCCATCATCAAAGAG
	pL21 PTEN 3	GTCGACTGCAGAATTtcaCTACTTCTTCTTCTTGGCCTGG CGG CCTTCTTGGTGGCGGCGGGCCTCTTGACTTTTGTA ATTTGT
pL21 PTEN C124A	pL21 PTEN 5	ctactctagagctagcgaattcCAACCATGgattacaaggatcatg acattga ctacaaagacgatgacgacaagcacgacggcATGA CAGCCATCATCAAAGAG
	PTEN C124A F	TTGCAGCAATTCACTGTAAAGCTGGAAAGGG
	PTEN C124A R	CCCTTTCCAGCTTTACAGTGAATTGCTGCAA
	pL21 PTEN 3	GTCGACTGCAGAATTtcaCTACTTCTTCTTCTTGGCCT GGCCGGCCTTCTTGGTGGCGGCGGGCCTCTTGACTTT TGTAATTTGT

pL21 PTEN wildtype and C124A plasmid map:

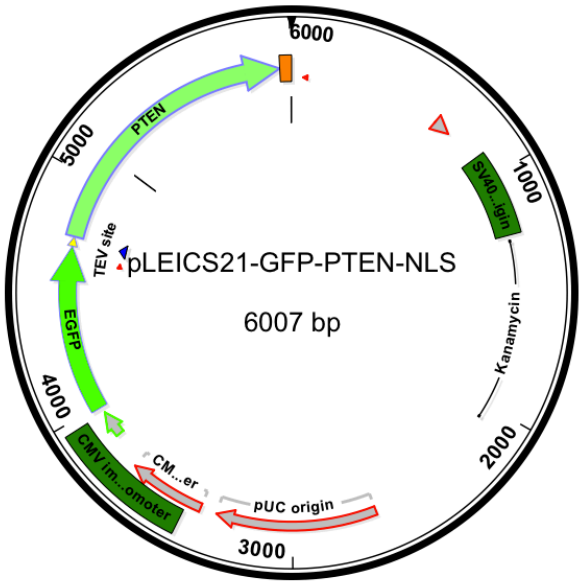

Sequencing results for pL21 PTEN wildtype:

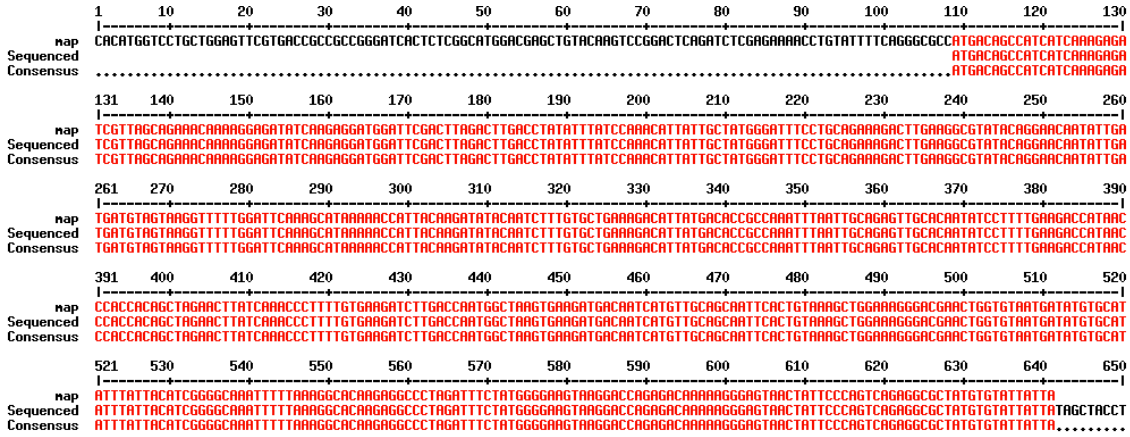

Sequencing results for pL21 PTEN C124A:

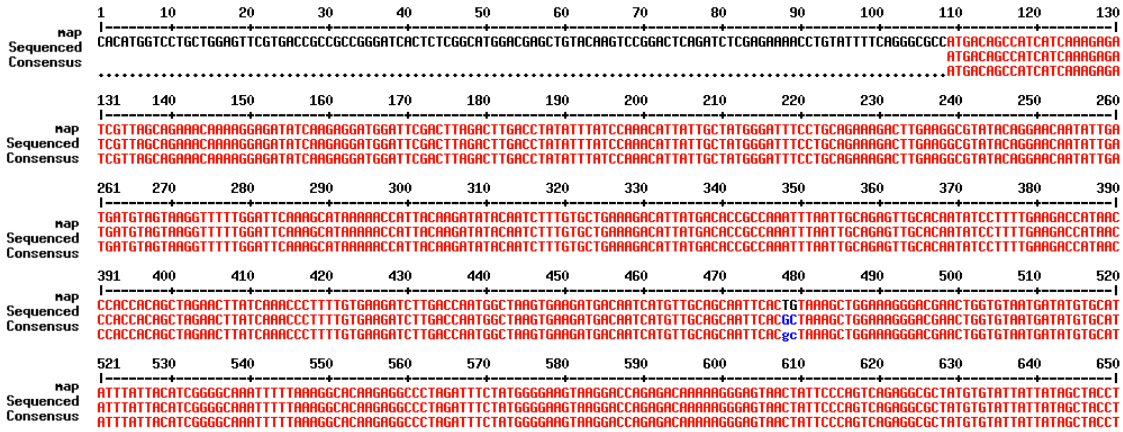

Table A3 5 Human IPMK vectors

Plasmid	Vector	Protein	Domain	Mutation	Tag	Inducible	Resistance
pL38-2x Flag IPMK	pLeics38	IPMK	Full length	None	Flag IRES Neo	No	Ampicillin
pL38 IPMK	pLeics38	IPMK	Full length	None	IRES Neo	No	Ampicillin
pL38 IPMK D144A	pLeics38	IPMK	Full length	D144A	IRES Neo	No	Ampicillin
PB TET IPMK	(Glover et al, 2013)	IPMK	Full length	None	Flag	TET/Dox	Ampicillin

Table A3 6 IPMK cloning primer sequences

Plasmid	Primers used	Sequence
pL38-2x Flag-IPMK	37-IP-Flag5	CTACTCTAGAGCTAGCGAATTCCAACCATGgattacaaggatcatgacattgactacaaagacgatgacgacaagcacgacggcATGGCAACAGAGCCACCATCC
	37-IP-3	GGATCCGATTTAAATTCGAATTCtcaATTGTCTAAAATACTTCGAAG
pL38 IPMK (no flag)	pL37 IPMK 5	CTACTCTAGAGCTAGCGAATTCCAACCATGATGGCAACAGAGCCACCATCC
	pL38 IPMK 3	GGATCCGATTTAAATTCGAATTCtcaATTGTCTAAAATACTTCGAAG
pL38 IPMK D144A	37-IP-Flag5	CTACTCTAGAGCTAGCGAATTCCAACCATGgattacaaggatcatgacattgactacaaagacgatgacgacaagcacgacggcATGGCAACAGAGCCACCATCC
	IPMK D114A F	AGCCCTGTATAATGGCTGTAAAGATAGGGC
	IPMK D114A R	GCCCTATCTTTACAGCCATTATACAGGGCT
	pL38 IPMK 3	GGATCCGATTTAAATTCGAATTCtcaATTGTCTAAAATACTTCGAAG
PB TET IPMK	TET IPMK pA 5’	TCAGATCGCCACTAGTCGAgttaatTTGTTCAACCATGgattacaaggatcatgacatt
	TET IPMK pA 3’	agaaggcatgaacatggttagcagaggGTTTCAATTGTCTAAAATACTTCGAAGTACAGA

pL38 2x FLAG-IPMK wildtype plasmid map:

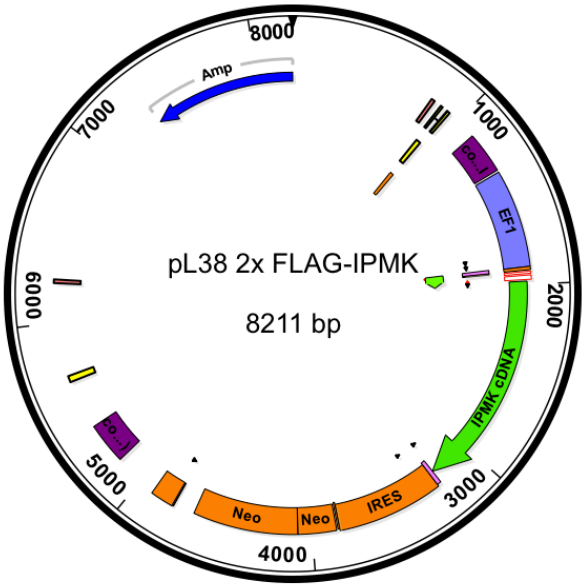

Sequencing results for pL38 2x FLAG-IPMK IRES Neo:

```
                1         10        20        30        40        50        60        70        80        90        100       110       120       130
                |---------+---------+---------+---------+---------+---------+---------+---------+---------+---------+---------+---------+---------|
map             CCTACTCTAGAGCTAGCGAATTCCAACCATGGATTACAAGGATCATGACATTGACTACAAAGACGATGACGACAAGCACGACGGCATGGCAACAGAGCCACCATCCCCCCTCCGGGTCGAGGCGCCGGGC
Sequenced                                                                   GATGACGACAAGCACGACGGCATGGCAACAGAGCCACCATCCCCCCTCCGGGTCGAGGCGCCGGGC
Consensus       ............................................................GATGACGACAAGCACGACGGCATGGCAACAGAGCCACCATCCCCCCTCCGGGTCGAGGCGCCGGGC

                131       140       150       160       170       180       190       200       210       220       230       240       250       260
                |---------+---------+---------+---------+---------+---------+---------+---------+---------+---------+---------+---------+---------|
map             CCCCCAGAAATGCGGACCTCACCGGCGATCGAGTCCACCCCTGAGGGCACCCCGCAGCCGGCGGGCGGCAGACTCCGCTTCCTCAACGGCTGCGTGCCCCTCTCGCATCAGGTGGCCGGGCACATGTACG
Sequenced       CCCCCAGAAATGCGGACCTCACCGGCGATCGAGTCCACCCCTGAGGGCACCCCGCAGCCGGCGGGCGGCAGACTCCGCTTCCTCAACGGCTGCGTGCCCCTCTCGCATCAGGTGGCCGGGCACATGTACG
Consensus       CCCCCAGAAATGCGGACCTCACCGGCGATCGAGTCCACCCCTGAGGGCACCCCGCAGCCGGCGGGCGGCAGACTCCGCTTCCTCAACGGCTGCGTGCCCCTCTCGCATCAGGTGGCCGGGCACATGTACG

                261       270       280       290       300       310       320       330       340       350       360       370       380       390
                |---------+---------+---------+---------+---------+---------+---------+---------+---------+---------+---------+---------+---------|
map             GGAAGGACAAAGTGGGTATACTGCAACATCCAGATGGCACAGTTTTGAAACAGTTACAACCACCTCCAAGGGGCCCAAGAGAGCTGGAATTCTATAATATGGTTTATGCTGCTGACTGTTTTGATGGTGT
Sequenced       GGAAGGACAAAGTGGGTATACTGCAACATCCAGATGGCACAGTTTTGAAACAGTTACAACCACCTCCAAGGGGCCCAAGAGAGCTGGAATTCTATAATATGGTTTATGCTGCTGACTGTTTTGATGGTGT
Consensus       GGAAGGACAAAGTGGGTATACTGCAACATCCAGATGGCACAGTTTTGAAACAGTTACAACCACCTCCAAGGGGCCCAAGAGAGCTGGAATTCTATAATATGGTTTATGCTGCTGACTGTTTTGATGGTGT

                391       400       410       420       430       440       450       460       470       480       490       500       510       520
                |---------+---------+---------+---------+---------+---------+---------+---------+---------+---------+---------+---------+---------|
map             TCTTCTAGAGCTACGAAAATATTTGCCAAAATATTATGGCATCTGGTCACCTCCCACTGCACCAAACGATTTATACCTAAAACTGGAAGATGTGACCCATAAATTTAATAAGCCCTGTATAATGGATGTA
Sequenced       TCTTCTAGAGCTACGAAAATATTTGCCAAAATATTATGGCATCTGGTCACCTCCCACTGCACCAAACGATTTATACCTAAAACTGGAAGATGTGACCCATAAATTTAATAAGCCCTGTATAATGGATGTA
Consensus       TCTTCTAGAGCTACGAAAATATTTGCCAAAATATTATGGCATCTGGTCACCTCCCACTGCACCAAACGATTTATACCTAAAACTGGAAGATGTGACCCATAAATTTAATAAGCCCTGTATAATGGATGTA
```

pL38 IPMK IRES WT/D144A Neo plasmid map:

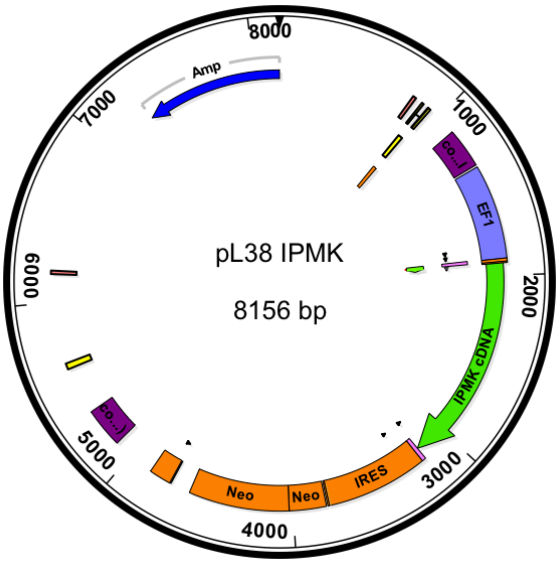

Sequencing results for pL38 IPMK IRES Neo (no flag):

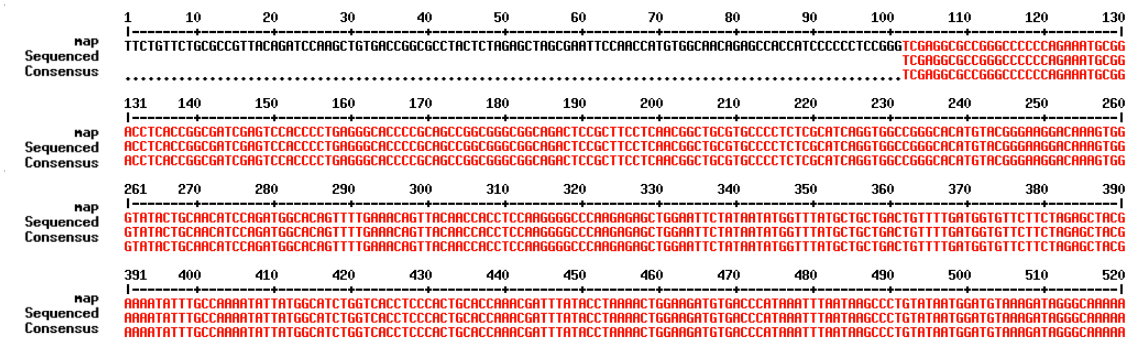

Sequencing results for pL38 IPMK D144A IRES Neo:

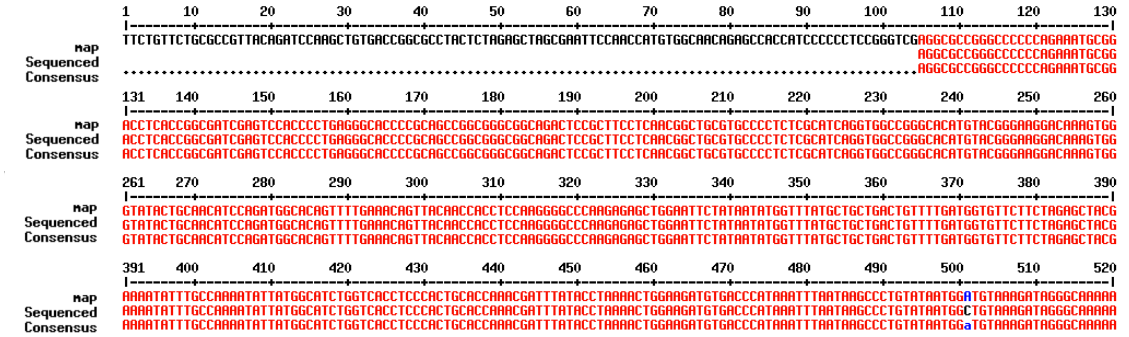

PB TET IPMK plasmid map:

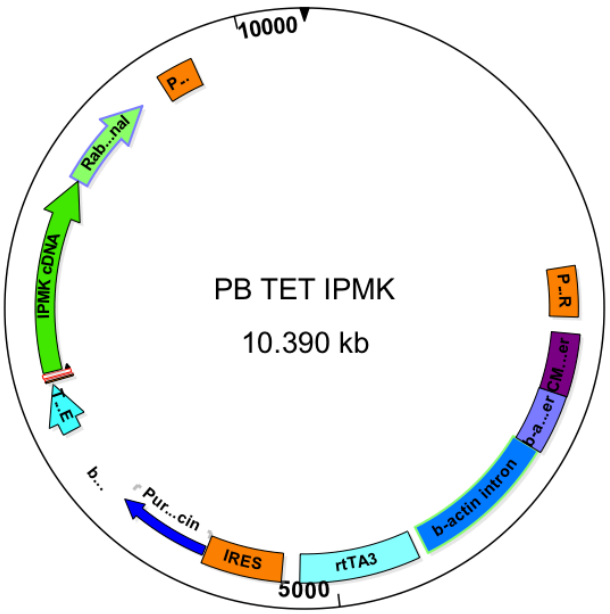

Sequencing results for PB TET IPMK:

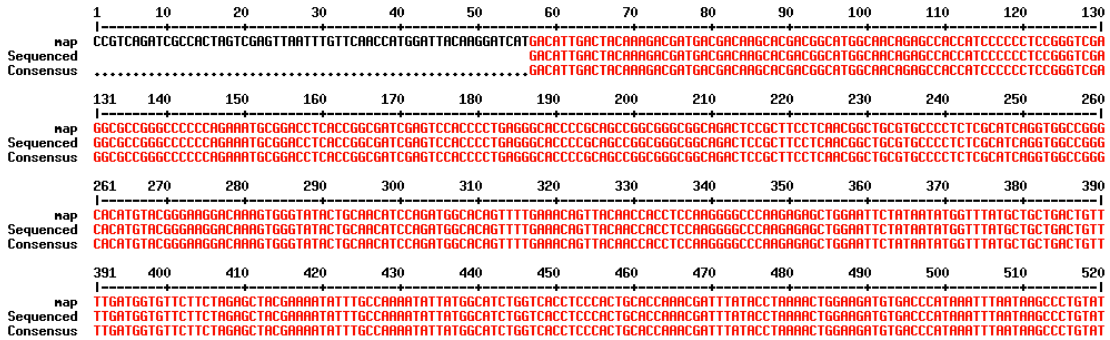

Table A3 7 Plasmids used in Reporter assay experiments

Plasmid	Vector	Protein	Domain (amino acids)	Mutation	Tag	Resistance
TkLuc	(Cowley et al, 2004)	Luciferase	Full length	None	Gal4 UAS	Amp
B-gal	(Cowley et al, 2004)	B-galactosidase	Full length	None	None	Amp
MadN35	(Ayer et al, 1996)	Mad	1-35	None	Gal4 DBD	Amp
SMRT-PJW1216	pLeics84	SMRT	Xt-DAD 350-480	None	Gal4 DBD	Amp
HDAC3-PJW371	pcDNA3	HDAC3	Full length	None	None	Amp
HDAC3 R265A-PJW1341	pLeics12	HDAC3	Full length	R265A	None	Amp
HDAC3:5m PJW801	pLeics12	HDAC3	Full length	H17C,G21A K25I,R265P R301A	None	Amp
pL38-2x Flag IPMK	pLeics38	IPMK	Full length	None	Flag IRES Neo	Amp

Table A3 8 Plasmids used for flag resin pull down experiments

Plasmid	Vector	Protein	Domain (amino acids)	Mutation	Tag	Resistance
SMRT-PJW1002	pLeics12	SMRT	Xt-DAD 350-480	None	Flag	Ampicillin
HDAC3-PJW371	pcDNA3	HDAC3	Full length	None	None	Ampicillin
pL21 SopB	pLeics21	SopB	Full length	None	eGFP	Kanamycin
pL21 SopB C460A	pLeics21	SopB	Full Length	C460A	eGFP	Kanamycin
pL21 PTEN	pLeics21	PTEN	Full length	None	eGFP	Kanamycin
pL21 PTEN C124A	pLeics21	PTEN	Full length	C124A	eGFP	Kanamycin
pL38 IPMK	pLeics38	IPMK	Full length	None	IRES Neo	Ampicillin
pL38 IPMK D144A	pLeics38	IPMK	Full length	D144A	IRES Neo	Ampicillin

References:

Abranches, E., Silva, M., Pradier, L., Schulz, H., Hummel, O., Henrique, D. & Bekman, E. (2009) Neural Differentiation of Embryonic Stem Cells In Vitro: A Road Map to Neurogenesis in the Embryo. *Plos One*, 4(7), 14.

Agalioti, T., Chen, G. Y. & Thanos, D. (2002) Deciphering the transcriptional histone acetylation code for a human gene. *Cell*, 111(3), 381-392.

Agger, K., Cloos, P. A. C., Christensen, J., Pasini, D., Rose, S., Rappsilber, J., Issaeva, I., Canaani, E., Salcini, A. E. & Helin, K. (2007) UTX and JMJD3 are histone H3K27 demethylases involved in HOX gene regulation and development. *Nature*, 449(7163), 731-U10.

Alland, L., David, G., Hong, S. L., Potes, J., Muhle, R., Lee, H. C., Hou, H., Chen, K. & DePinho, R. A. (2002) Identification of mammalian Sds3 as an integral component of the Sin3/histone deacetylase corepressor complex. *Molecular and Cellular Biology*, 22(8), 2743-2750.

Allfrey, V. G., Faulkner, R. & Mirsky, A. E. (1964) Acetylation and methylation of histones and their possible role in the regulation of RNA synthesis. *Proceedings of the National Academy of Sciences of the United States of America*, 51, 786-94.

Allfrey, V. G., Littau, V. C. & Mirsky, A. E. (1963) On the role of of histones in regulation ribonucleic acid synthesis in the cell nucleus. *Proceedings of the National Academy of Sciences of the United States of America*, 49, 414-21.

Ambrosetti, D. C., Basilico, C. & Dailey, L. (1997) Synergistic activation of the fibroblast growth factor 4 enhancer by Sox2 and Oct-3 depends on protein-protein interactions facilitated by a specific spatial arrangement of factor binding sites. *Molecular and Cellular Biology*, 17(11), 6321-6329.

Andres, M. E., Burger, C., Peral-Rubio, M. J., Battaglioli, E., Anderson, M. E., Grimes, J., Dallman, J., Ballas, N. & Mandel, G. (1999) CoREST: A functional corepressor required for regulation of neural-specific gene expression. *Proceedings of the National Academy of Sciences of the United States of America*, 96(17), 9873-9878.

Ang, S. L., Wierda, A., Wong, D., Stevens, K. A., Cascio, S., Rossant, J. & Zaret, K. S. (1993) The formation and maintenance of the definitive endoderm lineage in the mouse - involvement of HNF3/forkhead proteins. *Development*, 119(4), 1301-1315.

Arrar, M., de Oliveira, C. A. F. & McCammon, J. A. (2013a) Inactivating mutation in histone deacetylase 3 stabilizes its active conformation. *Protein Science*, 22(10), 1306-1312.

Arrar, M., Turnham, R., Pierce, L., de Oliveira, C. A. F. & McCammon, J. A. (2013b) Structural insight into the separate roles of inositol tetraphosphate and deacetylase-activating domain in activation of histone deacetylase 3. *Protein Science*, 22(1), 83-92.

Avilion, A. A., Nicolis, S. K., Pevny, L. H., Perez, L., Vivian, N. & Lovell-Badge, R. (2003) Multipotent cell lineages in early mouse development depend on SOX2 function. *Genes & Development*, 17(1), 126-140.

Ayer, D. E., Laherty, C. D., Lawrence, Q. A., Armstrong, A. P. & Eisenman, R. N. (1996) Mad proteins contain a dominant transcription repression domain. *Molecular and Cellular Biology*, 16(10), 5772-5781.

Ayer, D. E., Lawrence, Q. A. & Eisenman, R. N. (1995) Mad-max transcriptional repression is mediated by ternary complex-formation with mammalian homologs of yeast repressor Sin3. *Cell*, 80(5), 767-776.

Azevedo, C. & Saiardi, A. (2006) Extraction and analysis of soluble inositol polyphosphates from yeast. *Nature Protocols*, 1(5), 2416-2422.

Azuara, V., Perry, P., Sauer, S., Spivakov, M., Jorgensen, H. F., John, R. M., Gouti, M., Casanova, M., Warnes, G., Merkenschlager, M. & Fisher, A. G. (2006) Chromatin signatures of pluripotent cell lines. *Nature Cell Biology*, 8(5), 532-U189.

Bain, G., Kitchens, D., Yao, M., Huettner, J. E. & Gottlieb, D. I. (1995) Embryonic stem-cells express neuronal properties in-vitro. *Developmental Biology*, 168(2), 342-357.

Bain, G., Ray, W. J., Yao, M. & Gottlieb, D. I. (1996) Retinoic acid promotes neural and represses mesodermal gene expression in mouse embryonic stem cells in culture. *Biochemical and Biophysical Research Communications*, 223(3), 691-694.

Bakowski, M. A., Braun, V., Lam, G. Y., Yeung, T., Do Heo, W., Meyer, T., Finlay, B. B., Grinstein, S. & Brumell, J. H. (2010) The Phosphoinositide Phosphatase SopB Manipulates Membrane Surface Charge and Trafficking of the Salmonella-Containing Vacuole. *Cell Host & Microbe*, 7(6), 453-462.

Ballabeni, A., Park, I.-H., Zhao, R., Wang, W., Lerou, P. H., Daley, G. Q. & Kirschner, M. W. (2011) Cell cycle adaptations of embryonic stem cells. *Proceedings of the National Academy of Sciences of the United States of America*, 108(48), 19252-19257.

Baltus, G. A., Kowalski, M. P., Tutter, A. V. & Kadam, S. (2009) A Positive Regulatory Role for the mSin3A-HDAC Complex in Pluripotency through Nanog and Sox2. *Journal of Biological Chemistry*, 284(11), 6998-7006.

Banerjee, T. & Chakravarti, D. (2011) A Peek into the Complex Realm of Histone Phosphorylation. *Molecular and Cellular Biology*, 31(24), 4858-4873.

Bannister, A. J. & Kouzarides, T. (1996) The CBP co-activator is a histone acetyltransferase. *Nature*, 384(6610), 641-643.

Bannister, A. J., Zegerman, P., Partridge, J. F., Miska, E. A., Thomas, J. O., Allshire, R. C. & Kouzarides, T. (2001) Selective recognition of methylated lysine 9 on histone H3 by the HP1 chromo domain. *Nature*, 410(6824), 120-124.

Bantscheff, M., Hopf, C., Savitski, M. M., Dittmann, A., Grandi, P., Michon, A. M., Schlegl, J., Abraham, Y., Becher, I., Bergamini, G., Boesche, M., Delling, M., Dumpelfeld, B., Eberhard, D., Huthmacher, C., Mathieson, T., Poeckel, D., Reader, V., Strunk, K., Sweetman, G., Kruse, U., Neubauer, G., Ramsden, N. G. & Drewes, G. (2011) Chemoproteomics profiling of HDAC inhibitors reveals selective targeting of HDAC complexes. *Nature Biotechnology*, 29(3), 255-U124.

Barker, C. J., Illies, C. & Berggren, P.-O. (2010) HPLC separation of inositol polyphosphates. *Methods in molecular biology (Clifton, N.J.)*, 645, 21-46.

Barker, C. J., Wright, J., Hughes, P. J., Kirk, C. J. & Michell, R. H. (2004) Complex changes in cellular inositol phosphate complement accompany transit through the cell cycle. *Biochemical Journal*, 380, 465-473.

Berger, S. L. (2007) The complex language of chromatin regulation during transcription. *Nature*, 447(7143), 407-412.

Berger, S. L., Kouzarides, T., Shiekhattar, R. & Shilatifard, A. (2009) An operational definition of epigenetics. *Genes & Development*, 23(7), 781-783.

Bernstein, B. E., Mikkelsen, T. S., Xie, X. H., Kamal, M., Huebert, D. J., Cuff, J., Fry, B., Meissner, A., Wernig, M., Plath, K., Jaenisch, R., Wagschal, A., Feil, R., Schreiber, S. L. & Lander, E. S. (2006) A bivalent chromatin structure marks key developmental genes in embryonic stem cells. *Cell*, 125(2), 315-326.

Bernstein, B. E., Tong, J. K. & Schreiber, S. L. (2000) Genomewide studies of histone deacetylase function in yeast. *Proceedings of the National Academy of Sciences of the United States of America*, 97(25), 13708-13713.

Berridge, M. J. & Irvine, R. F. (1989) Inositol phosphates and cell signaling. *Nature*, 341(6239), 197-205.

Bertos, N. R., Gilquin, B., Chan, G. K. T., Yen, T. J., Khochbin, S. & Yang, X. J. (2004) Role of the tetradecapeptide repeat domain of human histone deacetylase 6 in cytoplasmic retention. *Journal of Biological Chemistry*, 279(46), 48246-48254.

Bhaskara, S., Chyla, B. J., Amann, J. M., Knutson, S. K., Cortez, D., Sun, Z.-W. & Hiebert, S. W. (2008) Deletion of histone deacetylase 3 reveals critical roles in S phase progression and DNA damage control. *Molecular Cell*, 30(1), 61-72.

Bhaskara, S., Knutson, S. K., Jiang, G., Chandrasekharan, M. B., Wilson, A. J., Zheng, S., Yenamandra, A., Locke, K., Yuan, J.-l., Bonine-Summers, A. R., Wells, C. E., Kaiser, J. F., Washington, M. K., Zhao, Z., Wagner, F. F., Sun, Z.-W., Xia, F., Holson, E. B., Khabele, D. & Hiebert, S. W. (2010) Hdac3 Is Essential for the Maintenance of Chromatin Structure and Genome Stability. *Cancer Cell*, 18(5), 436-447.

Bird, A. (2002) DNA methylation patterns and epigenetic memory. *Genes & Development*, 16(1), 6-21.

Blind, R. D., Suzawa, M. & Ingraham, H. A. (2012) Direct Modification and Activation of a Nuclear Receptor-PIP2 Complex by the Inositol Lipid Kinase IPMK. *Science Signaling*, 5(229).

Boyer, L. A., Lee, T. I., Cole, M. F., Johnstone, S. E., Levine, S. S., Zucker, J. R., Guenther, M. G., Kumar, R. M., Murray, H. L., Jenner, R. G., Gifford, D. K., Melton, D. A., Jaenisch, R. & Young, R. A. (2005) Core transcriptional regulatory circuitry in human embryonic stem cells. *Cell*, 122(6), 947-956.

Boyer, L. A., Mathur, D. & Jaenisch, R. (2006) Molecular control of pluripotency. *Current Opinion in Genetics & Development*, 16(5), 455-462.

Bradley, A., Evans, M., Kaufman, M. H. & Robertson, E. (1984) Formation of germ-line chimeras from embryo-derived teratocarcinoma cell-lines. *Nature*, 309(5965), 255-256.

Bradner, J. E., Mak, R., Tanguturi, S. K., Mazitschek, R., Haggarty, S. J., Ross, K., Chang, C. Y., Bosco, J., West, N., Morse, E., Lin, K., Shen, J. P., Kwiatkowski, N. P., Gheldof, N., Dekker, J., DeAngelo, D. J., Carr, S. A., Schreiber, S. L., Golub, T. R. & Ebert, B. L. (2010) Chemical genetic strategy identifies histone deacetylase 1 (HDAC1) and HDAC2 as therapeutic targets in sickle cell disease. *Proceedings of the National Academy of Sciences of the United States of America*, 107(28), 12617-12622.

Brownell, J. E. & Allis, C. D. (1996) Special HATs for special occasions: Linking histone acetylation to chromatin assembly and gene activation. *Current Opinion in Genetics & Development*, 6(2), 176-184.

Brownell, J. E., Zhou, J. X., Ranalli, T., Kobayashi, R., Edmondson, D. G., Roth, S. Y. & Allis, C. D. (1996) Tetrahymena histone acetyltransferase A: A homolog to yeast Gcn5p linking histone acetylation to gene activation. *Cell*, 84(6), 843-851.

Burdon, T., Smith, A. & Savatier, P. (2002) Signalling, cell cycle and pluripotency in embryonic stem cells. *Trends in Cell Biology*, 12(9), 432-438.

Caffrey, J. J., Darden, T., Wenk, M. R. & Shears, S. B. (2001) Expanding coincident signaling by PTEN through its inositol 1,3,4,5,6-pentakisphosphate 3-phosphatase activity. *Febs Letters*, 499(1-2), 6-10.

Cao, J. & Yan, Q. (2012) Histone ubiquitination and deubiquitination in transcription, DNA damage response, and cancer. *Frontiers in oncology*, 2, 26-26.

Capecchi, M. R. (1989) Altering the genome by homologous recombination. *Science*, 244(4910), 1288-1292.

Carrozza, M. J., Li, B., Florens, L., Suganuma, T., Swanson, S. K., Lee, K. K., Shia, W. J., Anderson, S., Yates, J., Washburn, M. P. & Workman, J. L. (2005) Histone H3 methylation by Set2 directs deacetylation of coding regions by Rpd3S to suppress spurious intragenic transcription. *Cell*, 123(4), 581-592.

Castelo-Branco, G. G., Lilja, T., Wallenborg, K., Falcao, A. M., Marques, S. C., Gracias, A., Solum, D., Paap, R., Walfridsson, J., Teixeira, A. I., Rosenfeld, M. G., Jepsen, K. & Hermanson, O. (2014) Neural Stem Cell Differentiation Is Dictated by Distinct Actions of Nuclear Receptor Corepressors and Histone Deacetylases. *Stem Cell Reports*, 3(3), 502-515.

Chakraborty, S. & Yutzey, K. E. (2012) Tbx20 regulation of cardiac cell proliferation and lineage specialization during embryonic and fetal development in vivo. *Developmental Biology*, 363(1), 234-246.

Chambers, I., Colby, D., Robertson, M., Nichols, J., Lee, S., Tweedie, S. & Smith, A. (2003) Functional expression cloning of Nanog, a pluripotency sustaining factor in embryonic stem cells. *Cell*, 113(5), 643-655.

Chang, S. C. & Majerus, P. W. (2006) Inositol polyphosphate multikinase regulates inositol 1,4,5,6-tetrakisphosphate. *Biochemical and Biophysical Research Communications*, 339(1), 209-216.

Chen, J. D. & Evans, R. M. (1995) A transcriptional co-repressor that interacts with nuclear hormone receptors. *Nature*, 377(6548), 454-457.

Choi, H. K., Choi, K. C., Kang, H. B., Kim, H. C., Lee, Y. H., Haam, S., Park, H. G. & Yoon, H. G. (2008) Function of multiple Lis-homology domain/WD-40 repeat-containing proteins in feed-forward transcriptional repression by silencing mediator for retinoic and thyroid receptor/nuclear receptor corepressor complexes. *Molecular Endocrinology*, 22(5), 1093-1104.

Chokas, A. L., Trivedi, C. M., Lu, M. M., Tucker, P. W., Li, S. R., Epstein, J. A. & Morrisey, E. E. (2010) Foxp1/2/4-NuRD Interactions Regulate Gene Expression and Epithelial Injury Response in the Lung via Regulation of Interleukin-6. *Journal of Biological Chemistry*, 285(17), 13304-13313.

Choudhary, C., Kumar, C., Gnad, F., Nielsen, M. L., Rehman, M., Walther, T. C., Olsen, J. V. & Mann, M. (2009) Lysine Acetylation Targets Protein Complexes and Co-Regulates Major Cellular Functions. *Science*, 325(5942), 834-840.

Codina, A., Love, J. D., Li, Y., Lazar, M. A., Neuhaus, D. & Schwabe, J. W. R. (2005) Structural insights into the interaction and activation of histone deacetylase 3 by nuclear receptor corepressors. *Proceedings of the National Academy of Sciences of the United States of America*, 102(17), 6009-6014.

Communi, D. & Erneux, C. (1996) Identification of an active site cysteine residue in human type I Ins(1,4,5)P-3 5-phosphatase by chemical modification and site-directed mutagenesis. *Biochemical Journal*, 320, 181-186.

Cowley, S. M., Iritani, B. M., Mendrysa, S. M., Xu, T., Cheng, P. F., Yada, J., Liggitt, H. D. & Eisenman, R. N. (2005) The mSin3A chromatin-modifying complex is essential for embryogenesis and T-cell development. *Molecular and Cellular Biology*, 25(16), 6990-7004.

Cowley, S. M., Kang, R. S., Frangioni, J. V., Yada, J. J., Degrand, A. M., Radhakrishnan, I. & Eisenman, R. N. (2004) Functional analysis of the Mad1-mSin3A repressor-corepressor interaction reveals determinants of specificity, affinity, and transcriptional response. *Molecular and Cellular Biology*, 24(7), 2698-2709.

Creaven, M., Hans, F., Mutskov, V., Col, E., Caron, C., Dimitrov, S. & Khochbin, S. (1999) Control of the histone-acetyltransferase activity of Tip60 by the HIV-1 transactivator protein, Tat. *Biochemistry*, 38(27), 8826-8830.

Creyghton, M. P., Cheng, A. W., Welstead, G. G., Kooistra, T., Carey, B. W., Steine, E. J., Hanna, J., Lodato, M. A., Frampton, G. M., Sharp, P. A., Boyer, L. A., Young, R. A. & Jaenisch, R. (2010) Histone H3K27ac separates active from poised enhancers and predicts developmental state. *Proceedings of the National Academy of Sciences of the United States of America*, 107(50), 21931-21936.

Dangond, F., Henriksson, M., Zardo, G., Caiafa, P., Ekstrom, T. J. & Gray, S. G. (2001) Differential expression of class IHDACs: Roles of cell density and cell cycle. *International Journal of Oncology*, 19(4), 773-777.

Das, C., Lucia, M. S., Hansen, K. C. & Tyler, J. K. (2009a) CBP/p300-mediated acetylation of histone H3 on lysine 56. *Nature*, 459(7243), 113-U123.

Das, C., Lucia, M. S., Hansen, K. C. & Tyler, J. K. (2009b) CBP/p300-mediated acetylation of histone H3 on lysine 56. *Nature*, 459(7243), 113-7.

De Ruijter, A. J. M., Van Gennip, A. H., Caron, H. N., Kemp, S. & Van Kuilenburg, A. B. P. (2003) Histone deacetylases (HDACs): characterization of the classical HDAC family. *Biochemical Journal*, 370, 737-749.

Delcuve, G. P., Khan, D. H. & Davie, J. R. (2012) Roles of histone deacetylases in epigenetic regulation: emerging paradigms from studies with inhibitors. *Clinical Epigenetics*, 4, 13.

Dhalluin, C., Carlson, J. E., Zeng, L., He, C., Aggarwal, A. K. & Zhou, M. M. (1999) Structure and ligand of a histone acetyltransferase bromodomain. *Nature*, 399(6735), 491-496.

Ding, S., Wu, X. H., Li, G., Han, M., Zhuang, Y. & Xu, T. (2005) Efficient transposition of the piggyBac resource (PB) transposon in mammalian cells and mice. *Cell*, 122(3), 473-483.

Doetschman, T. C., Eistetter, H., Katz, M., Schmidt, W. & Kemler, R. (1985) The invitro development of blastocyst-derived embryonic stem-cell lines - formation of visceral yolk-sac, blood islands and myocardium. *Journal of Embryology and Experimental Morphology*, 87(JUN), 27-&.

Dovey, O. M., Foster, C. T., Conte, N., Edwards, S. A., Edwards, J. M., Singh, R., Vassiliou, G., Bradley, A. & Cowley, S. M. (2013) Histone deacetylase 1 and 2 are

essential for normal T-cell development and genomic stability in mice. *Blood*, 121(8), 1335-1344.

Dovey, O. M., Foster, C. T. & Cowley, S. M. (2010a) Emphasizing the positive A role for histone deacetylases in transcriptional activation. *Cell Cycle*, 9(14), 2700-2701.

Dovey, O. M., Foster, C. T. & Cowley, S. M. (2010b) Histone deacetylase 1 (HDAC1), but not HDAC2, controls embryonic stem cell differentiation. *Proceedings of the National Academy of Sciences of the United States of America*, 107(18), 8242-8247.

Dubois, E., Dewaste, V., Erneux, C. & Messenguy, F. (2000) Inositol polyphosphate kinase activity of Arg82/ArgRIII is not required for the regulation of the arginine metabolism in yeast. *Febs Letters*, 486(3), 300-304.

Dufort, D., Schwartz, L., Harpal, K. & Rossant, J. (1998) The transcription factor HNF3 beta is required in visceral endoderm for normal primitive streak morphogenesis. *Development*, 125(16), 3015-3025.

Dukes, J. D., Lee, H., Hagen, R., Reaves, B. J., Layton, A. N., Galyov, E. E. & Whitley, P. (2006) The secreted Salmonella dublin phosphoinositide phosphatase, SopB, localizes to PtdIns(3)P-containing endosomes and perturbs normal endosome to lysosome trafficking. *Biochemical Journal*, 395, 239-247.

Dupont, C., Armant, D. R. & Brenner, C. A. (2009) Epigenetics: Definition, Mechanisms and Clinical Perspective. *Seminars in Reproductive Medicine*, 27(5), 351-357.

Eckmann, L., Rudolf, M. T., Ptasznik, A., Schultz, C., Jiang, T., Wolfson, N., Tsien, R., Fierer, J., Shears, S. B., Kagnoff, M. F. & Traynor-Kaplan, A. E. (1997) D-myo-inositol 1,4,5,6-tetrakisphosphate produced in human intestinal epithelial cells in response to Salmonella invasion inhibits phosphoinositide 3-kinase signaling pathways. *Proceedings of the National Academy of Sciences of the United States of America*, 94(26), 14456-14460.

El Alami, M., Messenguy, F., Scherens, B. & Dubois, E. (2003) Arg82p is a bifunctional protein whose inositol polyphosphate kinase activity is essential for nitrogen and PHO gene expression but not for Mcm1p chaperoning in yeast. *Molecular Microbiology*, 49(2), 457-468.

Emmett, M. J., Lim, H. W., Jager, J., Richter, H. J., Adlanmerini, M., Peed, L. C., Briggs, E. R., Steger, D. J., Ma, T., Sims, C. A., Baur, J. A., Pei, L. M., Won, K. J., Seale, P., Gerhart-Hines, Z. & Lazar, M. A. (2017) Histone deacetylase 3 prepares brown adipose tissue for acute thermogenic challenge. *Nature*, 546(7659), 544-+.

Endo-Streeter, S., Tsui, M.-K. M., Odom, A. R., Block, J. & York, J. D. (2012) Structural Studies and Protein Engineering of Inositol Phosphate Multikinase. *Journal of Biological Chemistry*, 287(42), 35360-35369.

Endoh, M., Endo, T. A., Endoh, T., Isono, K., Sharif, J., Ohara, O., Toyoda, T., Ito, T., Eskeland, R., Bickmore, W. A., Vidal, M., Bernstein, B. E. & Koseki, H. (2012) Histone

H2A Mono-Ubiquitination Is a Crucial Step to Mediate PRC1-Dependent Repression of Developmental Genes to Maintain ES Cell Identity. *Plos Genetics*, 8(7), 10.

Evans, A. L., Faial, T., Gilchrist, M. J., Down, T., Vallier, L., Pedersen, R. A., Wardle, F. C. & Smith, J. C. (2012) Genomic Targets of Brachyury (T) in Differentiating Mouse Embryonic Stem Cells. *Plos One*, 7(3).

Evans, M. J. & Kaufman, M. H. (1981) Establishment in culture of pluripotential cells from mouse embryos. *Nature*, 292(5819), 154-156.

Feldman, N., Gerson, A., Fang, J., Li, E., Zhang, Y., Shinkai, Y., Cedar, H. & Bergman, Y. (2006) G9a-mediated irreversible epigenetic inactivation of Oct-3/4 during early embryogenesis. *Nature Cell Biology*, 8(2), 188-U55.

Feng, D., Liu, T., Sun, Z., Bugge, A., Mullican, S. E., Alenghat, T., Liu, X. S. & Lazar, M. A. (2011) A Circadian Rhythm Orchestrated by Histone Deacetylase 3 Controls Hepatic Lipid Metabolism. *Science*, 331(6022), 1315-1319.

Feng, Y. C., Wente, S. R. & Majerus, P. W. (2001) Overexpression of the inositol phosphatase SopB in human 293 cells stimulates cellular chloride influx and inhibits nuclear mRNA export. *Proceedings of the National Academy of Sciences of the United States of America*, 98(3), 875-879.

Fierz, B., Chatterjee, C., McGinty, R. K., Bar-Dagan, M., Raleigh, D. P. & Muir, T. W. (2011) Histone H2B ubiquitylation disrupts local and higher-order chromatin compaction. *Nature Chemical Biology*, 7(2), 113-119.

Finley, M. F. A., Devata, S. & Huettner, J. E. (1999) BMP-4 inhibits neural differentiation of murine embryonic stem cells. *Journal of Neurobiology*, 40(3), 271-287.

Finnin, M. S., Donigian, J. R., Cohen, A., Richon, V. M., Rifkind, R. A., Marks, P. A., Breslow, R. & Pavletich, N. P. (1999) Structures of a histone deacetylase homologue bound to the TSA and SAHA inhibitors. *Nature*, 401(6749), 188-193.

Fischle, W., Dequiedt, F., Fillion, M., Hendzel, M. J., Voelter, W. & Verdin, E. (2001) Human HDAC7 histone deacetylase activity is associated with HDAC3 in vivo. *Journal of Biological Chemistry*, 276(38), 35826-35835.

Fischle, W., Dequiedt, F., Hendzel, M. J., Guenther, M. G., Lazar, M. A., Voelter, W. & Verdin, E. (2002) Enzymatic activity associated with class IIHDACs is dependent on a multiprotein complex containing HDAC3 and SMRT/N-CoR. *Molecular Cell*, 9(1), 45-57.

Fischle, W., Tseng, B. S., Dormann, H. L., Ueberheide, B. M., Garcia, B. A., Shabanowitz, J., Hunt, D. F., Funabiki, H. & Allis, C. D. (2005) Regulation of HP1-chromatin binding by histone H3 methylation and phosphorylation. *Nature*, 438(7071), 1116-1122.

Forneris, F., Binda, C., Dall'Aglio, A., Fraaije, M. W., Battaglioli, E. & Mattevi, A. (2006) A highly specific mechanism of histone H3-K4 recognition by histone demethylase LSD1. *Journal of Biological Chemistry*, 281(46), 35289-35295.

Foster, C. T., Dovey, O. M., Lezina, L., Luo, J. L., Gant, T. W., Barlev, N., Bradley, A. & Cowley, S. M. (2010) Lysine-Specific Demethylase 1 Regulates the Embryonic Transcriptome and CoREST Stability. *Molecular and Cellular Biology*, 30(20), 4851-4863.

Frederick, J. P., Mattiske, D., Wofford, J. A., Megosh, L. C., Drake, L. Y., Chiou, S. T., Hogan, B. L. M. & York, J. D. (2005) An essential role for an inositol polyphosphate multikinase, Ipk2, in mouse embryogenesis and second messenger production. *Proceedings of the National Academy of Sciences of the United States of America*, 102(24), 8454-8459.

Fujii, M. & York, J. D. (2005) A role for rat inositol polyphosphate kinases rIPK2 and rIPK1 in inositol pentakisphosphate and inositol hexakisphosphate production in rat-1 cells. *Journal of Biological Chemistry*, 280(2), 1156-1164.

Fujita, N., Jaye, D. L., Kajita, M., Geigerman, C., Moreno, C. S. & Wade, P. A. (2003) MTA3, a Mi-2/NuRD complex subunit, an invasive growth pathway in breast. *Cell*, 113(2), 207-219.

Fussner, E., Ching, R. W. & Bazett-Jones, D. P. (2011) Living without 30 nm chromatin fibers. *Trends in Biochemical Sciences*, 36(1), 1-6.

Gao, L., Cueto, M. A., Asselbergs, F. & Atadja, P. (2002) Cloning and functional characterization of HDAC11, a novel member of the human histone deacetylase family. *Journal of Biological Chemistry*, 277(28), 25748-25755.

Gao, Y. & Wang, H.-Y. (2007) Inositol pentakisphosphate mediates Wnt/beta-catenin signaling. *Journal of Biological Chemistry*, 282(36).

Garcea, R. L. & Alberts, B. M. (1980) Comparative studies of histone acetylation in nucleosomes, nuclei, and intact-cells - evidence for special factors which modify acetylase action. *Journal of Biological Chemistry*, 255(23), 1454-1463.

Glover, J. D., Taylor, L., Sherman, A., Zeiger-Poli, C., Sang, H. M. & McGrew, M. J. (2013) A Novel Piggybac Transposon Inducible Expression System Identifies a Role for Akt Signalling in Primordial Germ Cell Migration. *Plos One*, 8(11), 9.

Goldberg, A. D., Allis, C. D. & Bernstein, E. (2007) Epigenetics: A landscape takes shape. *Cell*, 128(4), 635-638.

Gonzalez, B., Schell, M. J., Letcher, A. J., Veprintsev, D. B., Irvine, R. F. & Williams, R. L. (2004) Structure of a human inositol 1,4,5-trisphosphate 3-kinase: Substrate binding reveals why it is not a phosphoinositide 3-kinase. *Molecular Cell*, 15(5), 689-701.

Gordillo, M., Evans, T. & Gouon-Evans, V. (2015) Orchestrating liver development. *Development*, 142(12), 2094-2108.

Gregoire, S., Xiao, L., Nie, J., Zhang, X., Xu, M., Li, J., Wong, J., Seto, E. & Yang, X.-J. (2007) Histone deacetylase 3 interacts with and deacetylates myocyte enhancer factor 2. *Molecular and Cellular Biology*, 27(4), 1280-1295.

Gregoretti, I. V., Lee, Y. M. & Goodson, H. V. (2004) Molecular evolution of the histone deacetylase family: Functional implications of phylogenetic analysis. *Journal of Molecular Biology*, 338(1), 17-31.

Grozinger, C. M., Hassig, C. A. & Schreiber, S. L. (1999) Three proteins define a class of human histone deacetylases related to yeast Hda1p. *Proceedings of the National Academy of Sciences of the United States of America*, 96(9), 4868-4873.

Grozinger, C. M. & Schreiber, S. L. (2000) Regulation of histone deacetylase 4 and 5 and transcriptional activity by 14-3-3-dependent cellular localization. *Proceedings of the National Academy of Sciences of the United States of America*, 97(14), 7835-7840.

Grozinger, C. M. & Schreiber, S. L. (2002) Deacetylase enzymes: biological functions and the use of small-molecule inhibitors. *Chemistry & Biology*, 9(1), 3-16.

Guenther, M. G., Barak, O. & Lazar, M. A. (2001) The SMRT and N-CoR corepressors are activating cofactors for histone deacetylase 3. *Molecular and Cellular Biology*, 21(18), 6091-6101.

Guenther, M. G., Lane, W. S., Fischle, W., Verdin, E., Lazar, M. A. & Shiekhattar, R. (2000) A core SMRT corepressor complex containing HDAC3 and TBL1, a WD40-repeat protein linked to deafness. *Genes & Development*, 14(9), 1048-1057.

Haberland, M., Mokalled, M. H., Montgomery, R. L. & Olson, E. N. (2009a) Epigenetic control of skull morphogenesis by histone deacetylase 8. *Genes & Development*, 23(14), 1625-1630.

Haberland, M., Montgomery, R. L. & Olson, E. N. (2009b) The many roles of histone deacetylases in development and physiology: implications for disease and therapy. *Nature Reviews Genetics*, 10(1), 32-42.

Hakimi, M. A., Bochar, D. A., Chenoweth, J., Lane, W. S., Mandel, G. & Shiekhattar, R. (2002) A core-BRAF35 complex containing histone deacetylase mediates repression of neuronal-specific genes. *Proceedings of the National Academy of Sciences of the United States of America*, 99(11), 7420-7425.

Hansen, J. C., Tse, C. & Wolffe, A. P. (1998) Structure and function of the core histone N-termini: more than meets the eye. *Biochemistry*, 37(51), 17637-17641.

Hassig, C. A., Fleischer, T. C., Billin, A. N., Schreiber, S. L. & Ayer, D. E. (1997) Histone deacetylase activity is required for full transcriptional repression by mSin3A. *Cell*, 89(3), 341-347.

Hatch, A. J., Odom, A. R. & York, J. D. (2017) Inositol phosphate multikinase dependent transcriptional control. *Advances in biological regulation*.

Haub, O. & Goldfarb, M. (1991) EXPRESSION OF THE FIBROBLAST GROWTH FACTOR-5 GENE IN THE MOUSE EMBRYO. *Development*, 112(2), 397-&.

He, Y. F., Li, B. Z., Li, Z., Liu, P., Wang, Y., Tang, Q. Y., Ding, J. P., Jia, Y. Y., Chen, Z. C., Li, L., Sun, Y., Li, X. X., Dai, Q., Song, C. X., Zhang, K. L., He, C. & Xu, G. L. (2011) Tet-Mediated Formation of 5-Carboxylcytosine and Its Excision by TDG in Mammalian DNA. *Science*, 333(6047), 1303-1307.

Hebbes, T. R., Thorne, A. W. & Cranerobinson, C. (1988) A direct link between core histone acetylation and transcriptionally active chromatin. *Embo Journal*, 7(5), 1395-1402.

Hebert, J. M., Boyle, M. & Martin, G. R. (1991) Messenger-rna localization studies suggest that murine fgf-5 plays a role in gastrulation. *Development*, 112(2), 407-415.

Hendrich, B., Guy, J., Ramsahoye, B., Wilson, V. A. & Bird, A. (2001) Closely related proteins MBD2 and MBD3 play distinctive but interacting roles in mouse development. *Genes & Development*, 15(6), 710-723.

Herrmann, B. G., Labeit, S., Poustka, A., King, T. R. & Lehrach, H. (1990) Cloning of the t-gene required in mesoderm formation in the mouse. *Nature*, 343(6259), 617-622.

Holtzinger, A., Rosenfeld, G. E. & Evans, T. (2010) Gata4 directs development of cardiac-inducing endoderm from ES cells. *Developmental Biology*, 337(1), 63-73.

Hong, L., Schroth, G. P., Matthews, H. R., Yau, P. & Bradbury, E. M. (1993) Studies of the dna-binding properties of histone h4 amino terminus - thermal-denaturation studies reveal that acetylation markedly reduces the binding constant of the h4 tail to dna. *Journal of Biological Chemistry*, 268(1), 305-314.

Hook, S. S., Orian, A., Cowley, S. M. & Eisenman, R. N. (2002) Histone deacetylase 6 binds polyubiquitin through its zinc finger (PAZ domain) and copurifies with deubiquitinating enzymes. *Proceedings of the National Academy of Sciences of the United States of America*, 99(21), 13425-13430.

Horlein, A. J., Naar, A. M., Heinzel, T., Torchia, J., Gloss, B., Kurokawa, R., Ryan, A., Kamel, Y., Soderstrom, M., Glass, C. K. & Rosenfeld, M. G. (1995) LIGAND-INDEPENDENT REPRESSION BY THE THYROID-HORMONE RECEPTOR-MEDIATED BY A NUCLEAR RECEPTOR CO-REPRESSOR. *Nature*, 377(6548), 397-404.

Hota, S. K. & Bruneau, B. G. (2016) ATP-dependent chromatin remodeling during mammalian development. *Development*, 143(16), 2882-2897.

Hubbert, C., Guardiola, A., Shao, R., Kawaguchi, Y., Ito, A., Nixon, A., Yoshida, M., Wang, X. F. & Yao, T. P. (2002) HDAC6 is a microtubule-associated deacetylase. *Nature*, 417(6887), 455-458.

Hubner, M. R., Eckersley-Maslin, M. A. & Spector, D. L. (2013) Chromatin organization and transcriptional regulation. *Current Opinion in Genetics & Development*, 23(2), 89-95.

Irvine, R. F. & Schell, M. J. (2001) Back in the water: The return of the inositol phosphates. *Nature Reviews Molecular Cell Biology*, 2(5), 327-338.

Ishizuka, T. & Lazar, M. A. (2003) The N-CoR/histone deacetylase 3 complex is required for repression by thyroid hormone receptor. *Molecular and Cellular Biology*, 23(15), 5122-5131.

Itoh, T., Fairall, L., Muskett, F. W., Milano, C. P., Watson, P. J., Arnaudo, N., Saleh, A., Millard, C. J., El-Mezgueldi, M., Martino, F. & Schwabe, J. W. R. (2015) Structural and functional characterization of a cell cycle associated HDAC1/2 complex reveals the structural basis for complex assembly and nucleosome targeting. *Nucleic Acids Research*, 43(4), 2033-2044.

Jacobs, S. A., Taverna, S. D., Zhang, Y. N., Briggs, S. D., Li, J. M., Eissenberg, J. C., Allis, C. D. & Khorasanizadeh, S. (2001) Specificity of the HP1 chromo domain for the methylated N-terminus of histone H3. *Embo Journal*, 20(18), 5232-5241.

Jamaladdin, S., Kelly, R. D. W., O'Regan, L., Dovey, O. M., Hodson, G. E., Millard, C. J., Portolano, N., Fry, A. M., Schwabe, J. W. R. & Cowley, S. M. (2014) Histone deacetylase (HDAC) 1 and 2 are essential for accurate cell division and the pluripotency of embryonic stem cells. *Proceedings of the National Academy of Sciences of the United States of America*, 111(27), 9840-9845.

Jepsen, K., Hermanson, O., Onami, T. M., Gleiberman, A. S., Lunyak, V., McEvilly, R. J., Kurokawa, R., Kumar, V., Liu, F., Seto, E., Hedrick, S. M., Mandel, G., Glass, C. K., Rose, D. W. & Rosenfeld, M. G. (2000) Combinatorial roles of the nuclear receptor corepressor in transcription and development. *Cell*, 102(6), 753-763.

Jepsen, K., Solum, D., Zhou, T. Y., McEvilly, R. J., Kim, H. J., Glass, C. K., Hermanson, O. & Rosenfeld, M. G. (2007) SMRT-mediated repression of an H3K27 demethylase in progression from neural stem cell to neuron. *Nature*, 450(7168), 415-U8.

Jin, B., Li, Y. & Robertson, K. D. (2011) DNA methylation: superior or subordinate in the epigenetic hierarchy? *Genes & cancer*, 2(6), 607-17.

Juan, L. J., Shia, W. J., Chen, M. H., Yang, W. M., Seto, E., Lin, Y. S. & Wu, C. W. (2000) Histone deacetylases specifically down-regulate p53-dependent gene activation. *Journal of Biological Chemistry*, 275(27), 20436-20443.

Kadosh, D. & Struhl, K. (1998) Histone deacetylase activity of Rpd3 is important for transcriptional repression in vivo. *Genes & Development*, 12(6), 797-805.

Kaji, K., Caballero, I. M., MacLeod, R., Nichols, J., Wilson, V. A. & Hendrich, B. (2006) The NuRD component Mbd3 is required for pluripotency of embryonic stem cells. *Nature Cell Biology*, 8(3), 285-292.

Kalb, R., Latwiel, S., Baymaz, H. I., Jansen, P., Muller, C. W., Vermeulen, M. & Muller, J. (2014) Histone H2A monoubiquitination promotes histone H3 methylation in Polycomb repression. *Nature Structural & Molecular Biology*, 21(6), 569-571.

Kan, L. X., Israsena, N., Zhang, Z. L., Hu, M., Zhao, L. R., Jalali, A., Sahni, V. & Kessler, J. A. (2004) Sox1 acts through multiple independent pathways to promote neurogenesis. *Developmental Biology*, 269(2), 580-594.

Kanai-Azuma, M., Kanai, Y., Gad, J. M., Tajima, Y., Taya, C., Kurohmaru, M., Sanai, Y., Yonekawa, H., Yazaki, K., Tam, P. P. L. & Hayashi, Y. (2002) Depletion of definitive gut endoderm in Sox17-null mutant mice. *Development*, 129(10), 2367-2379.

Kao, H. Y., Lee, C. H., Komarov, A., Han, C. C. & Evans, R. M. (2002) Isolation and characterization of mammalian HDAC10, a novel histone deacetylase. *Journal of Biological Chemistry*, 277(1), 187-193.

Keller, G. (2005) Embryonic stem cell differentiation: emergence of a new era in biology and medicine. *Genes & Development*, 19(10), 1129-1155.

Keller, G. M. (1995) In-vitro differentiation of embryonic stem-cells. *Current Opinion in Cell Biology*, 7(6), 862-869.

Kelly, R. D. W. & Cowley, S. M. (2013) The physiological roles of histone deacetylase (HDAC) 1 and 2: complex co-stars with multiple leading parts. *Biochemical Society Transactions*, 41, 741-749.

Kim, E., Tyagi, R., Lee, J.-Y., Park, J., Kim, Y.-r., Beon, J., Chen, P. Y., Cha, J. Y., Snyder, S. H. & Kim, S. (2013) Inositol polyphosphate multikinase is a coactivator for serum response factor-dependent induction of immediate early genes. *Proceedings of the National Academy of Sciences of the United States of America*, 110(49), 19938-19943.

Kim, J., Guermah, M., McGinty, R. K., Lee, J. S., Tang, Z. Y., Milne, T. A., Shilatifard, A., Muir, T. W. & Roeder, R. G. (2009) RAD6-Mediated Transcription-Coupled H2B Ubiquitylation Directly Stimulates H3K4 Methylation in Human Cells. *Cell*, 137(3), 459-471.

Klose, R. J., Yamane, K., Bae, Y. J., Zhang, D. Z., Erdjument-Bromage, H., Tempst, P., Wong, J. M. & Zhang, Y. (2006) The transcriptional repressor JHDM3A demethylates trimethyl histone H3 lysine 9 and lysine 36. *Nature*, 442(7100), 312-316.

Knutson, S. K., Chyla, B. J., Amann, J. M., Bhaskara, S., Huppert, S. S. & Hiebert, S. W. (2008) Liver-specific deletion of histone deacetylase 3 disrupts metabolic transcriptional networks. *Embo Journal*, 27(7), 1017-1028.

Kobayashi, T. & Kageyama, R. (2010) Hes1 regulates embryonic stem cell differentiation by suppressing Notch signaling. *Genes to Cells*, 15(7), 689-698.

Kodaka, Y., Rabu, G. & Asakura, A. (2017) Skeletal Muscle Cell Induction from Pluripotent Stem Cells. *Stem Cells International*, 16.

Koipally, J., Renold, A., Kim, J. & Georgopoulos, K. (1999) Repression by Ikaros and Aiolos is mediated through histone deacetylase complexes. *Embo Journal*, 18(11), 3090-3100.

Kolupaeva, V. & Janssens, V. (2013) PP1 and PP2A phosphatases - cooperating partners in modulating retinoblastoma protein activation. *Febs Journal*, 280(2), 627-643.

Kouzarides, T. (2007) Chromatin modifications and their function. *Cell*, 128(4), 693-705.

Kubo, A., Shinozaki, K., Shannon, J. M., Kouskoff, V., Kennedy, M., Woo, S., Fehling, H. J. & Keller, G. (2004) Development of definitive endoderm from embryonic stem cells in culture. *Development*, 131(7), 1651-1662.

Kunath, T., Saba-El-Leil, M. K., Almousailleakh, M., Wray, J., Meloche, S. & Smith, A. (2007) FGF stimulation of the Erk1/2 signalling cascade triggers transition of pluripotent embryonic stem cells from self-renewal to lineage commitment. *Development*, 134(16), 2895-2902.

Lagger, G., O'Carroll, D., Rembold, M., Khier, H., Tischler, J., Weitzer, G., Schuettengruber, B., Hauser, C., Brunmeir, R., Jenuwein, T. & Seiser, C. (2002) Essential function of histone deacetylase 1 in proliferation control and CDK inhibitor repression. *Embo Journal*, 21(11), 2672-2681.

Laherty, C. D., Yang, W. M., Sun, J. M., Davie, J. R., Seto, E. & Eisenman, R. N. (1997) Histone deacetylases associated with the mSin3 corepressor mediate Mad transcriptional repression. *Cell*, 89(3), 349-356.

Lahm, A., Paolini, C., Pallaoro, M., Nardi, M. C., Jones, P., Neddermann, P., Sambucini, S., Bottomley, M. J., Lo Surdo, P., Carfi, A., Koch, U., De Francesco, R., Steinkuhler, C. & Gallinari, P. (2007) Unraveling the hidden catalytic activity of vertebrate class Ila histone deacetylases. *Proceedings of the National Academy of Sciences of the United States of America*, 104(44), 17335-17340.

Lan, F., Collins, R. E., De Cegli, R., Alpatov, R., Horton, J. R., Shi, X. B., Gozani, O., Cheng, X. D. & Shi, Y. (2007) Recognition of unmethylated histone H3 lysine 4 links BHC80 to LSD1-mediated gene repression. *Nature*, 448(7154), 718-U14.

Larsson, O., Barker, C. J., Sjoholm, A., Carlqvist, H., Michell, R. H., Bertorello, A., Nilsson, T., Honkanen, R. E., Mayr, G. W., Zwiller, J. & Berggren, P. O. (1997) Inhibition of phosphatases and increased Ca2+ channel activity by inositol hexakisphosphate. *Science*, 278(5337), 471-474.

Law, J. A. & Jacobsen, S. E. (2010) Establishing, maintaining and modifying DNA methylation patterns in plants and animals. *Nature Reviews Genetics*, 11(3), 204-220.

Lee, D. Y., Hayes, J. J., Pruss, D. & Wolffe, A. P. (1993) A positive role for histone acetylation in transcription factor access to nucleosomal dna. *Cell*, 72(1), 73-84.

Lee, H., Rezai-Zadeh, N. & Seto, E. (2004a) Negative regulation of histone deacetylase 8 activity by cyclic AMP-dependent protein kinase A. *Molecular and Cellular Biology*, 24(2), 765-773.

Lee, J. H., Hart, S. R. L. & Skalnik, D. G. (2004b) Histone deacetylase activity is required for embryonic stem cell differentiation. *Genesis*, 38(1), 32-38.

Lee, M. G., Wynder, C., Bochar, D. A., Hakimi, M. A., Cooch, N. & Shiekhattar, R. (2006a) Functional interplay between histone demethylase and deacetylase enzymes. *Molecular and Cellular Biology*, 26(17), 6395-6402.

Lee, M. G., Wynder, C., Cooch, N. & Shiekhattar, R. (2005) An essential role for CoREST in nucleosomal histone 3 lysine 4 demethylation. *Nature*, 437(7057), 432-435.

Lee, M. K., Tuttle, J. B., Rebhun, L. I., Cleveland, D. W. & Frankfurter, A. (1990) The expression and posttranslational modification of a neuron-specific beta-tubulin isotype during chick embryogenesis. *Cell Motility and the Cytoskeleton*, 17(2), 118-132.

Lee, T. I., Jenner, R. G., Boyer, L. A., Guenther, M. G., Levine, S. S., Kumar, R. M., Chevalier, B., Johnstone, S. E., Cole, M. F., Isono, K., Koseki, H., Fuchikami, T., Abe, K., Murray, H. L., Zucker, J. P., Yuan, B. B., Bell, G. W., Herbolsheimer, E., Hannett, N. M., Sun, K. M., Odom, D. T., Otte, A. P., Volkert, T. L., Bartel, D. P., Melton, D. A., Gifford, D. K., Jaenisch, R. & Young, R. A. (2006b) Control of developmental regulator's by polycomb in human embryonic stem cells. *Cell*, 125(2), 301-313.

Leitch, H. G., McEwen, K. R., Turp, A., Encheva, V., Carroll, T., Grabole, N., Mansfield, W., Nashun, B., Knezovich, J. G., Smith, A., Surani, M. A. & Hajkova, P. (2013) Naive pluripotency is associated with global DNA hypomethylation. *Nature Structural & Molecular Biology*, 20(3), 311-316.

Lendahl, U., Zimmerman, L. B. & McKay, R. D. G. (1990) CNS stem-cells express a new class of intermediate filament protein. *Cell*, 60(4), 585-595.

Li, B., Gogol, M., Carey, M., Pattenden, S. G., Seidel, C. & Workman, J. L. (2007) Infrequently transcribed long genes depend on the Set2/Rpd3S pathway for accurate transcription. *Genes & Development*, 21(11), 1422-1430.

Li, J. W., Wang, J., Wang, J. X., Nawaz, Z., Liu, J. M., Qin, J. & Wong, J. M. (2000) Both corepressor proteins SMRT and N-CoR exist in large protein complexes containing HDAC3. *Embo Journal*, 19(16), 4342-4350.

Li, M., Pevny, L., Lovell-Badge, R. & Smith, A. (1998) Generation of purified neural precursors from embryonic stem cells by lineage selection. *Current Biology*, 8(17), 971-974.

Li, Q., Zhou, H., Wurtele, H., Davies, B., Horazdovsky, B., Verreault, A. & Zhang, Z. G. (2008) Acetylation of histone H3 lysine 56 regulates replication-coupled nucleosome assembly. *Cell*, 134(2), 244-255.

Liang, J., Wan, M., Zhang, Y., Gu, P. L., Xin, H. W., Jung, S. Y., Qin, J., Wong, J. M., Cooney, A. J., Liu, D. & Zhou, S. Y. (2008) Nanog and Oct4 associate with unique transcriptional repression complexes in embryonic stem cells. *Nature Cell Biology*, 10(6), 731-739.

Liu, P. Y., Dou, X. Y., Liu, C., Wang, L. B., Xing, C., Peng, G. D., Chen, J., Yu, F., Qiao, Y. B., Song, L., Wu, Y. X., Yue, C. M., Li, J. S., Han, J. D. J., Tang, K. & Jing, N. H. (2015) Histone deacetylation promotes mouse neural induction by restricting Nodal-dependent mesendoderm fate. *Nature Communications*, 6, 14.

Liu, X., Villalta, P. W. & Sturla, S. J. (2009) Simultaneous determination of inositol and inositol phosphates in complex biological matrices: quantitative ion-exchange chromatography/tandem mass spectrometry. *Rapid Communications in Mass Spectrometry*, 23(5), 705-712.

Loh, Y. H., Wu, Q., Chew, J. L., Vega, V. B., Zhang, W. W., Chen, X., Bourque, G., George, J., Leong, B., Liu, J., Wong, K. Y., Sung, K. W., Lee, C. W. H., Zhao, X. D., Chiu, K. P., Lipovich, L., Kuznetsov, V. A., Robson, P., Stanton, L. W., Wei, C. L., Ruan, Y. J., Lim, B. & Ng, H. H. (2006) The Oct4 and Nanog transcription network regulates pluripotency in mouse embryonic stem cells. *Nature Genetics*, 38(4), 431-440.

Loh, Y. H., Yang, L., Yang, J. C., Li, H., Collins, J. J. & Daley, G. Q. (2011) Genomic Approaches to Deconstruct Pluripotency, in Chakravarti, A. & Green, E. (eds), *Annual Review of Genomics and Human Genetics, Vol 12*. Annual Review of Genomics and Human Genetics. Palo Alto: Annual Reviews, 165-185.

Lolas, M., Valenzuela, P. D. T., Tjian, R. & Liu, Z. (2014) Charting Brachyury-mediated developmental pathways during early mouse embryogenesis. *Proceedings of the National Academy of Sciences of the United States of America*, 111(12), 4478-4483.

Losito, O., Szijgyarto, Z., Resnick, A. C. & Saiardi, A. (2009) Inositol Pyrophosphates and Their Unique Metabolic Complexity: Analysis by Gel Electrophoresis. *Plos One*, 4(5).

Loss, O., Wu, C. T., Riccio, A. & Saiardi, A. (2013) Modulation of inositol polyphosphate levels regulates neuronal differentiation. *Molecular Biology of the Cell*, 24(18), 2981-2989.

Lu, J. R., McKinsey, T. A., Nicol, R. L. & Olson, E. N. (2000) Signal-dependent activation of the MEF2 transcription factor by dissociation from histone deacetylases. *Proceedings of the National Academy of Sciences of the United States of America*, 97(8), 4070-4075.

Luger, K., Mader, A. W., Richmond, R. K., Sargent, D. F. & Richmond, T. J. (1997) Crystal structure of the nucleosome core particle at 2.8 angstrom resolution. *Nature*, 389(6648), 251-260.

Luger, K. & Richmond, T. J. (1998a) DNA binding within the nucleosome core. *Current Opinion in Structural Biology*, 8(1), 33-40.

Luger, K. & Richmond, T. J. (1998b) The histone tails of the nucleosome. *Current Opinion in Genetics & Development*, 8(2), 140-146.

Ma, Y. Q., Kanakousaki, K. & Buttitta, L. (2015) How the cell cycle impacts chromatin architecture and influences cell fate. *Frontiers in Genetics*, 6, 18.

MacLean, B., Tomazela, D. M., Shulman, N., Chambers, M., Finney, G. L., Frewen, B., Kern, R., Tabb, D. L., Liebler, D. C. & MacCoss, M. J. (2010) Skyline: an open source document editor for creating and analyzing targeted proteomics experiments. *Bioinformatics*, 26(7), 966-968.

Madsen, A. S. & Olsen, C. A. (2012) Profiling of Substrates for Zinc-dependent Lysine Deacylase Enzymes: HDAC3 Exhibits Decrotonylase Activity In Vitro. *Angewandte Chemie-International Edition*, 51(36), 9083-9087.

Maehama, T. & Dixon, J. E. (1998) The tumor suppressor, PTEN/MMAC1, dephosphorylates the lipid second messenger, phosphatidylinositol 3,4,5-trisphosphate. *Journal of Biological Chemistry*, 273(22), 13375-13378.

Maeshima, K. & Eltsov, M. (2008) Packaging the genome: the structure of mitotic chromosomes. *Journal of Biochemistry*, 143(2), 145-153.

Maeshima, K., Hihara, S. & Eltsov, M. (2010) Chromatin structure: does the 30-nm fibre exist in vivo? *Current Opinion in Cell Biology*, 22(3), 291-297.

Mal, A., Sturniolo, M., Schiltz, R. L., Ghosh, M. K. & Harter, M. L. (2001) A role for histone deacetylase HDAC1 in modulating the transcriptional activity of MyoD: inhibition of the myogenic program. *Embo Journal*, 20(7), 1739-1753.

Marks, H., Kalkan, T., Menafra, R., Denissov, S., Jones, K., Hofemeister, H., Nichols, J., Kranz, A., Stewart, A. F., Smith, A. & Stunnenberg, H. G. (2012) The Transcriptional and Epigenomic Foundations of Ground State Pluripotency. *Cell*, 149(3), 590-604.

Martello, G. & Smith, A. (2014) The Nature of Embryonic Stem Cells, in Schekman, R. & Lehmann, R. (eds), *Annual Review of Cell and Developmental Biology, Vol 30*. Annual Review of Cell and Developmental Biology. Palo Alto: Annual Reviews, 647-675.

Martello, G., Sugimoto, T., Diamanti, E., Joshi, A., Hannah, R., Ohtsuka, S., Goettgens, B., Niwa, H. & Smith, A. (2012) Esrrb Is a Pivotal Target of the Gsk3/Tcf3 Axis Regulating Embryonic Stem Cell Self-Renewal. *Cell Stem Cell*, 11(4), 491-504.

Martin, G. R. (1981) Isolation of a pluripotent cell-line from early mouse embryos cultured in medium conditioned by teratocarcinoma stem-cells. *Proceedings of the National Academy of Sciences of the United States of America-Biological Sciences*, 78(12), 7634-7638.

Martinez-Balbas, M. A., Bauer, U. M., Nielsen, S. J., Brehm, A. & Kouzarides, T. (2000) Regulation of E2F1 activity by acetylation. *Embo Journal*, 19(4), 662-671.

Masui, S., Nakatake, Y., Toyooka, Y., Shimosato, D., Yagi, R., Takahashi, K., Okochi, H., Okuda, A., Matoba, R., Sharov, A. A., Ko, M. S. H. & Niwa, H. (2007) Pluripotency governed by Sox2 via regulation of Oct3/4 expression in mouse embryonic stem cells. *Nature Cell Biology*, 9(6), 625-U26.

Mateo, F., Vidal-Laliena, M., Jesus Pujol, M. & Bachs, O. (2010) Acetylation of cyclin A: a new cell cycle regulatory mechanism. *Biochemical Society Transactions*, 38, 83-86.

Matsuda, T., Nakamura, T., Nakao, K., Arai, T., Katsuki, M., Heike, T. & Yokota, T. (1999) STAT3 activation is sufficient to maintain an undifferentiated state of mouse embryonic stem cells. *Embo Journal*, 18(15), 4261-4269.

McKinsey, T. A., Zhang, C. L., Lu, J. R. & Olson, E. N. (2000) Signal-dependent nuclear export of a histone deacetylase regulates muscle differentiation. *Nature*, 408(6808), 106-111.

McMahon, J. A., Takada, S., Zimmerman, L. B., Fan, C. M., Harland, R. M. & McMahon, A. P. (1998) Noggin-mediated antagonism of BMP signaling is required for growth and patterning of the neural tube and somite. *Genes & Development*, 12(10), 1438-1452.

Meshorer, E., Yellajoshula, D., George, E., Scambler, P. J., Brown, D. T. & Mistell, T. (2006) Hyperdynamic plasticity in pluripotent embryonic of chromatin proteins stem cells. *Developmental Cell*, 10(1), 105-116.

Metzger, E., Imhof, A., Patel, D., Kahl, P., Hoffmeyer, K., Friedrichs, N., Muller, J. M., Greschik, H., Kirfel, J., Ji, S., Kunowska, N., Beisenherz-Huss, C., Gunther, T., Buettner, R. & Schule, R. (2010) Phosphorylation of histone H3T6 by PKC beta(I) controls demethylation at histone H3K4. *Nature*, 464(7289), 792-U175.

Millard, C. J., Fairall, L. & Schwabe, J. W. R. (2014) Towards an understanding of the structure and function of MTA1. *Cancer and Metastasis Reviews*, 33(4), 857-867.

Millard, C. J., Varma, N., Saleh, A., Morris, K., Watson, P. J., Bottrill, A. R., Fairall, L., Smith, C. J. & Schwabe, J. W. R. (2016) The structure of the core NuRD repression complex provides insights into its interaction with chromatin. *Elife*, 5, 21.

Millard, C. J., Watson, P. J., Celardo, I., Gordiyenko, Y., Cowley, S. M., Robinson, C. V., Fairall, L. & Schwabe, J. W. R. (2013) Class I HDACs Share a Common Mechanism of Regulation by Inositol Phosphates. *Molecular Cell*, 51(1), 57-67.

Milon, B. C., Cheng, H. B., Tselebrovsky, M. V., Lavrov, S. A., Nenasheva, V. V., Mikhaleva, E. A., Shevelyov, Y. Y. & Nurminsky, D. I. (2012) Role of Histone Deacetylases in Gene Regulation at Nuclear Lamina. *Plos One*, 7(11), 9.

Miska, E. A., Karlsson, C., Langley, E., Nielsen, S. J., Pines, J. & Kouzarides, T. (1999) HDAC4 deacetylase associates with and represses the MEF2 transcription factor. *Embo Journal*, 18(18), 5099-5107.

Mitsui, K., Tokuzawa, Y., Itoh, H., Segawa, K., Murakami, M., Takahashi, K., Maruyama, M., Maeda, M. & Yamanaka, S. (2003) The homeoprotein Nanog is required for maintenance of pluripotency in mouse epiblast and ES cells. *Cell*, 113(5), 631-642.

Montgomery, R. L., Davis, C. A., Potthoff, M. J., Haberland, M., Fielitz, J., Qi, X. X., Hill, J. A., Richardson, J. A. & Olson, E. N. (2007) Histone deacetylases 1 and 2 redundantly regulate cardiac morphogenesis, growth, and contractility. *Genes & Development*, 21(14), 1790-1802.

Montgomery, R. L., Hsieh, J., Barbosa, A. C., Richardson, J. A. & Olson, E. N. (2009) Histone deacetylases 1 and 2 control the progression of neural precursors to neurons during brain development. *Proceedings of the National Academy of Sciences of the United States of America*, 106(19), 7876-7881.

Montgomery, R. L., Potthoff, M. J., Haberland, M., Qi, X. X., Matsuzaki, S., Humphries, K. M., Richardson, J. A., Bassel-Duby, R. & Olson, E. N. (2008) Maintenance of cardiac energy by histone deacetylase 3 metabolism in mice. *Journal of Clinical Investigation*, 118(11), 3588-3597.

Montpetit, B., Thomsen, N. D., Helmke, K. J., Seeliger, M. A., Berger, J. M. & Weis, K. (2011) A conserved mechanism of DEAD-box ATPase activation by nucleoporins and InsP(6) in mRNA export. *Nature*, 472(7342), 238-242.

Morrisey, E. E., Tang, Z. H., Sigrist, K., Lu, M. M., Jiang, F., Ip, H. S. & Parmacek, M. S. (1998) GATA6 regulates HNF4 and is required for differentiation of visceral endoderm in the mouse embryo. *Genes & Development*, 12(22), 3579-3590.

Murry, C. E. & Keller, G. (2008) Differentiation of embryonic stem cells to clinically relevant populations: Lessons from embryonic development. *Cell*, 132(4), 661-680.

Musselman, C. A., Lalonde, M. E., Cote, J. & Kutateladze, T. G. (2012) Perceiving the epigenetic landscape through histone readers. *Nature Structural & Molecular Biology*, 19(12), 1218-1227.

Nakano, T., Kodama, H. & Honjo, T. (1994) Generation of lymphohematopoietic cells from embryonic stem-cells in culture. *Science*, 265(5175), 1098-1101.

Nalaskowski, M. M., Deschermeier, C., Fanick, W. & Mayr, G. W. (2002) The human homologue of yeast ArgRIII protein is an inositol phosphate multikinase with predominantly nuclear localization. *Biochemical Journal*, 366, 549-556.

Nathan, D., Ingvarsdottir, K., Sterner, D. E., Bylebyl, G. R., Dokmanovic, M., Dorsey, L. A., Whelan, K. A., Krsmanovic, M., Lane, W. S., Meluh, P. B., Johnson, E. S. & Berger, S. L. (2006) Histone sumoylation is a negative regulator in Saccharomyces cerevisiae and shows dynamic interplay with positive-acting histone modifications. *Genes & Development*, 20(8), 966-976.

Nichols, J., Zevnik, B., Anastassiadis, K., Niwa, H., Klewe-Nebenius, D., Chambers, I., Scholer, H. & Smith, A. (1998) Formation of pluripotent stem cells in the mammalian embryo depends on the POU transcription factor Oct4. *Cell*, 95(3), 379-391.

Nielsen, T. K., Hildmann, C., Dickmanns, A., Schwienhorst, A. & Ficner, R. (2005) Crystal structure of a bacterial class 2 histone deacetylase homologue. *Journal of Molecular Biology*, 354(1), 107-120.

Nishikawa, S., Hirashima, M., Matsuyoshi, N. & Kodama, H. (1998) Progressive lineage analysis by cell sorting and culture identifies FLK1(+)VE-cadherin(+) cells at a diverging point of endothelial and hemopoietic lineages. *Development*, 125(9), 1747-1757.

Niwa, H., Burdon, T., Chambers, I. & Smith, A. (1998) Self-renewal of pluripotent embryonic stem cells is mediated via activation of STAT3. *Genes & Development*, 12(13), 2048-2060.

Niwa, H., Miyazaki, J. & Smith, A. G. (2000) Quantitative expression of Oct-3/4 defines differentiation, dedifferentiation or self-renewal of ES cells. *Nature Genetics*, 24(4), 372-376.

Norris, F. A., Wilson, M. P., Wallis, T. S., Galyov, E. E. & Majerus, P. W. (1998) SopB, a protein required for virulence of Salmonella dublin, is an inositol phosphate phosphatase. *Proceedings of the National Academy of Sciences of the United States of America*, 95(24), 14057-14059.

Norton, V. G., Imai, B. S., Yau, P. & Bradbury, E. M. (1989) Histone acetylation reduces nucleosome core particle linking number change. *Cell*, 57(3), 449-457.

Nowak, S. J. & Corces, V. G. (2004) Phosphorylation of histone H3: a balancing act between chromosome condensation and transcriptional activation. *Trends in Genetics*, 20(4), 214-220.

Oberoi, J., Fairall, L., Watson, P. J., Yang, J. C., Czimmerer, Z., Kampmann, T., Goult, B. T., Greenwood, J. A., Gooch, J. T., Kallenberger, B. C., Nagy, L., Neuhaus, D. & Schwabe, J. W. R. (2011) Structural basis for the assembly of the SMRT/NCoR core transcriptional repression machinery. *Nature Structural & Molecular Biology*, 18(2), 177-U239.

Odom, A. R., Stahlberg, A., Wente, S. R. & York, J. D. (2000) A role for nuclear inositol 1,4,5-trisphosphate kinase in transcriptional control. *Science*, 287(5460), 2026-2029.

Oehme, I., Deubzer, H. E., Wegener, D., Pickert, D., Linke, J. P., Hero, B., Kopp-Schneider, A., Westermann, F., Ulrich, S. M., von Deimling, A., Fischer, M. & Witt, O. (2009) Histone Deacetylase 8 in Neuroblastoma Tumorigenesis. *Clinical Cancer Research*, 15(1), 91-99.

Ogryzko, V. V., Schiltz, R. L., Russanova, V., Howard, B. H. & Nakatani, Y. (1996) The transcriptional coactivators p300 and CBP are histone acetyltransferases. *Cell*, 87(5), 953-959.

Okabe, S., ForsbergNilsson, K., Spiro, A. C., Segal, M. & McKay, R. D. G. (1996) Development of neuronal precursor cells and functional postmitotic neurons from embryonic stem cells in vitro. *Mechanisms of Development*, 59(1), 89-102.

Olins, A. L. & Olins, D. E. (1973) Spheroid chromatin units (nu bodies). *Journal of Cell Biology*, 59(2), A252-A252.

Olson, E. N. (2006) Gene regulatory networks in the evolution and development of the heart. *Science*, 313(5795), 1922-1927.

Orchiston, E. A., Bennett, D., Leslie, N. R., Clarke, R. G., Winward, L., Downes, C. P. & Safrany, S. T. (2004) PTEN M-CBR3, a versatile and selective regulator of inositol 1,3,4,5,6-pentakisphosphate (Ins(1,3,4,5,6)P-5) - Evidence for Ins(1,3,4,5,6)P-5 as a proliferative signal. *Journal of Biological Chemistry*, 279(2), 1116-1122.

Pagliuca, F. W., Collins, M. O., Lichawska, A., Zegerman, P., Choudhary, J. S. & Pines, J. (2011) Quantitative Proteomics Reveals the Basis for the Biochemical Specificity of the Cell-Cycle Machinery. *Molecular Cell*, 43(3), 406-417.

Pavri, R., Zhu, B., Li, G. H., Trojer, P., Mandal, S., Shilatifard, A. & Reinberg, D. (2006) Histone H2B monoubiquitination functions cooperatively with FACT to regulate elongation by RNA polymerase II. *Cell*, 125(4), 703-717.

Pena, P. V., Hom, R. A., Hung, T., Lin, H., Kuo, A. J., Wong, R. P. C., Subach, O. M., Champagne, K. S., Zhao, R., Verkhusha, V. V., Li, G., Gozani, O. & Kutateladze, T. G. (2008) Histone H3K4me3 binding is required for the DNA repair and apoptotic activities of ING1 tumor suppressor. *Journal of Molecular Biology*, 380(2), 303-312.

Perrett, C. A. & Zhou, D. G. (2013) Salmonella type III effector SopB modulates host cell exocytosis. *Emerging Microbes & Infections*, 2, 8.

Pflum, M. K. H., Tong, J. K., Lane, W. S. & Schreiber, S. L. (2001) Histone deacetylase I phosphorylation promotes enzymatic activity and complex formation. *Journal of Biological Chemistry*, 276(50), 47733-47741.

Pon, J. R. & Marra, M. A. (2016) MEF2 transcription factors: developmental regulators and emerging cancer genes. *Oncotarget*, 7(3), 2297-2312.

Qiao, Y. B., Wang, R., Yang, X. F., Tang, K. & Jing, N. H. (2015) Dual roles of histone H3 lysine 9 acetylation in human embryonic stem cell pluripotency and neural differentiation (vol 290, pg 2508, 2015). *Journal of Biological Chemistry*, 290(16), 9949-9949.

Qu, X.-B., Pan, J., Zhang, C. & Huang, S.-Y. (2008) Sox17 facilitates the differentiation of mouse embryonic stem cells into primitive and definitive endoderm in vitro. *Development Growth & Differentiation*, 50(7), 585-593.

Rea, S., Eisenhaber, F., O'Carroll, N., Strahl, B. D., Sun, Z. W., Schmid, M., Opravil, S., Mechtler, K., Ponting, C. P., Allis, C. D. & Jenuwein, T. (2000) Regulation of chromatin structure by site-specific histone H3 methyltransferases. *Nature*, 406(6796), 593-599.

Reichert, N., Choukrallah, M.-A. & Matthias, P. (2012) Multiple roles of class I HDACs in proliferation, differentiation, and development. *Cellular and Molecular Life Sciences*, 69(13), 2173-2187.

Ridsdale, J. A., Hendzel, M. J., Delcuve, G. P. & Davie, J. R. (1990) Histone acetylation alters the capacity of the h1 histones to condense transcriptionally active competent chromatin. *Journal of Biological Chemistry*, 265(9), 5150-5156.

Rohwedel, J., Maltsev, V., Bober, E., Arnold, H. H., Hescheler, J. & Wobus, A. M. (1994) Muscle-cell differentiation of embryonic stem-cells reflects myogenesis in-vivo - developmentally-regulated expression of myogenic determination genes and functional expression of ionic currents. *Developmental Biology*, 164(1), 87-101.

Rossetto, D., Avvakumov, N. & Cote, J. (2012) Histone phosphorylation A chromatin modification involved in diverse nuclear events. *Epigenetics*, 7(10), 1098-1108.

Rothbart, S. B. & Strahl, B. D. (2014) Interpreting the language of histone and DNA modifications. *Biochimica Et Biophysica Acta-Gene Regulatory Mechanisms*, 1839(8), 627-643.

Ruizcarrillo, A., Wangh, L. J. & Allfrey, V. G. (1975) PROCESSING OF NEWLY SYNTHESIZED HISTONE MOLECULES. *Science*, 190(4210), 117-128.

Ruthenburg, A. J., Allis, C. D. & Wysocka, J. (2007) Methylation of lysine 4 on histone H3: Intricacy of writing and reading a single epigenetic mark. *Molecular Cell*, 25(1), 15-30.

Ruthenburg, A. J., Li, H. T., Milne, T. A., Dewell, S., McGinty, R. K., Yuen, M., Ueberheide, B., Dou, Y. L., Muir, T. W., Patel, D. J. & Allis, C. D. (2011) Recognition of a Mononucleosomal Histone Modification Pattern by BPTF via Multivalent Interactions. *Cell*, 145(5), 692-706.

Sabari, B. R., Tang, Z. Y., Huang, H., Yong-Gonzalez, V., Molina, H., Kong, H. E., Dai, L. Z., Shimada, M., Cross, J. R., Zhao, Y. M., Roeder, R. G. & Allis, C. D. (2015) Intracellular Crotonyl-CoA Stimulates Transcription through p300-Catalyzed Histone Crotonylation. *Molecular Cell*, 58(2), 203-215.

Sahakian, E., Powers, J. J., Chen, J., Deng, S. L., Cheng, F., Distler, A., Woods, D. M., Rock-Klotz, J., Sodre, A. L., Youn, J.-I., Woan, K. V., Villagra, A., Gabrilovich, D., Sotomayor, E. M. & Pinilla-Ibarz, J. (2015) Histone deacetylase 11: A novel epigenetic regulator of myeloid derived suppressor cell expansion and function. *Molecular Immunology*, 63(2), 579-585.

Saiardi, A., Erdjument-Bromage, H., Snowman, A. M., Tempst, P. & Snyder, S. H. (1999) Synthesis of diphosphoinositol pentakisphosphate by a newly identified family of higher inositol polyphosphate kinases. *Current Biology*, 9(22), 1323-1326.

Saiardi, A., Nagata, E., Luo, H. B. R., Sawa, A., Luo, X. J., Snowman, A. M. & Snyder, S. H. (2001) Mammalian inositol polyphosphate multikinase synthesizes inositol 1,4,5-trisphosphate and an inositol pyrophosphate. *Proceedings of the National Academy of Sciences of the United States of America*, 98(5), 2306-2311.

Saunders, A., Huang, X., Fidalgo, M., Reimer, M. H., Faiola, F., Ding, J. J., Sanchez-Priego, C., Guallar, D., Saenz, C., Li, D. & Wang, J. L. (2017) The SIN3A/HDAC Corepressor Complex Functionally Cooperates with NANOG to Promote Pluripotency. *Cell Reports*, 18(7), 1713-1726.

Savatier, P., Huang, S., Szekely, L., Wiman, K. G. & Samarut, J. (1994) CONTRASTING PATTERNS OF RETINOBLASTOMA PROTEIN EXPRESSION IN MOUSE EMBRYONIC STEM-CELLS AND EMBRYONIC FIBROBLASTS. *Oncogene*, 9(3), 809-818.

Shah, Z. H., Jones, D. R., Sommer, L., Foulger, R., Bultsma, Y., D'Santos, C. & Divecha, N. (2013) Nuclear phosphoinositides and their impact on nuclear functions. *Febs Journal*, 280(24), 6295-6310.

Shears, S. B. (2004) How versatile are inositol phosphate kinases? *Biochemical Journal*, 377, 265-280.

Shears, S. B., Ganapathi, S. B., Gokhale, N. A., Schenk, T. M. H., Wang, H., Weaver, J. D., Zaremba, A. & Zhou, Y. (2012) Defining signal transduction by inositol phosphates. *Sub-cellular biochemistry*, 59, 389-412.

Shen, M. M. & Leder, P. (1992) Leukemia inhibitory factor is expressed by the preimplantation uterus and selectively blocks primitive ectoderm formation invitro. *Proceedings of the National Academy of Sciences of the United States of America*, 89(17), 8240-8244.

Shen, X. T., Xiao, H., Ranallo, R., Wu, W. H. & Wu, C. (2003) Modulation of ATP-dependent chromatin-remodeling complexes by inositol polyphosphates. *Science*, 299(5603), 112-114.

Shi, Y. & Whetstine, J. R. (2007) Dynamic regulation of histone lysine methylation by demethylases. *Molecular Cell*, 25(1), 1-14.

Shi, Y. J., Lan, F., Matson, C., Mulligan, P., Whetstine, J. R., Cole, P. A., Casero, R. A. & Shi, Y. (2004) Histone demethylation mediated by the nuclear arnine oxidase homolog LSD1. *Cell*, 119(7), 941-953.

Shi, Y. J., Matson, C., Lan, F., Iwase, S., Baba, T. & Shi, Y. (2005) Regulation of LSD1 histone demethylase activity by its associated factors. *Molecular Cell*, 19(6), 857-864.

Shi, Y. J., Sawada, J., Sui, G. C., Affar, E. B., Whetstine, J. R., Lan, F., Ogawa, H., Luke, M. P. S., Nakatani, Y. & Shi, Y. (2003) Coordinated histone modifications mediated by a CtBP co-repressor complex. *Nature*, 422(6933), 735-738.

Shogren-Knaak, M. & Peterson, C. L. (2006) Switching on chromatin - Mechanistic role of histone H4-K16 acetylation. *Cell Cycle*, 5(13), 1361-1365.

Singh, A. P. & Archer, T. K. (2014) Analysis of the SWI/SNF chromatin-remodeling complex during early heart development and BAF250a repression cardiac gene transcription during P19 cell differentiation. *Nucleic Acids Research*, 42(5), 2958-2975.

Smith, A. G. (2001) Embryo-derived stem cells: Of mice and men. *Annual Review of Cell and Developmental Biology*, 17, 435-462.

Smith, A. G., Heath, J. K., Donaldson, D. D., Wong, G. G., Moreau, J., Stahl, M. & Rogers, D. (1988) Inhibition of pluripotential embryonic stem-cell differentiation by purified polypeptides. *Nature*, 336(6200), 688-690.

Snow, M. H. L. (1977) GASTRULATION IN MOUSE - Growth and regionalization of epiblast. *Journal of Embryology and Experimental Morphology*, 42(DEC), 293-303.

Sobel, R. E., Cook, R. G., Perry, C. A., Annunziato, A. T. & Allis, C. D. (1995) Conservation of deposition-related acetylation sites in newly synthesized histones h3 and h4. *Proceedings of the National Academy of Sciences of the United States of America*, 92(4), 1237-1241.

Sokol, S. Y. (2011) Maintaining embryonic stem cell pluripotency with Wnt signaling. *Development*, 138(20), 4341-4350.

Somoza, J. R., Skene, R. J., Katz, B. A., Mol, C., Ho, J. D., Jennings, A. J., Luong, C., Arvai, A., Buggy, J. J., Chi, E., Tang, J., Sang, B. C., Verner, E., Wynands, R., Leahy, E. M., Dougan, D. R., Snell, G., Navre, M., Knuth, M. W., Swanson, R. V., McRee, D. E. & Tari, L. W. (2004) Structural snapshots of human HDAC8 provide insights into the class I histone deacetylases. *Structure*, 12(7), 1325-1334.

Steger, D. J., Haswell, E. S., Miller, A. L., Wente, S. R. & O'Shea, E. K. (2003) Regulation of chromatin remodeling by inositol polyphosphates. *Science*, 299(5603), 114-116.

Sterner, D. E. & Berger, S. L. (2000) Acetylation of histones and transcription-related factors. *Microbiology and Molecular Biology Reviews*, 64(2), 435-+.

Stevenson-Paulik, J., Chiou, S.-T., Frederick, J. P., dela Cruz, J., Seeds, A. M., Otto, J. C. & York, J. D. (2006) Inositol phosphate metabolomics: Merging genetic perturbation with modernized radiolabeling methods. *Methods*, 39(2), 112-121.

Strahl, B. D. & Allis, C. D. (2000) The language of covalent histone modifications. *Nature*, 403(6765), 41-45.

Sun, Z., Feng, D., Fang, B., Mullican, S. E., You, S. H., Lim, H. W., Everett, L. J., Nabel, C. S., Li, Y., Selvakumaran, V., Won, K. J. & Lazar, M. A. (2013) Deacetylase-Independent

Function of HDAC3 in Transcription and Metabolism Requires Nuclear Receptor Corepressor. *Molecular Cell*, 52(6), 769-782.

Sun, Z., Miller, R. A., Patel, R. T., Chen, J., Dhir, R., Wang, H., Zhang, D., Graham, M. J., Unterman, T. G., Shulman, G. I., Sztalryd, C., Bennett, M. J., Ahima, R. S., Birnbaum, M. J. & Lazar, M. A. (2012) Hepatic Hdac3 promotes gluconeogenesis by repressing lipid synthesis and sequestration. *Nature Medicine*, 18(6), 934-+.

Suter, D. M., Tirefort, D., Julien, S. & Krause, K. H. (2009) A Sox1 to Pax6 Switch Drives Neuroectoderm to Radial Glia Progression During Differentiation of Mouse Embryonic Stem Cells. *Stem Cells*, 27(1), 49-58.

Tada, S., Era, T., Furusawa, C., Sakurai, H., Nishikawa, S., Kinoshita, M., Nakao, K., Chiba, T. & Nishikawa, S. I. (2005) Characterization of mesendoderm: a diverging point of the definitive endoderm and mesoderm in embryonic stem cell differentiation culture. *Development*, 132(19), 4363-4374.

Tahiliani, M., Koh, K. P., Shen, Y. H., Pastor, W. A., Bandukwala, H., Brudno, Y., Agarwal, S., Iyer, L. M., Liu, D. R., Aravind, L. & Rao, A. (2009) Conversion of 5-Methylcytosine to 5-Hydroxymethylcytosine in Mammalian DNA by MLL Partner TET1. *Science*, 324(5929), 930-935.

Tam, P. P. L. & Behringer, R. R. (1997) Mouse gastrulation: the formation of a mammalian body plan. *Mechanisms of Development*, 68(1-2), 3-25.

Tan, M. J., Luo, H., Lee, S., Jin, F. L., Yang, J. S., Montellier, E., Buchou, T., Cheng, Z. Y., Rousseaux, S., Rajagopal, N., Lu, Z. K., Ye, Z., Zhu, Q., Wysocka, J., Ye, Y., Khochbin, S., Ren, B. & Zhao, Y. M. (2011) Identification of 67 Histone Marks and Histone Lysine Crotonylation as a New Type of Histone Modification. *Cell*, 146(6), 1015-1027.

Taplick, J., Kurtev, V., Kroboth, K., Posch, M., Lechner, T. & Seiser, C. (2001) Homo-oligomerisation and nuclear localisation of mouse histone deacetylase 1. *Journal of Molecular Biology*, 308(1), 27-38.

Taunton, J., Hassig, C. A. & Schreiber, S. L. (1996) A mammalian histone deacetylase related to the yeast transcriptional regulator Rpd3p. *Science*, 272(5260), 408-411.

Taverna, S. D., Li, H., Ruthenburg, A. J., Allis, C. D. & Patel, D. J. (2007) How chromatin-binding modules interpret histone modifications: lessons from professional pocket pickers. *Nature Structural & Molecular Biology*, 14(11), 1025-1040.

Thoma, F., Koller, T. & Klug, A. (1979) Involvement of histone-h1 in the organization of the nucleosome and of the salt-dependent superstructures of chromatin. *Journal of Cell Biology*, 83(2), 403-427.

Thompson, S., Clarke, A. R., Pow, A. M., Hooper, M. L. & Melton, D. W. (1989) Germ line transmission and expression of a corrected hprt gene produced by gene targeting in embryonic stem-cells. *Cell*, 56(2), 313-321.

Torchy, M. P., Hamiche, A. & Klaholz, B. P. (2015) Structure and function insights into the NuRD chromatin remodeling complex. *Cellular and Molecular Life Sciences*, 72(13), 2491-2507.

Trivedi, C. M., Luo, Y., Yin, Z., Zhang, M. Z., Zhu, W. T., Wang, T., Floss, T., Goettlicher, M., Noppinger, P. R., Wurst, W., Ferrari, V. A., Abrams, C. S., Gruber, P. J. & Epstein, J. A. (2007) Hdac2 regulates the cardiac hypertrophic response by modulating Gsk3 beta activity. *Nature Medicine*, 13(3), 324-331.

Tropepe, V., Hitoshi, S., Sirard, C., Mak, T. W., Rossant, J. & van der Kooy, D. (2001) Direct neural fate specification from embryonic stem cells: A primitive mammalian neural stem cell stage acquired through a default mechanism. *Neuron*, 30(1), 65-78.

Tsai, S. C. & Seto, E. (2002) Regulation of histone deacetylase 2 by protein kinase CK2. *Journal of Biological Chemistry*, 277(35), 31826-31833.

Tsukada, Y., Fang, J., Erdjument-Bromage, H., Warren, M. E., Borchers, C. H., Tempst, P. & Zhang, Y. (2006) Histone demethylation by a family of JmjC domain-containing proteins. *Nature*, 439(7078), 811-816.

Unnikrishnan, A., Gafken, P. R. & Tsukiyama, T. (2010) Dynamic changes in histone acetylation regulate origins of DNA replication. *Nature Structural & Molecular Biology*, 17(4), 430-U68.

Urvalek, A. M. & Gudas, L. J. (2014) Retinoic Acid and Histone Deacetylases Regulate Epigenetic Changes in Embryonic Stem Cells. *Journal of Biological Chemistry*, 289(28), 19519-19530.

Valinluck, V. & Sowers, L. C. (2007) Endogenous cytosine damage products alter the site selectivity of human DNA maintenance methyltransferase DNMT1. *Cancer Research*, 67(3), 946-950.

Vannini, A., Volpari, C., Filocamo, G., Casavola, E. C., Brunetti, M., Renzoni, D., Chakravarty, P., Paolini, C., De Francesco, R., Gallinari, P., Steinkuhler, C. & Di Marco, S. (2004) Crystal structure of a eukaryotic zinc-dependent histone deacetylase, human HDAC8, complexed with a hydroxamic acid inhibitor. *Proceedings of the National Academy of Sciences of the United States of America*, 101(42), 15064-15069.

Varga-Weisz, P. (2001) ATP-dependent chromatin remodeling factors: Nucleosome shufflers with many missions. *Oncogene*, 20(24), 3076-3085.

Vassilev, L. T. (2006) Cell cycle synchronization at the G(2)/M phase border by reversible inhibition of CDK1. *Cell Cycle*, 5(22), 2555-2556.

Vempati, R. K., Jayani, R. S., Notani, D., Sengupta, A., Galande, S. & Haldar, D. (2010) p300-mediated Acetylation of Histone H3 Lysine 56 Functions in DNA Damage Response in Mammals. *Journal of Biological Chemistry*, 285(37), 28553-28564.

Verbsky, J., Lavine, K. & Majerus, P. W. (2005a) Disruption of the mouse inositol 1,3,4,5,6-pentakisphosphate 2-kinase gene, associated lethality, and tissue distribution of 2-kinase expression. *Proceedings of the National Academy of Sciences of the United States of America*, 102(24), 8448-8453.

Verbsky, J. W., Chang, S. C., Wilson, M. P., Mochizukim, Y. & Majerus, P. W. (2005b) The pathway for the production of inositol hexakisphosphate in human cells. *Journal of Biological Chemistry*, 280(3), 1911-1920.

Vermeulen, M., Eberl, H. C., Matarese, F., Marks, H., Denissov, S., Butter, F., Lee, K. K., Olsen, J. V., Hyman, A. A., Stunnenberg, H. G. & Mann, M. (2010) Quantitative Interaction Proteomics and Genome-wide Profiling of Epigenetic Histone Marks and Their Readers. *Cell*, 142(6), 967-980.

Verreault, A., Kaufman, P. D., Kobayashi, R. & Stillman, B. (1996) Nucleosome assembly by a complex of CAF-1 and acetylated histones H3/H4. *Cell*, 87(1), 95-104.

Vidal, M. & Gaber, R. F. (1991) Rpd3 encodes a 2nd factor required to achieve maximum positive and negative transcriptional states in saccharomyces-cerevisiae. *Molecular and Cellular Biology*, 11(12), 6317-6327.

Vidal-Laliena, M., Gallastegui, E., Mateo, F., Martinez-Balbas, M., Pujol, M. J. & Bachs, O. (2013) Histone Deacetylase 3 Regulates Cyclin A Stability. *Journal of Biological Chemistry*, 288(29), 21096-21104.

Vignali, M., Hassan, A. H., Neely, K. E. & Workman, J. L. (2000) ATP-dependent chromatin-remodeling complexes. *Molecular and Cellular Biology*, 20(6), 1899-1910.

Viiri, K. M., Janis, J., Siggers, T., Heinonen, T. Y. K., Valjakka, J., Bulyk, M. L., Maki, M. & Lohi, O. (2009) DNA-Binding and -Bending Activities of SAP30L and SAP30 Are Mediated by a Zinc-Dependent Module and Monophosphoinositides. *Molecular and Cellular Biology*, 29(2), 342-356.

Walther, C. & Gruss, P. (1991) PAX-6, A MURINE PAIRED BOX GENE, IS EXPRESSED IN THE DEVELOPING CNS. *Development*, 113(4), 1435-1449.

Wang, A. H., Kruhlak, M. J., Wu, J., Bertos, N. R., Vezmar, M., Posner, B. I., Bazett-Jones, D. P. & Yang, X. J. (2000) Regulation of histone deacetylase 4 by binding of 14-3-3 proteins. *Molecular and Cellular Biology*, 20(18), 6904-6912.

Wang, H. B., Wang, L. J., Erdjument-Bromage, H., Vidal, M., Tempst, P., Jones, R. S. & Zhang, Y. (2004) Role of histone H2A ubiquitination in polycomb silencing. *Nature*, 431(7010), 873-878.

Wang, H. M. & Stillman, D. J. (1990) Invitro regulation of a sin3-dependent dna-binding activity by stimulatory and inhibitory factors. *Proceedings of the National Academy of Sciences of the United States of America*, 87(24), 9761-9765.

Wang, J. X., Scully, K., Zhu, X., Cai, L., Zhang, J., Prefontaine, G. G., Krones, A., Ohgi, K. A., Zhu, P., Garcia-Bassets, I., Liu, F., Taylor, H., Lozach, J., Jayes, F. L., Korach, K. S., Glass, C. K., Fu, X. D. & Rosenfeld, M. G. (2007) Opposing LSD1 complexes function in developmental gene activation and repression programmes. *Nature*, 446(7138), 882-887.

Wang, L. & Chen, Y.-G. (2016) Signaling Control of Differentiation of Embryonic Stem Cells toward Mesendoderm. *Journal of Molecular Biology*, 428(7), 1409-1422.

Wang, X. W., Spandidos, A., Wang, H. J. & Seed, B. (2012) PrimerBank: a PCR primer database for quantitative gene expression analysis, 2012 update. *Nucleic Acids Research*, 40(D1), D1144-D1149.

Wang, Z. B., Zang, C. Z., Cui, K. R., Schones, D. E., Barski, A., Peng, W. Q. & Zhao, K. J. (2009) Genome-wide Mapping of HATs and HDACs Reveals Distinct Functions in Active and Inactive Genes. *Cell*, 138(5), 1019-1031.

Wang, Z. B., Zang, C. Z., Rosenfeld, J. A., Schones, D. E., Barski, A., Cuddapah, S., Cui, K. R., Roh, T. Y., Peng, W. Q., Zhang, M. Q. & Zhao, K. J. (2008) Combinatorial patterns of histone acetylations and methylations in the human genome. *Nature Genetics*, 40(7), 897-903.

Watson, P. J., Fairall, L., Santos, G. M. & Schwabe, J. W. R. (2012) Structure of HDAC3 bound to co-repressor and inositol tetraphosphate. *Nature*, 481(7381), 335-U114.

Watson, P. J., Millard, C. J., Riley, A. M., Robertson, N. S., Wright, L. C., Godage, H. Y., Cowley, S. M., Jamieson, A. G., Potter, B. V. L. & Schwabe, J. W. R. (2016) Insights into the activation mechanism of class I HDAC complexes by inositol phosphates. *Nature Communications*, 7, 13.

Wei, W., Liu, X., Chen, J., Gao, S., Lu, L., Zhang, H., Ding, G., Wang, Z., Chen, Z., Shi, T., Li, J., Yu, J. & Wong, J. (2017) Class I histone deacetylases are major histone decrotonylases: evidence for critical and broad function of histone crotonylation in transcription. *Cell research*.

Wei, Y., Yu, L. L., Bowen, J., Gorovsky, M. A. & Allis, C. D. (1999) Phosphorylation of histone H3 is required for proper chromosome condensation and segregation. *Cell*, 97(1), 99-109.

Wen, Y. D., Perissi, V., Staszewski, L. M., Yang, W. M., Krones, A., Glass, C. K., Rosenfeld, M. G. & Seto, E. (2000) The histone deacetylase-3 complex contains nuclear receptor corepressors. *Proceedings of the National Academy of Sciences of the United States of America*, 97(13), 7202-7207.

Weng, L. P., Brown, J. L. & Eng, C. (2001) PTEN coordinates G(1) arrest by down-regulating cyclin D1 via its protein phosphatase activity and up-regulating p27 via its lipid phosphatase activity in a breast cancer model. *Human Molecular Genetics*, 10(6), 599-604.

Whetstine, J. R., Nottke, A., Lan, F., Huarte, M., Smolikov, S., Chen, Z. Z., Spooner, E., Li, E., Zhang, G. Y., Colaiacovo, M. & Shi, Y. (2006) Reversal of histone lysine trimethylation by the JMJD2 family of histone demethylases. *Cell*, 125(3), 467-481.

Wickramasinghe, V. O., Savill, J. M., Chavali, S., Jonsdottir, A. B., Rajendra, E., Gruner, T., Laskey, R. A., Babu, M. M. & Venkitaraman, A. R. (2013) Human Inositol Polyphosphate Multikinase Regulates Transcript-Selective Nuclear mRNA Export to Preserve Genome Integrity. *Molecular Cell*, 51(6), 737-750.

Widom, J. & Klug, A. (1985) Structure of the 300a chromatin filament - x-ray-diffraction from oriented samples. *Cell*, 43(1), 207-213.

Wilder, P. J., Kelly, D., Brigman, K., Peterson, C. L., Nowling, T., Gao, Q. S., McComb, R. D., Capecchi, M. R. & Rizzino, A. (1997) Inactivation of the FGF-4 gene in embryonic stem cells alters the growth and/or the survival of their early differentiated progeny. *Developmental Biology*, 192(2), 614-629.

Wilkinson, G., Dennis, D. & Schuurmans, C. (2013) PRONEURAL GENES IN NEOCORTICAL DEVELOPMENT. *Neuroscience*, 253, 256-273.

Willhoft, O., Bythell-Douglas, R., McCormack, E. A. & Wigley, D. B. (2016) Synergy and antagonism in regulation of recombinant human INO80 chromatin remodeling complex. *Nucleic Acids Research*, 44(17), 8179-8188.

Williams, R. L., Hilton, D. J., Pease, S., Willson, T. A., Stewart, C. L., Gearing, D. P., Wagner, E. F., Metcalf, D., Nicola, N. A. & Gough, N. M. (1988) Myeloid-leukemia inhibitory factor maintains the developmental potential of embryonic stem-cells. *Nature*, 336(6200), 684-687.

Wilson, A. J., Byun, D. S., Popova, N., Murray, L. B., L'Italien, K., Sowa, Y., Arango, D., Velcich, A., Augenlicht, L. H. & Mariadason, J. M. (2006) Histone deacetylase 3 (HDAC3) and other class IHDACs regulate colon cell maturation and p21 expression and are deregulated in human colon cancer. *Journal of Biological Chemistry*, 281(19), 13548-13558.

Wilson, M. H., Coates, C. J. & George, A. L. (2007) PiggyBac transposon-mediated gene transfer in human cells. *Molecular Therapy*, 15(1), 139-145.

Wilson, M. S. C., Bulley, S. J., Pisani, F., Irvine, R. F. & Saiardi, A. (2015) A novel method for the purification of inositol phosphates from biological samples reveals that no phytate is present in human plasma or urine. *Open Biology*, 5(3), 9.

Wilting, R. H., Yanover, E., Heideman, M. R., Jacobs, H., Horner, J., van der Torre, J., DePinho, R. A. & Dannenberg, J. H. (2010) Overlapping functions of Hdac1 and Hdac2 in cell cycle regulation and haematopoiesis. *Embo Journal*, 29(15), 2586-2597.

Wolffe, A. P. & Hayes, J. J. (1999) Chromatin disruption and modification. *Nucleic Acids Research*, 27(3), 711-720.

Worley, J., Luo, X. X. & Capaldi, A. P. (2013) Inositol Pyrophosphates Regulate Cell Growth and the Environmental Stress Response by Activating the HDAC Rpd3L. *Cell Reports*, 3(5), 1476-1482.

Wysocka, J., Swigut, T., Xiao, H., Milne, T. A., Kwon, S. Y., Landry, J., Kauer, M., Tackett, A. J., Chait, B. T., Badenhorst, P., Wu, C. & Allis, C. D. (2006) A PHD finger of NURF couples histone H3 lysine 4 trimethylation with chromatin remodelling. *Nature*, 442(7098), 86-90.

Xu, R., Paul, B. D., Smith, D. R., Tyagi, R., Rao, F., Khan, A. B., Blech, D. J., Vandiver, M. S., Harraz, M. M., Guha, P., Ahmed, I., Sen, N., Gallagher, M. & Snyder, S. H. (2013a) Inositol polyphosphate multikinase is a transcriptional coactivator required for immediate early gene induction. *Proceedings of the National Academy of Sciences of the United States of America*, 110(40), 16181-16186.

Xu, R., Sen, N., Paul, B. D., Snowman, A. M., Rao, F., Vandiver, M. S., Xu, J. & Snyder, S. H. (2013b) Inositol Polyphosphate Multikinase Is a Coactivator of p53-Mediated Transcription and Cell Death. *Science Signaling*, 6(269).

Xue, Y. T., Wong, J. M., Moreno, G. T., Young, M. K., Cote, J. & Wang, W. D. (1998) NURD, a novel complex with both ATP-dependent chromatin-remodeling and histone deacetylase activities. *Molecular Cell*, 2(6), 851-861.

Yamaguchi, T., Cubizolles, F., Zhang, Y., Reichert, N., Kohler, H., Seiser, C. & Matthias, P. (2010) Histone deacetylases 1 and 2 act in concert to promote the G1-to-S progression. *Genes & Development*, 24(5), 455-469.

Yang, M. J., Gocke, C. B., Luo, X. L., Borek, D., Tomchick, D. R., Machius, M., Otwinowski, Z. & Yu, H. T. (2006) Structural basis for CoREST-dependent demethylation of nucleosomes by the human LSD1 histone demethylase. *Molecular Cell*, 23(3), 377-387.

Yang, W. M., Inouye, C., Zeng, Y. Y., Bearss, D. & Seto, E. (1996) Transcriptional repression by YY1 is mediated by interaction with a mammalian homolog of the yeast global regulator RPD3. *Proceedings of the National Academy of Sciences of the United States of America*, 93(23), 12845-12850.

Yang, W. M., Tsai, S. C., Wen, Y. D., Fejer, G. & Seto, E. (2002) Functional domains of histone deacetylase-3. *Journal of Biological Chemistry*, 277(11), 9447-9454.

Yang, W. M., Yao, Y. L., Sun, J. M., Davie, J. R. & Seto, E. (1997) Isolation and characterization of cDNAs corresponding to an additional member of the human histone deacetylase gene family. *Journal of Biological Chemistry*, 272(44), 28001-28007.

Yang, X. J. & Seto, E. (2008) The Rpd3/Hda1 family of lysine deacetylases: from bacteria and yeast to mice and men. *Nature Reviews Molecular Cell Biology*, 9(3), 206-218.

Yang, Y., Huang, Y., Wang, Z., Wang, H.-t., Duan, B., Ye, D., Wang, C., Jing, R., Leng, Y., Xi, J., Chen, W., Wang, G., Jia, W., Zhu, S. & Kang, J. (2016) HDAC10 promotes lung cancer proliferation via AKT phosphorylation. *Oncotarget*, 7(37), 59388-59401.

Yao, Y. L. & Yang, W. M. (2003) The metastasis-associated proteins 1 and 2 form distinct protein complexes with histone deacetylase activity. *Journal of Biological Chemistry*, 278(43), 42560-42568.

Ye, F., Chen, Y., Hoang, T., Montgomery, R. L., Zhao, X. H., Bu, H., Hu, T., Taketo, M. M., van Es, J. H., Clevers, H., Hsieh, J., Bassel-Duby, R., Olson, E. N. & Lu, Q. R. (2009) HDAC1 and HDAC2 regulate oligodendrocyte differentiation by disrupting the beta-catenin-TCF interaction. *Nature Neuroscience*, 12(7), 829-U35.

Yin, F., Lan, R. F., Zhang, X. M., Zhu, L. Y., Chen, F. F., Xu, Z. S., Liu, Y. Q., Ye, T., Sun, H., Lu, F. & Zhang, H. (2014) LSD1 Regulates Pluripotency of Embryonic Stem/Carcinoma Cells through Histone Deacetylase 1-Mediated Deacetylation of Histone H4 at Lysine 16. *Molecular and Cellular Biology*, 34(2), 158-179.

Ying, Q.-L., Wray, J., Nichols, J., Batlle-Morera, L., Doble, B., Woodgett, J., Cohen, P. & Smith, A. (2008) The ground state of embryonic stem cell self-renewal. *Nature*, 453(7194), 519-U5.

Ying, Q. L., Nichols, J., Chambers, I. & Smith, A. (2003a) BMP induction of Id proteins suppresses differentiation and sustains embryonic stem cell self-renewal in collaboration with STAT3. *Cell*, 115(3), 281-292.

Ying, Q. L., Stavridis, M., Griffiths, D., Li, M. & Smith, A. (2003b) Conversion of embryonic stem cells into neuroectodermal precursors in adherent monoculture. *Nature Biotechnology*, 21(2), 183-186.

Yoon, H. G., Chan, D. W., Huang, Z. Q., Li, J. W., Fondell, J. D., Qin, J. & Wong, J. M. (2003) Purification and functional characterization of the human N-CoR complex: the roles of HDAC3, TBL1 and TBLR1. *Embo Journal*, 22(6), 1336-1346.

York, J. D. (2006) Regulation of nuclear processes by inositol polyphosphates. *Biochimica Et Biophysica Acta-Molecular and Cell Biology of Lipids*, 1761(5-6), 552-559.

York, J. D., Odom, A. R., Murphy, R., Ives, E. B. & Wente, S. R. (1999) A phospholipase C-dependent inositol polyphosphate kinase pathway required for efficient messenger RNA export. *Science*, 285(5424), 96-100.

You, A., Tong, J. K., Grozinger, C. M. & Schreiber, S. L. (2001) CoREST is an integral component of the CoREST-human histone deacetylase complex. *Proceedings of the National Academy of Sciences of the United States of America*, 98(4), 1454-1458.

You, S.-H., Lim, H.-W., Sun, Z., Broache, M., Won, K.-J. & Lazar, M. A. (2013) Nuclear receptor co-repressors are required for the histone-deacetylase activity of HDAC3 in vivo. *Nature Structural & Molecular Biology*, 20(2), 182-187.

Yu, J. J., Li, Y., Ishizuka, T., Guenther, M. G. & Lazar, M. A. (2003) A SANT motif in the SMRT corepressor interprets the histone code and promotes histone deacetylation. *Embo Journal*, 22(13), 3403-3410.

Zamir, I., Harding, H. P., Atkins, G. B., Horlein, A., Glass, C. K., Rosenfeld, M. G. & Lazar, M. A. (1996) A nuclear hormone receptor corepressor mediates transcriptional silencing by receptors with distinct repression domains. *Molecular and Cellular Biology*, 16(10), 5458-5465.

Zhang, J. S., Kalkum, M., Chait, B. T. & Roeder, R. G. (2002) The N-CoR-HDAC3 nuclear receptor corepressor complex inhibits the JNK pathway through the integral subunit GPS2. *Molecular Cell*, 9(3), 611-623.

Zhang, X. H., Ozawa, Y., Lee, H., Wen, Y. D., Tan, T. H., Wadzinski, B. E. & Seto, E. (2005) Histone deacetylase 3 (HDAC3) activity is regulated by interaction with protein serine/threonine phosphatase 4. *Genes & Development*, 19(7), 827-839.

Zhang, Y., Iratni, R., ErdjumentBromage, H., Tempst, P. & Reinberg, D. (1997) Histone deacetylases and SAP18, a novel polypeptide, are components of a human Sin3 complex. *Cell*, 89(3), 357-364.

Zhang, Y., LeRoy, G., Seelig, H. P., Lane, W. S. & Reinberg, D. (1998) The dermatomyositis-specific autoantigen Mi2 is a component of a complex containing histone deacetylase and nucleosome remodeling activities. *Cell*, 95(2), 279-289.

Zhang, Y., Ng, H. H., Erdjument-Bromage, H., Tempst, P., Bird, A. & Reinberg, D. (1999) Analysis of the NuRD subunits reveals a histone deacetylase core complex and a connection with DNA methylation. *Genes & Development*, 13(15), 1924-1935.

Zhang, Y. & Reinberg, D. (2001) Transcription regulation by histone methylation: interplay between different covalent modifications of the core histone tails. *Genes & Development*, 15(18), 2343-2360.

Zhao, R., Nakamura, T., Fu, Y., Lazar, Z. & Spector, D. L. (2011) Gene bookmarking accelerates the kinetics of post-mitotic transcriptional re-activation. *Nature Cell Biology*, 13(11), 1295-U39.

Zimmermann, S., Kiefer, F., Prudenziati, M., Spiller, C., Hansen, J., Floss, T., Wurst, W., Minucci, S. & Gottlicher, M. (2007) Reduced body size and decreased intestinal tumor rates in HDAC2-mutant mice. *Cancer Research*, 67(19), 9047-9054.

Zupkovitz, G., Grausenburger, R., Brunmeir, R., Senese, S., Tischler, J., Jurkin, J., Rembold, M., Meunier, D., Egger, G., Lagger, S., Chiocca, S., Propst, F., Weitzer, G. & Seiser, C. (2010) The Cyclin-Dependent Kinase Inhibitor p21 Is a Crucial Target for Histone Deacetylase 1 as a Regulator of Cellular Proliferation. *Molecular and Cellular Biology*, 30(5), 1171-1181.